Chemotherapeutic Drug Cytotoxicity Enhancement in Human Cells in Culture

by Séamus Coyle B.Sc. M.Med.Sc

A thesis submitted for the degree of Ph.D.

Dublin City University

The research work described in this thesis was carried out under the supervision of

Professor Martin Clynes

National Cell & Tissue Culture Centre
School of Biological Sciences

August 1996

I hereby certify that this material, which I now submit for the assessment on the programme of study leading to the award of Ph.D. is entirely my own work and has not been taken from the work of others save and to the extent that such work has been cited and acknowledged within the text of my work.

Signed: Séamus Coyle **ID. No.:** 92700845

Date: 19-9-1996

TABLE OF CONTENTS

Abstract

Chemotherapeutic Drug Cytotoxicity Enhancement in Human Cells in Culture

Séamus Coyle

This thesis examined the effect of combinations of different drugs on toxicity to cancer cells *in vitro*. Combinations of a known anticancer agent with one of a series of coded non-toxic compounds known to be safe for human use were assayed. Significant enhancement of toxicity of adriamycin and vincristine but not 5-fluorouracil, was observed with three compounds from the series. Studies in a wide range of cellular models showed that this combination effect was not observed in cells overexpressing P-glycoprotein and that the mechanism involved was not inhibition of P-glycoprotein.

An assay was developed to analyse how synergy was affected when cells were exposed to the compounds at different times relative to chemotherapeutic drug pulse exposure. Activity of the active compounds was observed only during 24 hours subsequent to 2 hours drug exposure. Pre-treatment or treatment at later times was ineffective.

Flow cytometric analysis was used to determine the cell cycle distribution of these test compounds in DLKP-SQ, a human lung carcinoma clonal cell line. U-1 (active in the combination assay) on its own was shown to induce a transient G_1/S arrest. There was no apparent effect on the cell cycle distribution using A-1 (inactive) or N-1 (active). A combination of adriamycin and U-1 caused an increased delay in the G_1 phase and the S phase compared to adriamycin alone. Vincristine in combination with U-1 displayed an increased G_2/M arrest compared to vincristine treated cells alone. DLKP-SQ treated with 5-fluorouracil alone and in combination showed no effect on cell cycle distribution.

Time lapse videomicroscopic studies demonstrated that vincristine induced apoptosis within 24 hours and the rate of apoptosis increased in the combination. Cells underwent apoptosis 24 hours after treatment with adriamycin but surprisingly there was no significant difference in the rate of apoptosis between adriamycin alone and in combination.

To investigate if the combination effect was due to interference with proteins controlling cell cycle progress, the levels of cyclin E and CDK2 were determined using western blotting; Cyclin E/CDK2 kinase activity was also measured.

Abstract

Chemotherapeutic Drug Cytotoxicity Enhancement in Human Cells in Culture

Séamus Coyle

This thesis examined the effect of combinations of different drugs on toxicity to cancer cells *in vitro*. Combinations of a known anticancer agent with one of a series of coded non-toxic compounds known to be safe for human use were assayed. Significant enhancement of toxicity of adriamycin and vincristine but not 5-fluorouracil, was observed with three compounds from the series. Studies in a wide range of cellular models showed that this combination effect was not observed in cells overexpressing P-glycoprotein and that the mechanism involved was not inhibition of P-glycoprotein.

An assay was developed to analyse how synergy was affected when cells were exposed to the compounds at different times relative to chemotherapeutic drug pulse exposure. Activity of the active compounds was observed only during 24 hours subsequent to 2 hours drug exposure. Pre-treatment or treatment at later times was ineffective.

Flow cytometric analysis was used to determine the cell cycle distribution of these test compounds in DLKP-SQ, a human lung carcinoma clonal cell line. U-1 (active in the combination assay) on its own was shown to induce a transient G_1/S arrest. There was no apparent effect on the cell cycle distribution using A-1 (inactive) or N-1 (active). A combination of adriamycin and U-1 caused an increased delay in the G_1 phase and the S phase compared to adriamycin alone. Vincristine in combination with U-1 displayed an increased G_2/M arrest compared to vincristine treated cells alone. DLKP-SQ treated with 5-fluorouracil alone and in combination showed no effect on cell cycle distribution.

Time lapse videomicroscopic studies demonstrated that vincristine induced apoptosis within 24 hours and the rate of apoptosis increased in the combination. Cells underwent apoptosis 24 hours after treatment with adriamycin but surprisingly there was no significant difference in the rate of apoptosis between adriamycin alone and in combination.

To investigate if the combination effect was due to interference with proteins controlling cell cycle progress, the levels of cyclin E and CDK2 were determined using western blotting; Cyclin E/CDK2 kinase activity was also measured.

Abbreviations

ABC	ATP binding cassette
ActD	Actinomycin D
Adr	Adriamycin
AMSA	Amsacrine
ATCC	American Tissue Culture Collection
ATP	Adenosine tri-phosphate
bp	Base pair
BSA	Bovine serum albumin
BSO	DL-Buthionine-[S,R]-sulfoximine
$CaCl_2$	Calcium chloride
CAK	Cdc2-activating kinase
$CaPO_4$	Calcium phosphate
CDI	Cyclin dependent kinase inhibitor
cDNA	Complementary deoxyribonucleic acid
CDK	Cyclin dependent kinase
CHO	Chinese hampster ovary
CHX	Cycloheximide
CI	Combination Index
CML	Chronic myelocytic leukeamia
CsCl	Cesium chloride
CTL	Cytotoxic T-cell
CysA	Cyclosporin A
Da	Dalton
DEM	Minimum essential medium eagle's
DEPC	Diethyl pyrocarbonate
DHFR	Dihydrofolate reductase
DMEM	Dulbeccos mimimum eagle's medium
DMSO	Dimethyl sulphoxide
DNA	Deoxyribonucleic acid

DTT	DL-Dithiothreitol
ECL	Enhanced chemiluminescence
EDTA	Ethylene glycol-bis(ß-aminoethylether)-N,N,N',N'-tetraacetic acid
FCS	Foetal calf serum
5-FU	5-Fluorouracil
GSH	Glutathione
GST	Glutathione-S-transferase
HCl	Hydrochloric acid
Hepes	4-(2-hydroxyethyl)-1-piperazine ethane sulphonic acid
HPLC	High pressure liquid chromatography
IC-50	Drug concentration at 50% survival
ICE	Interleukin-1ß-converting enzyme
IMS	Industrial methylated spirits
Kcl	Potassium chloride
LRP	Lung resistance-related protein
MEX	Methylxanthine
MDR	Multidrug resistance
MHC	Major histocompatibility complex
$MgCl_2$	Magnesium chloride
mRNA	Messenger ribonucleic acid
MRP	Multidrug resistance related protein
MT	Metallothionein
NaCl	Sodium chloride
NADPH	Nicotine adenine dinucleotide phosphate
$NaHCO_2$	Sodium bicarbonate
NaH_2PO_4	Monosodium phosphate
Na_2HPO_4	Disodium phosphate
NaOH	Sodium hydroxide
NSCLC	Non-small cell lung carcinoma
OD	Optical Density
PBS	Phosphate buffered saline
PCNA	Proliferating cell nuclear antigen

PCR	Polymerase chain reaction
PIPES	Piperazine-N,N'-bis[2-ethanesulphonic acid
PMSF	Phenylmethylsulphonyl fluoride
Rb	Retinablastoma protein
RNA	Ribonucleic acid
rRNA	Ribosomal ribonucleic acid
rpm	revolutions per minute
RT	Reverse transcriptase
SCLC	Small cell lung carcinoma
SDS	Sodium dodedecyl sulphate
TAP	Transporter-related with antigen presentation
TBS	Tris buffered saline
TC	Test compound
TEMED	N,N,N',N'-Tetramethyl-ethylenediamine
TGF-ß	Transforming growth factor ß
Thr	Threonine
Tris	Tris(hydroxymethyl)aminomethane hydrochloride
Tyr	Tyrosine
UV	Ultraviolet
Vcr	Vincristine
Ver	Verapamil
VM-26	Tenopside
VP-16	Etoposide

1.0 Introduction

1.1 Introduction

The human body is a finely tuned organism. It has evolved defense mechanisms to the environmental stresses (radiation, UV light, chemicals) which it is exposed to in everyday life. Over 200 different types of cells act in synchrony so that the body can survive and function properly.

When something goes wrong in any one cell, it may die off or the altered cell may remain undetected by the body. In the latter case it might be allowed to survive until it evolved into a neoplastic cell in which some of the controls on the cell's proliferation would be abrogated.

The common human cancers are cancers that involve epithelial cells such as those lining the gastrointestinal tract (GIT), the lungs, cells in the breast and the outer surface layers of the body. Human skin is completely replaced every 6 weeks, 10,000 million epithelial cells are shed and replaced in the colon every day and 300,000 million blood and lymphatic cells are destroyed and replaced every 24 hours (Evans, 1993). These tissues comprise of and their function is dependent on, normal proliferating cells. The emergence of cancer is a consequence of the failure to control cell proliferation.

1.3 million new cases of cancer occur each year in Europe and there are 840,000 deaths. There are 7500 deaths in Ireland which is higher than the European per capita average.

At present the only way of treating cancer is by surgery, radiotherapy or chemotherapy or a combination of any of these.

1.2 Chemotherapy

The idea of using drugs to treat cancer has been in existence for over 500 years when preparations of silver, zinc and mercury were used. The usefulness of drugs in the treatment of cancer was first documented in 1865 when Lissamer gave potassium arsenite to a patient with leukaemia and noticed a positive effect. However, successful systemic cancer chemotherapy was not developed until 1942 when Gilman, Goodman, Lindskog and Dougherty used nitrogen mustard in a patient with lymphosarcoma (Pratt *et al.*, 1994). Subsequently a number of chemotherapeutic drugs have been developed for clinical use. These drugs are members of a number of specific drug classes, including the anthracycline antibiotics, the Vinca alkaloids, epipodophyllotoxins, antimetabolites, covalent inhibitors of DNA and non-covalent inhibitors of DNA.

Chemotherapy is most useful against tumours with a high proportion of dividing cells. However, some normal tissues e.g. bone marrow and GIT, also have a high proportion of dividing cells. The clinical effectiveness of a chemotherapeutic drug necessitates that doses administered must allow enough cells in a patients normal tissues (bone marrow, GIT etc) to survive and allow the patient to recover, while killing malignant tumour cells *in vivo* .

Tumours with a high growth fraction rate e.g. leukaemia and lymphoma, can generally be effectively treated by chemotherapy. The more common malignant tumours, the solid tumours including colorectal, lung and breast tumours usually have a low proportion of dividing cells and are consequently less susceptible to treatment by chemotherapy alone.

1.2.1 Anthracyclines

The anthracyclines are antibiotics isolated from different Streptomyces species and include adriamycin (also called doxorubicin), daunorubicin and epirubicin. Adriamycin which has the most common clinical usage, is used for a variety of carcinomas including breast,

bladder, endometrium, lung, ovaries, stomach and thyroid; bone and soft tissue sarcomas; paediatric solid tumours; lymphoid and myelogenous tumours.
It was first isolated in Italian soil samples from Streptomyces peucetium var caesius. It is generally administered by intravenous infusion at a dose of 60mg/m², repeated after 21 days. Clearance of the drug from the body follows a 2 phase pharmokinetic profile. The first ½ life (α t½) lasts approximately 10 minutes. The second ½ life (ß t½) lasts approximately 30 hours. The longer ß t½ represents the slow release of adriamycin from tissue depots in the body because of the ability of adriamycin to intercalate with DNA and perhaps elsewhere in cellular vesicles and membranes.

The metabolism of adriamycin is outlined in Figure 1.2.1. The major metabolic step is the reduction of adriamycin to doxorubicinol by cytoplasmic NADPH-dependent aldoketo reductases. Doxorubicinol, which is still an active cytotoxic agent, and doxorubicin are split into less active aglycones and the free amino sugar by microsomal glycosides. These aglycones are demethylated and conjugated to a sulphate or glucuronide ester, and excreted principally in the bile (Pratt *et al.,* 1994).

As with all chemotherapeutic drugs, doxorubicin has serious side effects. A carcinogen and a mutagen, it also causes immunosuppression. The main limiting characteristic of adriamycin is that it can cause a cardiotoxic reaction. This cardiotoxicity is also a feature of other anthracycline drugs.

The primary mechanism of action of adriamycin is due to its ability to bind to DNA and RNA. Intercalation by the aglycone moiety between adjacent DNA base pairs in the double helix, results in the inhibition of replication, transcription, RNA and protein synthesis, stabilisation of topoisomerase II-DNA complex, which causes protein-associated DNA strand breaks, and free radical mediated cytotoxicity. Adriamycin and other anthracyclines are also metal chelators with high stability constants for transition metal ions such as iron. Ferric-adriamycin complexes have been shown to degrade deoxyribose and cleave DNA (DeGraff *et al.,* 1994) . The cytotoxicity induced by adriamycin can occur in the absence of significant DNA damage. When adriamycin is chemically altered

so that its ability to bind to DNA and RNA is decreased, there is a corresponding decrease in cytotoxicity (Pratt *et al.*, 1994). At high concentrations of adriamycin, synthesis of DNA and RNA is inhibited although this is not critical for cytotoxicity (Pratt *et al.*, 1994).

Active oxygen species induced by adriamycin can cause single strand DNA breaks, lipid peroxidation and disruption of cell membrane function and integrity (Skladanowski and Konopa, 1993) although the overall effect on cytotoxicity is thought to be minor. However, the active oxygen species play a major role in the ability of adriamycin to induce cardiotoxicity (Pratt *et al.*, 1994).

Adriamycin has been shown to be active throughout the cell cycle, however the effect is greatest in exponential cells compared to plateau phase cells. Cells which have been synchronised in the S or the G_2 phase are more sensitive to cytotoxicity than cells in G_1 (Krishan and Frei, 1976). Low concentrations of adriamycin induce G_2 arrest, higher concentrations or exposure to drug for longer periods of time induce a G_1 arrest and a delay in S phase traverse (Barlogie *et al.*, 1976).

1.2.2 Vinca Alkaloids

The Vinca alkaloids are extracted from the periwinkle plant Catharanthus rosea. The periwinkle plants have been used in folk medicine for centuries and a claim that extracts could cause hypoglycaemia led to the discovery of vincristine and vinblastine. The relatively low toxicity of vincristine for normal marrow cells makes it unusual compared to other chemotherapeutic agents. For this reason it is often included in combination chemotherapy with other myelosuppressive agents. It is used to treat acute leukaemia (adult and children), Hodgkin's lymphoma, aggressive non-Hodgkin's lymphoma, small cell lung cancer, Wilm's tumour, neuroblastoma, rhabdomyosarcoma and Ewing's sarcoma (Pratt *et al.*, 1994).

Given as a bolus intravenous injection, vincristine leaves the body's circulation by triexponential kinetics, having α and ß ½ lives of 2-5 minutes and 50-150 minutes respectively, the terminal ½ life lasts approximately 85 hours. It is primarily eliminated by a combination of hepatic metabolism and biliary excretion. Approximately 5-25% of the parent drug and metabolites can be recovered in urine. Although there is relatively little toxicity to normal marrow cells, the dose-limiting toxicity of vincristine is predominantly peripheral neuropathy.

Vincristine is an antimitotic agent and acts by disrupting the mitotic spindle and as a consequence arrests cells in the mitotic phase. It binds to free tubulin dimers to form paracrystalline aggregates; this interrupts microtubule polymerisation and causes the dissolution of the microtubules (Pratt *et al.,* 1994). Some studies have shown that inhibition of cell proliferation by vincristine appears to be due to spindle microtubule perturbation rather than depolymerisation of the microtubules (Jordan *et al.,* 1991; Jordan *et al.,* 1992). Several other cellular processes unrelated to microtubule perturbation which are affected by the vinca alkaloids include RNA, DNA and lipid biosynthesis, cyclic nucleotide and glutathione metabolism and calmodulin-dependent ATPase activity (Jordan *et al.,* 1991).

Figure 1.2.1 The major metabolic pathway for doxorubicin in humans (Pratt *et al.*, 1994).

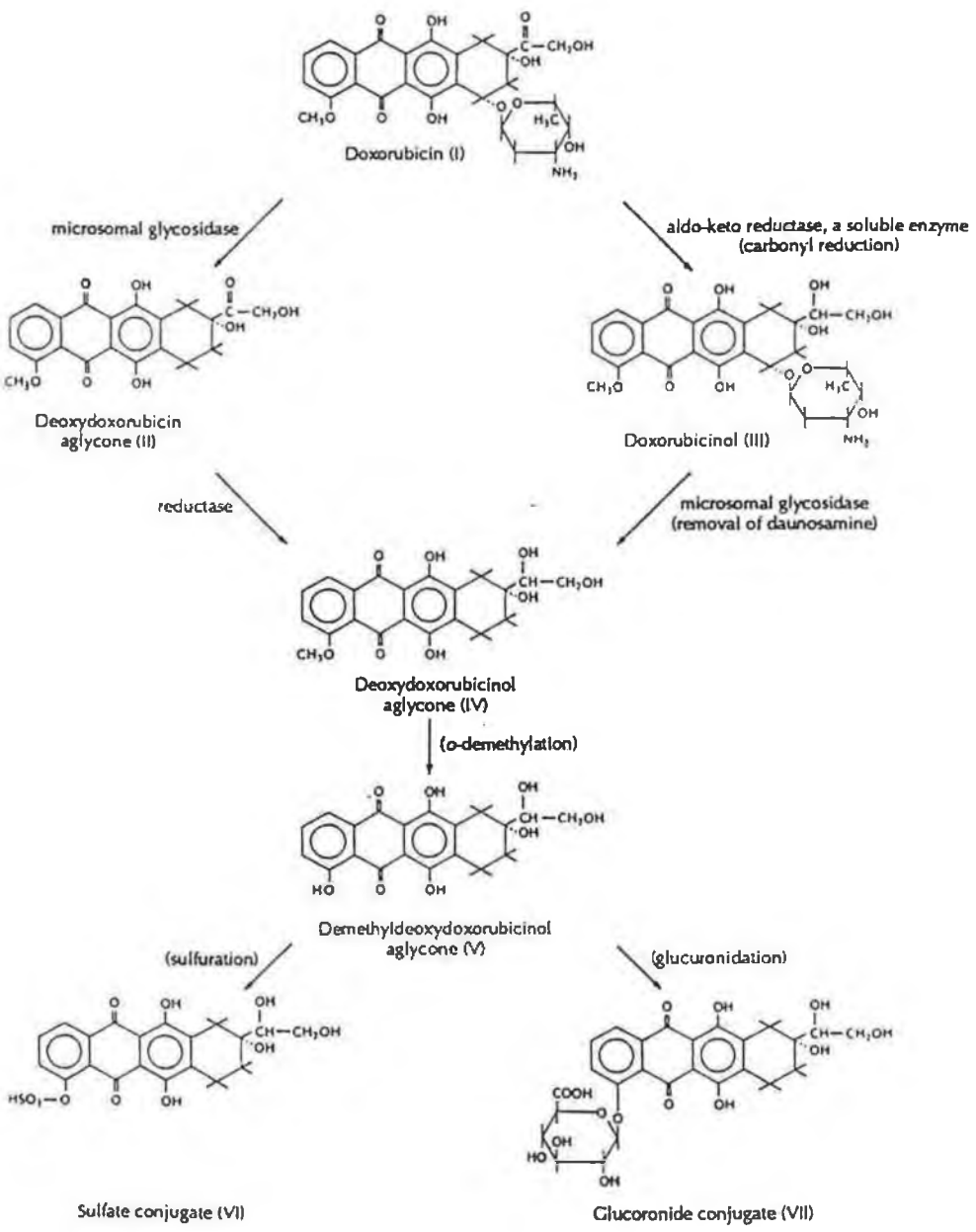

1.2.3 Epipodophyllotoxins

These include etopside (VP-16) and tenopside (VM-26) which are semisynthetic derivatives of podophyllotoxin, a microtubule inhibitor found in extracts of the mandrake plant. Active against a number of cancers, VP-16 is used clinically in testicular and small-cell lung cancer.

VP-16 can be administered orally or intravenously. Metabolism follows a biphasic kinetics with a terminal ½-life of 4-8 hours. Approximately 30-50% of the drug can be recovered in urine and approximately 20% has been recovered as metabolites including hydroxy acids and glucuronide and sulphate conjugates. A portion of the administered drug (20-30%) is frequently unaccounted for, possibly due to tight binding to tissue proteins (Pratt *et al.,* 1994).

Limitations in the use of VP-16 derive from its myelosuppressive actions, primarily leucopenia, other effects include nausea, diarrhoea mucositis and hypotension.

Initially VP-16 was thought to inhibit microtubule function but was subsequently shown to inhibit topoisomerase II. Topoisomerase II decatenates DNA. It binds to double stranded DNA making a transient double strand break. The enzyme is activated by sites on chromosomes where two double helices cross over each other. When the topoisomerase binds to such a crossing site, it; 1) breaks one double helix reversibly to create a DNA "gate"; 2) causes the second, nearby double helix to pass through this break; 3) reseals the break and dissociates from the DNA. In this way topoisomerase II efficiently separates two interlocked DNA circles (Alberts *et al.,* 1994).

A schematic of drug induced topoisomerase II inhibition is given in Figure 1.2.3. Topoisomerase II-mediated cytotoxicity is achieved by drug stabilisation of the complex formed between cleaved DNA and the covalently bound enzyme (Liu, 1989). Stabilisation of the complex interferes with the cleavage / religation action of topoisomerase II resulting in double strand breaks.

1.2.4 Antipyrimidines

Antipyrimidines were developed during attempts to synthesise analogs that could inhibit uracil utilization by tumours. The rationale used was to substitute fluorine for the hydroxyl atom in the 5 position in the pyrimidine ring of uracil, since fluorine added to acetic acid (fluoroacetic acid) is a rat poison. From this, 5-fluorouracil was developed and this was the first antipyrimidine. 5-Fluorouracil is direct inhibitor of thymidylate synthase which is the key enzyme in thymidine nucleotide production. Because steady-state pools of thymidine nucleotides are small, DNA synthesis is inhibited until the drug is withdrawn and new thymidylate synthase can be made (Pratt *et al.*, 1994). 5-Fluorouracil can also incorporate into RNA and DNA, inhibiting transcription, translation and the intracellular distribution of mRNA (Pratt *et al.*, 1994). It is commonly used to treat common solid tumours including colorectal, breast, head and neck, gastric and pancreatic cancers. Other antipyrimidines have been developed including cytosine arabinoside, which is widely used in antileukaemic therapy.

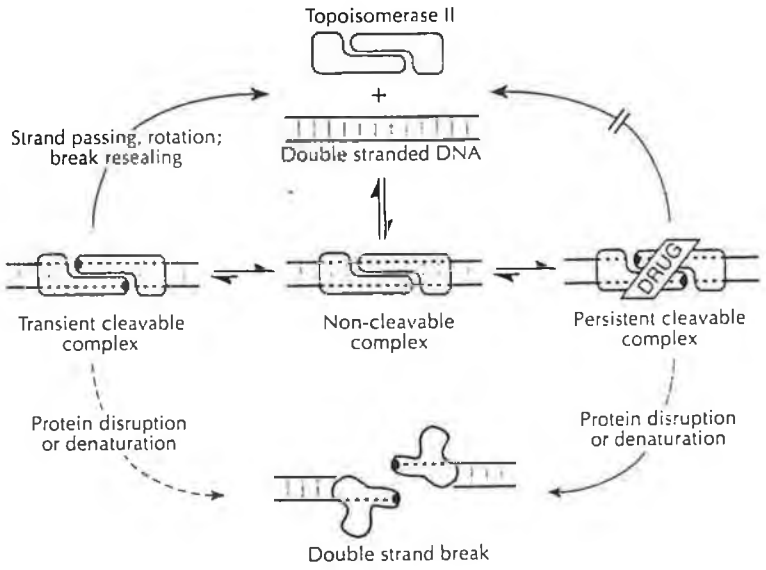

Figure 1.2.3: DNA damage induced by inhibition of topoisomerase II. Temporary double-strand breaks are induced by topoisomerase II in the course of its normal catalytic cycle, by formation of a cleavable complex. Disruption of this complex, which results in a permanent double-strand break, occurs infrequently in the absence of drugs. Inhibitors of topoisomerase II cause the cleavable complex to persist, thereby increasing the probability that the cleavable complex will be converted to an irreversible double strand break (Pratt *et al.*, 1994).

1.3 The Cell Cycle

One of the general findings of chemotherapy is that chemotherapeutic drugs work best on proliferating cells even if the mode of action of the drug is not cell cycle specific. A lot of attention has now focused on the role of the cell cycle.

The cell cycle is the process that a cell must undergo in order to replicate. It is composed of four different phases; G_1 (Gap 1) which is a growth phase; the S phase, during which DNA is replicated; G_2 (Gap 2) where the cell pauses as it prepares to divide; mitosis (M) (see Figure 1.3.1).

Figure 1.3.1

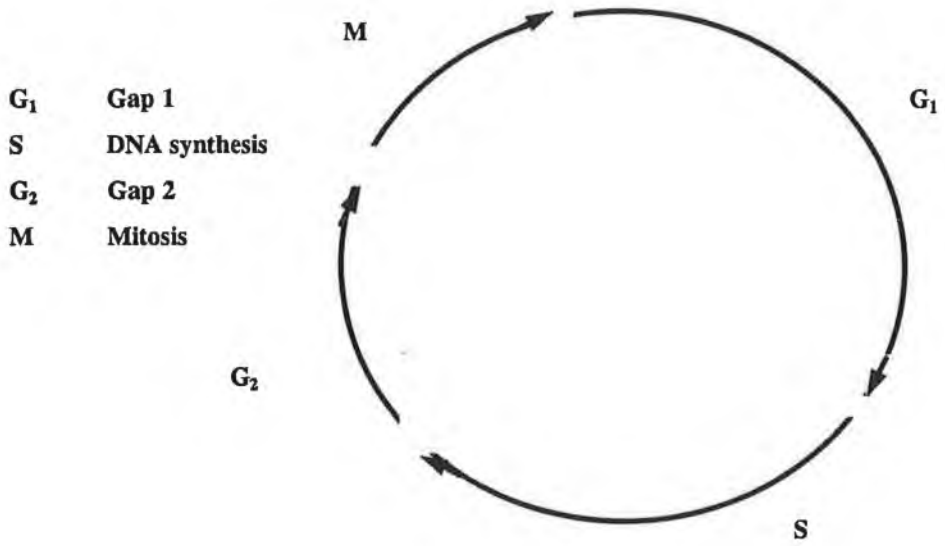

The four phases of the cell cycle are controlled by the actions of specific serine/threonine kinases, the cdc-2 related proteins. The cdc-2 related proteins all need to bind a protein called a cyclin in order to become active, thus they are called cyclin-dependent-kinases (CDKs). At present there are 8 CDKs and more than 10 cyclins known.

During various stages of the cell cycle different cyclins bind to different CDKs e.g., cyclin A binds to CDK2 during the S phase and to CDK1 during G_2. The cyclins can be broadly classed as being G_1/S cyclins or G_2/M cyclins (see Table 1.3.1).

Table 1.3.1

G_1/S cyclins	G_2/M cyclins
Cyclin A	Cyclin A
Cyclin C	Cyclin B1
Cyclin D (1-3)	Cyclin B2
Cyclin E	Cyclin H

At present 8 different kinases have been identified that bind a cyclin. Several other structurally related proteins are known, and some of these may be re-classified as CDKs if they are shown to bind a cyclin (Table 1.3.2).

Table 1.3.2

Cyclin dependent kinases and related proteins (Pines, 1993)

Name	Identity to cdc2 kinase domain (%)	Cyclin bound
cdc2 (CDK1)	100	Cyclin B (1-2)
CDK2	65	Cyclin A, D(1-3), E
CDK3	66	?
CDK4	44	Cyclin D (1-3)
CDK5	57	Cyclin D (1-3)
CDK6	47	Cyclin D (1-3)
PICTAIRE (1-3)	51-55	?
PITAIRE	42	?
$p58^{GTA}$	42	?
$p40^{Mo15}$ / CDK7	40	Cyclin H

1.3.1 G_1 phase

After mitosis, most cells in the body enter a quiescent state called G_0. Entry into the cell cycle can be stimulated by growth factors which regulate cell proliferation through a complex network of intracellular signalling cascades which ulitimately regulate gene transcription and the assembly and activation of the cell cycle control system. As yet no direct evidence between the signalling pathways and the cell cycle proteins have been shown.

At a point called the restriction (R) during G_1, the cells become independent of serum and commit to initiating DNA replication (Pardee, 1989). The CDK complexes that have been most closely linked to regulating the R point are those regulated by the D-type cyclins. In different cell types the 3 D-type cyclins are differentially expressed (Lew *et*

al., 1991; Matsushime *et al.*, 1991). The D-type cyclins can bind to a number of CDKs (CDK2, CDK4, CDK5 and CDK6) although they appear to predominantly act with CDK4 and CDK6. Although cyclin D and CDK4 levels are almost constant in cycling cells the cyclin D/CDK4 complex forms as the cells reach the R point and dissociate once the cells enter the S phase. Transcription of these cyclins is GF dependent e.g. CDK4 synthesis can be regulated by TGF-ß (Ewen *et al.*, 1993), and because both D cyclins mRNAs and proteins turn over rapidly their levels quickly decrease when growth factors are withdrawn (Matsushime *et al.*, 1991). This has led to the concept that the D-type cyclins act primarily as growth factor sensors integrating external cellular signals with cell cycle progression (Sherr, 1993).

Only two substrates are known for the cyclin D/CDK4 complexes:

(i) Retinoblastoma tumour suppressor protein Rb

(ii) Components of the E2F family of transcription factors

Rb is a tumour suppressor gene which acts as a cell brake. Rb is underphosphorylated throughout G_1 and phosphorylated at the G_1/S transition. Once phosphorylated, Rb leaves the nucleus, thus removing its suppressing activity. As the cell progresses through the cell cycle Rb is phosphorylated (at multiple sites) by different CDK complexes, until the M/G_1 transition, where it becomes dephosphorylated and returns to the nucleus (Weinberg, 1995). The hypophosphorylated form of Rb is able to block cells in G_1 phase and it binds and potentially sequesters large numbers of proteins including the transcription factor E2F (Chellappan *et al.*, 1991).

The D type cyclin/CDK complexes may phosphorylate and inactivate Rb in mid-G_1 phase and it has been suggested that cyclin-D1 and Rb form a negative feedback loop in late G_1 phase because cells that lack Rb also have less cyclin D1 (Sherr, 1993). Thus hypophosphorylated Rb may stimulate Cyclin D1 transcription and subsequently cyclin D1 - CDK4/6 would inactivate Rb allowing cells to progress into S phase and concomitantly down-regulate cyclin D1 synthesis (Weinberg, 1995).

During G_1, E2F is bound to Rb. At the restriction point, Rb phosphorylation by the cyclin/CDK complexes, causes a conformational change, which releases E2F and allows it to bind to DNA and activate transcription (Ludlow *et al.*, 1990). E2F transcription factors are thought to regulate the early response genes such as c-myc and B-myb, and the synthesis of cell cycle dependent proteins required for S phase e.g. DNA polymerase α, thymidine kinase, ribonucleotide reductase and dihydrofolate reductase. E2F is a heterodimer composed of an E2F family member and a DP family member. There are at present 5 E2F proteins and 3 DP proteins are known but the most detailed analysis have been performed with E2F-1 and DP-1 (La Thangue, 1994; Muller, 1995).

1.3.2 S phase

Once cells pass the R point they must pass into S phase. The transition from G_1 into S is controlled by the cyclin E/CDK2 complex and this is essential for the cell to begin DNA replication. Cyclin E mRNA and protein levels and the activity of the cyclin E/CDK2 complex all peak at the G_1/S transition, sharply decreasing as the cells progress through the mid and late S phase (Dulic *et al.*, 1992). Thus the cyclin E/CDK2 complex has a role in the initiation of DNA replication (Knoblich *et al.*, 1994). When cyclin E is overexpressed in cells, the cells progress through G_1 and into the S phase at a faster rate . These cells also have a diminished requirement for growth factors, indicating that cyclin E may overlap with the D-type cyclins in integrating growth factor signal transduction into the cell cycle (Ohtsubo and Roberts, 1993). The activation of the cyclin E/CDK 2 complex also appears to be the point at which radiation damage in the G_1 phase can delay the cell cycle (Dulic *et al.*, 1994).

Cyclin E/CDK2 associates with E2F and p107 (Lees *et al.*, 1992). Cyclin E and p107 bind to the E2F sub-unit E2F-4, while E2F-1, -2 or -3 may associate with Rb, DP-1 is common to both complexes (Lees *et al.*, 1992). Very little is known about the substrates of cyclin E but it is thought to be a potential regulator of Rb (Sherr, 1993) and to activate E2F and thus transcription of S phase genes.

Once cells enter the S phase cyclin E is rapidly degraded. It is replaced by cyclin A which also forms a complex with CDK2 and this is required for continued DNA replication. E2F-4/DP-1 and p107, which bind to cyclin E at the G_1/S transition, then form a complex with cyclin A/CDK2 (Lees *et al.*, 1992). Cyclin A/CDK2 is also thought to phosphorylate E2F-1 and therefore inhibit E2F-1/DP-1 DNA-binding activity (Krek *et al.*, 1994; Xu *et al.*, 1994). Thus cyclin A/CDK2 might inactivate E2F and turn off G_1/S phase genes (Krek *et al.*, 1994). The exact role of cyclin A/cdk2 in continued DNA replication is not known.

1.3.3. G_2/M phase

The most widely studied CDK is the $p34^{cdc2}$ kinase. $p34^{cdc2}$'s regulation has been extensively studied and is important because it controls the G_2/M transition. This has immediate applications to chemotherapy since DNA-damaging chemotherapeutic drugs often cause a cell cycle arrest in G_2 (Sorenson and Eastman, 1988; Tsao *et al.*, 1992; Demarcq *et al.*, 1994). $p34^{cdc2}$ kinase is active during the G_2 and M phase and binds the mitotic cyclins i.e. cyclin A, cyclin B1 or cyclin B2. Once activated $p34^{cdc2}$ kinase catalyses the breakdown of the nuclear envelope, the organisation of the mitotic spindle and the packaging of the chromatin (DNA) for mitosis. Because the actions of this kinase are so potent (i.e. dissociation of the nucleus) its regulation is tightly controlled (see Figure 1.3.2).

Activation of $p34^{cdc2}$ is rapid and produces an all or nothing effect. Once cyclin B and cdc2 combine the complex is immediately phosphorylated on Thr-161, stabilising the complex. Phosphorylation on a homologous site appears to be required for activation of all CDKs. The kinase that phosphorylates this site is the cdc2-activating kinase (CAK). CAK is itself a CDK and is a complex between cyclin H and CDK7 and as such also needs to be phosphorylated at a similar site to become active (Fisher and Morgan, 1994). Phosphorylation at two sites overlapping the ATP-binding site (Tyr-15 and Thr-14), keeps

$p34^{cdc2}$ in a catalytically inactive state (Solomon *et al.*, 1990; Krek and Nigg, 1991). One of these inhibitory kinases is wee1 which phosphorylates Tyr-15 (Parker and Piwnica-Worms, 1992) and can itself be inactivated by another protein kinase nim1 and can also be phosphorylated. Other unknown kinases also act on $p34^{cdc2}$ (Parker *et al.*, 1993).

Since tyrosine phosphorylation plays an important role in restraining $p34^{cdc2}$ activity, the regulation of tyrosine dephosphorylation becomes a crucial step in $p34^{cdc2}$ activation. Cdc25C is a tyrosine phosphatase which specifically removes the inhibitory tyrosine phosphate on $p34^{cdc2}$ that is generated by wee1. Cdc25C itself appears to be regulated by several complex pathways.

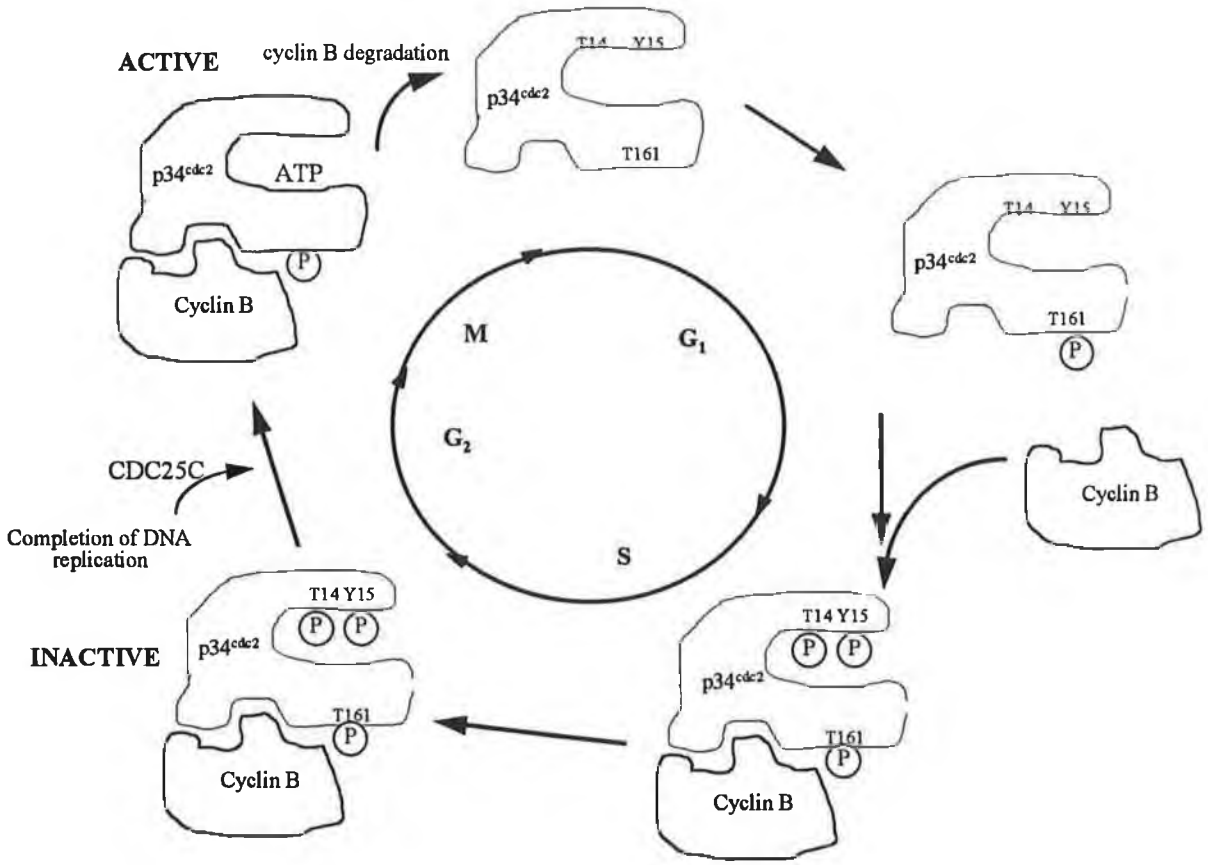

Figure 1.3.2: Regulation of p34cdc2 activity during the cell cycle. Cyclin B association with p34cdc2 occurs during interphase, possibly regulated by Thr 161 phosphorylation of p34cdc2. Sufficient cyclin B can be accumulated early in the cell cycle for subsequent protein kinase activation. Phosphorylation of Thr 14 and Tyr 15 in the ATP-binding site of p34cdc2 prevents protein kinase activation for the remainder of interphase. Dephosphorylation of Thr14 and Tyr15 by cdc25C brings about protein kinase activation, but this cannot usually occur unless DNA replication is completed (Norbury and Nurse, 1992).

1.3.4 Cyclin Dependent Kinase Inhibitors

Cyclin dependent kinases inhibiters (CDIs) can bind and inhibit the function of CDKs and are an extra control mechanism by which CDKs can be regulated. Most CDIs inhibit the progression of the cell cycle, some respond to extracellular signals while others are involved in intrinsic steps of the cycle. CDIs (*in vitro*) act by binding to the cyclin, the kinase or to the cyclin-CDK complex and inhibiting the function of cyclin-CDK complexes while not covalently modifying either the cyclin or the CDK (Peter and Herskowitz, 1994).

At present there are six mammalian CDIs identified, p14, p15, p16, p21, p27 and p28. These CDIs can be roughly divided into two groups, one group which have a broad affinity for different cyclins (p21 and p27) and the other which have a more specific mechanism of action (p15 and p16) (see Table 1.3.4).

p21 and p27 can both bind to cyclins A, B, D(1-3) and E. p27 is produced in response to TGF-ß and inhibits cyclin E/CDK2 kinase activity (Polyak *et al.*, 1994). p21 is a protein whose gene expression can be induced by p53 (Dulic *et al.*, 1994). p53 is necessary for a G_1 check-point control which senses DNA damage (fibroblasts lacking p53 do not respond to DNA damage induced by radiation). This will then lead to a transient arrest in G_1 since p21 inhibits the CDK complexes (Dulic *et al.*, 1994). It is also possible that p21 inhibits proliferating cell nuclear antigen (PCNA; a small protein which binds to DNA polymerase δ during DNA replication) (Fotedar *et al.*, 1996). Recent work has shown that p21 can (*in vitro*) inhibit DNA replication directly. This means that p21 has a dual role in response to DNA damage, by inhibiting CDK complexes it prevents transition from G_1 to S and may also directly block DNA replication by inhibiting PCNA (Chen *et al.*, 1995; Fotedar *et al.*, 1996).

Table 1.3.4 **Major Cyclin-CDK Cell Cycle Complexes**

Cell Cycle Phase	Cyclin-CDK complex	Inhibitors				
		p15	p16	p18	p21	p27
G_1	Cyclin D - CDK4/6	+	+	+	+	+
G_1/S	Cyclin E - CDK2	-	-	-	+	+
S	Cyclin A - CDK2	-	-	-	+	-
G_2/M	Cyclin B - cdc2	-	-	-	+	-

1.4 Chemotherapy and the Cell Cycle

1.4.1 G_2 arrest

The most common effect of DNA-damaging drugs is the accumulation of cells in the G_2 phase. These drugs include cisplatin (Sorenson and Eastman, 1988; Demarcq *et al.*, 1994), campothecin (Tsao *et al.*, 1992), VP-16 (Wood *et al.*, 1995), adriamycin (Barlogie *et al.*, 1976), bleomycin, X-rays and nitrosurea compounds (Rao, 1980). Active DNA synthesis is required before a cell will arrest in G_2 (Tsao *et al.*, 1992).

Arrest in G_2 is thought to allow time for the repair of DNA damage (Lücke-Huhle, 1982). This idea is supported by the increased radiosensitivity of yeast mutants which are unable to arrest in G_2 (Lücke-Huhle, 1982).

It is proposed that there are two distinct check-point mechanisms in mammalian G_2 (Downes *et al.,* 1994); one sensitive to DNA damage and another which is sensitive to the catenation state of DNA (this includes the decatenatory activity of topoisomerase II) (Downes *et al.,* 1994; Ishida *et al.,* 1994). Downes et al showed that ICRF-193 (an epipodophyllotoxin analogue which selectively binds topoisomerase II but does not induce DNA strand breaks) blocks entry but not exit from mitosis. Compounds which are able to circumvent this G_2 arrest e.g. caffeine, result in malformed condensed chromosomes (Downes *et al.,* 1994). This also highlights the important role topoisomerase II has in mitosis.

1.4.2 G_2 and p34cdc2

DNA damaging chemotherapeutic drugs often cause a cell cycle arrest in G_2. Research investigating the role of the cell cycle and chemotherapeutic drugs has consistently shown that the activity of p34cdc2 kinase is inhibited (Lock and Ross, 1990; Lock and Ross, 1990; Steinmann *et al.,* 1991; Lock, 1992; Lock and Keeling, 1993; O'Connor *et al.,* 1993; Demarcq *et al.,* 1994). Since activation of $p34^{cdc2}$ kinase results in the transition of cells from G_2 into mitosis inactivation of this kinase induces a G_2 arrest.

Studies using chemotherapeutic drugs and radiation have shown that they can exert their effect in different ways on p34cdc2 kinase activity. CA46 (human lymphoma) cells treated with nitrogen mustard, showed that the cyclin A/cdk2 complex remained active while the activity of cyclin B/cdc2 and cyclin A/cdc2 decreased (O'Connor *et al.,* 1993). Cyclin B accumulation was altered in HeLa cells treated with campothecin (Tsao *et al.,* 1992). Studies using ionising radiation on HeLa cells which induced G_2 arrest showed a decrease in cyclin B levels while cyclin A levels increased. In control cells the levels of cyclin A

and cyclin B both increased (Muschel *et al.*, 1991; Muschel *et al.*, 1993). This suggests that cells proceed through the S phase but are inhibited in G_2.

Brief exposure of both CHO and HeLa cells to VP-16 inhibits mitotic progress. Cell cycle arrest in G_2 showed a concomitant increase in cyclin B levels and accumulation of hyperphosphorylated p34cdc2. Inactivation of p34cdc2 was due to the inhibition of dephosphorylation of a tyrosine residue (Lock and Ross, 1990; Lock and Ross, 1990) and a threonine residue, both in the active site (Lock, 1992).

p34cdc2 kinase is regulated by the complex interaction of a number of protein kinases and phosphatases. Since tyrosine phosphorylation plays an important role in restraining $p34^{cdc2}$ activity, the regulation of tyrosine dephosphorylation becomes a crucial step in $p34^{cdc2}$ activation. Cdc25C is a tyrosine phosphatase which specifically removes the inhibitory tyrosine phosphate on $p34^{cdc2}$ that is generated by wee1. When phosphorylated cdc25C becomes active and dephosphorylates p34cdc2 at the active site, thus activating it.

G_2 arrested HeLa cells treated with campothecin have unaltered levels of cdc25C (Tsao *et al.*, 1992). No activation of cdc25C was found in nitrogen mustard treated G_2 arrested CA46 cells (O'Connor *et al.*, 1994). This suggests that the G_2 check-points preventing entry into mitosis in the presence of unreplicated or damaged DNA, suppress the initiation of the cdc2-cdc25C autocatalytic feedback loop, which normally brings about the rapid activation of cdc2. Therefore p34cdc2 inhibition is a result of the inactivation of some unknown factor early in its control.

In drug resistant cells drug-induced G_2 arrest depends on the amount of chemotherapeutic drugs getting into the cell. In a CHO/VpmR-5 drug resistant cell line, VP-16 concentrations differing by a factor of 10 were needed to induce the equivalent inhibition of p34cdc2 kinase in the sensitive CHO parent. This is equivalent to the degree of resistance displayed by the VpmR-5 cell line (Lock and Ross, 1990). Thus for VP-16 treated cells, damage caused to the cells' DNA appears a prerequisite for the cellular

process resulting in the inhibition of p34cdc2 kinase activity and G_2 arrest i.e. it is the DNA damage caused by chemotherapeutic drugs which causes inhibition of p34cdc2.

Despite the ability of chemotherapeutic agents to induce an arrest in G_2, there are some compounds which have the ability to overcome this arrest. These include okadaic acid (which is a type 2A phosphatase inhibitor) (Symthe and Newport, 1992), 2-aminopurine (Bunch *et al.,* 1994), 6-dimethyl-aminopurine (two protein kinase inhibitors) and the methylxanthines (MEX). The MEXs (which include caffeine and pentoxifylline) enhance the *in vitro* cytotoxicity of X-irradiation (Hain *et al.,* 1994), UV light and alkylating agents (Byfield *et al.,* 1981; Das *et al.,* 1982).

Exposure to caffeine after a brief VP-16 exposure is known to release G_2 arrest and increase mitotic death (Lock *et al.,* 1994). Premature chromosome condensation, a feature of some G_2 arrested cell lines when exposed to caffeine, needs cyclin B and p34cdc2 to be intact (Steinmann *et al.,* 1991; Lock *et al.,* 1994). Activation of p34cdc2 kinase activity is a common response to caffeine exposure (Symthe and Newport, 1992; Hain *et al.,* 1993; O'Connor *et al.,* 1993; Bunch *et al.,* 1994; Lock *et al.,* 1994). Pentoxifylline reverts the activity of cyclin A/cdc2 and cyclin B/cdc2 kinases to control levels in CA46 cells treated with nitrogen mustard (O'Connor *et al.,* 1993). However, Bunch et al (1994) demonstrated that dephosphorylation of p34cdc2 kinase is not enough to induce mitosis in all systems .

Not all cell lines showed enhanced cytotoxicity when exposed to caffeine. Caffeine did not circumvent cell cycle blocks induced by replication inhibitors or UV radiation in SVM Indian muntjac DM87 cells. Similarly, G_2 arrest induced by τ-irradiation or VP-16 in HeLa was caffeine insensitive (Musk *et al.,* 1988; Downes *et al.,* 1994).

MEXs are also reported to reduce the cytotoxicity of DNA damaging anti-topoisomerase drugs (including doxorubicin, mitoxantrone, VP-16 and ellipticine). Intercalation between the drug and the MEX can lead to a decrease in the effective drug concentration available

(Traganos *et al.*, 1991) (Traganos *et al.*, 1993) while inhibition of RNA synthesis may also be a possible mechanism (Perez *et al.*, 1994).

1.5 Apoptosis

Even though the mechanism of action of chemotherapeutic agents is known to the extent that some cellular targets have been identified, it is unknown how or why they are more toxic to cancer cells than normal cells. How these drugs cause a cell to die is at present a major focus of research worldwide.

Apoptosis is a mechanism of cell death whereby a cell actively dismantles itself. It is characterised by a detachment of the apoptotic cell from surrounding cells, a decrease in cell volume, membrane blebbing, condensation of the nucleus and endonucleolytic cleavage of DNA into nucleosomal-length fragments. Finally the cell content is packaged into numerous apoptotic bodies which can be phagocytosed by surrounding cells.

Under normal physiological conditions, the stimuli which induce apoptosis are diverse and vary from normal physiological signals, such as hormones that trigger selection of cells during differentiation, to the removal of cells that have sustained some form of damage. Cells can also be primed to undergo apoptosis by the removal of either some intracellular apoptosis inhibitory factor or the withdrawal of important extracellular components such as serum or growth factors. Non-physiological conditions which induce apoptosis include radiation, hyperthermia, calcium influx, glucocorticoids and cytotoxic agents.

The regular and controlled nature of apoptosis implies that the process is under genetic control. Research into the nematode Caenorhabditis elegans has provided a detailed cascade of the genetic factors involved. Three genes (ced3, ced4, and ced9) are involved in the death of the cell and two groups of genes (ced1, ced6, ced7 & ced8 and ced2, ced5

& ced10) appear to be involved in parallel pathways implicated in the phagocytosis of apoptotic bodies. Another gene, nuc1, which encodes for a nuclease, is involved in degrading the DNA of the apoptotic cell. Mutations in this gene still results in apoptosis but there is no degradation of DNA (Hall and Lane, 1994).

1.5.1 Bcl-2

The ced-9 gene is essential for development and protects cells from apoptosis. It exhibits partial homology to the mammalian proto-oncogene product bcl-2 (Hengartner and Horwitz, 1994) and expression of bcl-2 in C.elegans blocks apoptosis (Vaux *et al.*, 1992).

The bcl-2 gene was first identified at the t(14:18) translocation in human follicular lymphoma and was subsequently shown to be expressed in all haematopoietic cell types having a renewing stem cell population (Korsmeyer, 1992). The gene is also expressed in other cell types that have an extended life span (Allsopp *et al.*, 1993; Merry *et al.*, 1994). The bcl-2 gene encodes a 26 kDa intracellular membrane associated protein which is localised to mitochondria, endoplasmic reticulum and nuclear membranes (Chen-Levy and Cleary, 1990; Nguyen *et al.*, 1993).

Mice lacking bcl-2 complete embryonic development and appear normal during the first week after birth. Consequently, the mice begin to show growth retardation, and have small external ears and immature facial features. The mice die young. These mice show apoptosis in the embryonic kidney and hypoplastic renal development, which progresses to severe polycystic kidney disease. There is apoptotic involution of the thymus and spleen and an almost complete loss of lymphocytes (Veis *et al.*, 1993).

Apart from its role in protecting against physiologic cell death, deregulation of bcl-2 in non-Hodgkin's lymphoma cells rendered the cells resistant to a range of drugs (including

dexamethasone, methotrexate and VP-16) commonly used to treat the disease (Miyashita and Reed, 1993). However, the gene is not protective in all situations i.e. Fas/FasL. Monoclonal antibodies raised against the Fas (APO-1) cell curface protein have cell killing activity, reviewed in (Nagata and Suda, 1995). Therefore there is a bcl-2 independent mechanism of apoptosis. Protection by bcl-2 against the potentially lethal effects of exogenous and endogenous factors (including radiation, various peptides, heat, and other gene products) provides a basis for categorising bcl-2-dependent and bcl-2 independent pathways to cell death (Reed, 1994).

Bcl-2 is the original member of an increasing multigene family. Members of the family are in two functional categories, those that inhibit and those that promote apoptosis. The inhibitors of apoptosis include bcl-2 (Vaux *et al.,* 1992), Bcl-x_L (Boise *et al.,* 1993), Mcl-1 (Kozopas *et al.,* 1993), Adenovirus E1B 19K Epstein-Barr virus BHRF1 and Ced-9 (Hengartner and Horwitz, 1994). The promotors include Bax (Oltvai *et al.,* 1993), Bak (Chittenden *et al.,* 1995; Chittenden *et al.,* 1995; Farrow *et al.,* 1995), Nbk/Bik1 (Boyd *et al.,* 1995), Bad (Yang *et al.,* 1995) and Bcl-x_S (Boise *et al.,* 1993) (see Table 1.5.1).

Bcl-2 family members interact with each other forming both homo and heterodimers. Bax counters bcl-2 activity, accelerating apoptotic cell death but only after a death-inducing signal. When bcl-2 is excess, bcl-2 homodimers and heterodimers predominate and cells are protected from apoptosis. When bax is in excess, bax homodimers predominate and cells are susceptible to apoptosis (Oltvai *et al.,* 1993; Oltvai and Korsmeyer, 1994). A number of biological systems indicate that, during development, cells vary in their inherent sensitivity or resistance to a given death stimulus. The ratio of bcl-2:bax represents one cell-autonomous rheostat that predetermines a cell's life or death response to an apoptotic stimulus.

Other interactions between Bcl-2 family members include Bcl-2 and Bak (Chittenden *et al.,* 1995; Chittenden *et al.,* 1995), Bcl-x_S (Boise *et al.,* 1993) or Bad (Yang *et al.,* 1995); Bcl-x_L and Bcl-x_S (Boise *et al.,* 1993); E1B 19K and Bak (Farrow *et al.,* 1995),

Bax or Nbk/Bik1 (Han and White, 1995); Bcl-x_L and Bak (Farrow *et al.,* 1995) (see Table 1.5.2).

Three conserved regions within Bcl-2-related proteins have been identified, bcl-1 homology 1 (BH1), homology 2 (BH2) (Yin *et al.,* 1994) and homology 3 (BH3) (Chittenden *et al.,* 1995; Chittenden *et al.,* 1995). These conserved motifs control protein-protein interactions. Selected mutations within BH1 or BH2 of bcl-2 disrupt its heterodimerisation with bax, but not its homodimerisation, and destroy the ability of bcl-2 to counter apoptosis (Yin *et al.,* 1994), demonstrating that bcl-2 must heterodimerise with bax to function.

The difference between Bcl-x_L and Bcl-x_S is that Bcl-x_L contains the BH1 and BH2 domains, which will inhibit apoptosis, while the short version, bcl-x_S, lacks those motifs and favours death (Boise *et al.,* 1993).

The ability of the bcl-2 family proteins to dimerise is not restricted to proteins within the family. Bcl-2 can dimerise with R-ras which accelerates apoptosis (Wang *et al.,* 1995), while Bag-1 enhances the ability of bcl-2 to block apoptosis (Takayama *et al.,* 1995) (see Table 1.5.3).

Another protein implicated in resistance to apoptosis is the bcr-abl oncoprotein. In chronic myelocytic leukeamia (CML) cells, translocation of the c-abl gene from chromosome 7 to chromosome 22 leads to the formation of a bcr-abl fusion protein. This results in the up-regulation of abl tyrosine kinase activity. Transfection of v-abl in HL-60 resulted in the acquisition of resistance to spontaneous and induced apoptosis (McGahon *et al.,* 1994). CML cells isolated from newly diagnosed, untreated patients showed increased resistance to spontaneous or drug-induced apoptosis comared to normal granuolcytes. The CML cell line, K562, is more resistant to apoptosis compared to cell lines derived from other types of leukaemias. Antisense strategies, which reduce the levels of fusion protein in K562 cells restored sensitivity to apoptosis (McGahon *et al.,* 1994).

Table 1.5.1

Bcl-2 family members

Apoptotic protectors	Apoptotic inducers
Bcl-2	Bax
Bcl-x_L	Bak
Mcl-1	Nbk/Bik1
E1B 19K	Bcl-x_S
BHRF1	Bad
Ced-9	
bcr-abl	

Table 1.5.2

Bcl-2 family interactions

Bcl-2 + Bax

Bcl-2 + Bak

Bcl-2 + Bcl-x_S

Bcl-2 + Bad

Bcl-x_L + Bcl-x_S

E1B 19K + Bak

E1B 19K + Bax

E1B 19K + Nbk/Bik1

Bcl-x_L + Bak

Table 1.5.3

Proteins which interact with Bcl-2 family members

Apoptotic protectors	Apoptotic inducers
Bcl-2 + Bag-1	Bcl-2 + R-ras

1.5.2 ICE / Apoptotic proteases

The ced-3 protein may act as a cysteine protease which may have an important role in the execution pathway of apoptosis in both C.elegans and mammalian cells. ced-3 has close homology with the human interleukin-1ß-converting enzyme (ICE). ICE is a cysteine protease with a novel specificity for aspartic acid. ICE is comprised of two sub-units (p20 and p10) both of which can be autocatalytically derived from an inactive 45 kDa proenzyme (Thornberry *et al.*, 1992). Transient overproduction of ICE or CED-3 will cause Rat-1 fibroblast cells to die. This effect of ICE can be countered by bcl-2 (Miura *et al.*, 1993).

There is another protease with specificity for aspartic acid, a serine protease called Granzyme B, also known as fragmentin 2. Granzyme B is stored within the cytolytic granules of cytotoxic T cells (CTL), and it is transferred upon CTL attack to recognised target cells (Heusel *et al.*, 1994).

Other ICE-like genes have been identified; NEDD-1/ICH-1 demonstrates only 29% identity and 52% similarity with ICE but the sequence QACRG, which contains the active

cysteine residue required for the proteolytic activity of ICE, is conserved. Overproduction of this protein will induce cell death that can be blocked by bcl-2 (Kumar *et al.,* 1994; Wang *et al.,* 1994). However, Wang et al (1994) also noted a truncated version of ICH-1 generated by alternative RNA splicing. This truncated version (ICH-1_S) begins to diverge immediately following the QACRG active site and terminates shortly downstream. When overproduced, ICH-1_S countered the death-inducing effect of the full length ICH-1_L protein. This system provides another example of positive/negative regulation of apoptosis encoded within the same gene or gene family.

Transcription factors such as myc, fos, jun and p53 are intimately associated with cellular proliferation and are also important in apoptosis. The transcription factor c-rel will induce apoptosis in bone marrow cells when expressed at high levels (Abbadie *et al.,* 1993). c-fos is expressed immediately prior to apoptosis in many cells *in vivo* (Smeyne *et al.,* 1993). Deregulated c-myc expression is a potent inducer of apoptosis. Overexpression of c-myc during cell cycle arrest, e.g. following deprivation of growth factors or forcible arrest with cytostatic drugs induces apoptosis (Evan *et al.,* 1994). Expression of the c-myc gene is rapidly induced upon addition of serum to quiescent cells, and its expression is followed by mitosis. However, overexpression of c-myc in quiescent rat-1 fibroblasts maintained without serum leads to apoptosis (Evan *et al.,* 1992). This is most likely due to regulation of gene transcription by the myc-max heterodimer (Evan *et al.,* 1992). Thus, the induction of c-myc in cells grown in the presence of appropriate growth factors or co-expression of other 'survival genes' such as bcl-2, causes cell proliferation. In the absence of these factors, c-myc expression causes cell death.

The complexity of pathways which induce apoptosis and the variety of unique proteins in the ICE and bcl-2 families argues for the existence of different pathways each using one or more family members to regulate induction of apoptosis within a given tissue or for a particular differentiation program (Martin *et al.,* 1995).

1.6 Apoptosis and Chemotherapy

Research into apoptosis from a cancer research perspective has focused on three main areas; oncogenesis i.e. the ability to acquire genes (e.g. bcl-2) which prevent apoptosis and therefore prolong the life of a cell; tumour homeostasis i.e. the growth of a tumour is now thought to be a balance between the rate of apoptosis and mitosis within the tumour mass (Staunton and Gaffney, 1995); and the mechanism of action of cytotoxic drugs.

The exact mechanisms by which chemotherapeutic agents are cytotoxic are unclear. Several chemotherapeutic agents commonly used in the treatment of both solid and haematologic malignancies have been shown to be able to induce apoptosis in a number of cell lines *in vitro*. These include cisplatin (Demarcq *et al.,* 1994), adriamycin (Ling *et al.,* 1993; Skladanowski and Konopa, 1993; Smith *et al.,* 1994), DNA alkylating agents (O'Connor *et al.,* 1991; Gorczyca *et al.,* 1993; O'Connor *et al.,* 1993), macromolecular synthesis inhibitors (Gorczyca *et al.,* 1993) and other topoisomerase I and II inhibitors (Solary *et al.,* 1994; Dubrez *et al.,* 1995). The kinetics of cell death by each of these agents varies depending upon the cells under study.

As discussed previously, chemotherapeutic drugs cause DNA damage, this damage disrupts the cell cycle, induces cell cycle perturbations and initiates cell death. Arrest of the cell cycle in G_1 or G_2 in response to DNA damage is the result of activation of p53. p53 mediated arrest leads to either the repair of the damaged DNA and cell recovery or the induction of apoptosis. In p53 negative cells, apoptosis can still occur by a p53-independent mechanism (Lowe *et al.,* 1993). p53 has also been shown to have a direct effect on apoptosis by downregulating bcl-2 expression and upregulating bax expression (Miyashita *et al.,* 1994).

p53 induction in response to DNA damage activates the expression of a number of genes $p21^{WAF1/CIP1}$, GADD45, mdm2, bax and cyclin G, the function of which has yet to be determined (Enoch and Norbury, 1995; Miyashita and Reed, 1995).

Induction of the p21 protein will lead to a transient arrest in G_1 and G_2 since p21 inhibits the CDK complexes (Section 1.3.4). As an inhibitor of the CDKs, p21 contributes to G_1 arrest by preventing the phosphorylation of Rb. Hypophosphorylated Rb binds to and inactivates the E2F family of transcription factors which control the expression of proteins important for entry into S-phase.

p53 acts as a specific transactivator of the GADD45 gene (Kastan *et al.*, 1992; Zhan *et al.*, 1994) though other types of DNA damage induce GADD45 by p53-independent mechanisms (Kastan *et al.*, 1992; Zhan *et al.*, 1993). Overexpression of GADD45 inhibits colony formation in clonogenic assays (Zhan *et al.*, 1994), suggesting a role in cellular proliferation and/or cell survival. The mechanism of action of GADD45 is unknown although there is a physical association between gadd45 protein and PCNA ((Smith *et al.*, 1994). It is thought that gadd45 participates in the DNA repair process and that overexpression of gadd45 inhibits DNA synthesis (Smith *et al.*, 1994).

The mdm2 oncoprotein is also transcriptionally activated by p53 following DNA damage (Perry *et al.*, 1993; Chen *et al.*, 1994; Price and Park, 1994) . mdm2 is a 54kDa nuclear phosphoprotein which forms complexes with both wild-type and mutant p53. This interaction inhibits wild-type p53-directed transcription of target genes (Oliner *et al.*, 1993; Chen *et al.*, 1994). It has been suggested that the mdm2 may serve as an element of a feedback loop with p53 (Chen *et al.*, 1994; Price and Park, 1994). p53 induces the expression of mdm2, which in turn binds to and inactivates p53. mdm2 may be involved in cellular recovery from the cell cycle arrest caused by p53 induction, allowing the cells to resume cycling after the DNA damage has been repaired (Kastan *et al.*, 1995).

1.7 Cell Cycle and Apoptosis

The role of cell cycle proteins in apoptosis is unclear. It has been proposed that apoptosis may be a result of aberrant cell cycle control, i.e. apoptosis may be a consequence of conflicting growth regulatory signals which lead to an unsuccessful attempt at traversing the cell cycle (Freeman *et al.,* 1994; Kastan *et al.,* 1995).

Apoptosis has a number of features i.e. cell rounding, nuclear envelope breakdown and chromatin condensation, which are also characteristic of mitosis. This has led researchers to investigate the role of cyclin B/cdk2 and cyclin B/cdc2 during apoptosis.

In YAC lymphoma cells, cyclin B/cdc2 was found to be essential during serine protease induced apoptosis (Shi *et al.,* 1994). Overexpression of Wee1 has been found to inhibit this effect (Chen *et al.,* 1995). Cyclin B/cdc2 kinase activity was also found to be elevated in HL-60 cells treated with camptothecin or etopside (Shimizu *et al.,* 1995). In A1.1 hybridoma cells induced to undergo apoptosis when the T receptor is cross-linked with anti-CD3 antibodies, apoptosis was blocked with cyclin antisense oligonucleotides (Fotedar *et al.,* 1995). However, no cdc2 kinase activity was found during apoptosis in FT-210 cells (Martin *et al.,* 1995), an embryonic fibroblast cell line during chromatin condensation (Oberhammer *et al.,* 1994), thymocytes, which die during G_0 (Norbury *et al.,* 1994) and neurons (Freeman *et al.,* 1994).

The role of cyclin A is less clear. Rat fibroblasts undergoing apoptosis increase cyclin A mRNA levels while cyclins B, C, D1 and E remain unaffected, and deregulated expression of cyclin-A was found to be sufficient to induce apoptosis in cells exposed to low serum (Hoang *et al.,* 1994). HeLa cells arrested in S phase have increased cyclin A kinase activity when induced to undergo S phase apoptosis by caffeine, okadaic acid, staurosporine, di-methylaminepurine or TNF-α (Meikrnatz *et al.,* 1994). HIV-1 Tat protein induced apoptosis in CD4 T-lymphocytes has elevated levels of CDK2 and cdc2 activity which can be inhibited by antisense oligonucleotides to cyclin A, B and E (Li *et al.,* 1995). However, there has been no increase in cyclin A levels in HL-60 cells (Dou *et*

al., 1995; Shimizu *et al.,* 1995) and neurons (Freeman *et al.,* 1994) undergoing apoptosis. HL-60 cells exposed to cytosine arabinoside increase cyclin E kinase activity (Dou *et al.,* 1995).

Thus although CDK2/cdc2 activity is induced during apoptosis in some systems there is no evidence that it is necessary. Other studies have shown the involvement of other cell cycle proteins. Cyclin D1 expression is selectively induced in post-mitotic neurons undergoing programmed cell death (Freeman *et al.,* 1994; Kranenburg *et al.,* 1996). Overexpression of p58 PITSLRE, a CDK-related kinase, was found to initiate apoptosis and the kinase activity of p58 was elevated during Fas induced apoptosis in human T cells (Lahti *et al.,* 1995).

Fotedar *et al* (1995) suggest that there are at least 2 apoptotic pathways in T cell death; one which is dependent on activation through surface receptors (e.g. anti-CD3) leading to cyclin B-dependent cell death during G_2/M and a second (e.g. dexamethasone-induced pathway) which is independent of cell activation and cyclin B.

While there is a single apoptotic pathway and a single effector molecule in Caenorhabditis elegans, this is not the case in higher eukaryotic cells. The variety of unique proteins in the ICE and bcl-2 families argues for the existence of different pathways each using one or more family members to regulate induction of apoptosis. Cdc2, as a member of a larger family of CDK effectors, participates in some of these apoptotic pathways, although it is unknown whether all pathways would necessarily involve a CDK effector (Martin *et al.,* 1995).

1.8 Necrosis

Necrosis is a passive mode of cell death, characterised by an increase in cell volume which ultimately leads to cell lysis. Necrosis is not genetically influenced, does not appear to

require expression of new mRNAs or proteins and would seem to be uncontrollable in terms of drug intervention (Dive and Hickman, 1991).

It is thought that necrosis is initiated by cellular damage that disrupts osmotic balance. Ions, especially Ca^{++}, enter the cell passively and the cell swells with H_2O because of ion influx. Increasing Ca^{++} can also inhibit some enzymatic pathways e.g. ATP production and stimulate others e.g. proteolysis. An early fall in ATP precedes a fatal disruption of the ionic gradients within the cell. The cell ruptures to spill out degradative lysosomal enzymes which mediate an inflammatory reaction in the immediate locality.

The choice to between dying actively by apoptosis or passively by necrosis, appears to depend on the severity of the injury inflicted on the cell. Higher doses of cytotoxic drugs tend to cause necrosis rather than apoptosis, although this effect was not evident with VP-16 (Marks and Fox, 1991).

HL-60 cells exposed to melphalan or chlorambucil, showed that the mode of cell death depended on the levels of intracellular reduced glutathione (GSH). Reducing the levels of GSH induced necrosis at concentrations that would normally induce apoptosis. The monocytic cell line, U937 and the chronic myelogenous leukaemia line, K562, have been found to be more resistant to melphalan or chlorambucil and were found to contain higher levels of GSH as compared to the HL-60 line (Fernandes and Cotter, 1994). This suggests that intracellular levels of GSH might preset the injury-levels the cell can sustain before it becomes too damaged to undergo apoptosis and dies by necrosis.

1.9 Multidrug Resistance

Successful systemic cancer chemotherapy was not developed until 1942 when Gilman, Goodman, Lindskog and Dougherty used nitrogen mustard in a patient with lymphosarcoma. However, the clinical course of this first patient treated is reflected in the use of anticancer drugs today. He was administered nitrogen mustard for 10 days. Within that time there was a noticeable regression of the tumour. However, about 3½ weeks after initiation of therapy the total white blood cell count decreased down to 200 cells/cubic millimeter. Subsequently, the bone marrow gradually recovered, but so did the tumour. A second, shorter course of treatment produced a transient improvement, and a third course had virtually no effect. Thus, the therapy-limiting effect of marrow toxicity and the development of drug resistance, both of which are still problems in cancer chemotherapy, were observed in the first patient.

Approximately 50% of patients with cancer can be cured by surgery and radiation therapy since their tumours have not spread. Of the remaining 50%, 10% are curable with systemic chemotherapy, including children with leukaemia and sarcomas and adults with testicular cancer and choriocarcinoma. However, the majority of metastatic cancers are not currently curable by chemotherapy or by any other kind of therapy. These cancers fall into two categories; cancers which are intrinsically resistant to chemotherapy (i.e. there is no significant response to chemotherapy); and those cancers which respond initially to chemotherapy but then acquire resistance during the course of therapy.

When a population resistant to an administered drug develops, this new population may also be resistant to a number of other chemotherapy drugs, even if they are structurally dissimilar and have different modes of action. This is called Multidrug Resistance (MDR).

1.9.1 P-glycoprotein

Currently the best understood mechanism of MDR is the resistance mediated by the MDR1 gene product, P-glycoprotein (P-170). P-glycoprotein is a 170 kDa glycoprotein, 1280 amino acids in length and consists of 12 transmembrane domains and two nucleotide binding sites (see figure 1.9.1). It acts as an energy-dependent transmembrane efflux pump that actively transports chemotherapeutic agents out of the cell. Several structurally and functionally unrelated agents, including anthracyclines (doxorubicin, daunorubicin), vinca alkaloids (vincristine, vinblastine), epipodophyllotoxins (VP-16, VM-26), taxanes (paclitaxel, docetaxel), and actinomycin D are substrates for P-glycoprotein.

There are two human MDR genes, MDR1 and MDR3 (Roninson *et al.,* 1986; Van der Bliek *et al.,* 1986). However only full cDNA from the MDR1 gene can confer the MDR phenotype (Gros *et al.,* 1986; Ueda *et al.,* 1987). Although P-glycoprotein is believed to be a pump that actively effluxes drugs from resistant cells (Dano, 1973; Safa *et al.,* 1987), the actual mechanism for this activity is not understood.

P-glycoprotein is a member of the ATP binding cassette (ABC) superfamily of transport systems which includes over 30 proteins that share extensive sequence similarity and domain organisation (Hyde *et al.,* 1990). There are marked similarities in sequence and apparent structure between P-glycoprotein and a number of prokaryotic transport proteins (Chen *et al.,* 1986; Higgins, 1989); including HLYB, the ATP-binding haemolysin export protein in Escherichia coli (Felmelee *et al.,* 1985; Blight and Holland, 1990); pfMDR, the MDR gene in Malaria parasites Plasmodium falciparum (Foote *et al.,* 1989); CFTR, the product of the cystic fibrosis (Riordan *et al.,* 1989; Hyde *et al.,* 1990).

P-glycoprotein expression has been detected in a number of normal tissues; liver, adrenal gland, pancreas, kidney colon and jejunum (Fojo *et al.,* 1987). Localisation within these tissues appears to be extremely specific; apical surface of epithelial cells in liver, kidney, colon, and jejunum; biliary canalicular front of hepatocytes; on small biliary and pancreatic ductules; on the adrenal cortex (Thiebaut *et al.,* 1987; Sugawara *et al.,* 1988)

human placenta (Sugawara *et al.*, 1988) and is expressed in specialised endothelial cells in the brain and testis (Cordon-Cardo *et al.*, 1990).

The localisation of P-glycoprotein to specialised cells in human tissues indicates that it might be involved in transepithelial secretion of toxic substances or unknown cellular metabolites into the bile or the lumen of the GI tract. The fact that the MDR1 gene can be co-induced with the P450A1 gene probably supports this (Burt and Thorgeirsson, 1988).

Expression of the MDR1 gene is in general, high in those tumours which derive from tissues that naturally express high levels of P-glycoprotein i.e. tumours derived from the colon, kidney, liver and pancreas. In poorly differentiated tumours of the kidney and colon the levels may often be lower because of the altered differentiation state of these tumours . Expression of the MDR1 gene is sometimes high in leukaemias, lymphomas and some other tissues that do not normally express the MDR1 gene. Several tumour types have low levels of the MDR1 gene and are known to be drug sensitive. These include Wilm's tumour and cancer of the ovary and breast (see Table 1.9.1). However a number of tumours exhibit low levels of MDR1 expression but are resistant to chemotherapy, for example adenocarcinoma of the lung and non small cell lung cancer (Pastan and Gottesman, 1991).

Table 1.9.1

MDR expression in untreated Human Cancers

High	Sometimes High	Low
Colon	Acute Leukaemias	SCLC
Kidney	Lymphomas	NSCLC
Liver	NSCLC-NE	Gastric
Adrenal	CML	Oesophageal
Pancreas	Neuroblastoma	Ovary
		Wilm's
		Head and Neck
		Myeloma
		Breast

Table 1.9.2

Cancers in which MDR1 expression has been found to increase after chemotherapy

Acute Leukaemias
Breast
Lymphomas
Multiple Myeloma
Neuroblastoma
Ovary
Pheochromocytoma
Rhabdomyosarcoma
Sarcomas

1.9.2 Multidrug Resistance Related Protein

Despite the widespread occurence of drug resistance in human lung tumours, overexpression of P-glycoprotein is infrequent. This implies that alternative mechanisms of resistance exist (Cole *et al.,* 1992).

Overexpression of the Multidrug Resistance Related Protein (MRP) is sufficient to confer multidrug resistance (Cole *et al.,* 1992). MRP is a 1531-amino acid, 190-kDa glycoprotein, that is overexpressed in a number of non-P-glycoprotein MDR cell lines (Krishnamachary and Center, 1993; Zaman *et al.,* 1993). MRP has been detected in a number of normal human tissues, including lung, stomach, colon, peripheral blood macrophages, thyroid, testis, nerve, bladder, adrenal, ovary, pancreas, gall-bladder, duodenum, heart, muscle, placenta, brain, kidney, liver and spleen (Cole *et al.,* 1992; Zaman *et al.,* 1993).

MRP has minor sequence homology to P-glycoprotein but it is most related to the ABC-transporter encoded by the pgpA gene of Leishmania tarentolae. This protein is involved in low level oxyanion (arsenite) resistance, rather than resistance to hydrophobic drugs (Zaman *et al.,* 1993).

MRP functions as an ATP dependent export pump for endogenous as well as exogenous glutathione, glucuronidated and sulfated conjugates (Jedlitschky *et al.,* 1996).

MRP-transfected cell lines demonstrated a 5-15 fold more resistant profile to adriamycin, daunorubicin, epirubicin, vincristine and VP-16, ≤3 fold resistance to taxol, vinblastine and colchicine and no cross resistance was observed to 9-alkyl anthracyclines, mitoxantrone or cisplatin. There was also cross resistance to some heavy metal anions including arsenite, arsenate, and trivalent and pentavalent antimonials but not to cadmium chloride. Thus, the MDR phenotype conferred by MRP is similar but not identical to that conferred by P-glycoprotein (Cole *et al.,* 1994).

MRP is predominantly located in the endoplasmic reticulum of resistant cells but lower levels are also contained in the plasma membrane (Krishnamachary and Center, 1993).

Because the cellular accumulation of chemotherapeutic drugs appears unchanged in MRP overexpressing cell lines it is thought that MRP may participate directly in the active transport of drugs into subcellular organelles or influence drug distribution indirectly (Cole *et al.,* 1992; Krishnamachary and Center, 1993)

Immunohistochemical examination of 61 human cell lines demonstrated that some of the most sensitive cell lines had a relatively high expression of MRP suggesting that resistance may not be a simple function of the level of MRP (Izquierdo *et al.,* 1996).

1.9.3 Transporter-related with Antigen Presentation

Another member of the ABC-transporter superfamily which has been found to be overexpressed in a number of MDR cell lines of different histogenic origin is the Transporter-related with Antigen Presentation (TAP) (Izquierdo, 1996). TAP is a heterodimer formed by the TAP1 and TAP2 gene products and a plays a role in MHC class I restricted antigen presentation by mediating peptide translocation over the endoplasmic reticulum membrane (Neefjes *et al.,* 1993).

Transfection of the TAP genes into mutant lymphoblastoid cells lacking TAP genes, showed a 2-3 fold increase in resistance to VP-16, vincristine and adriamycin. High concentrations of VP-16 or vincristine were able to inhibit the TAP-mediated transport of a model peptide into the endoplasmic reticulum (Izquierdo, 1996).

1.9.4 Lung Resistance-related Protein

Lung resistance-related protein (LRP) was first identified as a 110 kDa vesicular protein overexpressed in a non-P-glycoprotein MDR lung cell line (Scheper *et al.,* 1993). LRP expression was seen in bronchus, digestive tract, renal proximal tubules, keratinocytes, macrophages, and the adrenal cortex, varying levels were observed in other organs. Expression of LRP in normal tissues parallels that of other drug-resistance related proteins

such as P-glycoprotein and MRP (Izquierdo *et al.,* 1996). The LRP gene was found to be located on chromosome 16p11.2, 27 cM, proximal to the MRP gene (16p13.1) (Izquierdo, 1996). When it was cloned and sequenced it was found to be the major component of vaults (Scheffer *et al.,* 1995).

Vaults were first identified by negative staining and transmission EM in 1986, as contaminant particles of clathrin-coated vesicle preparations derived from rat liver (Kedersha and Rome, 1986). Vaults were subsequently isolated from various species including a lower eukaryote Dictyostelium discoideum, amphibians, avians, and mammals and are highly conserved among different species supporting the notion that their function is essential to eukaryotic cells (Kedersha *et al.,* 1990).

As found with LRP in normal human tissues, the expression of vaults in other species is most abundant in epithelial cells (i.e. rat intestine) and macrophages (rat alveolar macrophages) (Kedersha *et al.,* 1990). In rats, vaults are ribonucleoprotein particles composed of a major vault protein of 104kDa (accounting for >70% of the mass and is equivalent to LRP), three minor proteins of 210, 192 and 54kDa and a small RNA molecule. These are assembled in a barrel-like structure of approx. 57 x 32 nm with a molecular mass of about 13MDa, which is 3 times the size of a ribosome. The vault particle has 2-fold symmetry, and each half can be opened into a flower-like structure which contains eight petals surrounding a central ring (Kedersha *et al.,* 1991). These dynamic structural variations are likely to play a role in vault function. Most vaults are present in the cytoplasm and most cells contain thousands of vaults although there precise function is unknown (Chugani *et al.,* 1993).

Vaults structure and localisation support a transport function for this particle which could involve a variety of substances. It is thought that vaults may play a role in drug resistance by regulating the nucleocytoplasmic transport of drugs.

Low levels of LRP positivity were seen in testicular cancer, neuroblastoma and acute myeloid leukaemia, intermediate levels in ovarian cancer and high levels in colon, renal and pancreatic carcinomas (Izquierdo *et al.,* 1996). MRP and LRP were found to be widely expressed in a panel of 61 human cancer cell lines as opposed to the low frequency of expression of P-glycoprotein. LRP was also found to be a superior marker of *in vitro* drug resistance compared to P-glycoprotein and MRP (Izquierdo *et al.,* 1996). Positivity

of LRP in primary ovarian cancer was significantly associated with a worse response to chemotherapy, a shorter progression-free interval and shorter overall survival (Izquierdo *et al.,* 1995).

1.10 Alternative Mechanisms of Resistance

The above mechanisms do not account for all the types of resistance observed.

1.10.1 Topoisomerase II

Alterations in topoisomerase II can lead to resistance to anthracyclines and the epipodophyllotoxins (De Isabella *et al.,* 1990) but not to the vinca alkaloids. Changes in topoisomerase-II can occur via a number of mechanisms;

i) Quantitative changes

A number of cell lines selected for resistance to VP-16 have decreased topoisomerase-II content (Ferguson *et al.,* 1988; Liu *et al.,* 1989; Heenan, 1994). A decrease in cellular content of topoisomerase-II in many instances contributes to MDR. This results in a decreased number of drug-induced topoisomerase-II DNA strands breaks and thus confers resistance to topoisomerase-II drugs. The decrease in topoisomerase-II content can be caused by gene inactivation e.g. gene rearrangement and/or hypermethylation (Tan *et al.,* 1989), leading diminished transcription, or possibly post-translational events (Deffie *et al.,* 1992).

ii) Decreased drug-induced DNA cleavage

In a CHO cell line selected for resistance to VM-26, the cellular amounts and catalytic activity of topoisomerase-II were equal in resistant and wild-type cells. The topoisomerase-II cleaved DNA normally but was insensitive to drug inhibition of religation (Glisson *et al.*, 1986; Sullivan *et al.*, 1989). Subsequently the normal allele of topoisomerase-II was found to be lost and a point mutation was found (Chan *et al.*, 1993). Further mutations in the gene which confer decreased cleavage and religation activity due to alterations in ATP binding has been described (Danks *et al.*, 1989).

iii) Differential expression of topoisomerase-II isoforms

In various resistant cell lines there can be alterations in isoform expression compared to the parent cell line. For example, an m-AMSA-resistant P388 cell line, in which the content of the p170 topoisomerase-II isoform was reduced, whereas there was no difference in expression of the p180 isoform (Drake *et al.*, 1987).

iv) Altered subcellular distribution of topoisomerase-II

In a VM-26-resistant CCRF-CEM cell line less topoisomerase-II was detected in the nuclear matrix, whereas the amount of total nuclear topoisomerase-II was equal in resistant and sensitive cells. The catalytic activity of topoisomerase-II in nuclear matrix preparations were reduced 6-7 fold in the resistant cell lines. It is thought that a mutation in the enzyme may impair its incorporation into the nuclear matrix (Fernandes *et al.*, 1990).

v) Changes in extrinsic factors modulating topoisomerase-II activity

Cytosolic proteins may modulate the activity of topoisomerase-II. A VP-16-resistant human melanoma cell line, where drug uptake was unchanged and the catalytic activity and drug-induced DNA strand breaks mediated by isolated topoisomerase-II were similar

from resistant and sensitive cells had decreased drug-induced cleavage in whole cells although it was unchanged in isolated nuclei (Campain *et al.*, 1993).

The formation of an m-AMSA-induced topoisomerase-II-DNA complex in isolated nuclei was reduced compared to whole cells from the murine mastocytoma cell line K21 (Darkin and Ralph, 1989). When protein from cytoplasmic extracts was added, complex formation was increased to the same level as in whole cells. This protein was tentatively identified as a type of casein kinase (Darkin-Rattray and Ralph, 1991). Thus, the resistance of quiescent cells to topoisomerase-II-active drugs may be explained by decreased activation of topoisomerase-II.

vi) Phosphorylation of Topoisomerase-II

Stimulation of topoisomerase-II activity has been shown by phosphorylation *in vivo* (Ackerman *et al.*, 1988). Casein kinase II (Ackerman *et al.*, 1985), protein kinase C (Rottmann *et al.*, 1987) and a cAMP-independent protein kinase (Sander *et al.*, 1984) have been shown to phosphorylate topoisomerase-II *in vitro*. Changes in phosphorylation of topoisomerase-II caused by mutations in protein kinases or phosphorylation sites on topoisomerase-II could result in drug resistance. Although this has yet to be proven, it has been shown that phosphorylation of topoisomerase-II decreases its sensitivity to drug-induced DNA cleavage, while increasing the overall catalytic activity (DeVore *et al.*, 1992).

1.10.2 Glutathione S-transferases

Many active chemotherapeutic agents are electrophiles and are subject to conjugation with molecules such as glutathione and glucuronic acid to facilitate transport, metabolism and ultimately excretion. In almost all animal models of carcinogenesis there is overexpression

of conjugation enzymes, amongst which the glutathione S-transferases (GSTs) have been most extensively studied. Many human cancers show overexpression of GSTs, although a significant proportion of liver and breast carcinomas may show no expression at all, despite being resistant to drugs metabolised by these enzymes (Harrison, 1995).

GSTs are a family of multifunctional enzymes which play an important role in the detoxification of cytotoxic compounds and mediate the conjugation of cytotoxic drugs and carcinogens with reduced glutathione. GSTs are a widely distributed family of enzymes, expressed in most normal tissues. In general, the enzymes are rather low in catalytic activity but present in high abundance, accounting for approximately 6% of liver cytosolic protein. Overexpression of GSTs (GST-π is the most commonly elevated isoenzyme) is commonly associated with increased P-glycoprotein expression in leukaemias (Gekeler *et al.,* 1992) leading to the hypothesis that GSTs may serve the drug efflux pump with its substrate, thereby increasing the efficiency of drug exclusion from the cell. However, clear evidence for a direct metabolic role of GSTs in tumour cell resistance is still lacking.

1.10.3 Bcl-2 / p53

Alterations in levels of proteins involved in the apoptotic pathway may prevent drug-induced cell death. The tumour suppressor gene p53 acts as a sensor in cells detecting DNA strand breakage and preventing a cell from proliferating whilst bearing damaged or mutated DNA (Kastan *et al.,* 1991). In some systems p53 causes cell cycle arrest at the G_1-S interface, but in other situations p53 commits a cell to die by apoptosis (Clarke *et al.,* 1993). Thus, in mouse thymocytes, absence of p53 confers resistance to the topoisomerase II inhibitor VP-16, even though this drug can kill lymphoid cells in and out of the cell cycle (Dive and Wyllie,).

Overexpression of bcl-2 oncogene in lymphoma cell lines (Miyashita and Reed, 1993), murine FL5.12 (Walton *et al.,* 1993) and neuroblastoma cells (Dole *et al.,* 1994) confers drug resistance and is of proven clinical significance.

Increased levels of bcl-2 and decreased levels of bax may elevate drug resistance and thereby cause a broad spectrum of drug resistance (R. NicAmhlaoibh, personal communication).

Elevations of the bcl-2 : bax ratio do not prevent drug-induced apoptosis but rather shifts the dose response curve so that an increased concentration of drug is required to achieve an equivalent tumour cell kill.

Overexpression of bcl-x_S in MCF-7 cells induces sensitisation to apoptosis induced by low concentrations of VP-16 and Taxol (Sumantran *et al.,* 1995). Overexpression of bcl-x_L inhibited both cisplatin and cyclophosphamide induced cell death in the shep-1 cell line (Dole *et al.,* 1995) and decreased the cytotoxicity of bleomycin, cisplatin, VP-16 and vincristine in FL5.12 murine cells. Overexpression of bcl-x_L did not prevent cells from undergoing cell cycle arrest in response to these drugs rather it prevented the treated cells from undergoing apoptosis (Minn *et al.,* 1995).

1.10.4 Metallothioneins

Metallothioneins (MT) are intracellular proteins of low molecular weight (6-7 kDa) that are characterised by a high content of cysteine and the ability to bind heavy metals. Most tissues have a basel level of MT although their physiological function is not well understood. MT have been demonstrated in a variety of malignancies including colorectal, testicular germ cell, ovarian and lung tumours. The synthesis of MT by tumour cells has been proposed as a possible mechanism for the intracellular inactivation of metal-containing chemotherapeutic agents such as cisplatin. Cells transfected with MT were found to be resistant to cisplatin, chlorobucil, melphalan and doxorubicin. Cells of various origins selected for cisplatin resistance often, but not always show an increased MT

expression. In human NSCLC a significant relationship was found between MT expression and doxorubicin resistance *in vitro* (Mattern and Volm, 1995).

1.10.5 DNA repair mechanisms

The DNA repair protein, O6-alkylguanine DNA alkyltransferase is a major contributor to the resistance to nitrosurea, triazine class of alkylating agents (Gerson and Wilson 1995). DNA repair is a vast subject, directly involving up to 200 different genes (Harrison, 1995) reviewed in Friedburg (Friedberg, 1985). In general, two fundamental reactions are involved in cellular responses to DNA damage; (i) repair of the damage and (ii) tolerance of the damage. Different DNA repair mechanisms are shown in Table 1.10.1.

Table 1.10.1

Mechanisms of drug repair, modulations of which may be important in altering tumour sensitivity to drugs

Mechanism	Function	Drugs affected
Mismatch repair	Removal of mismatched bases	cisplatin
Excision repair	Removal of drug/DNA adducts	Alkylating agents
Recombination	Double-strand break repair	Bleomycin, irradiation
Other	Dealkylation and deamination	Nitrosoureas

The reality of MDR is not as simple as just explained and may involve more than one mechanism coexpressed in the same cell. Resistant cells in situ are usually not more than 5 to 10 fold resistant compared to *in vitro* models whereby resistance may increase 100- or 1000- fold (Simon and Schindler, 1994).

1.11 MDR circumvention:

The best understood mechanism of MDR is the resistance mediated by P-glycoprotein. Should this protein be inhibited then there is a restoration of cytotoxic drug accumulation in MDR cells. This is the present rational for the circumvention of MDR and two approaches are being taken; pharmacological intervention and genetic antisense technology.

1.11.1 Pharmacological circumvention

A number of compounds have been identified which inhibit the efflux of chemotherapeutic drugs by P-glycoprotein and reverse cellular resistance in eperimental systems. These chemosensitisers may block cytotoxic drug efflux by acting as competive or noncompetive inhibitors, perhaps by binding to similar drug substrate binding sites, or to other chemosensitiser binding sites that cause allosteric changes resulting in inhibition of cytotoxic drug binding (Ford, 1995). The majority of chemosensitisers described to date may be grouped into six broad categories, based on their primary pharmacologic activity; calcium channel blockers; calmodulin antagonists; steroids and hormonal analogues; cyclosporines; dipyridamole; miscellaneous other compounds (see Table 1.11.1).

Table 1.11.1 Selected pharmacologic agents with ability to reverse multidrug resistance (Ford, 1995)

Calcium channel blockers	*Immunosuppressive Drugs*
Verapamil	Cyclosporin A
Nifedipine	SDZ PSC 833
Niguldipine	SDZ 280-446
Bepridil	FK506
PAK-200	Rapamycin
Ro11-2933	
	Antibiotics
Calmodulin Antagonists	Cefoperazone
Trifluoperazine	Ceftriaxone
Prochlorperazine	Erythromycin
Fluphenazine	
Trans-Flupenthixol	*Miscellaneous Compounds*
	Dipyridamol
Vinca Alkaloid Analogs	BIBW 22
Vindoline	Quinidine
Thaliblastine	Chloroquine
	Terfenadine
Steroidal Agents	Reserpine
Progesterone	Amiodarone
Tamoxifen	Methodone
Toremifene	S 9788
Megestrol acetate	GF 120918
17ß-Estradiol glucuronide	Tolyphorphin

A number of these compounds demonstrate circumvention ability *in vitro* but are too toxic for use *in vivo*. Verapamil, cyclosporin A and quinine have been used in early clinical trials, but the results have been disappointing so far.

Verapamil inhibits the P-glycoprotein-associated, energy-dependent drug efflux and is a potent and effective antagonist of resistance to a number of drugs in most MDR cell lines *in vitro*. Verapamil inhibits the binding of many chemotherapeutic drugs as well as other chemosensitisers to P-glycoprotein suggesting that the mechanism of action of verapamil is through blocking the binding of drugs to P-glycoprotein (Ford, 1995). Spoelstra *et al* demonstrated that verapamil was actively transported by P-glycoprotein

and that verapamil and daunorubicin were non-competing substrates for P-glycoprotein. Therefore the effectiveness of verapamil as a MDR antagonist may be compromised because it may be extruded by P-glycoprotein (Spoelstra *et al.,* 1994). The use of verapamil in humans is limited by its cardiovascular effects at plasma concentrations in the 2 to 6μM range, which are needed for the antagonism of MDR *in vitro*. Therefore more potent and less toxic chemosensitising agents other than verapamil have been investigated e.g. Ro11-2933, which is ten fold more potent than verapamil with plasma levels *in vivo* of less than 2μM effective *in vitro* (Ford, 1995).

Cyclosporin A, a hydrophobic cyclic peptide of 11 amino acids that is widely used in human organ transplantation, has been found to reverse resistance in MDR cells but not sensitive cells. Interestingly, cyclosporin A apparently does not inhibit the function of MRP in combination with doxorubicin, vincristine or mitoxantrone (van der Graaf *et al.,* 1994). Cyclosporin A has been found to act as a P-glycoprotein substrate and antagonise P-glycoprotein at least in part through competitive inhibition of cytotoxic drugs efflux (Ford, 1995). However because of the profound pharmacologic effects of cyclosporin A *in vivo* (Erlichman *et al.,* 1993), there has been an interest in developing the anti-MDR activity of other, less immunosuppressive or nephrotoxic cyclosporine analogues e.g. PSC 833 and PSC 280-446.

Attempts at chemomodulation of P-glycoprotein has been investigated using various P-glycoprotein antagonists. A lack of specificity (calcium antagonists) or toxic effects (cyclosporin A) however, result in a limited clinical application of these chemomodulators. Therefore a more specific modulation of MDR is necessary for an improved reduction in drug resistance.

1.11.2 Genetic circumvention

The results of circumvention compounds in clinical trials have been disappointing due to non-specific or toxic effects of the circumvention agent. Other alternatives such as molecular approaches may improve attempts at the reversal of MDR. A more specific interference with P-glycoprotein expression achieved by modern antisense technology may be more promising approach..

Ribozymes are RNA molecules which have catalytic activity. They were first discovered when the large ribosomal RNA (rRNA) precursor of *Tetrahymena thermophila* could self-splice the intron and as the RNA component of the *E.coli* RNase P, an RNA-protein which could cleave the leader segment from precursor transfer RNA molecules. Subsequently the hammerhead ribozyme and hairpin ribozyme were discovered in viroids (helper viruses found in plants) and the hepatitis delta virus ribozyme was found in the hepatitis delta virus. These latter ribozymes cleave RNA which is synthesised in a rolling circle into individual RNA transcripts. Further research demonstrated that these RNA molecules with self-splicing activity could be manipulated to target specific RNA molecules. Once paired to a target site, the manipulated ribozymes can cleave single stranded RNA and thus functionally destroy the RNA target and several substrate molecules can be turned over by one molecule of catalytic RNA. The high specificity of ribozymes in RNA cleavage reactions has provided a new method in controlling gene expression artificially and this makes ribozymes potentially useful therapeutic agents.

The hammerhead ribozyme is the smallest of the ribozymes. Figure 1.11.2.1 shows the hammerhead ribozyme bound to a substrate. The non-based paired nucleotides of stem II make up the catalytic core. The substrate and the ribozyme hybridise to form stem I and stem III, orienting the -UH- nucleotides of the substrate over the catalytic core. The GUC nucleotide triplet is thought to yield the highest rate of cleavage compared to other cleavage triplet sequences. The hammerhead ribozyme has been the best characterised ribozyme with respect to optimised target sequence, conserved nucleotides sequences within the catalytic core, and the kinetic parameters. The target RNA cleavage sites have

the least constraints with respect to sequence and therefore are the most abundant sites compared to the other ribozyme types (Sullivan, 1994).

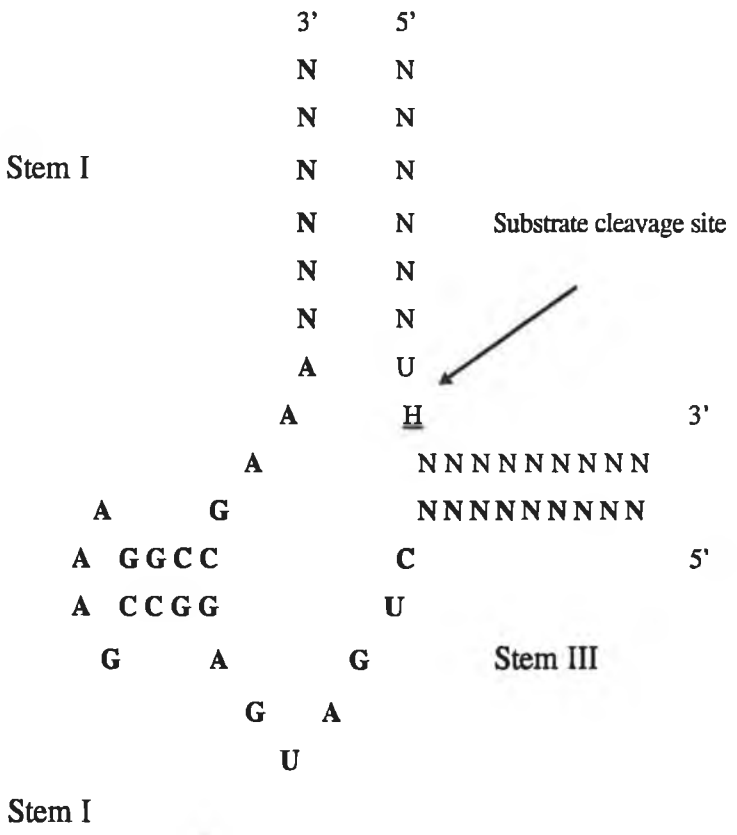

Figure 1.11.2.1 **Structure of the hammerhead ribozyme.**

The hammerhead ribozyme is in bold. Stem I and stem III are the binding arms and stem II is a part of the catalytic core. The H represents the cleaveage site of the the substrate RNA and may be an adenine, cytosine or uridine (Sullivan, 1994).

A hammerhead ribozyme which cleaves the 3'-end of the GUC sequence in codon 880 of mdr1 RNA was transfected into the pancreatic carcinoma cell line EPP85-181RDB , which is 1,600 fold-more resistant to daunorubicin than the parental cell line. Ribozyme decreased the level of mdr1 mRNA expression, inhibited the formation of P-glycoprotein and reduced the cell's resistance to daunorubicin. Cell clones that showed ribozyme

expression were only 5.3-fold more resistant than the parental cell line (Holm *et al.*, 1994). This ribozyme was also effective in two adriamycin resistant human lung carcinoma cell lines DLKP-A and SK-MES-1/Adr (Daly *et al.*, 1996).

Other researchers with different ribozymes have successfully reduced P-glycoprotein expression in the human colon adenocarcinoma cell line LoVo, a mouse sarcoma cell line S-180, a human oral epidermoid carcinoma cell line KB (Bertram *et al.*, 1995) and a human plueral mesothelioma cell line (Kiehntopf *et al.*, 1994). Interestingly, the expression of the *c-fos* ribozyme in A2780S human ovarian carcinoma cells, not only decreased the expression of *c-fos* but also the expression of the mdr1 gene, *c-jun* and mutant p53. Reversal of the MDR phenotype by an anti-MDR ribozyme occured one-fourth as rapidly as that induced by the anti-*fos* ribozyme (Scanlon *et al.*, 1994).

1.12 Non-MDR chemosensitisers

There are a number of other non-chemotherapeutic drugs which enhance chemotherapeutic cytotoxicity by mechanisms other than reversal of drug resistance (reviewed in Stewart and Evans, 1989). These include buthionine sulfoximine (BSO) and other glutathionine depletors, the nitroimidazoles and the methylxanthines.

Glutathione helps to protect cells both by reacting with cytotoxic electrophile drug derivatives and by reacting with drug generated reactive oxygen compounds such as peroxides (Pratt *et al.*, 1994). High glutathione levels were found to be associated with decreased DNA cross-link formation by some chemotherapy drugs. This reduction in DNA cross-link formation was probably due to intracellular drug inactivation by the glutathione rather than an increased rate of DNA repair (Stewart and Evans, 1989). BSO is structural analogue of γ-glutamylcysteine, which reduces cellular glutathione levels, by irreversibly inhibiting γ-glutamylcysteine synthetase, the first enzyme involved in *de novo* glutathione synthesis (Pratt *et al.*, 1994). BSO also inhibits glutahtione transferase activity, and inhibits the uptake of cystine, a precursor of glutathione (Stewart and Evans,

1989). While BSO decreased glutathione concentrations in most normal tissues, the degree of glutathione reduction in these normal tissues has not been as great as in tumour tissues. Chemotherapy toxicity to normal tissues (including bone marrow) was generally not augmented at BSO doses that enhanced chemotherapy efficacy against tumours (Lee *et al.,* 1987; Stewart and Evans, 1989; Siemann and Beyers, 1993).

The nitroimidazoles also potentiate the effect of numerous chemotherapeutic drugs against hypoxic tumour cells. Although their mechanism of action is not well understood they are thought to act by decreasing tumour cell thiols, increasing DNA damage (in part from inhibition of repair processes) and possibly alterating tumour vasculature (Stewart and Evans, 1989).

The methylxanthines, which include caffeine and pentoxifylline, have also been found to potentiate the cytotoxic effect of chemotherapeutic drugs (Das *et al.,* 1982; Hain *et al.,* 1993; Hain *et al.,* 1994). The actual mechansim of action of methylxanthines is unclear although they are thought to act by interfering with the repair of DNA, preventing G_2 arrest and prematurely inducung mitosis (Fingert *et al.,* 1986; Schlegel and Pardee, 1986; Lock *et al.,* 1994) or inhibiting the induction of, or indirectly inhibiting with post-replication repair mechanisms (Schiano *et al.,* 1991). Methylxanthines are also reported to reduce the cytotoxicity of DNA damaging anti-topoisomerase drugs (including adriamycin, mitoxantrone, VP-16 and ellipticine). Intercalation between the drug and methylxanthine can lead to a decrease in the effective drug concentration available (Traganos *et al.,* 1991; Traganos *et al.,* 1993), while inhibition of RNA synthesis may also be a possible mechanism (Perez *et al.,* 1994).

1.13 Aims of this thesis

The aims of this thesis were to examine the effect of combinations of different drugs on toxicity to sensitive and multidrug resistant cancer cells *in vitro*. Combinations of existing anticancer agents were analysed. Combinations of anticancer drugs and a variety of chemosensitivity drugs used at nontoxic levels were then studied. Cellular models transfected with the MDR1 gene and an anti-MDR1 ribozyme were also developed. Combinations of a known anticancer agent with one of a series of coded non-toxic compounds known to be safe for human use were examined in a number of cell lines. The effects of adding these compounds at different times after chemotherapeutic drug treatment were investigated. The rate and timing of apoptosis, progress through the cell cycle and levels of cell cycle-related proteins then were examined.

2.0 Materials and Methods

2.1 WATER

Ultrapure water was used in the preparation of all media and solutions. This water was purified by a reverse osmosis system (Millipore Milli-RO 10 Plus, Elgastat UHP) to a standard of 12 - 18 MΩ/cm resistance.

2.2 GLASSWARE

Solutions pertaining to cell culture and maintenance were prepared and stored in sterile glass bottles. Bottles (and lids) and all other glassware used for any cell-related work were prepared as follows:- all glassware and lids were soaked in a 2% (v/v) solution of RBS-25 (AGB Scientific) for at least 1 hour. after which they were scrubbed and rinsed several times in tap water. They were then washed by machine using Neodisher detergent which is an organic, phosphate-based acid detergent, rinsed twice with distilled water, once with ultrapure water and sterilised by autoclaving.

2.3 STERILISATION

Water, glassware and all thermostable solutions were sterilised by autoclaving at 120°C for 20 min. under pressure of 1bar. Thermolabile solutions were filtered through a 0.22μm sterile filter (Millipore, millex-gv). Low protein-binding filters were used for all protein-containing solutions.

2.4 MEDIA PREPARATION

The basal media used during routine cell culture were prepared according to the formulations shown in Table 2.4.1. 10X media were added to sterile ultrapure water, buffered with HEPES and $NaHCO_3$ and adjusted to a pH of 7.45 - 7.55 using sterile 1.5M

NaOH and 1.5M HCl. The media were then filtered through sterile 0.22μm bell filters (Gelman; G.1423S) and stored in 500ml sterile bottles at 4°C. Sterility checks were carried out on each 500ml bottle of medium as described in Section 2.5.5.

The basal media were stored at 4°C up to their expiry dates as specified on each individual 10X medium container. Prior to use, 100ml aliquots of basal media were supplemented with 2mM L-glutamine (Gibco; 043-05030) and 5% foetal calf serum (Sigma; F7524, Batch #13H 3389) and this was used as routine culture medium. This was stored for up to 2 weeks at 4°C, after which time, fresh culture medium was prepared.

Table 2.4.1 Preparation of basal media

	DMEM (Gibco 042-02501M)	**Hams F12** (Gibco 042-01430M)	**MEM** (Gibco 074-01700N)
10X Medium	500ml	Powder	500ml
Ultrapure H_20	4300ml	4700ml	4300ml
1M HEPES* Sigma H9136	100ml	100ml	100ml
7.5% $NaHCO_3$ BDH 30151	45ml	45ml	45ml

* HEPES = N-(2-Hydroxyethyl)piperazine-N'-(2-ethanesulfonic acid)

2.5 CELL LINES

All cell culture work was carried out in a class II down-flow re-circulating laminar flow cabinet (Nuaire Biological Cabinet) and any work which involved toxic compounds was carried out in a cytoguard (Gelman). Strict aseptic techniques were adhered to at all times. The laminar flow cabinet was swabbed with 70% industrial methylated spirits (IMS) before and after use, as were all items used in the cabinet. Each cell line was assigned

specific media and waste bottles and only one cell line was worked with at a time in the cabinet which was allowed to clear for 15min between different cell lines. The cabinet itself was cleaned each week with industrial detergents (Virkon; Antec. International, TEGO; TH.Goldschmidt Ltd.), as were the incubators.

The cell lines used during the course of this study, their sources and their basal media requirements are listed in Table 2.5.1. Basal medium was supplemented with 5-10% serum and 2mM L-glutamine. Lines were maintained in 25cm^2 flasks (Costar; 3050) or 75cm^2 flasks (Costar; 3075) at 37°C and fed every two to three days.

2.5.1 Subculture of Adherent Lines

During routine subculturing or harvesting of adherent lines, cells were removed from their flasks by enzymatic detachment.

1. Waste medium was removed from the flasks and rinsed with a pre-warmed (37°C) trypsin/EDTA (TV) solution (0.25% trypsin (Gibco; 043-05090), 0.01% EDTA (Sigma; EDS) solution in PBS A (Oxoid; BR14a)). The purpose of this was to sequester naturally occurring trypsin inhibitor which would be present in any residual serum.
2. Fresh TV was then placed on the cells (2ml/25cm^2 flask or 4ml/75cm^2 flask) and the flasks incubated at 37°C until the cells were seen to have detached (5 - 10 min).
3. The trypsin was deactivated by addition of a equal volume of growth medium (*i.e.* containing 5% serum).
4. The entire solution was transferred to a 30ml sterile universal tube (Sterilin; 128a) and centrifuged at 1,000 r.p.m. for 5 min.
5. The resulting cell pellet was resuspended in pre-warmed (37°C) fresh growth medium, counted (Section 2.5.2) and used to re-seed a flask at the required cell density or to set up an assay.

Table 2.5.1 Cell lines used during the course of this study

Cell line	Basal medium	Cell type	Source
DLKP (and all its derivatives)	ATCC[1]	Human lung squamous carcinoma	Dr.Grant NCTCC
SK-MES-1 (and all its derivatives	MEM[2]	Human lung squamous carcinoma	ATCC[3]

[1]ATCC consists of a 1:1 mixture of DMEM and Hams F12.

[2]MEM medium was supplemented with 1% (v/v) MEM Non-essential amino acids (NEAA) (Gibco; 043-01140) and 1mM sodium pyruvate for all lines

[3]ATCC = American Type Culture Collection

2.5.2 Cell Counting

Cell counting and viability determinations were carried out using a trypan blue (Gibco; 525) dye exclusion technique.

1. An aliquot of trypan blue was added to a sample from a single cell suspension in a ratio of 1:5.
2. After 3 min. incubation at room temperature, a sample of this mixture was applied to the chamber of a haemocytometer over which a glass coverslip had been placed.
3. Cells in the 16 squares of the four outer corner grids of the chamber were counted microscopically, an average per corner grid was calculated with the dilution factor being taken into account and final cell numbers were multiplied by 10^4 to determine the number of cells per ml (volume occupied by sample in chamber is 0.1cm x 0.1cm x 0.01cm *i.e.* 0.0001cm^3 therefore cell number x 10^4 is equivalent to cells per ml).

4. Non-viable cells were those which stained blue while viable cells excluded the trypan blue dye and remained unstained.

2.5.3 Cell Freezing

To allow long term storage of cell stocks, cells were frozen and cryo-preserved in liquid nitrogen at temperatures below -180°C. Once frozen properly, such stocks should last indefinitely.

1. Cells to be frozen were harvested in the log phase of growth (*i.e.* actively growing and approximately 50 - 70% confluent) and counted as described in Sections 2.5.2.
2. Pelleted cells were re-suspended in serum and an equal volume of a DMSO/serum (1:9, v/v). This solution was slowly added dropwise to the cell suspension to give
a final concentration of at least $5x10^6$ cells/ml.
3. 1.5ml aliquots of this suspension was placed in cryovials (Greiner; 122 278) which were then quickly placed in the vapour phase of liquid nitrogen containers (approximately -80°C).
4 After 2.5 - 3.5 hours, the cryovials were lowered down into the liquid nitrogen where they were stored until required.

2.5.4 Cell Thawing

1. Immediately prior to the removal of a cryovial from the liquid nitrogen stores for thawing, a sterile universal tube containing growth medium was prepared for the rapid transfer and dilution of thawed cells to reduce their exposure time to the DMSO freezing solution which is toxic at room temperature.
2. The suspension was centrifuged at 1,000 r.p.m. for 5 min., the DMSO-containing supernatant removed and the pellet re-suspended in fresh growth medium.

3. A viability count was carried out (Section 2.5.2) to determine the efficacy of the freezing/ thawing procedures
4. Thawed cells were placed into tissue culture flasks with the appropriate volume of medium (10ml/25cm^2 flask and 15ml/75cm^2 flask) and allowed to attach overnight.
5. After 24 hours, the cells were re-fed with fresh medium to remove any residual traces of DMSO.

2.5.5 Sterility Checks

Sterility checks were routinely carried out on all media, supplements and trypsin used for cell culture. Samples of basal media were inoculated into Columbia (Oxoid; CM331) blood agar plates, Sabauraud (Oxoid; CM217) dextrose and Thioglycollate (Oxoid; CM173) broths which should between them detect most contaminants including bacteria, fungus and yeast. Growth media (*i.e.* supplemented with serum and L-glutamine) were sterility checked at least 2 days prior to use by incubating samples at 37°C which were subsequently examined for turbidity and other indications of contamination.

2.6 *MYCOPLASMA* ANALYSIS

Mycoplasma examinations were carried out routinely (at least every 3 months) on all cell lines used in this study. These analyses were performed by Mary Heenan and William Nugent.

2.6.1 Indirect Staining Procedure

In this procedure, *Mycoplasma*-negative NRK cells (a normal rat kidney fibroblast line) were used as indicator cells. As such, these cells were incubated with supernatant from test cell lines and then examined for *Mycoplasma* contamination. NRK cells were used for this

procedure because cell integrity is well maintained during fixation. A fluorescent Hoechst stain was utilised which binds specifically to DNA and so will stain the nucleus of the cell in addition to any *Mycoplasma* DNA present. A *Mycoplasma* infection would thus be seen as small fluorescent bodies in the cytoplasm of the NRK cells and sometimes outside the cells.

1. NRK cells were seeded onto sterile coverslips in sterile Petri dishes at a cell density of $2x10^3$ cells per ml and allowed to attach over night at 37°C in a 5% CO_2, humidified incubator.
2. 1ml of cell-free (cleared by centrifugation at 1,000 r.p.m. for 5 min) supernatant from each test cell line was then inoculated onto a NRK Petri dish and incubated as before until the cells reached 20 - 50% confluency (4 - 5 days).
3. After this time, the waste medium was removed from the Petri dishes, the coverslips washed twice with sterile PBS A, once with a cold PBS/Carnoys (50/50) solution and fixed with 2ml of Carnoys solution (acetic acid:methanol-1:3) for 10 min.
4. The fixative was then removed and after air drying, the coverslips were washed twice in deionised water and stained with 2ml of Hoechst 33258 stain (BDH) (50ng/ml) for 10 min.

From this point on, work proceeded in the dark to limit quenching of the fluorescent stain.

5. The coverslips were rinsed three times in PBS.
6. They were then mounted in 50% (v/v) glycerol in 0.05M citric acid and 0.1M disodium phosphate and examined using a fluorescent microscope with a UV filter.

2.6.2 Direct Staining

The direct stain for *Mycoplasma* involved a culture method where test samples were inoculated onto an enriched *Mycoplasma* culture broth (Oxoid; CM403) - supplemented with 16% serum. 0.002% DNA (BDH; 42026), 2µg/ml fungizone (Gibco; 042 05920),

$2x10^3$ units penicillin (Sigma; Pen-3) and 10ml of a 25% (w/v) yeast extract solution - to optimise growth of any contaminants and incubated at 37°C for 48 hours. Sample of this broth were then streaked onto plates of *Mycoplasma* agar base (Oxoid; CM401) which had also been supplemented as above and the plates were incubated for 3 weeks at 37°C in a CO_2 environment. The plates were viewed microscopically at least every 7 days and the appearance of small, "fried egg" -shaped colonies would be indicative of a mycoplasma infection.

2.7 Toxicity assay

Due to the nature of the compounds tested in the assays, precautions were taken to limit the risks involved in their handling and disposal. All work involving toxic compounds was carried out in a Gelman "Cytoguard" laminar air flow cabinet (CG Series). All chemotherapeutic drugs were stored and disposed of as described in table 2.7.1.

Table 2.7.1

Cytotoxic Drug	Supplier	Inactivation	Storage
Adriamycin	Farmitalia	Hyperchlorite inactivation followed by autoclaving	Stock at 4°C
Carboplatinum	Bristol Myers Pharmaceuticals	Incineration	Store at room temperature
5-Fluorouracil	Farmitalia	NaOH inactivation followed by autoclaving	Store at room temperature
Vincristine	David Bull Laboratories Ltd	Autoclave	Store at 4°C
VP-16	Bristol Myers Pharmaceuticals	Incineration	Store at room temperature

All drugs were stored in the dark

2.7.1 Toxicity assay

Before setting up any assay, a cell line was pretreated so that it would be in the exponential phase of growth. Two days prior to the assay, the cells were subcultured into 75cm^2 flasks at a density of 2 x 10^5 cells/flask. The cell were allowed to attach overnight and the next day were fed with fresh medium.

1. Cells were harvested from a flask in the exponential phase of growth.
2. A cell suspension of 1x10^4 cells/ml was made up in growth medium and 100µl added into 96-well plates (Costar; 3599) and allowed to attach overnight at 37°C, 5% CO_2.
3. Drug dilutions (including a control with no drug) were prepared at 2X their final concentration in growth medium and 100µl added to each well in replicas of eight, giving final a concentration of 1X drug.
4. The plates were incubated for 6 days at 37°C and 5% CO_2 or until the control wells reached 80% confluency.
5. Cell survival was determined by acid phosphatase assay (Section 2.7.2).
6. The concentration of drug which causes 50% cell kill (the IC50 value) was calculated using the Chou and Talalay computer package (Section 2.7.5).

2.7.2 Acid Phosphatase Assay

1. After incubation for 6 days or until 80% confluency was reached in the control wells the plates were removed from the incubator and the medium discarded.
2. The wells were washed twice with PBS (100µl) and the PBS discarded. 100µl of phosphatase substrate (10mM *p*-nitrophenolphosphate (Sigma; 104-0), 0.1M sodium acetate (Sigma; S8625), 0.1% triton X-100 (BDH; 30632) pH 5.5) was added to each well.
3. Plates were then wrapped in aluminium foil and left in the dark at 37°C for 2 hours.
4. The enzyme reaction was stopped by the addition of 50µl of 1.0M NaOH.

5. The plate was read in a dual beam plate reader at 405nm (reference wavelength 620nm).

2.7.3 Circumvention assays

1. Cells were harvested from a flask in the exponential phase of growth.
2. A cell suspension of $1x10^4$ cells/ml was made up in growth medium and 100µl added into 96-well plates (Costar; 3599) and allowed to attach overnight at 37°C and 5% CO_2.
3. Drug dilutions (including a control with no drug) were prepared at 4X their final concentration in growth medium and 50µl added to each appropriate well, giving a final concentration of 1X drug.

All circumvention agents (DL-buthionine-[S,R]-sulphoximine (Sigma; B2640), cyclosporin A (Sandoz; Sandimmune), verapamil (Sigma; V4629) and the test compounds) were dissolved in media. A 2mg/ml stock solution of the test compounds U-1 or N-1, was prepared by dissolving 20mg in 250µl of DMSO, the volume made up to 10 mls with media and the resulting solution filter sterilised using a 0.22µm filter.

In assays where more than 2 drug were used in combination, 8X drug dilutions were prepared and 25µl added to the appropriate wells. The final volume in each well was always 200µl.

4. The plates were incubated for 6 days at 37°C and 5% CO_2 or until the control wells reached 80% confluency.
5. Cell survival was determined by the acid phosphatase assay (Section 2.7.2).
6. The combination index (CI value), which quantifies the synergistic, additive or antagonistic effect of a combination of drugs, was calculated using the Chou and Talalay computer package.

2.7.4 Chemotherapeutic drug pulse assays

1. Cells were harvested from a flask in the exponential phase of growth.
2. A cell suspension of $1x10^4$ cells/ml was made up in growth medium and 100µl added into 96-well plates (Costar; 3599) and allowed to attach overnight at 37°C and 5% CO_2.
3. Drug dilutions (including a control with no drug) were prepared at 2X their final concentration in growth medium and 100µl added to each well in replicas of eight, giving a final concentration of 1X drug for 2 hours.
4. Drug was removed from the wells by inverting and tapping the plates over an open vessel which had been swabbed with IMS. The wells were then washed twice with preheated sterile PBS, ensuring to remove as much PBS as possible after the final rinse.
5. Circumvention agent was prepared at 1X final concentration and added immediately after drug exposure, 24 hours, 48 hours or 72 hours after drug exposure as appropriate. Each time the circumvention agent was removed the cells were washed once with preheated sterile PBS.
6. The plates were incubated for a total of 6 days at 37°C and 5% CO_2 or until the control wells reached 80% confluency.
7. Cell survival was determined by acid phosphatase assay (Section 2.7.2).

2.7.5 IC50 calculation

The multiple drug effect analysis of Chou and was used to calculate the IC50 value of drugs on their own and the effects of combinations of drugs (Chou and Talalay, 1983; Chou and Talalay, 1984). This involved plotting of dose-effect curves for a drug or combination of drugs, at different concentrations using the median-effect equation [Equation 1].

$$fa/fu = (D/Dm)^m \qquad \text{[Equation 1]}$$

Where:

fa represents the fraction of cells affected by *D*.

fu represents the fraction of cells unaffected by *D* (i.e. *fa* = 1-*fu*).

D represents the dose of drug used.

Dm is the dose required for 50% inhibition of cell growth and is the IC50 value.

m is the coefficient of the sigmoidicity of the dose-effect curve; m = 1, m < 1 and m > 1 indicate hyperbolic, sigmoidal and negative sigmoidal dose-effect curves respectively for the inhibitory drug.

The above equation can be rearranged to give:

$$D = Dm\,[fa/(1-fa)]^{1/m} \qquad \text{[Equation 2]}$$

The values of *Dm* and *m* can be calculated by the median-effect plot of x = log (*D*) versus y = log (*fa/(1-fa)*). In the median-effect plot, *m* is the slope and log (*Dm*) is the x-intercept. The conformity of the data to the median-effect principle was checked by the linear correlation coefficient (r) of the median effect plot. Values of drug concentrations and their corresponding percentage inhibition (expressed as a fraction) were entered for computer analysis by the computer package, Dose effect analysis with microcomputers (Chou and Chou, 1987).

2.7.6 Combination Index calculation

The Combination Index value was calculated for a combination of two drugs using Equation 3:

$$CI = (D)_1 / (Dx)_1 + (D)_2 / (Dx)_2 \qquad \text{[Equation 3]}$$

Where,

$(D)_1$ is the concentration of drug 1 used in a combination with drug 2, $(D)_2$, that causes $x\%$ inhibition.

$(D)_2$ is the concentration of drug 2 used in a combination with drug 1, $(D)_1$, that causes $x\%$ inhibition.

$(Dx)_1$ is the concentration of drug 1 alone that causes $x\%$ inhibition.

$(Dx)_2$ is the concentration of drug 2 alone that causes $x\%$ inhibition.

Synergy is indicated by a CI value < 1, an additive effect is indicated by a CI value equal to 1 and antagonism is indicated by a CI value > 1. Analysis was carried out using Dose effect analysis with microcomputers (Chou and Chou, 1987).

Two examples are given below:

Example 1:

(a) drug 1 inhibits cell growth by 50% at 5μg/ml $(Dx)_1$

(b) drug 2 inhibits cell growth by 50% at 1μg/ml $(Dx)_2$

(c) a combination of the two drugs at 5μg/ml in a e.g. 4:1 ratio (i.e. 4 μg/ml drug 1 $(D)_1$ and 1μg/ml drug 2 $(D)_2$) inhibits cell growth by 50%.

$$CI = (D)_1 / (Dx)_1 + (D)_2 / (Dx)_2$$

Then,

$$\begin{aligned} CI &= 4/5 + 1/1 \\ &= 0.8 + 1 \\ &= 1.8 \\ &= \text{Antagonistic} \end{aligned}$$

Example 2:

(a) drug 1 inhibits cell growth by 50% at 5μg/ml $(Dx)_1$

(b) drug 2 inhibits cell growth by 50% at 1μg/ml $(Dx)_2$

(c) a combination of the two drugs at 1μg/ml in a e.g. 4:1 ratio (i.e. 0.8 μg/ml drug 1 $(D)_1$ and 0.2μg/ml drug 2 $(D)_2$) inhibits cell growth by 50%.

$$CI = (D)_1 / (Dx)_1 + (D)_2 / (Dx)_2$$

Then,

CI = 0.8/5 + 0.2/1

= 0.16 + .2

= 0.36

= Synergistic

2.8 Flow cytometry

1. Cells were seeded at 5 x 10^4cells/25cm^2 flask four days before experiments.
2. Drug dilutions (including a control with no drug) were prepared at 2X their final concentration in growth medium and added to each flask giving a final concentration of 1X drug for 2 hours.
3. Drug was removed from the flasks by pouring the drug into a sterile bottle. The flasks were then washed twice with preheated sterile PBS, removing as much PBS as possible after the final rinse.
4. Circumvention agent was prepared at 1X final concentration and added immediately after drug exposure.
5. Samples were collected for flow cytometry at various time points; media from the flasks were poured into labelled universals, the flasks were trypsinised into single cell suspensions and the trypsinised cells added to the labelled universals (this ensured that any floating cells were collected), pelleted and resuspended in 70% ethanol 30% PBS and kept at 4°C. The samples could be stored for up to 1 month.
6. On the day samples were analysed, cells were harvested and resuspended in PBS with 100µg/ml RNase (DNase free) (Boeringher Mannheim; 1 119 915) and 40µg/ml propidium iodide (Sigma; P4170).
7. Samples were analysed on a Becton Dickenson (FACScan) using an argon-ion laser tuned to 488nm measuring forward and orthogonal light scatter and red fluorescence. Cell cycle analysis was performed on the Lysis program.

2.9 Time-lapse videomicroscopy

Time-lapse videomicroscopy was carried out on a Nikon Diaphot inverted microscope (Micron Optical, Bray, Ireland) equipped with phase-contrast optics, linked to a Mitsubishi CCD-100 colour video camera. Images were recorded in S-VHS onto a Mitsubishi HS-S5600 video recorder with time lapse capabilities. Recording speed was set at 3.22 sec/field (480 hour mode), which at normal playback speed resulted in an acceleration factor of 160.

The temperature of the culture vessel was controlled by a Linkam CO102 warm stage controller. This controller was adjusted to keep the culture medium inside the vessel at 37°C, as measured using a TB3301 probe. All time-lapse video equipment was obtained from Laboratory Instruments (Ashbourne, Ireland).

Cells were seeded at 5 x 10^6cells/25cm^2 flask four days before experiments. Recording was started after cells were exposed to chemotherapeutic drug for two hours and washed twice with PBS.

Cell death was classified as apoptotic on the basis of morphological events starting with rounding up of adherent cells, subsequent cell shrinkage and/or breakup into apoptotic bodies. These cell death events were scored at the time when rounding up first occurred. Cell division was classified as mitotic on the basis of morphological events starting with rounding up of adherent cells, subsequent cytokinesis and readherance of daughter cells to the surface. Mitotic events were scored at the time when rounding up first occurred. Typically 100 cells in the microscope field were followed.

2.10 Western blot analysis

2.10.1 Sample preparation

1. Cells were seeded at 5 x 10^6cells/25cm^2 flask two days before experiments.
2. Drug dilutions (including a control with no drug) were prepared at 2X their final concentration in growth medium and added to each flask giving a final concentration of 1X drug for 2 hours.
3. Drug was removed from the flasks by pouring the drug into a sterile bottle. The flasks were then washed twice with preheated sterile PBS, removing as much PBS as possible after the final rinse.
4. Circumvention agent was prepared at 1X final concentration and added immediately after drug exposure.
5. Samples were collected at various time points i.e. the media from the flasks were poured into labelled universals, the flasks were trypsinised into single cell suspensions and the trypsinised cells added to the labelled universals (this ensured that any floating cells were collected), pelleted and stored at -80°C.
6. Cells were lysed by sonication (7 pulses at 50% power) in SDS-radioimmunoprecipitation assay (RIPA) buffer (50mM Tris (pH 7.5), 150mM NaCl, 1% nonidet P-40 (Sigma; N6507), 0.1% sodium dodecyl sulphate (SDS) (Riedel-de Häin; 62862), 1% sodium deoxycholate (Sigma; D5670)) containing protease inhibitors (1mM sodium orthovanadate (Sigma; S6508), 1mM DTT (Sigma; D5545), 1mM phenylmethylsulphonyl fluoride (PMSF) (Sigma; P7626), 25µg/ml leupeptin (Sigma; L2884), 25µg/ml aprotinin (Sigma; A1153), 1mM benzamidine (Sigma; B6506), 10mg/ml trypsin inhibitor (Sigma; T9003)).
7. Samples were centrifuged at 4,000rpm for 10 minutes.
8. The supernatant was collected and centrifuged for 1 hour at 13,000rpm.
9. Samples were collected, aliquoted and stored at -80°C.

2.10.2 Protein Quantitation

The protein levels were determined using the Bio-Rad protein assay kit (Bio-Rad; 500-0006).

1. Standard concentrations of bovine serum albumin (BSA) (Sigma; A9543) were prepared fresh.
2. 20µl of protein standard or unknown protein sample was added to an Eppendorf.
3. 1ml of diluted (1:5) dye reagent was added and the mixture vortexed.
4. The OD_{570} was measured against a reagent blank after 5 mins to 1 hour.
5. The concentration of the protein samples was determined from the plot of the OD_{595} of the BSA standards.

2.10.3 Gel electrophoresis

Proteins for western blot analysis were separated by SDS-polyacrylamide gel electrophoresis (SDS-PAGE). Resolving and stacking gels were prepared as outlined in Table 2.17.1 and poured into clean 10cm x 8cm gel cassettes which consisted of 1 glass and 1 aluminium plate, separated by 0.75cm plastic spacers. The resolving gel was poured first and allowed to set. The stacking gel was then poured and a comb was placed into the stacking gel in order to create wells for sample loading. Once set, the gels could be used immediately or wrapped in aluminium foil and stored at 4°C for 24 hours.

Table 2.10.1 Preparation of electrophoresis gels

	Resolving gel (15%)	**Stacking gel**
Acrylamide stock*	10ml	0.8ml
Distilled H_2O	5.7ml	3.6ml
1.875M-Tris/HCl, pH 8.8	4ml	-
1.25M-Tris/HCL, pH 6.8	-	0.5ml
10% SDS		
(Sigma; L4509)	150µl	50µl
10% Ammonium persulphate		

(Sigma; A1433)	50µl	17µl
TEMED		
(Sigma; T8133)	9µl	6µl

* Acrylamide stock = 29.1g acrylamide (Sigma; A8887) and 0.9g NN'-methylene bis-acrylamide (Sigma; N7256) made up to 100ml with distilled water.

Before samples were loaded onto the stacking gels, 10µg of protein was diluted in 5X loading buffer (2.5ml 1.25M-Tris/HCl, 1.0g SDS, 2.5ml mercaptoethanol (Sigma; M6250), 5.8ml glycerol and 0.1% bromophenol blue (Sigma; B8026) made up to 10ml with distilled water). The samples were then loaded including 5µl of molecular weight protein markers (Sigma; P1677). The gels were run at 250V, 45mA for approximately 1.5 hours. When the bromophenol blue dye front was seen to have reached the end of the gels, electrophoresis was stopped.

2.10.4 Western blotting

1. Following electrophoresis, the acrylamide gels were equilibrated in transfer buffer (25mM Tris, 192mM glycine (Sigma; G7126) pH 8.3 - 8.5 unadjusted) for 20 mins.
2. Protein in gels were transferred onto Hybond ECL nitrocellulose membranes (Amersham; RPN 2020D) by semi-dry electroblotting; Four sheets of Whatman 3mm filter paper were soaked in transfer buffer and placed on the cathode plate of the semi-dry blotting apparatus. Excess air was removed from between the filters by moving a glass pipette over the filter paper. Nitrocellulose, cut to the same size of the gel, was soaked in transfer buffer and placed over the filter paper, making sure there were no air bubbles.The acrylamide gel was placed over the nitrocellulose and four more sheets of presoaked filter paper were placed on top of the gel. Excess air was again removed by rolling the pipette over the filter paper. The proteins were transferred from the gel to the nitrocellulose at a current of 34mA at 15V for 30 mins.

All incubation steps from now on, including the blocking step, were carried out on a revolving apparatus to ensure even exposure of the nitrocellulose blot to all reagents.

3. The nitrocellulose membranes were blocked for 2 hours with fresh filtered 5% milk (Cadburys; Marvel skimmed milk) in TBS (125mM NaCl, 20mM Tris pH 7.5).
4. Membranes were probed overnight with cyclin-E antiserum (HE12) (Santa Cruz Biotechnology Inc; sc-247) diluted 1:1000 or CDK2 antiserum (M2) (Santa Cruz Biotechnology Inc.; sc-163) diluted 1:1000.
5. The primary antibody was removed and the membranes rinsed 3 times with TBS. The membranes were washed for 15 mins, and then twice for 5 mins in TBS.
6. Bound antibody was detected using enhanced chemiluminescence (ECL).

2.10.5 Enhanced chemiluminescence detection

Protein bands were developed using the Enhanced Chemiluminescence Kit (ECL) (Amersham; RPN2109) according to the manufacturers instructions.

1. Membranes were rinsed 3 times with TBS. The membranes were first washed for 15 mins and then washed twice for 5 mins.
2. Secondary antibody (1/1,000 dilution of anti-mouse IgG peroxidase conjugate (Sigma; A-6782) in TBS or a 1/1000 dilution of anti-rabbit IgG (Sigma; A-4914) in TBS) was added for 1hour.
3. The secondary antibody was removed and the membranes rinsed 3 times with TBS. The membranes were washed for 15 mins first, and then twice for 5 mins.
4. A sheet of parafilm was flattened over a smooth surface e.g. a glass plate, making sure all air bubbles were removed. The membrane was then placed on the parafilm, and excess fluid removed.

5. 1.5ml of ECL detection reagent 1 and 1.5ml of reagent 2 were mixed and covered over the membrane. Charges on the parafilm ensured the fluid stayed on the membrane.
6. The reagent was removed after one minute and the membrane wrapped in cling film.
7. The membrane was then exposed to autoradiographic film (Kodak; X-OMAT S) in an autoradiographic cassette for various times, depending on the signal.
9. The autoradiographic film was then developed.

2.10.6 Autoradiograph film processing

1. The exposed film was developed for 5mins in developer (Kodak; LX24), 1;6.5 dilution in water.
2. The film was briefly immersed in water and transferred to a Fixer solution (Kodak; FX-40) a 1:5 dilution in water, for 5mins.
3. The film was transferred to water for 5 mins and then air-dried.

2.11 Immunoprecipitation

Samples for all immunoprecipitation experiments were prepared as for western blotting (Section 2.10.1)

1. 100µg of total protein were centrifuged at 3000rpm at 4°C for 15 minutes.
2. The supernatant was transferred to another Eppendorf with 1µg of normal mouse IgG (Sigma; I-5381) and 20µl of agarose conjugate (Santa Cruz Biotechnology Inc.; sc-2001).
3. This was then centrifuged at 1,500rpm at 4°C for 5 minutes.

4. The supernatant was transferred to another Eppendorf with 10µl of mouse anti-cyclin E (HE(111)) (Santa Cruz Biotechnology Inc.; sc-248) for 1 hour at 4°C.
5. The solution was then incubated overnight at 4°C with 20µl of agarose conjugate.
6. The agarose beads were collected by centrifugation at 2,500rpm for 5 mins at 4°C.
7. The resulting pellet was washed 4 times with RIPA buffer.
8. After the final wash the supernatant was discarded and the pellet was resuspended in 50µl kinase buffer for kinase assays (see protein kinase assay, Section 2.12).

2.12 Protein kinase assay

1. 100μg of protein was immunoprecipitated and resuspended in 50μl kinase buffer (20mM Tris pH 7.5, 10mM $MgCl_2$ and 1mM DTT) see Section 2.11.
2. The agarose beads were collected by centrifugation at 2,500rpm for 5 mins at 4°C.
3. The resulting pellet was washed 2 times with kinase buffer.
4. The pellet was resuspended in 50μl of 100μg/ml histone H1 (Boehringer Mannheim; 223 549), 5μM adenosine-5'-triphosphate (ATP) (Boehringer Mannheim; 127 523) and 0.1μCi/ml [^{32}-P] ATP in kinase buffer for 30 mins at 30°C.
5. The reaction was stopped by adding 5X loading buffer and boiled for 4 mins. 20μl of the reaction mixture was run on a 15% SDS gel for 1 hour at 200mA and 1000V.
6. The gel was placed on three sheets of blotting paper and dried on a gel dryer (GS200, Savent, USA) for 3 hours at 70°C.
7. The sheet of blotting paper with the dried gel was placed in an autoradiographic cassette with autoradiography film and left at -80°C.
8. After 1 - 3 days the film was developed as in Section 2.10.6.
9. The levels of kinase activity was quantified by using a densitometer (Bio-Rad GS-670, imaging densitometer).

2.13 Plasmid DNA Isolation

2.13.1 Preparation of competent cells for transformation

1. 20ml of sterile LB-broth (10μg/ml tryptone (Oxoid; L42), 5μg/ml yeast extract (Oxoid; L21), 10μg/ml NaCl) was inoculated with JM 109 Escherichia coli in a 50ml universal and grown overnight at 37°C in a shaking incubator at 250rpm. 2.4mls of this overnight culture was inoculated in 400ml sterile LB-broth in a sterile 2l baffled flask and placed at 37°C at 250rpm until the absorbance at 590nm was exactly 0.375.
3. This culture was then aliquoted into pre-chilled 50ml universals and left on ice for 5-10 mins.
4. The cells were then centrifuged at 3000rpm at 4°C for 7 mins.
5. The supernatant was removed and the pellet resuspended in 10 mls of ice-cold sterile $CaCl_2$ (60mM $CaCl_2$ (Sigma; C7902), 15% glycerol, 10mM PIPES (Sigma; P9291) pH 7.0).
6. Cells were centrifuged again for 5 mins at 2500rpm at 4°C.
7. The resulting pellet was resuspended in 2mls of ice-cold $CaCl_2$ and left on ice for 12 - 24 hours.
8. The suspension was then aliquoted into -80°C pre-chilled sterile Eppendorfs and stored at -80°C.

2.13.2 Transformation of Escherichia coli

1. 10ng of plasmid DNA to be transformed was placed in a sterile Eppendorf.
2. 100μl of competent cells were taken directly from the freezer, thawed and added to the DNA.
3. The mixture was left on ice for 30 mins.

4. 1ml of LB-broth was added to this suspension, mixed gently by inversion and incubated at 37°C and 250rpm for 1 hour.
5. The cells were then pelleted for 1 - 2 mins at 13,000rpm and resuspended in 200µl LB-broth.
6. 200µl of this culture was spread on LB Agar plates (LB-broth and 25µg/ml agar (Sigma; A5054)) containing 100µg/ml ampicillin (Sigma; A9393) (ampicillin resistance was encoded for on the transformed plasmid).
7. The plates were incubated at 37°C overnight.
8. The resulting colonies were checked for the plasmid using a plasmid Miniprep.

2.13.3 Plasmid Miniprep

1. One colony (from a transformed plate) was removed and added to 10 ml of LB-broth containing ampicillin and incubated overnight at 37°C and 250 rpm.
2. 1.5mls of the overnight culture was placed in a sterile Eppendorf and the cells pelleted at 12,000rpm for 30 secs at 4°C.
3. The supernatant was removed and the pellet resuspended in 300µl STET (8% glucose (Riedel-de Häin; 16325), 5% triton X-100, 50mM Tris-HCl, 50mM EDTA).
4. 25µl of fresh 10mg/ml lysozyme (Sigma; L7001) solution was added to the cell suspension. This was then vortexed and boiled for 45 secs. The suspension was pelleted at 13,000rpm for 15 mins.
5. Approximately 210µl of the supernatant was removed.
6. 230µl of isopropanol (Riedel-de Häin; 33539) was mixed with the pellet and left for 10 mins at 4°C.
7. This was centrifuged at 13,000rpm for 5 mins.
8. The pellet was washed twice with 70% ethanol and then resuspended in 25µl of TE (10mM Tris-HCl, 1mM EDTA, pH 8.0) .

9. 1µl boiled RNase (10mg/ml) was added and left at 37°C for 15mins to remove RNA.

2.14 Transfection procedures

2.14.1 Electroporation

1. Cells were pretreated so that they were in the exponential phase of growth.
2. They were trypsinised at 4°C, spun down and resuspended in half the original volume using ice cold PBS (sterile and without Mg or Ca).
3. A cell count was performed and the cells were centrifuged at 1000rpm for 5mins resuspended at 1 x 10^6 cells/600µl in PBS at 0°C.
4. 600µl of the cell suspension was transferred to 200µl of TE in an electroporation cuvette (Bio-Rad; 165-2088) at 0°C.
5. 10µg of plasmid was added. The plasmid/cell suspension was mixed by holding the cuvette on the two "window sides" and flicking the bottom of the cuvette and then left for 5 minutes.
6. The dried cuvettes were placed in the holder of the electroporation apparatus at room temperature and one pulse delivered at the desired setting;

Cell line	**Settings**
DLKP	600V 25µF ∞Ω
SK-MES-1/Adr	250V 25µF ∞Ω

7. The electroporated cells were returned to ice for 10 minutes and then diluted 20-fold in non-selective medium. The cuvette was rinsed with the same medium to get all the transfected cells.
8. (i) The cells were plated out in 10cm diameter sterile petri dishes at 37°C and 5% CO_2.

or

(ii) The cells were plated out in 96-well plates at a density of 100 cells per well and incubated at 37°C and 5% CO_2.

2.14.2 Calcium phosphate co-precipitation

1. Cells were pretreated so that they were in the exponential phase of growth.
2. Cells were set up at 5 x 10_5 cells per 10cm petri dish and incubated at 37°C and 5% CO_2 overnight.
3. 10µg of pCH110 plasmid was added to 410µl of sterile H_2O and left overnight at 4°C.
4. The following day the plasmid was incubated at 37°C for 1 hour.
5. 60µl of 2M $CaCl_2$ was added dropwise into the plasmid using continuous vortexing.
6. This was immediately added dropwise to 480µl of 2X hepes buffer saline (HBS) (280mM NaCl, 50mM hepes, 1.5mM Na_2HPO_4, pH 7.12) with continuous vortexing and left for 30mins at room temperature.
7. The plasmid-$CaPO_4$ mixture was added dropwise to a petri dish of cells which had been set up the previous day. The plates were gently shaken to ensure even mixing and left for 4 hours at 37°C and 5% CO_2.
8. After 4 hours the media was removed and 5mls of 10% glycerol was added for 3 mins (this is critical).
9. The glycerol was then removed and the cells washed twice with 5mls of serum-free media.
10. 10mls of fresh growth media was then added and the cells incubated at 37°C.

2.15 Assay for ß-Galactosidase activity

This assay was used to optimise the transfection protocol for various cell lines. pCH110, which encodes for ß-galactosidase, was used as a marker plasmid. Its activity was detected as follows;

2.15.1 Preparation of cell extract

1. 24 hours after cells were transfected, they were rinsed twice with 10mls PBS.
2. 1ml of TEN (40mM Tris, 1mM EDTA, 150mM NaCl) was added and the cells were harvested using a cell scraper.
3. The harvested cells were centrifuged at 13,000rpm for 5mins.
4. The supernatant was removed with a pipette.
5. The pellet was resuspended in 60µl of 0.25M Tris-HCl pH 7.8. This cell suspension was left at -80°C for 5mins and then at 37°C for 5mins.
6. This freeze/thaw cycle was repeated 3 times.
7. The lysate was centrifuged at 13,000rpm for 5 mins and then the supernatant was transfered to a separate Eppendorf.

2.15.2 Assay

1. 100µl of fresh 15mg/ml chlorophenol red ß-D-galactopyranoside (CPRG) (Boehringer Mannheim; 884 308) was added to 400µl of buffer A (100mM NaH_2PO_4 adjusted to pH 7.2 with NaOH, 10mM KCl, 1mM $MgCl_2$, 10mM ß-mercaptoethanol added just before use) in an Eppendorf.
2. 50µl of cell extract was then added (one tube was left as a control) and left for 2 hours in a water bath at 37°C.
3. If there was no difference in colour between the control and the samples with the extract then the samples were incubated overnight (8 - 16 hours) at 37°C.

4. After a colour change the samples were diluted with 1.1mls (2 volumes) of buffer A without ß-mercaptoethanol.
5. The absorbance was read at 574nm using the control sample as a blank. The higher the absorbance value, the higher the ß-galactosidase activity. The activity of ß-galactosidase correlates to the efficiency of transfection of pCH110 into the cells.

2.16 Selection of Transfectants

Cells transfected with pHaMDR1/A (a kind gift from M. Gottesman, National Institutes of Health, Bethesda) were allowed to grow for 3 days in nonselective media and selected with 50µg/ml Adriamycin. MDR1 ribozyme (received as a gift from Dr.Kevin Scanlon, City of Hope Medical Centre, Los Angeles) transfected cells were allowed to grow for 24 hours in nonselective medium and selected with 400µg/ml geneticin (Sigma, G418). Untransfected cells were treated in the same way as a control.

2.16.1 Isolation of clonal transfectants

1. 5 days after transfection, each well was examined microscopically and those wells identified as containing a single colony were marked. The remaining wells contained no cells, had more than one colony or contained cells lying close to each other but it was not clear if they were clones or not. All such wells were disregarded.
2. The marked wells were fed every 6 - 7 days until they became confluent.
3. The cells were then removed from their wells by trypsinisation. This involved removing the waste medium from each well and adding 50µl trypsin.
4. The plates were then incubated at 37°C for approximately 5 min. After this time, cells which had not completely detached from the well surface were resuspended with a micropipette.

5. Each clonal population was then transferred to an individual well in a 24-well plate (Greiner; 662160) without centrifugation. Each well contained 1ml of growth medium which was sufficient to inactivate the trypsin.
6. When these wells were confluent (after 6 - 7 days), the clones were transferred into 6-well plates (Costar; 3516) in a similar manner to that of the previous transfer.
7. When these wells became confluent, the cells were transferred to 25cm^2 flasks and then to 75cm^2 flasks.
8. Frozen stocks were then prepared (Section 2.5.3).

2.17 RNA Extraction

The labile nature of RNA required that strict procedures were followed in the course of work involving RNA. This procedures included the wearing of gloves at all times that RNA-containing vessels were being used, the baking of all glassware and foil used to make up solutions and weigh compounds and most solutions and plastics were treated with 0.1% diethyl pyrocarbonate (DEPC) which is a strong inhibitor of RNases.

RNA was then extracted from cells as follows:-

1. Cells were grown in 175cm^2 flasks to approximately 80% confluency.
2. Waste medium was removed and the cells washed twice with DEPC-PBS
3. The cells were lysed in 25ml of 4M-guanidinium thiocyanate (GnSCn) solution (50g guanidinium thiocyanate (Sigma; G6639), 0.5g N-lauroyl sarcosine (Sigma; L5125) and 5ml of 1M-sodium citrate (RDH; 32320), pH 7.0 - brought up to 100ml with DEPC-water, filtered through a 0.45µm filter and supplemented with 700µl/ml β-mercaptoethanol and 330µl/100ml antifoam A (Sigma; A5758) prior to use).
4. 5.5ml of a 5.7M-cesium chloride solution (95.8g CsCl (Sigma; C3032) and 2.5ml of 1M-sodium citrate, pH 7.0 in 100ml water, filtered through a 0.22µm filter, treated with 0.1% DEPC and autoclaved) was placed into polyallomer

ultracentrifuge tubes and the cell lysates were then layered onto these CsCl cushions.

5. The lysates were centrifuged at 26,000 r.p.m. for 21 - 24 hours at 15°C in a swinging bucket centrifuge.
6. The tubes were then brought into a laminar flow cabinet and the supernatant removed from the tubes using a pasteur pipette, leaving approximately 1ml of CsCl in the bottom of the tube, below which lay the RNA pellet.
7. The tube was inverted and the bottom of the tube was cut away using a heated scalpel blade.
8. The pellet was rinsed with 95% ethanol and resuspended in 200µl DEPC-water. The solution was transferred to an Eppendorf and the bottom of the tube was rinsed with a further 200µl water which was added to the Eppendorf.
9. 40µl of 3M-sodium acetate was added to the RNA solution to give a final concentration of 0.3M-sodium acetate, and 2 volumes of ice-cold absolute ethanol were also added.
10. The Eppendorfs were stored at -80°C overnight and the RNA was then pelleted at 4°C at maximum speed in a microfuge.
11. The resulting pellet was washed with 70% ethanol, the supernatant removed and the pellet resuspended in 20µl DEPC-water.

RNA concentration was calculated by determining its OD at 260nm and using the following formula:-

$$OD_{260nm} \times \text{Dilution factor} \times 40 = \mu g/\mu l \text{ RNA}$$

The purity of the RNA extraction was calculated by determining its OD at 260nm and 280nm. An $A_{260} : A_{280}$ ratio of 2 is indicative of pure RNA and only those samples with ratios between 1.8 and 2.1 were used.

2.18 Reverse transcriptase reaction

Reverse transcriptase (RT) reactions were carried out in laminar flow cabinets using micropipettes which were specifically allocated to this work.

cDNA was formed using the following procedure:-

1µl oligo $(dT)^{12-18}$ primers (1µg/µl) (Promega; C1101)

1µl total RNA (1µg/µl)

3µl water

were mixed in an Eppendorf, heated to 70°C for 10 min and then chilled on ice. To this, the following were added:-

4µl of a 5x buffer (250mM-Tris/HCl pH 8.3, 375mM-KCl and 15mM-$MgCl_2$)

2µl DTT (100mM) (Gibco; 510-8025 SA)

1µl RNasin (40U/µl) (Promega; N2511)

1µl dNTPs (10mM of each dNTP)

6µl water

1µl Moloney murine leukemia virus-reverse transcriptase (MMLV-RT) (40,000U/µl) (Gibco; 510-8025 SA).

The solutions were mixed and the RT reaction was carried out by incubating the Eppendorfs at 37°C for 1 hour. The MMLV-RT enzyme was then inactivated by heating to 95°C for 2 min. The cDNA was stored at -20°C until required for use in PCR reactions as outlined in Section 2.18.

2.19 Polymerase chain reaction

A standardised polymerase chain reaction (PCR) procedure was followed in this study. The Eppendorf tubes used (Eppendorf; 0030 121 023) and the sterile water were DEPC-treated. All reagents had been aliquoted and were stored at -20°C and all reactions were carried out in a laminar flow cabinet.

Each PCR tube contained the following:-

24.5µl water

5µl 10x buffer* (100mM-Tris/HCl, pH 9.0, 50mM-KCl, 1% Triton X-100)

3µl 25mM-$MgCl_2$*

8µl dNTPs (1.25mM each of dATP, dCTP, dGTP and gTTP) (Promega; U1240)

1µl each of first and second strand target primers (250ng/µl)

1µl each of first and second strand endogenous control primer (250ng/µl)

0.5µl of 5U/µl *Taq* DNA polymerase enzyme*

5µl DNA or cDNA

*(Promega; N1862)

A drop of autoclaved mineral oil was placed in each reaction tube to prevent evaporation and the DNA was amplified by PCR (Techne; PHC-3) as follows:-

95°C for 1.5 min - to denature double-stranded DNA

30 cycles: 95°C for 1.5 min. - denature

55°C for 1 min - anneal

72°C for 3 min. - extend

72°C for 7 min. - extend

The reaction tubes were then stored at 4°C until analysed by gel electrophoresis as described in Section 2.19.

2.20 Electrophoresis of PCR products

1. A 3% agarose gel (NuSieve;GTG) was prepared in TBE buffer (5.4g Tris, 2.75g boric acid, 2ml 0.5M-EDTA pH 8.0 in 500ml water) and melted in a microwave oven.
2. After allowing to cool, 0.003% of a 10mg/ml ethidium bromide solution was added to the gel which was then poured into an electrophoresis apparatus

(BioRad). Combs were placed in the gel to form wells and the gel was allowed to set.

3. 10μl loading buffer (50% glycerol, 1mg/ml xylene cyanol, 1mg/ml bromophenol blue, 1mM EDTA) was added to each 50μl PCR sample and 10 - 20μl was run on the gel at 80mV for approximately 1 hour.
4. When the dye front was seen to have migrated the required distance, the gel was removed from the apparatus and examined on a transilluminator.

3.0 RESULT

3.1 Chemotherapeutic drug combinations

The use of multiple drugs in combination is standard in treating a patient with cancer. Clinical studies have shown that drug combinations generally produce higher response rates in treated populations than those produced by single agents alone. However, it is possible that some drug combinations may be antagonistic. This series of experiments investigated the use of common chemotherapeutic drugs in combination at three different ratios. Assays were performed as described in Section 2.7 and the combination index (CI) values were calculated as described in Section 2.7.6. These values indicate if a drug combination in synergistic, additive or antagonistic.

Three different ratios of adriamycin and carboplatin were used in combination in DLKP (Table 3.1.1). The results show that the ratios of adriamycin to carboplatin at 1:10 and 1:100 were antagonistic with the lowest CI value being 3. The ratio of adriamycin to carboplatin at 1:40 displayed some additive effects and a synergistic effect at high concentrations of the combination.

Combinations of adriamycin and carboplatin were assayed in DLKP-A (Table 3.1.2). The combination of adriamycin and carboplatin in a 1:40 ratio was additive although some concentrations did show synergy. The combination at ratios of 1:10 and 1:100 were antagonistic.

A combination of vincristine and carboplatin at ratios of 1:10, 1:40 and 1:100 were assayed in DLKP-A (Table 3.1.3). The combination at a ratio of 1:10 and 1:100 were antagonistic. The combination at a 1:40 ratio did show slight synergy at 5 and 7.5 μg/ml and an additive effects at higher concentrations.

A combination of adriamycin and vincristine at a ratios of 1:4 was assayed in DLKP (Table 3.1.4). Vincristine and adriamycin were antagonistic initially but then showed some

synergism at higher concentrations. Vincristine and adriamycin were assayed at ratios of 1:1, 4:1 and 1:4 in DLKP-A (Table 3.1.5). At each combination the CI values were antagonistic at lower concentrations but then showed some synergy at higher concentrations.

Vincristine and VP-16 were assayed at 1:1, 1:5 and 5:1 combination in DLKP (Table 3.1.6). The combinations were antagonistic initially but were synergistic at higher concentrations of the combinations. However, the percentage growth at the higher concentrations was very low (< 10%).

At ratios of 1:1, 1:5 and 5:1, vincristine and VP-16 were assayed in combination in DLKP-A (Table 3.1.7). This combination in DLKP-A did show synergy in each combination at all concentrations used.

The above results demonstrated that a combination of carboplatin and adriamycin/vincristine was additive in DLKP-A. The combinations of adriamycin plus vincristine were antagonistic in DLKP and DLKP-A. Vincristine plus VP-16 were antagonistic in DLKP but did show synergism in DLKP-A.

Table 3.1.1: Combination Index (CI) values for carboplatin and adriamycin at different ratios in combination in DLKP. Survival was calculated as percentage growth relative to that measured in a drug-free control and is the mean of eight replicates. The values also include the standard deviations. The Combination Index (CI) was calculated as outlined as in Section 2.7.6. CI value <1 represents synergistic toxicity, CI value $=1$ represents additive toxicity and CI value >1 antagonistic toxicity.

Combination 1 (adriamycin 1: carboplatin 10).

Concentration (ng/ml)	% Growth	CI values
Control	100±6	-
2.5	100±7	13
5	98±10	3
10	100±4	5
15	95±9	4.5
20	95±9	6
50	91±9	9
100	64±8	3

Combination 2 (adriamycin 1 : carboplatin 40)

Concentration (ng/ml)	% Growth	CI value
Control	100±10	-
0.05	102±7	>100
0.1	75±13	1.5
0.25	69±15	3
0.5	37±8	1.6
0.75	20±3	1
1	13±2	.81
2.5	7±2	1.13
5	7±1	2.7

Combination 3 (adriamycin 1: carboplatin 100).

Concentration (ng/ml)	% Growth	CI values
Control	100±4	-
0.05	100±8	-
0.1	104±12	>100
0.25	93±7	14
0.5	89±4	21
0.75	80±4	13.8
1	73±3	12
2.5	34±2	4.8
5	18±1	4.5

Table 3.1.2: Combination Index (CI) values for carboplatin and adriamycin in at different ratios in DLKP-A. Survival was calculated as percentage growth relative to that measured in a drug-free control and is the mean of eight replicates. The values also include the standard deviations. The Combination Index (CI) was calculated as outlined as in Section 2.7.6. CI value <1 represents synergistic toxicity, CI value $=1$ represents additive toxicity and CI value >1 antagonistic toxicity.

Combination 1 (adriamycin 1: carboplatin 10)

Concentration (μg/ml)	% Growth	CI values
Control	100±5	-
0.5	103±6	>100
0.75	103±8	>100
1	97±4	4.3
2.5	96±8	9
5	59±8	1.5
7.5	40±8	1.2
10	34±7	1.3

Combination 2 (adriamycin 1: carboplatin 40).

Concentration (μg/ml)	% Growth	CI values
Control	100±7	-
0.75	102±3	>100
1	99±8	16
2.5	90±6	3.5
5	47±6	0.92
7.5	36±3	0.94
10	30±3	1.01
15	30±4	1.56

Combination 3 (adriamycin 1: carboplatin 100).

Concentration (μg/ml)	% Growth	CI values
Control	100±11	-
0.5	99±4	5
0.75	104±6	>100
1	100±10	77
2.5	98±5	16
5	66±3	1.78
7.5	48±3	1.42
10	41±2	1.47
15	40±3	2.8

Table 3.1.3: Combination Index (CI) values for Carboplatin and Vincristine in DLKP-A. Survival was calculated as percentage growth relative to that measured in a drug-free control and is the mean of eight replicates. The values also include the standard deviations. The Combination Index (CI) was calculated as outlined as in Section 2.7.6. CI value < 1 represents synergistic toxicity, CI value $= 1$ represents additive toxicity and CI value > 1 antagonistic toxicity.

Combination 1 (vincristine 1: carboplatin 10)

Concentration (μg/ml)	% Growth	CI values
Control	100 ±7	-
0.5	85±7	88
0.75	89±7	-
1	86±3	10
2.5	66±8	26
5	44±4	4.7
7.5	25±5	4
10	17±4	4.6

Combination 2 (vincristine 1: carboplatin 40)

Concentration (μg/ml)	% Growth	CI values
Control	100±7	-
0.75	102±3	>100
1	99±8	16
2.5	90±6	3.5
5	47±6	0.92
7.5	36±3	0.94
10	30±3	1.01
15	30±4	1.56

Combination 3 (vincristine 1: carboplatin 100)

Concentration (μg/ml)	% Growth	CI values
Control	100±11	-
0.75	102±7	-
1	106±12	>100
2.5	88±9	5.6
5	56±8	3
7.5	37±7	2.5
10	26±4	2.3
15	17±2	2.2

Table 3.1.4: Combination Index (CI) values for adriamycin and vincristine at a ratio of 1:4 in DLKP. Survival was calculated as percentage growth relative to that measured in a drug-free control and is the mean of eight replicates. The values also include the standard deviations. The Combination Index (CI) was calculated as outlined as in Section 2.7.6. CI value < 1 represents synergistic toxicity, CI value $= 1$ represents additive toxicity and CI value > 1 antagonistic toxicity.

Concentration (n/ml)	% Growth	CI values
Control	100± 5	-
10	94±5	2.79
20	57±4	1.31
40	13±1	0.75
80	5	0.53
150	3	0.76
300	3	1.08

Table 3.1.5: Combination Index (CI) values for adriamycin and vincristine in DLKP-A. Survival was calculated as percentage growth relative to that measured in a drug-free control and is the mean of eight replicates. The values also include the standard deviations. The Combination Index (CI) was calculated as outlined as in Section 2.7.6. CI value <1 represents synergistic toxicity, CI value $=1$ represents additive toxicity and CI value >1 antagonistic toxicity.

Combination 1 (1 adriamycin : vincristine 1).

Concentration (μg/ml)	% Growth	CI values
Control	100±10	-
0.312	88±10	2.58
.625	56±8	1.28
1.25	30±4	1.06
2.5	9±2	0.67
5	7±1	1.14
7.5	7±1	1.59

Combination 2 (4 adriamycin : 1 Vincristine).

Concentration (μg/ml)	% Growth	CI values
Control	100±5	-
0.312	80±6	1.5
0.625	66±7	1.6
1.25	40±6	1.22
2.5	21±4	1.08
5	7±2	0.69
7.5	6±1	0.99

Combination 3 (1 adriamycin : 4 vincristine).

Concentration (μg/ml)	% Growth	CI values
Control	100±6	-
0.312	88±10	2.79
0.625	52±5	1.31
1.25	17±3	0.75
2.5	5±1	0.53
5	3±1	0.76
7.5	3±1	1.08

Table 3.1.7: Combination Index (CI) values for vincristine and VP-16 in DLKP-A. Survival was calculated as percentage growth relative to that measured in a drug-free control and is the mean of eight replicates. The values also include the standard deviations. The Combination Index (CI) was calculated as outlined as in Section 2.7.6. CI value <1 represents synergistic toxicity, CI value $=1$ represents additive toxicity and CI value >1 antagonistic toxicity.

Combination 1 (vincristine 1: VP-16 1)

Concentration (mg/ml)	% Growth	CI values
Control	100±8	-
0.05	97±8	0.2
0.125	97±4	0.48
0.25	95±8	0.79
0.5	68±11	0.535
1.25	8±2	0.31
2.5	6±1	0.55
3.75	8±2	0.95
5	9±2	1.3

Combination 2 (vincristine 1: VP-16 5)

Concentration (μg/ml)	% Growth	CI values
Control	100±9	-
0.05	94±7	-
0.125	95±9	0.22
0.25	95±14	0.45
0.5	92±9	0.72
1.25	19±4	0.48
2.5	7±1	0.56
3.75	7±1	0.88
5	7±1	1.13

Combination 3 (vincristine 5 : VP-16 1)

Concentration (μg/ml)	% Growth	CI values
Control	100±6	-
0.05	95±9	-
0.125	96±6	0.63
0.25	91±8	0.82
0.5	25±10	0.26
1.25	13±2	0.41
2.5	6±1	0.53
3.75	7±1	0.91
5	7±1	1.2

Table 3.1.6: Combination Index (CI) values for vincristine and VP-16 in DLKP. Survival was calculated as percentage growth relative to that measured in a drug-free control and is the mean of eight replicates. The values also include the standard deviations. The Combination Index (CI) was calculated as outlined as in Section 2.7.6. CI value <1 represents synergistic toxicity, CI value $=1$ represents additive toxicity and CI value >1 antagonistic toxicity.

Combination 1 (vincristine 1: VP-16 1)

Concentration (ng/ml)	% Growth	CI values
Control	100±4	-
0.5	56±7	8.38
1.25	12±1	0.53
2.5	5	0.21
5	4	0.32
12.5	3	0.41
25	2	0.38
37.5	2	0.41
50	2	0.60

Combination 2 (vincristine 1 : VP-16 5)

Concentration (ng/ml)	% Growth	CI values
Control	100±6	-
0.5	83±6	26.7
1.25	80±5	44.8
2.5	55±5	12.6
5	15±2	1.08
12.5	5	0.32
25	3	0.35
37.5	3	0.36
50	3	0.47

Combination 3 (vincristine 5: VP-16 1).

Concentration (ng/ml)	% Growth	CI values
Control	100±4	-
0.5	81±5	99
1.25	29±3	4.98
2.5	9±1	0.97
5	5	0.68
12.5	3	0.68
25	2	0.92
37.5	2	0.82
50	2	1.21

3.2 MDR circumvention

A number of compounds have been identified which inhibit the efflux of chemotherapeutic drugs by P-glycoprotein and reverse cellular resistance in experimental systems including verapamil, a calcium antagonist.

However, there are a number of non-chemotherapeutic drugs which enhance chemotherapeutic cytotoxicity by mechanisms other than the reversal of drug resistance. One of these drugs, buthionine sulfoximine (BSO), reduces cellular glutathione levels, by irreversibly inhibiting γ-glutamylcysteine synthetase, the first enzyme involved in *de novo* glutathione synthesis. Glutathione helps to protect cells both by reacting with cytotoxic drug derivatives and by reacting with drug generated reactive oxygen compounds.

This series of experiments was performed to investigate the efficacy of BSO plus a P-glycoprotein inhibitor (verapamil) in combination with adriamycin in DLKP and DLKP-A cell lines. DLKP is a human lung carcinoma cell line which is sensitive to chemotherapeutic drugs and DLKP-A is a MDR derivative of DLKP which overexpresses P-glycoprotein. Each experiment was performed twice as described in Section 2.7.3 and the combination Index (CI) value calculated as outlined in Section 2.7.6.

The cytotoxicity of BSO in combination with adriamycin in DLKP is given in Table 3.2.1 and the Combination Index (CI) values are given in Table 3.2.2. These results show that at higher concentrations of BSO, the CI value was approximately 1. This implies that there was an additive cytotoxic effect. A synergistic cytotoxic effect (i.e. CI value < 1) was observed at 10ng/ml adriamycin when 1μg/ml of BSO was used.

The cytotoxicity of BSO in combination with adriamycin in DLKP-A is given in Table 3.2.3 and the Combination Index (CI) values are given in Table 3.2.4. These results show that at the lowest concentration of BSO (1μg/ml), the CI values were less than 1. Thus

there was a synergistic toxic effect with all the concentrations adriamycin used. At higher concentrations of BSO, the CI values were in general antagonistic.

Verapamil in combination with adriamycin showed little enhanced cytotoxic effect in DLKP (Table 3.2.5), at the lower concentrations of BSO (0.125μg/ml and 0.25μg/ml), there was synergism in toxicity (Table 3.2.6). However, BSO plus verapamil in combination with adriamycin did not significantly enhance the toxicity of adriamycin alone compared to BSO alone with adriamycin (Table 3.2.7).

Verapamil did show enhanced cytotoxicity in combination with adriamycin in DLKP-A (Table 3.2.8). However, BSO did not significantly affect adriamycin toxicity (Table 3.2.9). The combination of BSO plus verapamil in combination was synergistic with adriamycin (Table 3.2.10), however it is not clear if this effect is to verapamil alone or the combination of BSO and verapamil. A more detailed experiment using a number of combinations of BSO and verapamil with adriamycin was then performed in DLKP-A (Table 3.2.11). This showed that the combination of BSO plus verapamil with adriamycin did seem to be synergistic. For example, when one concentration of verapamil was used and the concentration of BSO was increased then the toxicity of adriamycin was enhanced. Conversely, when one concentration of BSO was used and the concentration of verapamil was increased then the toxicity of adriamycin was also enhanced

Table 3.2.1: Effect of BSO on adriamycin toxicity to DLKP. Survival was calculated as percentage growth relative to that measured in a drug-free control and is the mean of eight replicates. The values also include the standard deviations.

	Adriamycin				
	Control	**5ng/ml**	**10ng/ml**	**15ng/ml**	**20ng/ml**
BSO 0μg/ml	100	57±5	29±3	24±4	15±2
BSO 0.25μg/ml		44±7	20±3	16±3	14±2
BSO 0.5μg/ml	77±8	44±5	20±2	17±1	14±1
BSO 1μg/ml		26±4	15±2	14±2	12±2

Table 3.2.2: Effect of BSO on adriamycin toxicity to DLKP. The Combination Index (CI) was calculated as outlined in Section 2.7.6. CI value <1 represents synergistic toxicity, CI value »1 represents additive toxicity and CI value >1 antagonistic toxicity.

	Adriamycin			
	5ng/ml	**10ng/ml**	**15ng/ml**	**20ng/ml**
BSO 1μg/ml	1.09	0.789	0.928	1.06
BSO 2.5μg/ml	1.49	0.971	1.14	1.26
BSO 5μg/ml	1.16	1.02	1.23	1.33

Table 3.2.3: Effect of BSO on adriamycin toxicity to DLKP-A. Survival was calculated as percentage growth relative to that measured in a drug-free control and is the mean of eight replicates. The values also include the standard.

	Adriamycin				
	0μg/ml	**0.5μg/ml**	**1μg/ml**	**2μg/ml**	**3μg/ml**
BSO 0μg/ml	100±7	71±11	48±15	18±4	12±3
BSO 1μg/ml	-	45±10	29±8	11±3	6±1
BSO 2.5μg/ml	56±13	82±6	55±5	26±3	15±2
BSO 5μg/ml	34±13	66±9	39±6	16±4	8±1

Table 3.2.4: Effect of BSO on adriamycin toxicity to DLKP-A. The Combination Index (CI) was calculated as outlined as in Section 2.7.6. CI value <1 represents synergistic toxicity, CI value »1 represents additive toxicity and CI value >1 antagonistic toxicity.

	Adriamycin			
	0.5μg/ml	**1μg/ml**	**2μg/ml**	**3μg/ml**
BSO 1μg/ml	0.975	0.868	0.691	0.688
BSO 2.5μg/ml	16	4	1.76	1.5
BSO 5μg/ml	8.8	3	1.3	0.95

Table 3.2.5: Effect of verapamil (Ver) on 15ng/ml adriamycin toxicity to DLKP. Survival was calculated as percentage growth relative to that measured in a drug-free control and is the mean of eight replicates. The values also include the standard deviations.

	Control	Adriamycin
Ver 0μg/ml	100±4	36±3
Ver 0.125μg/ml	104±5	34±2
Ver 0.25μg/ml	100±6	27±2
Ver 0.5μg/ml	114±8	28±3

Table 3.2.6: Effect of BSO on 15ng/ml adriamycin toxicity to DLKP. Survival was calculated as percentage growth relative to that measured in a drug-free control and is the mean of eight replicates. The values also include the standard deviations.

	Control	Adriamycin
BSO 0μg/ml	100±6	30±3
BSO 0.125μg/ml	97±5	12±1
BSO 0.25μg/ml	98±5	18±2
BSO 0.5μg/ml	100±5	20±5

Table 3.2.7: Effect of BSO plus verapamil (Ver) on 15ng/ml adriamycin toxicity to DLKP. Survival was calculated as percentage growth relative to that measured in a drug-free control and is the mean of eight replicates. The values also include the standard deviations.

	Control	Adr1	Adr2
0	100±2	30±2	7±1
Ver1 + BSO1	90±5	20±1	8±1
0	100	36±9	7±1
Ver2 + BSO2	94±24	13±2	7±1

Where:

Ver1 = 0.5μg/ml BSO1 = 0.5μg/ml Adr1 = 15ng/ml

Ver2 = 0.25μg/ml BSO2 = 0.25μg/ml Adr2 = 30ng/ml

Table 3.2.8: Effect of verapamil (Ver) on 2.5μg/ml adriamycin toxicity to DLKP-A. Survival was calculated as percentage growth relative to that measured in a drug-free control and is the mean of eight replicates. The values also include the standard deviations.

	Control	Adriamycin
Ver 0μg/ml	100±5	75±6
Ver 0.125μg/ml	100±8	26±2
Ver 0.25μg/ml	98±6	44±4
Ver 0.5μg/ml	101±7	62±4

Table 3.2.9: Effect of BSO on 2.5μg/ml adriamycin toxicity to DLKP-A. Survival was calculated as percentage growth relative to that measured in a drug-free control and is the mean of eight replicates. The values also include the standard deviations.

	Control	Adriamycin
BSO 0μg/ml	100±6	69±5
BSO 0.125μg/ml	100±6	63±4
BSO 0.25μg/ml	96±5	59±6
BSO 0.5μg/ml	97±5	56±5

Table 3.2.10: Effect of BSO plus verapamil (Ver) on adriamycin toxicity to DLKP-A. Survival was calculated as percentage growth relative to that measured in a drug-free control and is the mean of eight replicates. The values also include the standard deviations.

	Control	Adr1	Adr2
0	100±5	67±5	32±4
Ver1 + BSO1	99±5	20±1	8±1
0	100±10	56±5	21±4
Ver2 + BSO2	91±8	26±4	12±2

Where:

Ver1 = 0.5μg/ml BSO1 = 0.5μg/ml Adr1 = 2.5μg/ml

Ver2 = 0.25μg/ml BSO2 = 0.25μg/ml Adr2 = 5μg/ml

Table 3.2.11: Effect of BSO plus verapamil (Ver) on adriamycin toxicity to DLKP-A. Survival was calculated as percentage growth relative to that measured in a drug-free control and is the mean of eight replicates. The values also include the standard deviations.

	Control	Adr1	Adr2	Adr3
0	100±20	84±3	51±5	22±3
BSO1 + Ver1	100±7	80±6	42±5	14±2
0	100±14	88±20	59±5	27±3
BSO1 + Ver2	101±23	75±6	37±5	17±1
0	100±12	90±6	58±4	28±3
BSO1 + Ver3	99±12	63±6	31±3	17±1
0	100±7	90±5	51±4	21±2
BSO2 + Ver1	98±8	73±6	40±3	15±1
0	100±8	88±5	56±2	27±3
BSO2 + Ver2	95±7	75±6	44±2	21±1
0	100±4	90±6	52±6	26±4
BSO2 + Ver3	98±8	44±7	22±5	14±2
0	100±9	86±6	52±5	23±4
BSO3 + Ver1	101±9	75±6	43±4	16±2
0	100±5	80±4	46±3	20±3
BSO3 + Ver2	96±11	66±6	36±12	14±2
0	100±8	90±7	58±5	28±4
BSO3 + Ver3	99±7	63±6	31±4	17±3

Where:
Ver1 = 0.125μg/ml
Ver2 = 0.25μg/ml
Ver3 = 0.5μg/ml

BSO1 = 0.125μg/ml
BSO2 = 0.25μg/ml
BSO3 = 0.5μg/ml

Adr1 = 1.25μg/ml
Adr2 = 2.5μg/ml
Adr3 = 5μg/ml

3.3 MDR1 ribozyme transfection

Currently the best understood mechanism of MDR is the resistance mediated by the MDR1 gene product, P-glycoprotein (P-170) (see Section 1.9 and 1.10).

Attempts at chemomodulation of P-glycoprotein have been investigated using various P-glycoprotein antagonists. The results of circumvention compounds in clinical trials have been disappointing due to the non-specific effects (calcium antagonists) or toxic effects (cyclosporin A) of the circumvention agent. Therefore a more specific modulation of MDR is necessary for an improved reduction in drug resistance. At present, one alternative is to use antisense techniques to interfere with P-glycoprotein expression.

To test the efficacy of antisense *in vitro*, an anti-MDR1 hammerhead ribozyme was transfected into the adriamycin resistant human lung carcinoma cell line SK-MES-1/Adr. SK-MES-1/Adr is a derivative of the chemotherapeutic drug sensitive cell line SK-MES-1 (see Table 2.5.1), which was exposed to increasing concentrations of adriamycin. Its mechanism of drug resistance is primarily thought to be due to P-glycoprotein overexpression.

Before transfection of SK-MES-1/Adr with the MDR1 ribozyme, SK-MES-1/Adr was electroporated with the pCH110 ß-galactosidase reporter plasmid at various voltages in order to optimise transfection efficiency (see Section 2.14.4). ß-Galactosidase activity was assayed 24 hours after electroporation (see Section 2.15) and the results are given in Table 3.3.1 These show that increasing the voltage of electroporation beyond 250V decreased electroporation efficiency into SK-MES-1/Adr, as shown by highest OD_{570} value. Thus, the optimum voltage to electroporate SK-MES-1/Adr was determined to be 250V.

Three clones were isolated when SK-MES-1/Adr was electroporated with the anti-MDR1 ribozyme plasmid (see Section 2.14.4). These clones were selected in 96-well plates by continuous exposure to 200μg/ml geneticin in ATCC media (see Section 2.16).

Toxicity assays (see Section 2.7) were performed on each clone to adriamycin, vincristine and VP-16 and compared to SK-MES-1 and SK-MES-1/Adr (Figures 3.3.1 - 3.3.3). These graphs demonstrate that each clone displays a decreased resistance to adriamycin, vincristine and VP-16 compared to the resistant parent cell line, SK-MES-1/Adr. Clone #2 shows the least amount of chemosensitisation for each drug tested compared to clone #3 and clone #4. Clone #3 and clone #4 show a similar profile.

The IC50 values for adriamycin, vincristine and VP-16 of SK-MES-1, SK-MES-1/Adr and each ribozyme clone are given in Table 3.3.2. These values were calculated as described in Section 2.7.5. These values confirm Figures 3.3.1 - 3.3.3 and show that the IC50 values of the ribozyme clones were less than the resistant parent SK-MES-1/Adr.

The levels of resistance towards adriamycin, vincristine and VP-16 of SK-MES-1/Adr and each ribozyme clone was calculated from the IC50 values and are compared in Table 3.3.3. These fold resistance values show that the ribozyme transfectant clones had an approximately 50% decrease in resistance to adriamycin. Their resistance to vincristine and VP-16 varied with clone #2 demonstrating the least amount of chemosensitivity while clone #4 displayed the most.

RT-PCR analysis of RNA isolated from SK-MES-1, SK-MES-1/Adr and each ribozyme clone as described in Section 2.16 - 2.18, was performed (Figure 3.3.4). No MDR1 mRNA expression was detected in SK-MES-1. An increased expression of MDR1 mRNA was detected in SK-MES-1/Adr but the three MDR1 ribozyme transfectants expressed less than the resistant parent. Of the ribozyme transfectants, clone #4 expressed the least amount of MDR1 mRNA while clone #2 expressed the greatest amount MDR1 mRNA.

This experiment demonstrates the use of an anti-MDR1 ribozyme in a MDR cell line. Three clones were selected when SK-MES-1/Adr was transfected with the ribozyme plasmid. These clones were assayed for their resistance to adriamycin, vincristine and VP-16. All the clones displayed increased chemosensitivity to each drug with clone #4 being the most sensitive. RT-PCR analysis demonstrated that MDR1 mRNA expression was

decreased in the clones compared to the resistant parent SK-MES-1/Adr although there was no clone isolated in which MDR1 expression was completely abrogated. No MDR1 mRNA expression was observed in the sensitive parent SK-MES-1.

Table 3.3.1: Effect of various voltages on the electroporation efficiency of pCH110, a ß-galactosidase reporter plasmid, into SK-MES-1/Adr. The O.D. at 570nm represents ß-galactosidase activity (Section 2.14).

Voltage (V)	O.D. @ 570nm
0	0
250	0.031
500	0.002
750	0.007
1000	0.002
1250	0.002

Figure 3.3.1: Adriamycin toxicity profiles of SK-MES-1/Adr and the three MDR1 ribozyme clones. The error bars represent the standard deviation on the mean of eight replicates.

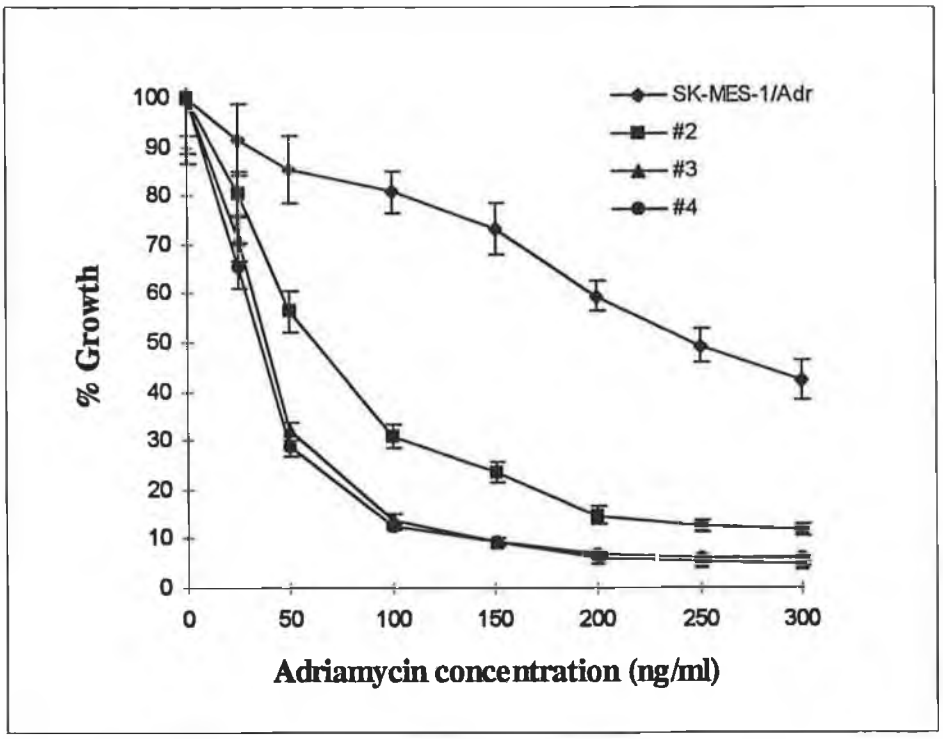

Figure 3.3.2: Vincristine toxicity profiles of SK-MES-1/Adr and the three MDR1 ribozyme clones. The error bars represent the standard deviation on the mean of eight replicates.

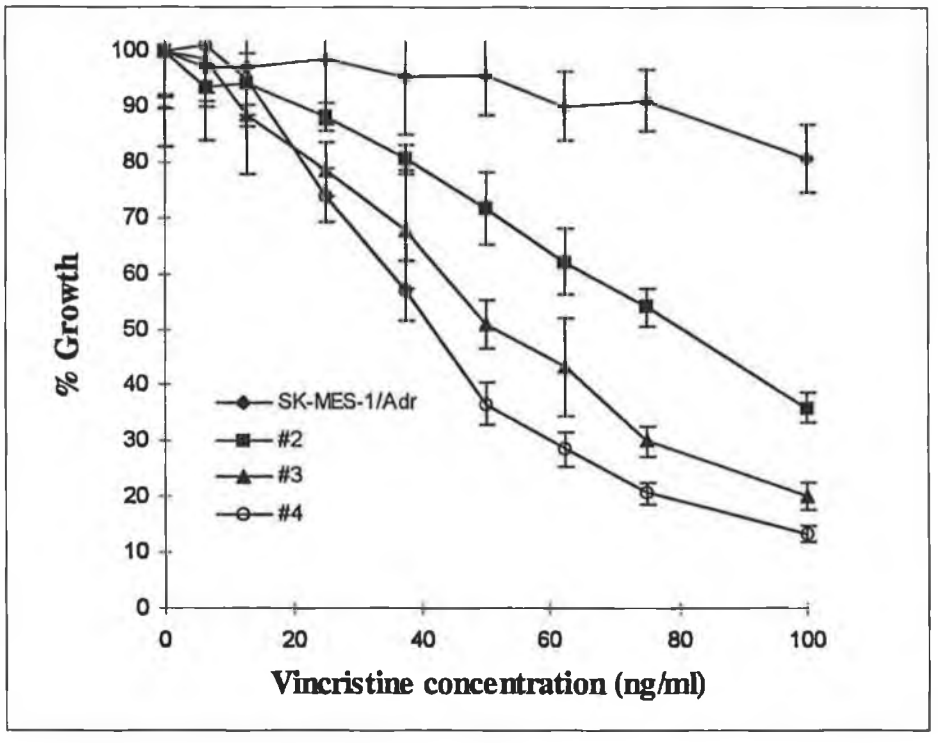

Figure 3.3.3: VP-16 toxicity profile of SK-MES-1/Adr and the three MDR1 ribozyme clones. The error bars represent the standard deviation on the mean of eight replicates.

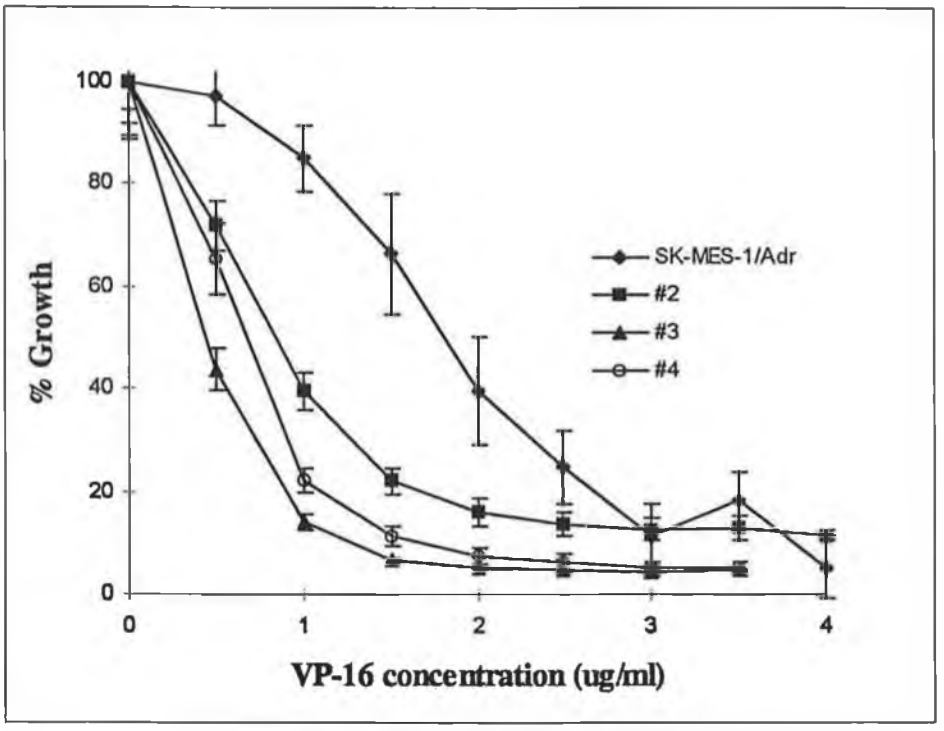

Table 3.3.2: The IC50 values of adriamycin, vincristine and VP-16 in SK-MES-1, SK-MES-1/Adr and three MDR1 ribozyme transfectant clones. IC50 values were calculated as described in Section 2.7.5. The values also include the standard deviations.

	Adriamycin (ng/ml)	Vincristine (ng/ml)	VP-16 (ng/ml)
SK-MES-1	24±16	2±1	333±117
SK-MES-1/Adr	274±109	220±28	2273±631
Clone #2	120±73	130±80	1624±897
Clone #3	108±71	150±91	1284±1054
Clone #4	117±36	91±27	1215±781

Table 3.3.3: Fold increase in resistance towards adriamycin, vincristine and VP-16 of SK-MES-1, SK-MES-1/Adr and three MDR1 ribozyme transfectant clones compared to SK-MES-1. The fold resistance was determined by dividing the average IC50 value for the cell line of interest by the corresponding average IC50 value for SK-MES-1. The values also include the standard deviations.

	Adriamycin	Vincristine	VP-16
SK-MES-1	1±0.7	1±0.5	1±0.4
SK-MES-1/Adr	11.5±4.5	104.5±13.4	6.8±1.9
Clone #2	5±3	61.9±38.2	4.9±2.7
Clone #3	4.5±3	71.3±43.4	3.9±3.3
Clone #4	4.9±1.5	43.3±13	3.7±2.4

Figure 3.3.4: Gel electrophoresis of the products of RT-PCR analysis of the MDR1 mRNA levels in SK-MES-1/Adr and the three MDR1 ribozyme clones. Two lanes were run per sample.

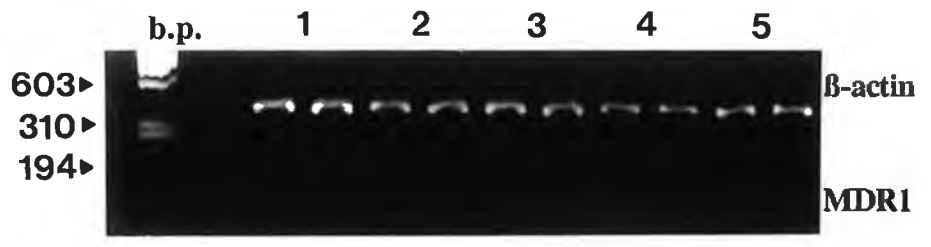

1 SK-MES-1

2 SK-MES-1/Adr MDR1 ribozyme #2

3 SK-MES-1/Adr MDR1 ribozyme #3

4 SK-MES-1/Adr MDR1 ribozyme #4

5 SK-MES-1/Adr

3.4 MDR1 gene transfection

MDR is a multifactorial phenomen with a number of resistance mechanisms co-expressed within a cell (see Section 1.9 and Section 1.10). DLKP-A is a MDR cell line derived from DLKP by sequential exposure to increasing concentrations of adriamycin. Nine clones were isolated from DLKP-A, each with different levels of resistance and a combination of resistance mechanisms (Heenan, 1994). However no clone solely expressed P-glycoprotein. Therefore DLKP was electroporated with the pHaMDR1/A plasmid, which encodes the full cDNA for the human MDR1 gene (Pastan *et al.,* 1988), to develop a low level resistance DLKP clone whose only mechanism of resistance was the expression of P-glycoprotein. These clones could then be investigated to determine their relative resistance profiles to different chemotherapeutic drugs and determine if they correlate with each other. They could also be compared to the resistance profiles to the resistant clones derived from DLKP-A.

Before transfection of DLKP with the MDR1 gene, DLKP was electroporated with the pCH110 ß-galactosidase reporter plasmid at various voltages in order to optimise transfection efficiency (see Section 2.14.4). ß-Galactosidase activity was assayed 24 hours after electroporation (see Section 2.15) and the results are given in Table 3.4.1. These show that increasing the voltage of electroporation up to 800V increased electroporation efficiency into DLKP, as shown by highest OD_{570} value. Thus, the optimum voltage to electroporate DLKP was determined to be 800V. Increasing the voltage further caused increased cell death and a decrease in transfection efficiency (results not shown).

Two clones were isolated when DLKP was transfected with the pHaMDR1/A plasmid (see Section 2.14.4). These clones were selected in 96-well plates by continuous exposure to 50ng/ml adriamycin in ATCC media (see Section 2.16). The adriamycin concentration represents approximately 3 times the IC50 value for DLKP, thus control cells did not survive when exposed to this concentration and clones selected were resistant to adriamycin. The concentration of adriamycin in the selection medium was not increased to a higher concentration because a relatively low resistant clone was preferred.

Toxicity assays (see Section 2.7) were performed on each clone to adriamycin, vincristine and VP-16 (Figures 3.4.1 - 3.4.3). These graphs demonstrate that each clone had an increased resistance to adriamycin, vincristine and VP-16 compared to the sensitive parent cell line, DLKP. Clone #1 demonstrated an increased resistance to adriamycin and vincristine compared to clone #2. In contrast clone #2 showed a greater resistance to VP-16. The IC50 values for adriamycin, vincristine and VP-16 of each clone are given in Table 3.4.2. These values were calculated as outlined in Section 2.7.5. The IC50 values determined for the clones are compared to the IC50 values of DLKP and DLKP-A as calculated by Dr. M. Heenan (Heenan, 1994). The values show that the MDR1 transfectants were more resistant to each chemotherapeutic drug tested compared to DLKP but were not as resistant as DLKP-A. The fold increase in resistance towards adriamycin, vincristine and VP-16 of DLKP-A and the MDR1 transfectants was calculated from the IC50 values (Table 3.4.3). These fold resistance values showed that clone #1 was over 2 fold as resistant as clone #2 to adriamycin and 1.5 fold more resistant to vincristine but that clone #2 was 1.7 fold more resistant to VP-16 than clone #1.

RT-PCR analysis of RNA isolated from DLKP, the two MDR1 transfectants and DLKP-A as described in Section 2.16 - 2.18, was performed (Figure 3.4.44). No MDR1 expression was detected in DLKP. An increased expression of MDR1 mRNA was detected in DLKP-A and the two MDR1 transfectants and the expression of MDR1 in DLKP-A was much greater than the two transfectant clones.

These results show that DLKP was successfully transfected with the MDR1 gene with two transfectant clones isolated. Toxicity assays were performed on each clone to determine their resistance profiles to adriamycin, vincristine and VP-16. These showed that the clones were more resistant to these chemotherapeutic drugs compared to the sensitive parent cell line DLKP. The toxicity data also demonstrated that clone #1 was more resistant to adriamycin and vincristine than clone #2 but that clone #2 was more resistant to VP-16 than clone #1. Thus even though these clones were derived from the same parent cell line and were transfected with the same plasmid, they displayed different resistance

profiles to the chemotherapeutic drugs tested. RT-PCR analysis confirmed increased expression of MDR1 mRNA in each clone.

Table 3.4.1: Effect of various voltages on the electroporation efficiency of pCH110, a ß-galactosidase reporter plasmid, into DLKP. The O.D. at 570nm represents ß-galactosidase activity (Section 2.15).

Voltage (V)	O.D. @ 570nm
0	0
200	0.017
400	0.046
600	0.055
800	0.077

Figure 3.4.1: Adriamycin toxicity profiles of DLKP pHaMDR1/A #1 and #2. The error bars represent the standard deviation on the mean of eight replicates.

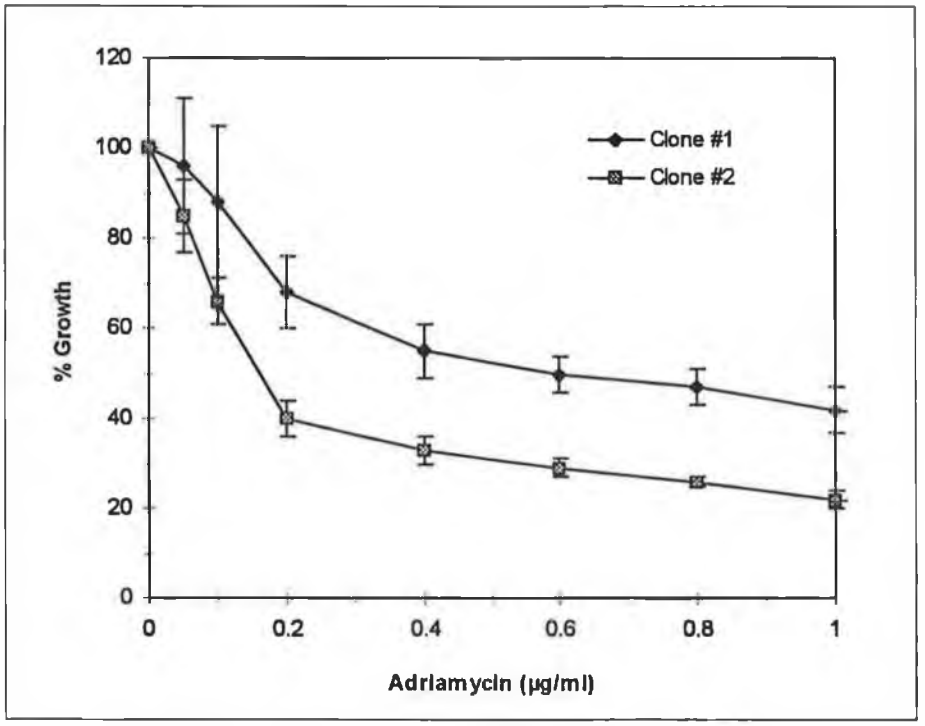

Figure 3.4.2: Vincristine toxicity profiles of DLKP pHaMDR1/A #1 and #2. The error bars represent the standard deviation on the mean of eight replicates.

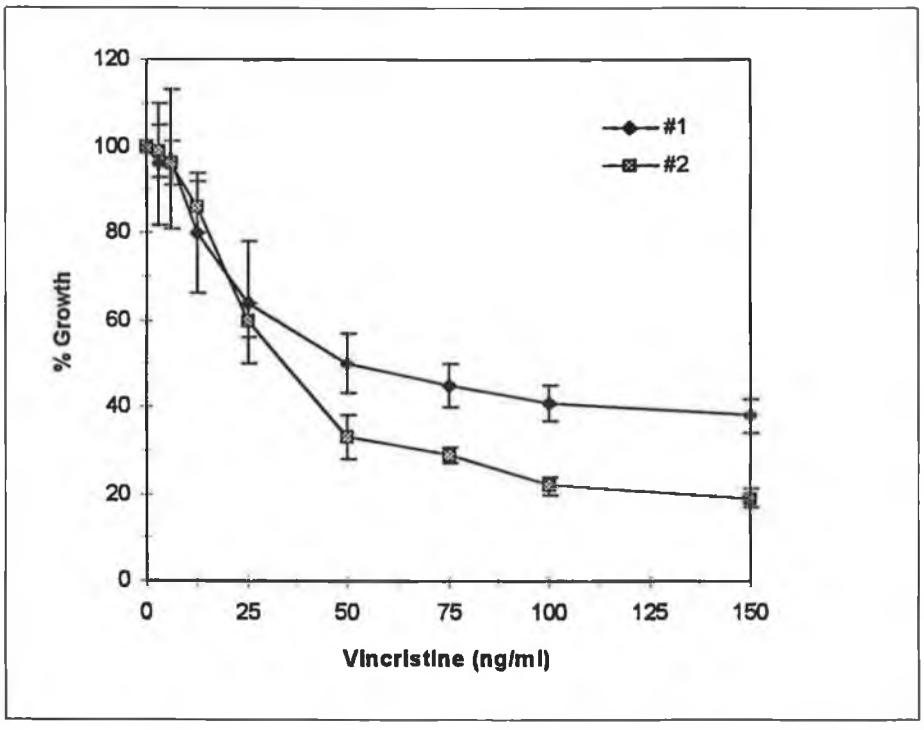

Figure 3.4.3: VP-16 toxicity profile of DLKP pHaMDR1/A #1 and #2. The error bars represent the standard deviation on the mean of eight replicates.

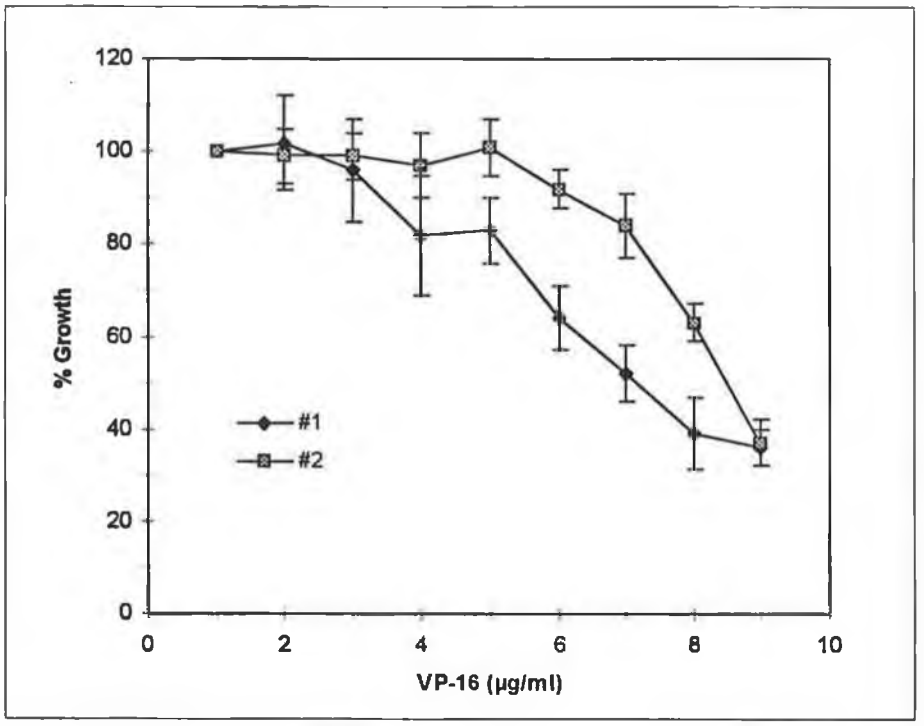

Table 3.4.2: The IC50 values of adriamycin, vincristine and VP-16 in DLKP pHaMDR1/A #1 and #2. IC50 values were calculated as outlined in Section 2.7.5. The IC50 values for DLKP and DLKP-A were calculated by Dr. M. Heenan (Heenan, 1994). The values also include the standard deviations.

	DLKP	**DLKP-A**	**DLKP pHaMDR1/A #1**	**DLKP pHaMDR1/A #2**
Adriamycin	14±8ng/ml	3660±1720ng/ml	520±212ng/ml	215±7ng/ml
Vincristine	1.1±0.3ng/ml	1680±790ng/ml	51±21ng/ml	33±15ng/ml
VP-16	86±40ng/ml	5230±690ng/ml	690±0ng/ml	1170±47ng/ml

Table 3.4.3: Fold increase in resistance towards adriamycin, vincristine and VP-16 of DLKP-A and the MDR1 transfectants. The fold resistance was determined by dividing the average IC50 value for the cell line of interest by the corresponding average IC50 value for DLKP. The IC50 values of DLKP and DLKP-A were calculated by Dr. M. Heenan (Heenan, 1994). The values also include the standard deviations.

	DLKP-A	**DLKP pHaMDR1/A #1**	**DLKP pHaMDR1/A #2**
Adriamycin	254 ± 119	37 ± 14.7	15 ± 0.5
Vincristine	1500 ± 705	45.5 ± 18.8	29.5 ± 13.1
VP-16	61 ± 8	8 ± 0	13.6 ± 0.5

Figure 3.4.4: Gel electrophoresis of the products of RT-PCR analysis of the MDR1 mRNA levels in DLKP, DLKP-A and the two MDR1 transfectant clones. Two lanes were run per sample.

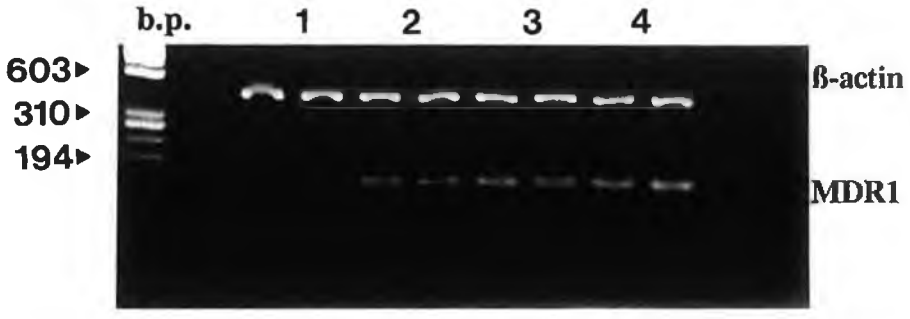

1 DLKP

2 DLKP pHaMDR1/A #1

3 DLKP pHaMDR1/A #2

4 DLKP-A

3.5 Test Compound Screening

There are a number of non-chemotherapeutic drugs which enhance chemotherapeutic cytotoxicity by mechanisms other than the reversal of drug resistance (reviewed in Stewart and Evans, 1989). These include buthionine sulfoximine (BSO) and other glutathione depletors, the nitroimidazoles and the methylxanthines. However none of these are in common clinical use. Thus, the need to test new non-chemotherapeutic drugs which enhances the cytotoxicity of chemotherapeutic drugs is needed more than ever. This series of experiments investigated possible cytotoxic synergy between adriamycin, a commonly used chemotherapeutic drug, and five selected non-chemotherapeutic test compounds. Two concentrations of adriamycin and three non-toxic concentrations of test compound were used in combination. and assays was performed as described in Section 2.7.3.. Seven cell lines were tested; DLKP (Table 3.5.1); DLKP pHaMDR1/A #2 (Table 3.5.2); DLKP-A-2B (Table 3.5.3); DLKP-A-2B IC7 (Table 3.5.4); SK-MES-1 (Table 3.5.5); SK-MES-1/Adr (Table 3.5.6); SK-MES-1/Adr mdr1 ribozyme #4 (Table 3.5.7).

The effect of two concentrations of adriamycin (10nM and 20 nM) was assayed in combination with five test compounds in DLKP, a chemotherapy drug sensitive human lung carcinoma cell line (Table 3.5.1). The test compounds N-1, O-1 and U-1 at non-toxic concentrations, each enhanced the cytotoxicity of adriamycin at 10nM and 20nM concentrations. The largest effect was observed at the highest concentration of test compound used. None of the concentrations of the test compounds A-1 or U-2 enhanced the cytotoxicity of adriamycin.

The five test compounds were also assayed in combination with adriamycin in DLKP pHaMDR1/A #2, a MDR1 transfectant of DLKP which is resistant to adriamycin (see Section 3.4). At the three concentrations of test compounds tested, none of the test compounds demonstrated any enhanced toxicity of adriamycin (Table 3.5.2).

From the results of testing DLKP and DLKP pHaMDR1/A #2, three test compounds were further assayed in five other cell lines. These were N-1 and U-1, both of which enhanced the toxicity of adriamycin in DLKP and A-1 which did not enhance adriamycin toxicity and was therefore used as a negative control.

DLKP-A-2B is a low level resistant clone derived from the MDR cell line DLKP-A (Heenan, 1994). DLKP-A-2B was tested to observe the effect of the test compounds in a cell line which expresses a number of MDR mechanisms including overexpression of P-glycoprotein. None of the test compounds assayed enhanced the toxicity of adriamycin (Table 3.3.3).

In order to further investigate the effect of the test compounds in MDR cell lines, DLKP-A-2B IC7 was also assayed. DLKP-A-2B IC7 is a MDR1 ribozyme transfectant of DLKP-A-2B, in which the expression of P-glycoprotein mRNA is inhibited (McBride, 1995). The test compounds N-1 and U-1 at non-toxic concentrations, each enhanced the cytotoxicity of adriamycin at 40nM and 80nM concentrations (Table 3.5.4). The largest effect was observed at the highest concentration of test compound used. None of the concentrations of the test compound A-1 significantly enhanced the cytotoxicity of adriamycin.

The test compounds N-1 and U-1 enhanced the toxicity of adriamycin at 5nM and 10nM in SK-MES-1, a chemotherapeutic drug sensitive cell line (Table 3.5.5). A-1 did not enhance the toxicity of adriamycin.

SK-MES-1/Adr is a MDR derivative of SK-MES-1, which was exposed to increasing concentrations of adriamycin. When this cell line was assayed with the test compounds in combination with adriamycin (Table 3.5.6), no enhancement of toxicity was observed.

A MDR1 ribozyme transfectant of SK-MES-1/Adr was then assayed with the test compounds. SK-MES-1/Adr MDR1 ribozyme clone #4 was the most sensitive clone obtained after transfection of SK-MES-1/Adr with a MDR1 ribozyme, although P-glycoprotein mRNA expression was not completely inhibited (see Section 3.3). No enhancement of toxicity was observed when this cell line was assayed with the test compounds in combination with adriamycin (Table 3.5.7).

The above results demonstrated that the test compounds N-1, O-1 and U-1 were shown to be synergistic at non-toxic levels in combination with adriamycin in DLKP but not DLKP pHaMDR1/A #2, whereas A-1 and U-2 exhibited no synergy. N-1 and U-1 exhibited synergy in DLKP-A-2B IC7 and SK-MES-1 but not in DLKP-A-2B, SK-MES-1/Adr and SK-MES-1/Adr mdr1 ribozyme #4. A-1 had no synergistic effect in any cell line assayed.

Table 3.5.1: Adriamycin in combination with the test compounds in DLKP. Survival was calculated as percentage growth relative to that measured in a drug-free control and is the mean of eight replicates. The values also include the standard deviations.

	[1]	[2]	[3]	Adr (10nM)	Adr + [1]	Adr + [2]	Adr + [3]
A-1	102±9	102±9	104±8	97±5	90±4	94±7	98±7
N-1	98±11	92±11	95±11	90±9	61±5	67±5	80±6
O-1	98±9	98±8	98±8	84±10	64±11	63±13	56±11
U-1	104±6	104±6	106±6	79±5	40±4	50±4	62±6
U-2	102±6	99±5	99±6	75±5	91±7	88±8	82±6

	[1]	[2]	[3]	Adr (20nM)	Adr + [1]	Adr + [2]	Adr + [3]
A-1	96±7	100±6	106±5	35±3	26±3	28±2	33±5
N-1	97±11	98±9	96±9	62±4	15±1	16±1	20±2
O-1	99±5	101±5	106±7	82±3	51±6	60±6	59±7
U-1	110±5	107±8	110±8	40±3	12±1	15±2	22±2
U-2	103±10	100±8	99±8	67±7	71±8	64±9	58±10

Test compound concentrations

[A-1] 1 = 140μM
[A-1] 2 = 70μM
[A-1] 3 = 35μM

[N-1] 1 = 8μM
[N-1] 2 = 4μM
[N-1] 3 = 2μM

[O-1] 1 = 240μM
[O-1] 2 = 120μM
[O-1] 3 = 60μM

[U-1] 1 = 17μM
[U-1] 2 = 8.5μM
[U-1] 3 = 4.25μM

[U-2] 1 = 5μM
[U-2] 2 = 2.5μM
[U-2] 3 = 1.25μM

Table 3.5.2: Adriamycin in combination with the test compounds in DLKP pHaMDR1/A #2. Survival was calculated as percentage growth relative to that measured in a drug-free control and is the mean of eight replicates. The values also include the standard deviations.

	[1]	[2]	[3]	Adr (180nM)	Adr + [1]	Adr + [2]	Adr + [3]
A-1	89±7	98±6	100±8	72±5	68±5	71±7	68±5
N-1	72±4	87±4	95±8	93±5	72±4	87±4	95±8
O-1	96±4	97±7	96±5	72±8	70±8	67±6	62±7
U-1	98±11	102±6	100±8	72±5	69±5	67±3	68±6
U-2	98±6	101±6	101±6	64±5	63±6	60±5	50±6

	[1]	[2]	[3]	Adr (360nM)	Adr + [1]	Adr + [2]	Adr + [3]
A-1	94±7	97±5	98±7	41±4	48±6	44±5	40±4
N-1	79±5	94±5	101±8	69±8	47±5	58±5	65±5
O-1	97±5	99±5	102±5	47±3	48±5	44±4	36±5
U-1	105±9	96±4	100±8	37±3	39±4	37±5	37±3
U-2	97±3	97±6	98±6	46±3	43±4	41±4	38±4

Test compound concentrations

[A-1] 1 = 140μM
[A-1] 2 = 70μM
[A-1] 3 = 35μM

[N-1] 1 = 8μM
[N-1] 2 = 4μM
[N-1] 3 = 2μM

[O-1] 1 = 240μM
[O-1] 2 = 120μM
[O-1] 3 = 60μM

[U-1] 1 = 17μM
[U-1] 2 = 8.5μM
[U-1] 3 = 4.25μM

[U-2] 1 = 5μM
[U-2] 2 = 2.5μM
[U-2] 3 = 1.25μM

Table 3.5.3: Adriamycin in combination with the test compounds in DLKP-A-2B. Survival was calculated as percentage growth relative to that measured in a drug-free control and is the mean of eight replicates. The values also include the standard deviations.

	[1]	[2]	[3]	Adr (100nM)	Adr + [1]	Adr + [2]	Adr + [3]
A-1	98±9	101±14	99±11	96±9	104±10	102±7	95±7
N-1	150±15	120±12	99±10	96±8	116±9	101±8	88±8
U-1	120±19	93±12	92±13	57±9	66±12	53±9	54±11

	[1]	[2]	[3]	Adr (200nM)	Adr + [1]	Adr + [2]	Adr + [3]
A-1	88±12	112±13	110±15	47±5	58±7	66±11	97±9
N-1	130±13	130±11	99±10	84±8	108±5	91±7	85±8
U-1	120±20	95±20	91±14	50±12	60±10	56±12	48±5

Test compound concentrations

[A-1] 1 = 140μM
[A-1] 2 = 70μM
[A-1] 3 = 35μM

[N-1] 1 = 8μM
[N-1] 2 = 4μM
[N-1] 3 = 2μM

[U-1] 1 = 17μM
[U-1] 2 = 8.5μM
[U-1] 3 = 4.25μM

Table 3.5.4: Adriamycin in combination with the test compounds in DLKP-A-2B IC7. Survival was calculated as percentage growth relative to that measured in a drug-free control and is the mean of eight replicates. The values also include the standard deviations.

	[1]	[2]	[3]	Adr (40nM)	Adr + [1]	Adr + [2]	Adr + [3]
A-1	90±7	99±7	125±6	76±4	58±4	63±5	93±6
N-1	72±4	104±7	102±6	81±7	18±1	26±2	32±2
U-1	105±6	107±7	103±6	79±5	25±2	33±4	53±4

	[1]	[2]	[3]	Adr (80nM)	Adr + [1]	Adr + [2]	Adr + [3]
A-1	88±11	92±9	83±10	26±5	19±3	20±4	13±2
N-1	107±5	107±5	106±3	34±3	16±2	25±2	15±2
U-1	102±5	99±5	99±7	32±4	15±1	15±1	17±1

Test compound concentrations

[A-1] 1 = 140μM [N-1] 1 = 8μM [U-1] 1 = 17μM

[A-1] 2 = 70μM [N-1] 2 = 4μM [U-1] 2 = 8.5μM

[A-1] 3 = 35μM [N-1] 3 = 2μM [U-1] 3 = 4.25μM

Table 3.5.5: Adriamycin in combination with the test compounds in SK-MES-1. Survival was calculated as percentage growth relative to that measured in a drug-free control and is the mean of eight replicates. The values also include the standard deviations.

	[1]	[2]	[3]	Adr (5nM)	Adr + [1]	Adr + [2]	Adr + [3]
A-1	74±5	88±4	98±5	100±5	73±4	85±5	94±6
N-1	94±4	99±7	100±8	103±6	87±4	92±5	98±6
U-1	98±5	100±5	100±7	102±5	89±6	100±5	94±6

	[1]	[2]	[3]	Adr (10nM)	Adr + [1]	Adr + [2]	Adr + [3]
A-1	73±3	86±5	93±5	93±6	69±3	82±5	87±5
N-1	91±6	95±4	94±4	91±8	69±3	70±4	89±4
U-1	98±8	101±4	101±6	93±7	61±4	80±5	88±6

Test compound concentrations

[A-1] 1 = 140μM
[A-1] 2 = 70μM
[A-1] 3 = 35μM

[N-1] 1 = 8μM
[N-1] 2 = 4μM
[N-1] 3 = 2μM

[U-1] 1 = 17μM
[U-1] 2 = 8.5μM
[U-1] 3 = 4.25μM

Table 3.5.6: Adriamycin in combination with the test compounds in SK-MES-1/Adr. Survival was calculated as percentage growth relative to that measured in a drug-free control and is the mean of eight replicates. The values also include the standard deviations.

	[1]	[2]	[3]	Adr (200nM)	Adr + [1]	Adr + [2]	Adr + [3]
A-1	74±6	88±8	95±7	97±7	77±5	92±8	98±9
N-1	80±13	101±12	103±10	104±13	82±8	103±10	97±13
U-1	102±14	104±10	103±10	97±8	94±8	96±8	99±13

	[1]	[2]	[3]	Adr (400nM)	Adr + [1]	Adr + [2]	Adr + [3]
A-1	71±7	85±6	92±7	93±7	85±9	101±6	109±7
N-1	73±8	94±10	98±11	90±11	65±7	87±10	85±11
U-1	92±9	95±10	99±10	89±12	86±10	89±10	85±15

Test compound concentrations

[A-1] 1 = 140μM
[A-1] 2 = 70μM
[A-1] 3 = 35μM

[N-1] 1 = 8μM
[N-1] 2 = 4μM
[N-1] 3 = 2μM

[U-1] 1 = 17μM
[U-1] 2 = 8.5μM
[U-1] 3 = 4.25μM

Table 3.5.7: Adriamycin in combination with the test compounds in SK-MES-1/Adr mdr1 ribozyme #4. Survival was calculated as percentage growth relative to that measured in a drug-free control and is the mean of eight replicates. The values also include the standard deviations.

	[1]	[2]	[3]	Adr (20nM)	Adr + [1]	Adr + [2]	Adr + [3]
A-1	77±7	81±8	91±8	87±8	67±6	77±6	85±7
N-1	82±9	86±9	95±6	97±7	82±8	85±5	90±13
U-1	97±8	99±9	100±6	96±8	86±8	88±7	90±9

	[1]	[2]	[3]	Adr (40nM)	Adr + [1]	Adr + [2]	Adr + [3]
A-1	77±4	85±6	97±7	98±12	74±6	82±6	93±9
N-1	84±7	87±9	96±7	94±7	79±7	83±6	88±8
U-1	94±14	96±5	100±10	93±7	87±7	87±5	87±6

Test compound concentrations

[A-1] 1 = 140μM
[A-1] 2 = 70μM
[A-1] 3 = 35μM

[N-1] 1 = 8μM
[N-1] 2 = 4μM
[N-1] 3 = 2μM

[U-1] 1 = 17μM
[U-1] 2 = 8.5μM
[U-1] 3 = 4.25μM

3.6 Drug Pulse / Scheduling Assays

There are a number of non-chemotherapeutic drugs which enhance chemotherapeutic cytotoxicity by mechanisms other than the reversal of drug resistance. However none of these are in common clinical use. Thus, the need to test new non-chemotherapeutic drugs which enhances the cytotoxicity of chemotherapeutic drugs is needed more than ever.

The results of the previous section (Section 3.5) described the effect of combining five test compounds with adriamycin. Three of these compounds were found to enhance the toxicity of adriamycin in three of seven cell lines assayed. However, due to the nature of the assay, which is an excellent assay for screening test compounds, no information could be derived about the mechanism of action of the active test compounds. To investigate the synergistic toxic effect of N-1, O-1 and U-1, an assay was developed to analyse how synergism was affected when cells were exposed to the test compounds at different times relative to adriamycin exposure (see Section 2.7.4). Briefly, cells were set up in 96-well plates and the following day, pulse treated with a chemotherapeutic drug for 2 hours, the drug was then removed and the cells washed twice in PBS, they were then exposed to a test compound for various time periods.

Initial experiments in DLKP demonstrated that there was a synergistic effect when DLKP was exposed to N-1 or U-1 during the first 24 hour time period after adriamycin exposure (Table 3.6.1). No synergism was observed when DLKP was exposed to the test compounds from 24 to 48 hours, 48 to 72 hours or from 72 to 96 hours.

Following on from these experiments a number of other test compounds were also assayed. These assays were performed on DLKP-SQ, which is a clone derived form DLKP (McBride, 1995). DLKP-SQ was used because it was a clonal population and therefore could also be used for subsequent flow cytometric analysis. The results of these assays are given in Table 3.6.2. N-1, O-1 and U-1 exhibited a synergistic effect during the first 24 hour period after a 2 hour pulse exposure to 1μM adriamycin. The test compounds

A-1, I-1 and U-2 had no effect. BSO showed an additive toxic effect with adriamycin but verapamil and cyclosporin A had no significant effect when added over this period.

Previous experiments demonstrated that the test compounds N-1, O-1 and U-1 were synergistic with adriamycin. These test compounds were also assayed using vincristine (Table 3.6.3) and 5-fluorouracil (Table 3.6.4). The test compounds showed a strong synergism in combination with vincristine, with an increase of 50% in cytotoxicity when N-1 was used. BSO was also used in combination with vincristine and there seems to be an enhancement of toxicity but this effect may be due to the additive toxicity of BSO. Combinations of the test compounds with 5-fluorouracil did not exert any synergistic cytotoxic effect.

In order to determine if pre-treatment of DLKP-SQ with the test compounds enhanced toxicity. Cells were pre-treated for 24 hours before pulse exposure to adriamycin. However, there was no enhanced cytotoxic effect with any test compound studied (Table 3.6.5).

Because treatment with N-1, O-1 or U-1 only worked during the first 24 hours after adriamycin treatment, the time period for exposure to a test compound was decreased to 10 hours. Using this time period N-1 exposure was assayed during adriamycin exposure and for the 10 hour periods after different adriamycin concentration pulse exposures (Table 3.6.6). The assay demonstrated that the greatest effect was observed during the first 10 hour period after adriamycin exposure (Table 3.6.6). No synergistic effect was observed when N-1 was added during adriamycin exposure.

Since the active test compounds exerted their synergistic effect during the first 24 hours after drug removal, cycloheximide (a protein synthesis inhibitor) and actinomycin D (an inhibitor of transcription and translation) were used to try and block the synergistic effect. Using a relatively non-toxic level of cycloheximide (75% cell survival) did not prevent the toxic effect of U-1 (Table 3.6.7). Actinomycin D in combination with U-1 after adriamycin exposure did not prevent the toxic effect of U-1 (Table 3.6.8).

The above results demonstrate that the active test compounds, N-1, O-1 and U-1 exert their synergistic cytotoxic effect during the first 24 hours post-treatment with adriamycin or vincristine but not 5-fluorouracil. Pretreatment with the test compounds for 24 hours has no enhanced toxic effect. Co-treatment of U-1 with cycloheximide or actinomycin D did not prevent the synergistic effect of U-1.

Table 3.6.1: Effect of exposing DLKP cells to 1μM adriamycin for 2 hours and then treating with a test compound (TC) for 24 hour periods from when adriamycin was removed. Survival was calculated as percentage growth relative to that measured in a drug-free control and is the mean of eight replicates. The values also include the standard deviations.

	Control	**TC 0-24hr**	**Adr (1μM)**	**Adr+TC 0-24hr**	**Adr +TC 24-48hr**	**Adr +TC 48-72hr**	**Adr+TC 72-96hr**
N-1 28μM	100±8	91±14	51±6	33±4	53±8	53±7	53±4
U-1 140μM	100±11	90±9	55±7	36±7	59±16	58±16	55±10

Table 3.6.2: DLKP-SQ pulse treated with 1μM adriamycin for 2 hours and then treating with a test compound (TC) from when 1μM adriamycin was removed for 24 hours and from 24 to 48 hours after drug removal. Survival was calculated as percentage growth relative to that measured in a drug-free control and is the mean of eight replicates. The values also include the standard deviations.

	Control	**TC 0-24hrs**	**TC 24-48hr**	**Adr (1μM)**	**Adr +TC 0-24hr**	**Adr +TC 24-48hr**
A-1 200μM	100±15	80±12	72±10	45±6	45±6	44±5
BSO 900μM	100±6	57±5	73±7	47±5	18±5	33±6
CysA 0.2μg/ml	100±10	90±8	81±9	52±6	45±7	47±5
I-1 60μM	100±17	91±15	92±14	52±9	62±10	53±7
N-1 28μM	100±19	106±21	93±17	46±7	29±4	40±5
O-1 130μM	100±12	109±16	107±7	56±9	37±7	54±14
U-1 140μM	100±13	88±12	81±8	46±3	30±2	45±3
U-2 1μM	100±16	105±11	77±9	44±5	39±6	41±7
Ver 1μM	100±12	113±9	115±9	53±8	46±6	48±5

Table 3.6.3: Effect of exposing cells to 60nM Vincristine for 2 hours and then treating with various compounds (TC) from when vincristine was removed, for 24 hours and from 24 to 48 hours after vincristine removal. Survival was calculated as percentage growth relative to that measured in a drug-free control and is the mean of eight replicates. The values also include the standard deviations.

	Control	**TC 0-24hrs**	**TC 24-48hr**	**Vcr (60nM)**	**Vcr+TC 0-24hr**	**Vcr+TC 24-48hr**
BSO 900μM	100±6	80±5	91±5	53±5	19±2	39±6
N-1 28μM	100±8	105±7	107±8	67±5	19±2	66±6
O-1 130μM	100±8	102±7	104±13	68±12	30±5	77±10
U-1 140μM	100±11	101±13	98±11	53±7	17±3	48±8

Table 3.6.4: Effect of exposing cells to 190μM 5-Fluorouracil for 2 hours and then treating with a compound (TC) from when 5-Fluorouracil was removed, for 24 hours and from 24 to 48 hours after 5-fluorouracil removal. Survival was calculated as percentage growth relative to that measured in a drug-free control and is the mean of eight replicates. The values also include the standard deviations.

	Control	**TC 0-24hrs**	**TC 24-48hr**	**5-FU (190μM)**	**FU+TC 0-24hr**	**FU+TC 24-48hr**
A-1 200μM	100±12	101±14	91±15	109±13	100±15	87±12
N-1 28μM	100±20	104±17	91±21	99±21	91±12	98±16
U-1 140μM	100±14	93±9	76±11	107±8	88±10	69±10

Table 3.6.5: Effect of pre-treating DLKP-SQ before pulse treating with 1μM adriamycin (Adr) for 2 hours. DLKP-SQ was exposed to a test compound for various time periods including 24 hours before drug exposure (-24 to 0), 24 hours before and after adriamycin treatment (-24 to 24) and for 24 hours after adriamycin treatment (0 to 24). All concentrations of test compounds used were less than 10% toxic. Survival was calculated as percentage growth relative to that measured in a drug-free control and is the mean of eight replicates. The values also include the standard deviations.

	Adr	**(-24 to 0)**	**(-24 to 24)**	**(0 to 24)**
U-1 140μM	71±6	68±8	33±4	35±4
N-1 28μM	75±7	75±9	41±4	38±6
A-1 200μM	86±8	78±7	74±12	93±14

Table 3.6.6: Effect of treating DLKP-SQ with N-1 during adriamycin exposure and for shorter time periods (10 hours) after 2 hours exposure to four concentrations of adriamycin. The table shows the effect of 28μM N-1 alone, adriamycin at various concentrations alone and adriamycin at the various concentrations in combination with N-1 during adriamycin exposure, for 10 hours after adriamycin exposure (0 - 10) and from 10 hours to 20 hours (10 - 20)Survival was calculated as percentage growth relative to that measured in a drug-free control and is the mean of eight replicates. The values also include the standard deviations.

[Adr]	**N-1**	**Adr**	**During Adr exposure**	**0 - 10**	**10 - 20**
0.25μM	90±12	88±10	87±8	96±14	102±13
0.5μM		76±11	74±10	63±8	65±9
1μM	94±13	30±6	34±5	22±4	29±4
2μM		15±3	13±3	6±2	6±1

Table 3.6.7: Effect of 50ng/ml cycloheximide (CHX) in combination with 140μM U-1 after 2 hours 1μM adriamycin exposure. Survival was calculated as percentage growth relative to that measured in a drug-free control and is the mean of eight replicates. The values also include the standard deviations.

	Control	1μM Adr
Control	100±22	56±10
U-1 (0 - 24)	81±14	35±5
CHX (0 - 24)	75±6	53±13
U-1 + CHX (0-24)	62±10	33±5

Table 3.6.8: Effect of 0.5ng/ml Actinomycin D (ActD) in combination with 140 μM U-1 after 2 hours 1μM adriamycin exposure. Survival was calculated as percentage growth relative to that measured in a drug-free control and is the mean of eight replicates. The values also include the standard deviations.

	Control	1μM Adr
Control	100±11	54±6
U-1 (0 - 24)	79±5	32±4
ActD (0 - 24)	72±6	44±3
U-1 + ActD (0-24)	56±4	26±3

3.7 DLKP pHaMDR1/A #2 Scheduling

Exposure of DLKP-SQ to a cytotoxic concentration of adriamycin, followed by treatment with a non-toxic concentration of an active test compound, results in an enhancement of adriamycin's toxicity. However, no effect of the test compounds was observed in any P-glycoprotein expressing cell line using the standard circumvention assay. Using the modified assay (see Section 2.7.4) i.e. pulse treatment with adriamycin, the effect of 6 test compounds was assayed on DLKP pHaMDR1/A #2.

DLKP pHaMDR1/A #2 was pulse treated with adriamycin and exposed to 6 test compounds for 24 hour periods (Table 3.7.1). When non-toxic levels of test compound were used after adriamycin exposure there was no enhanced toxicity compared to adriamycin alone . No synergistic effect with adriamycin was observed with any of the six test compounds assayed e.g. U-1 exposure did not enhance the toxicity of 1μM adriamycin compared to 1μM adriamycin exposure alone. A-1, I-1, O-1 and U-2 did show some increased toxicity in combination with adriamycin but this was probably due to the additive toxicity of the verapamil and the test compounds.

Because the test compounds had displayed no synergy with adriamycin in P-glycoprotein positive cells, verapamil was used in combination with the test compounds. Verapamil inhibits P-glycoprotein associated, energy-dependent drug-efflux in MDR cells, apparently by blocking the binding of drugs to P-glycoprotein (Ford, 1995). Using the test compounds and verapamil in combination with adriamycin, there was no restoration of the synergistic effect of the test compounds observed in DLKP (Table 3.7.2).

The above experiment was repeated using cyclosporin A instead of verapamil, in combination with U-1 (Table 3.7.3). Cyclosporin A is an immunosuppressive peptide which antagonises MDR through the inhibition of P-glycoprotein. At the lower concentration of adriamycin (0.25μM and 0.5μM) there was no enhanced toxicity with cyclosporin A or with cyclosporin A plus U-1 in combination. At 1μM and 2μM

adriamycin concentrations, cyclosporin A enhanced the toxicity of adriamycin. However, U-1 or U-1 plus cyclosporin did not enhance adriamycin toxicity.

These results show that the synergistic toxic effect observed between U-1 and adriamycin in DLKP was not restored in a DLKP pHaMDR1/A #2 when inhibitors of P-glycoprotein was used.

Table 3.7.1: DLKP pHaMDR1/A #2 pulse treated with 1μM adriamycin for 2 hours and treated with a test compound (TC) for 24 hour periods after adriamycin exposure. The table shows the drug-free control, test compound controls for 0-24 hours and 24-48 hours exposure, adriamycin alone and adriamycin in combination with a test compound for 0-24 hours and 24-48 hours. Survival was calculated as percentage growth relative to that measured in a drug-free control and is the mean of eight replicates. The values also include the standard deviations.

TC	Control	TC 0-24hrs	TC 24-48hr	Adr (1μM)	Adr+TC 0-24hr	Adr+TC 24-48hr
A-1 200μM	100±15	62±16	83±15	48±5	33±6	46±8
I-1 60μM	100±16	70±9	103±11	48±7	43±6	48±8
N-1 28μM	100±28	130±25	87±21	35±4	51±5	30±4
O-1 130μM	100±11	88±17	82±7	37±4	30±5	28±2
U-1 140μM	100±30	102±14	82±23	34±3	41±6	31±4
U-2 1μM	100±12	58±9	75±11	42±6	22±3	36±4

Table 3.7.2: Effect of combining test compounds with verapamil after 2 hours 1μM adriamycin (Adr) exposure pulse exposure in DLKP pHaMDR1/A #2. The table shows the drug-free control, the test compound (TC) alone for 24 hours, verapamil (Ver) for 24 hours, adriamycin alone, adriamycin in combination with verapamil and adriamycin in combination with verapamil plus a test compound for 24 hours. Survival was calculated as percentage growth relative to that measured in a drug-free control and is the mean of eight replicates. The values also include the standard deviations.

	Control	**TC 0-24hr**	**Ver 0-24 1μM**	**1μM Adr**	**Adr+Ver**	**Adr+Ver +TC**
A-1 200μM	100±15	62±16	67±13	48±5	32±6	39±4
I-1 60μM	100±16	70±9	74±21	48±7	39±6	42±5
N-1 28μM	100±28	130±25	112±9	35±4	43±6	47±5
O-1 130μM	100±11	88±17	69±8	37±4	22±4	21±3
U-1 140μM	100±30	102±19	99±18	34±3	36±5	38±7
U-2 1μM	100±12	58±9	75±11	42±6	30±4	27±2

Table 3.7.3: Effect of Cyclosporin A (CysA) in combination with U-1 in DLKP pHaMDR1/A #2 after 2 hours adriamycin exposure. The table shows the drug-free control, U-1 alone for 24 hours, cyclosporin A for 24 hours, adriamycin alone, adriamycin in combination with CysA and adriamycin in combination with CysA plus U-1 for 24 hours. Survival was calculated as percentage growth relative to that measured in a drug-free control and is the mean of eight replicates. The values also include the standard deviations.

[Adr]	Control	CysA 0.2μg/ml	U-1 140μM	CysA + U-1	Adr	Adr + CysA	Adr + CysA + U-1	Adr + U-1
0.25μM Adr	100±14	95±10	83±13	89±8	85±12	88±13	82±11	84±11
0.5μM Adr	100±15	113±19	95±10	98±18	102±20	104±13	92±12	91±9
1μM Adr	100±12	88±8	83±14		60±9	46±6	46±6	61±5
2μM Adr	100±12	94±19	88±14		52±7	19±5	19±5	51±3

3.8 Cell cycle distribution

The results from Section 3.6 demonstrated that the test compounds, N-1, O-1 and U-1 exert their synergistic cytotoxic effect during the first 24 hours post-treatment with adriamycin or vincristine but not 5-fluorouracil. These experiments were performed using a 7 day cell growth assay. In order to investigate the role of these test compounds on DLKP-SQ, flow cytometric analysis was used to determine the cell cycle distribution of treated samples. A flow cytometer measures the amount of fluorescence from an individual cell. Therefore, propidium iodide (which intercalates with DNA) stained cells, the amount of DNA fluorescence is measured and this can be used to determine the position of a cell in the cell cycle.

Flow cytometric analysis was used to determine the cell cycle distribution in DLKP-SQ pulse treated adriamycin, vincristine or 5-fluorouracil for 2 hours and to a test compound (A-1, N-1 or U-1) for 24 hours. Samples pulsed with a chemotherapeutic drug, followed by exposure to a test compound using conditions described in Section 2.8 were analysed to determine any effect on the cell cycle.

The effect of the test compounds N-1, U-1 and A-1, on the cell cycle distribution of DLKP-SQ is given in Figures 3.8.1 - 3.8.3. At 0 hours, test compound was added. 140μM U-1 treated cells showed an accumulation in the G_1 peak at 10 and 13 hours with corresponding decrease in the G_2/M peak, by 16 hours the cell cycle distribution resembled the normal cell cycle distribution of the control untreated sample at 0 hours (Figure 3.8.1). This accumulation in the G_1 peak suggests a delay or an arrest in G_1 transition into the S phase. DLKP-SQ exposed to 30μM N-1 also seemed to show an accumulation in the G_1 peak at 12 and 14 hours but by 16 hours resembled a normal cell cycle distribution (Figure 3.8.2). A-1 exposure did not appear to affect the cell cycle distribution (Figure 3.8.3).

U-1 in combination with 1μM adriamycin displayed an increased accumulation in G_1/ early S phase at 4 and 8 hours (Figure 3.8.4 (a)). By 12 and 15 hours there was a delayed

S peak evident compared to adriamycin alone (Figure 3.8.4 (b)), by 24 hours, U-1 treated samples were accumulated in the late S and G_2/M phase. N-1 in combination with 1μM adriamycin exhibited a delayed S phase peak at 12, 14 and 16 hours (Figure 3.8.5 (a)) compared to adriamycin alone (Figure 3.8.5 (b)). By 19 hours, N-1 treated samples were accumulated in the late S and G_2/M phase compared to the G_2/M peak in adriamycin alone. There seemed to be no difference in cell cycle distribution patterns of A-1 plus adriamycin and adriamycin alone (Figure 3.8.6 (a) and 3.8.6 (b)) with no evident increased delay in the S phase.

The cell cycle distribution profiles of DLKP-SQ treated with 50ng/ml vincristine in combination with U-1 are given in Figure 3.8.7 (a). From 10 to 24 hours there was a gradual decrease in the G_1 peak an increase in the G_2/M peak. In the vincristine alone treated sample there was an increase in the G_1 peak after G_2/M arrest at 18 hours with a large G_1 peak at 24 hours (Figure 3.8.7 (b)). Vincristine and N-1 in combination (Figure 3.8.8 (a)), displayed a similar profile to vincristine plus U-1. By 12 hours there was no G_1 peak and an accumulation of cells in the G_2/M peak, there was no G_1 peak by 24 hours compared to vincristine alone which showed an increase in G_1 by 16 hours (Figure 3.8.8 (b)). Vincristine plus A-1 (Figure 3.8.9) displayed little difference between vincristine alone (Figure 3.8.7 (b)).

DLKP-SQ treated with 190μM 5-fluorouracil alone or in combination with 140μM U-1 displayed no difference between the cell cycle distribution over time (Figure 3.8.10 and Figure 3.8.11).

Because of the increased G_1/S phase arrest and an increased S phase transition in DLKP-SQ treated with adriamycin plus N-1 or U-1, increasing concentrations of adriamycin alone were analysed. DLKP-SQ treated with 0.5μM adriamycin for 2 hours showed a decrease in the G_1 peak and an accumulation in the S phase at 12 hours (Figure 3.8.12), at 14 hours the G_1 peak further decreased and there was a peak at the late S phase. By 19 and 24 hours there was an accumulation in G_2/M. 1μM adriamycin treated samples showed a decrease in the G_1 peak and a peak in the early S phase at 12 hours (Figure

3.8.13). From 14 to 19 hours the S phase peak progresses through the S phase until at 24 hours the cells accumulate at G_2/M. 2μM adriamycin treated samples displayed a decrease in the G_1 peak and an accumulation in a peak at the early S phase by 12 hours (Figure 3.8.14). Over time the G_1 peak further decreased and the S phase peak further progressed through the S phase. By 24 hours this peak had reached the late S phase.

Increasing concentrations of vincristine were analysed to investigate if increasing concentrations increased G_2/M arrest as found when 50ng/ml plus U-1 or N-1 were used in combination. 25ng/ml vincristine for 2 hours caused a decrease in the G_1 peak and an accumulation in G_2/M by 12 hours (Figure 3.8.15). The G_1 peak gradually increased and the G_2 peak decreased at 14 ,16 and 19 hours. There seemed to be a normal cell cycle distribution by 24 hours. DLKP-SQ exposed to 50ng/ml (60nM) vincristine decreased the G_1 peak at 12 and 14 hours and cells accumulated in the G_2/M phase (Figure 3.8.16). The G_1 peak began to increase and the G_2/M peak decrease at 19 and 24 hours. 100ng/ml vincristine treated cells were delayed longer in the G_2/M phase with cells accumulated in G_2/M from 12 hours until 19 hours, and there was a slight increase in the G_1 peak at 24 hours (Figure 3.8.17).

These results showed that using an active test compound (U-1 or N-1) after adriamycin treatment caused an increased G_1/S phase arrest and a delayed S phase transition compared to adriamycin alone. Increasing concentrations of adriamycin also exhibited this effect. Vincristine in combination with U-1 or N-1 showed an increased G_2/M arrest compared to vincristine alone. This G_2/M arrest was further delayed when increasing concentrations of vincristine was used. DLKP-SQ treated with 190μM 5-fluorouracil alone or in combination with 140μM U-1 displayed no difference between the cell cycle distribution over time.

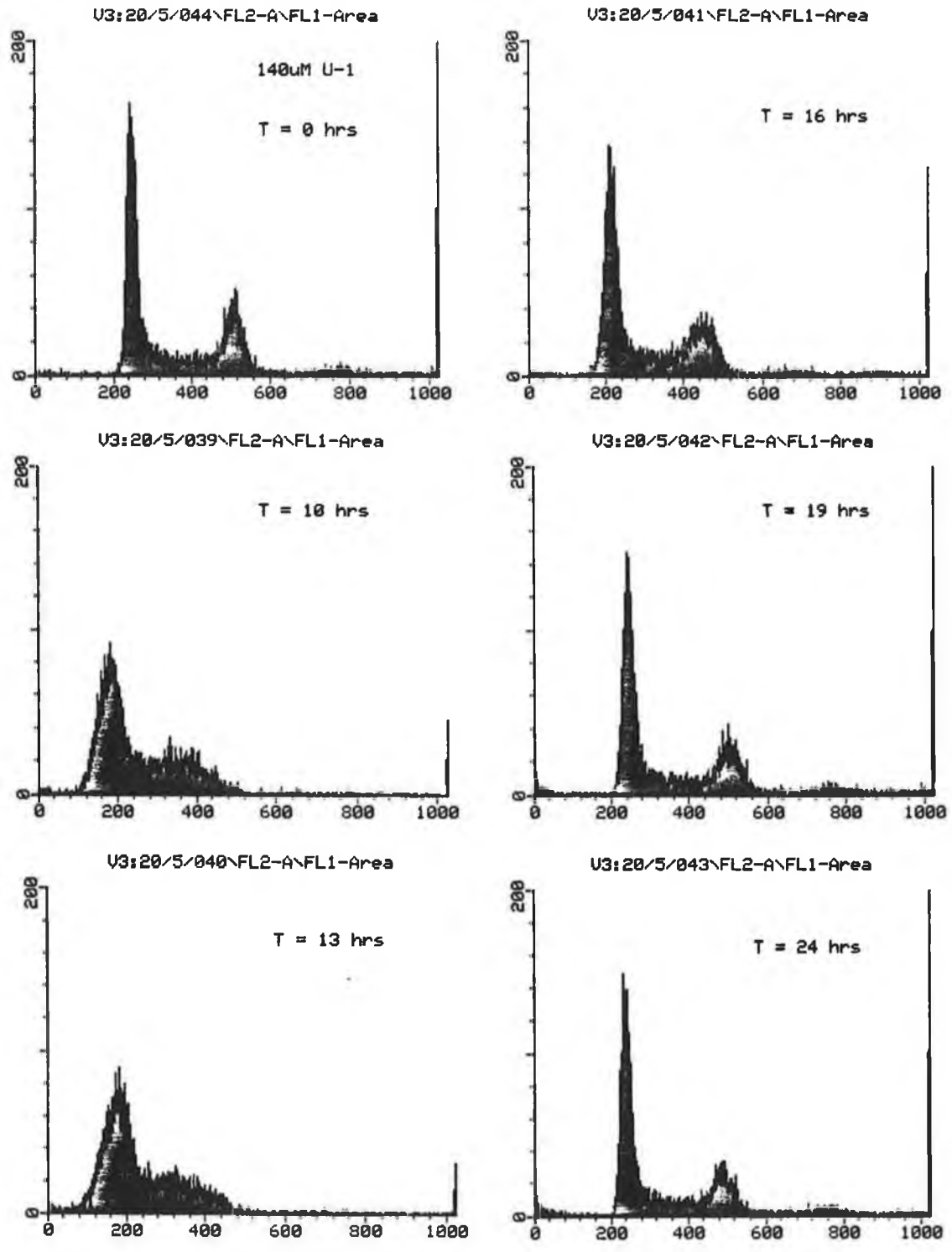

Figure 3.8.1: Cell cycle distribution of DLKP-SQ treated with 140μM U-1 for 24 hours. The graphs represent the DNA fluorescence as measured by flow cytometry of 10, 000 individual cells taken at different time points. The x-axis represents relative DNA fluorescence and the y-axis represents cell number. The left-hand peak is the G_1 peak and represents diploid cells. The peak on the right-hand is the G_2/M peak and represents tetraploid cells before cytokinesis of mitosis. Cells between the two peaks are in the S phase, i.e. cells which are replicating their DNA and thus have an increasing amount of DNA fluoresence.

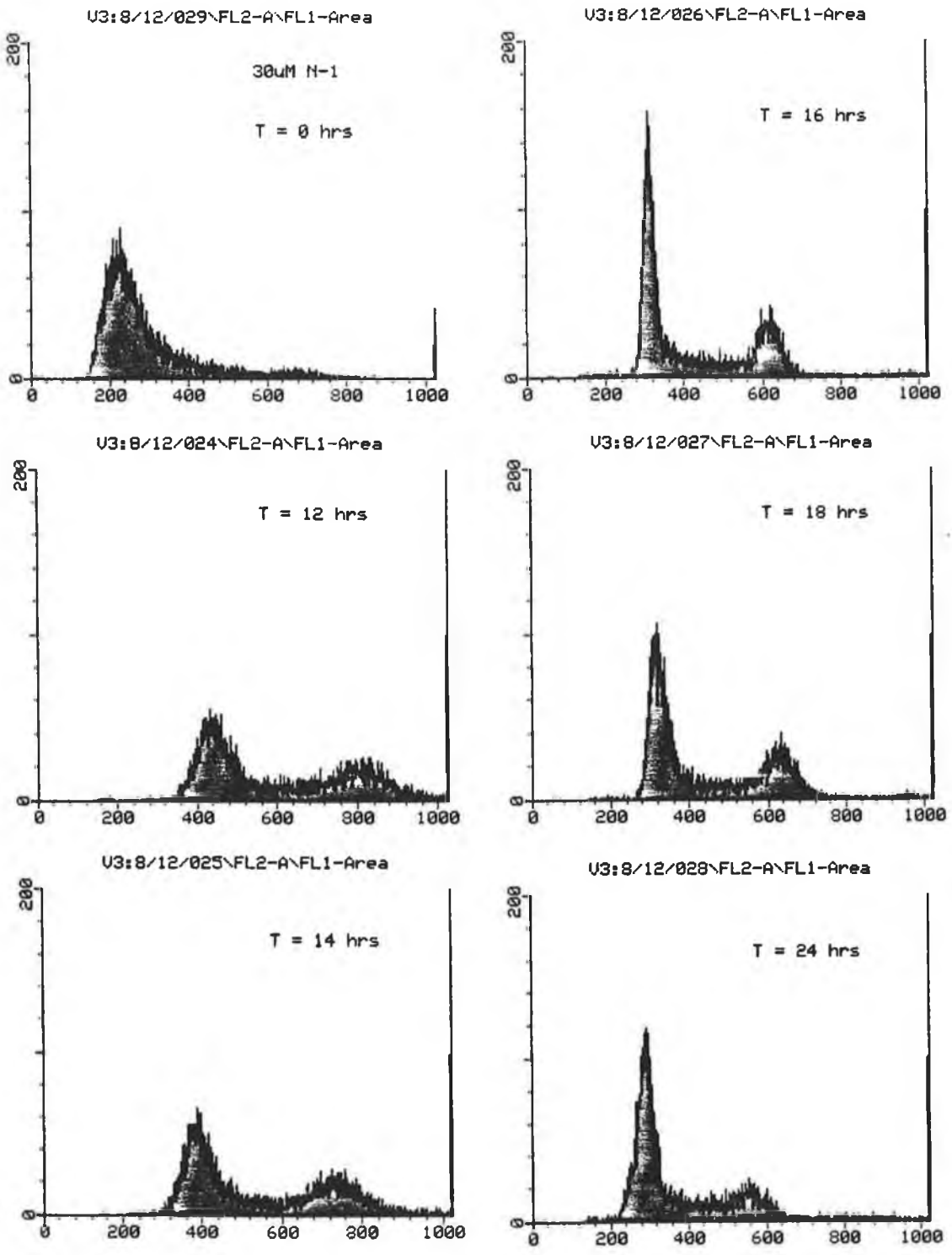

Figure 3.8.2: Cell cycle distribution of DLKP-SQ treated with 30μM N-1 for 24 hours. The graphs represent the DNA fluorescence as measured by flow cytometry of 10, 000 individual cells taken at different time points. The x-axis represents relative DNA fluorescence and the y-axis represents cell number. The left-hand peak is the G_1 peak and represents diploid cells. The peak on the right-hand is the G_2/M peak and represents tetraploid cells before cytokinesis of mitosis. Cells between the two peaks are in the S phase, i.e. cells which are replicating their DNA and thus have an increasing amount of DNA fluoresence.

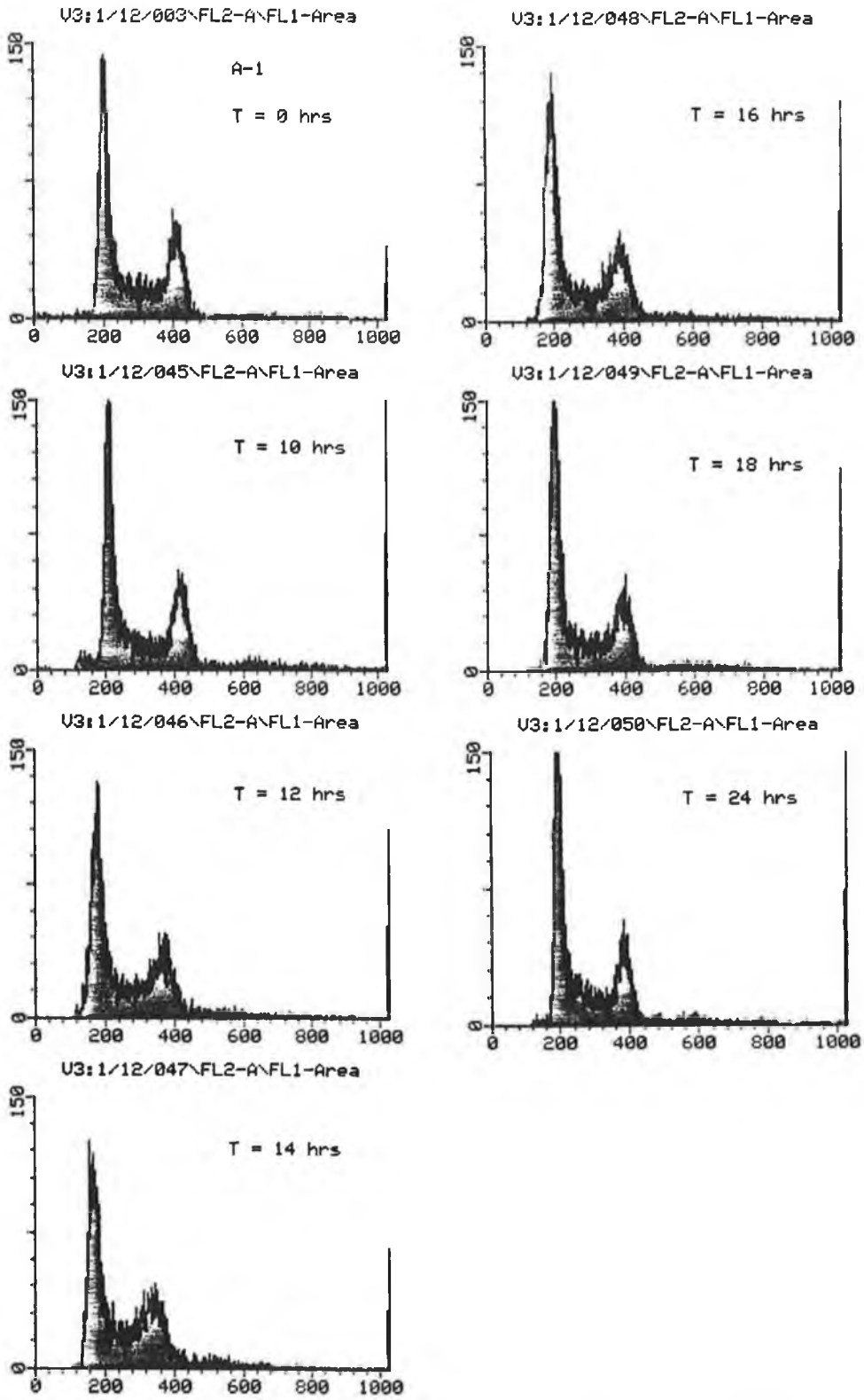

Figure 3.8.3: Cell cycle distribution of DLKP-SQ treated with 200μM A-1 for 24 hours. The graphs represent the DNA fluorescence as measured by flow cytometry of 10, 000 individual cells taken at different time points. The x-axis represents relative DNA fluorescence and the y-axis represents cell number. The left-hand peak is the G_1 peak and represents diploid cells. The peak on the right-hand is the G_2/M peak and represents tetraploid cells before cytokinesis of mitosis. Cells between the two peaks are in the S phase, i.e. cells which are replicating their DNA and thus have an increasing amount of DNA fluoresence.

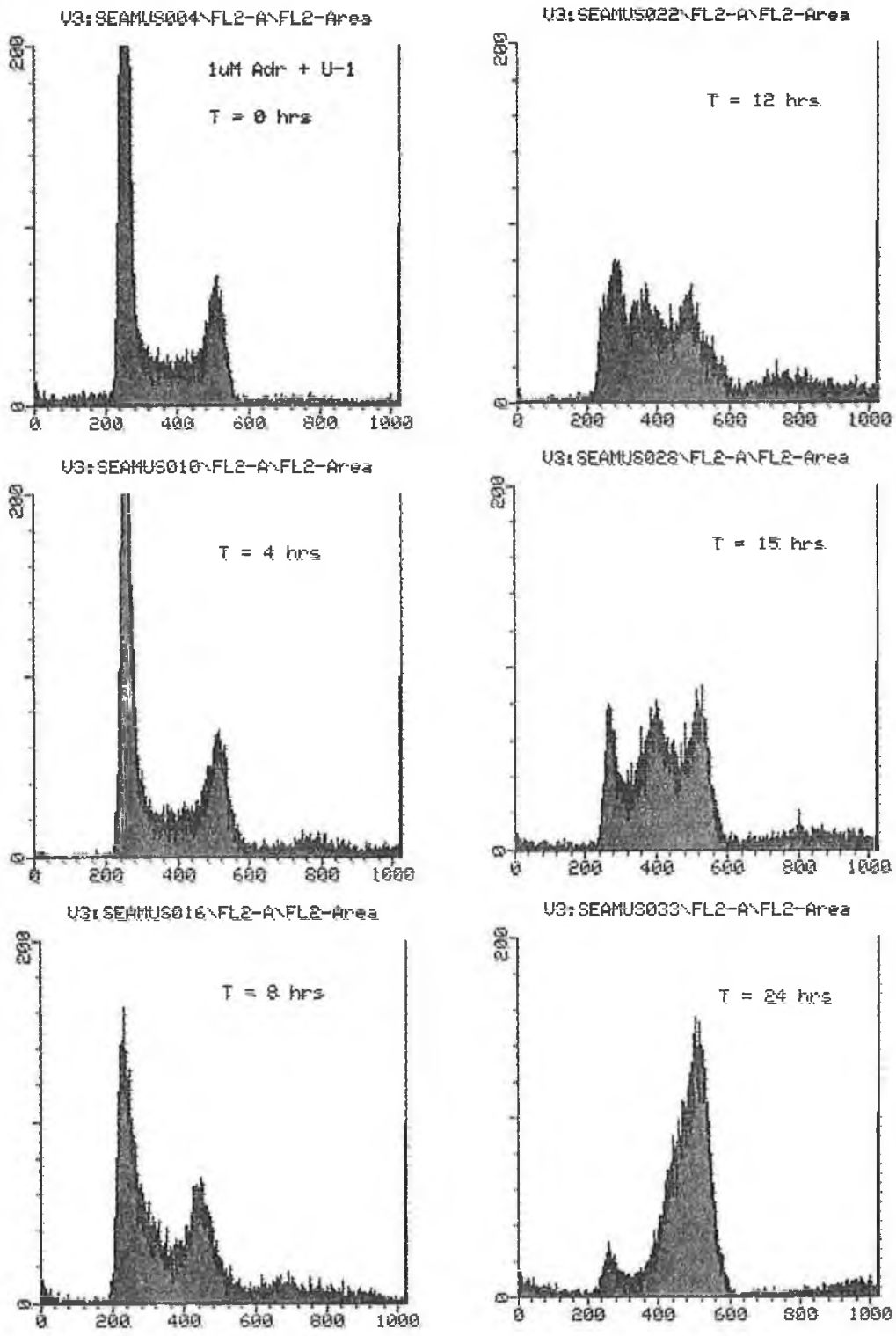

Figure 3.8.4 (a): Cell cycle distribution of DLKP-SQ treated 1μM adriamycin for 2 hours plus 140μM U-1 for 24 hours. The graphs represent the DNA fluorescence as measured by flow cytometry of 10, 000 individual cells taken at different time points. The x-axis represents relative DNA fluorescence and the y-axis represents cell number. The left-hand peak is the G_1 peak and represents diploid cells. The peak on the right-hand is the G_2/M peak and represents tetraploid cells before cytokinesis of mitosis. Cells between the two peaks are in the S phase, i.e. cells which are replicating their DNA and thus have an increasing amount of DNA fluoresence.

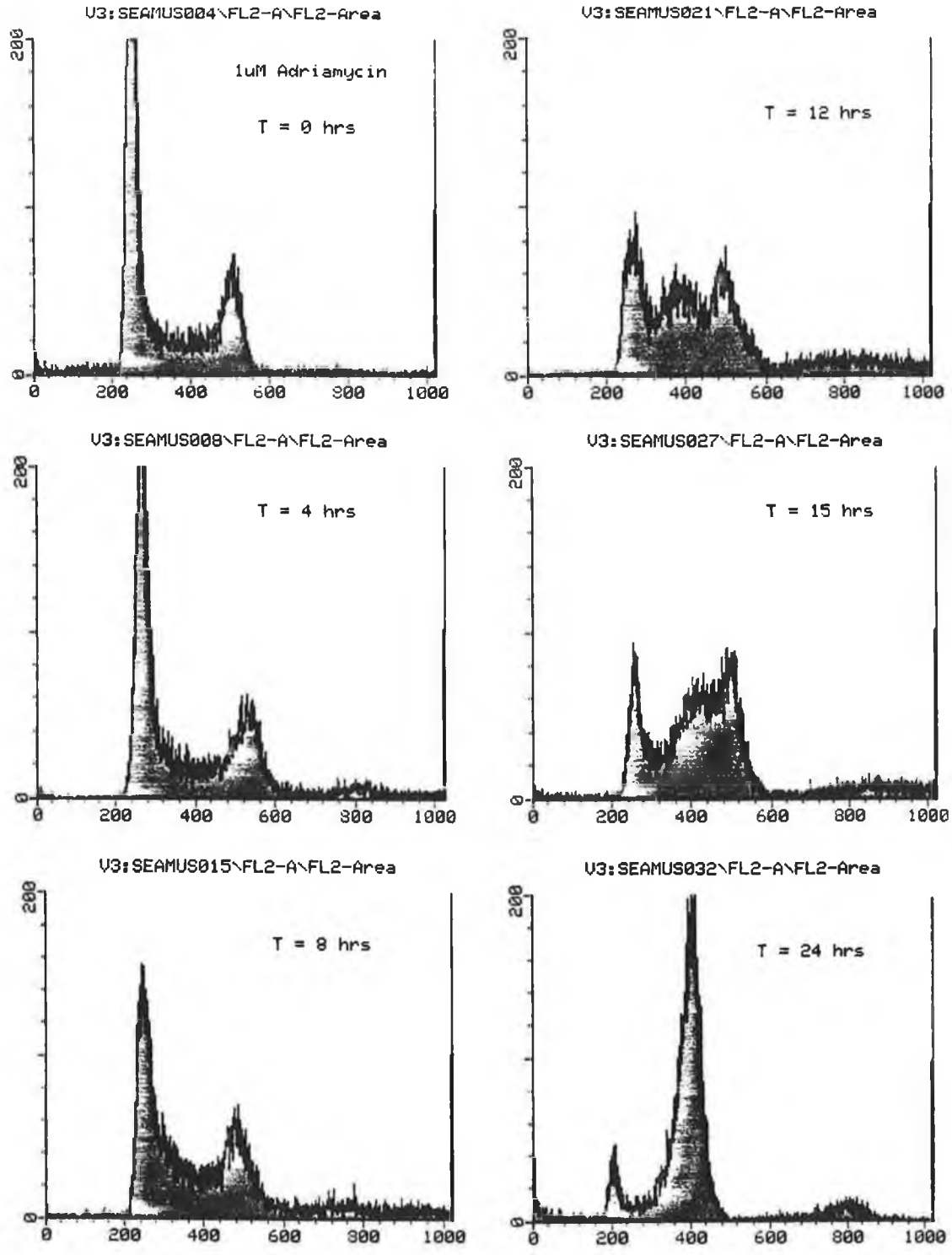

Figure 3.8.4 (b): Cell cycle distribution of DLKP-SQ treated with 1μM adriamycin for 2 hours. The graphs represent the DNA fluorescence as measured by flow cytometry of 10, 000 individual cells taken at different time points. The x-axis represents relative DNA fluorescence and the y-axis represents cell number. The left-hand peak is the G_1 peak and represents diploid cells. The peak on the right-hand is the G_2/M peak and represents tetraploid cells before cytokinesis of mitosis. Cells between the two peaks are in the S phase, i.e. cells which are replicating their DNA and thus have an increasing amount of DNA fluoresence.

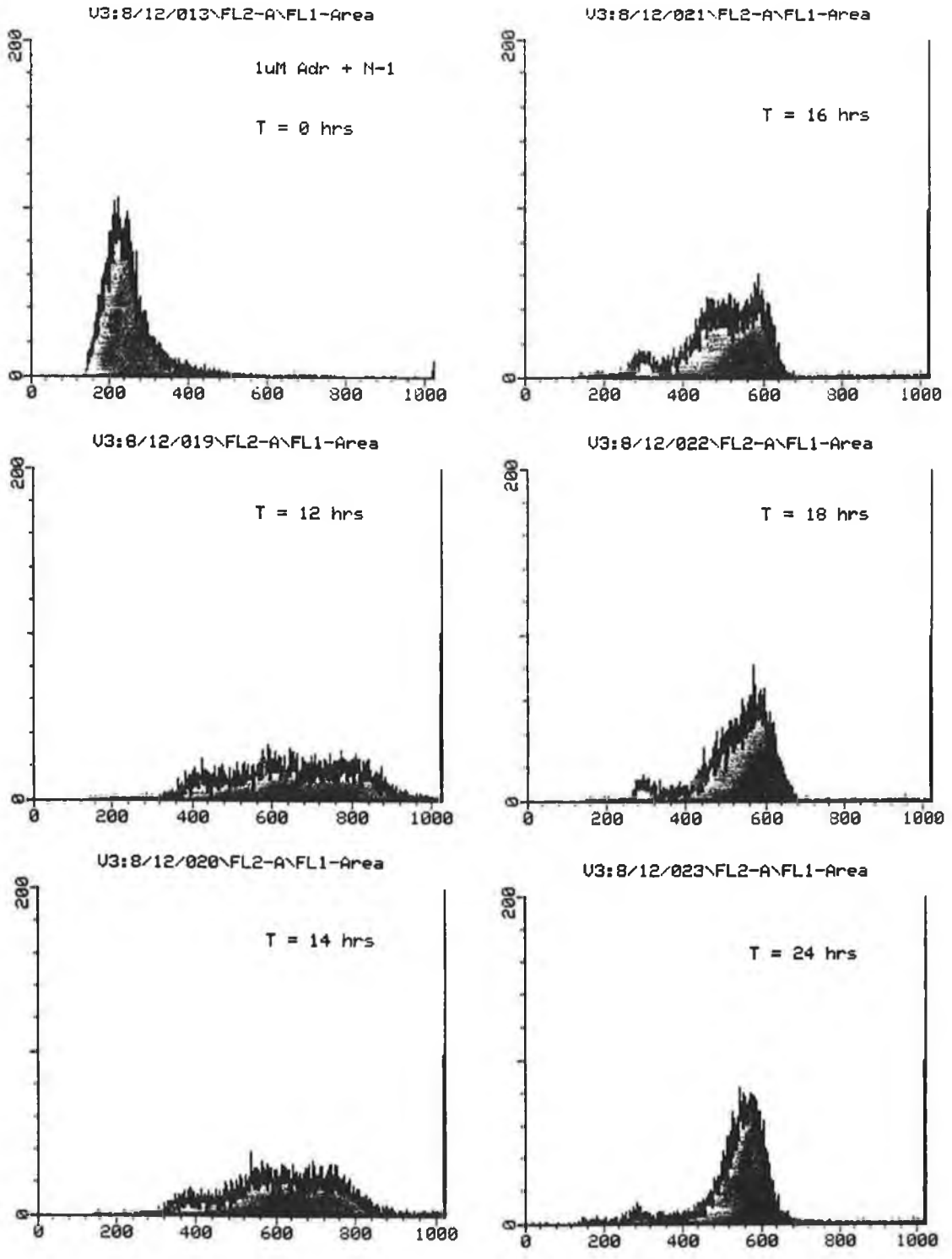

Figure 3.8.5 (a): Cell cycle distribution of DLKP-SQ treated 1μM adriamycin for 2 hours plus 30μM N-1 for 24 hours. The graphs represent the DNA fluorescence as measured by flow cytometry of 10, 000 individual cells taken at different time points. The x-axis represents relative DNA fluorescence and the y-axis represents cell number. The left-hand peak is the G_1 peak and represents diploid cells. The peak on the right-hand is the G_2/M peak and represents tetraploid cells before cytokinesis of mitosis. fluoresence. Cells between the two peaks are in the S phase, i.e. cells which are replicating their DNA and thus have an increasing amount of DNA fluoresence.

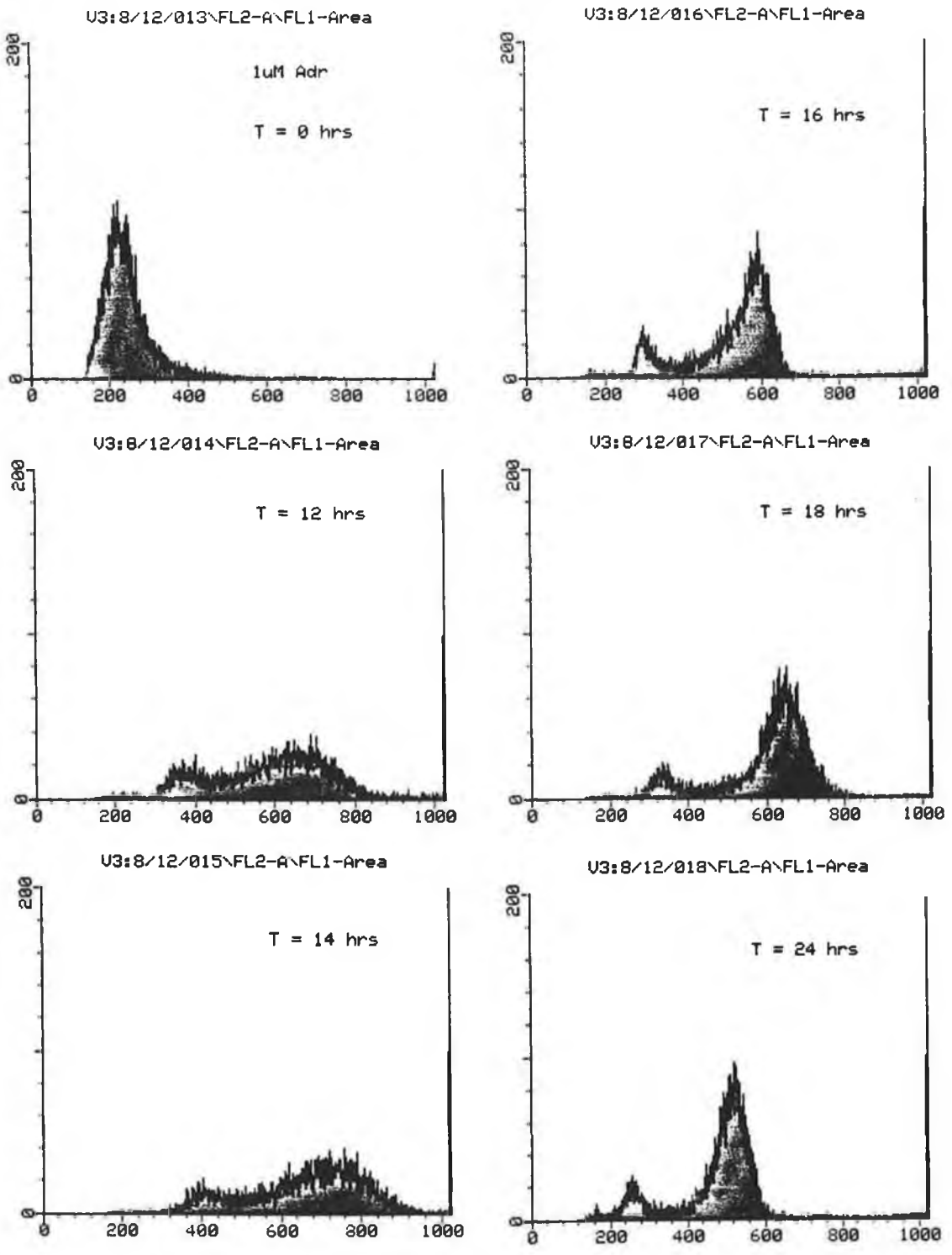

Figure 3.8.5 (b): Cell cycle distribution of DLKP-SQ treated with 1μM adriamycin for 2 hours. The graphs represent the DNA fluorescence as measured by flow cytometry of 10, 000 individual cells taken at different time points. The x-axis represents relative DNA fluorescence and the y-axis represents cell number. The left-hand peak is the G_1 peak and represents diploid cells. The peak on the right-hand is the G_2/M peak and represents tetraploid cells before cytokinesis of mitosis. Cells between the two peaks are in the S phase, i.e. cells which are replicating their DNA and thus have an increasing amount of DNA fluoresence.

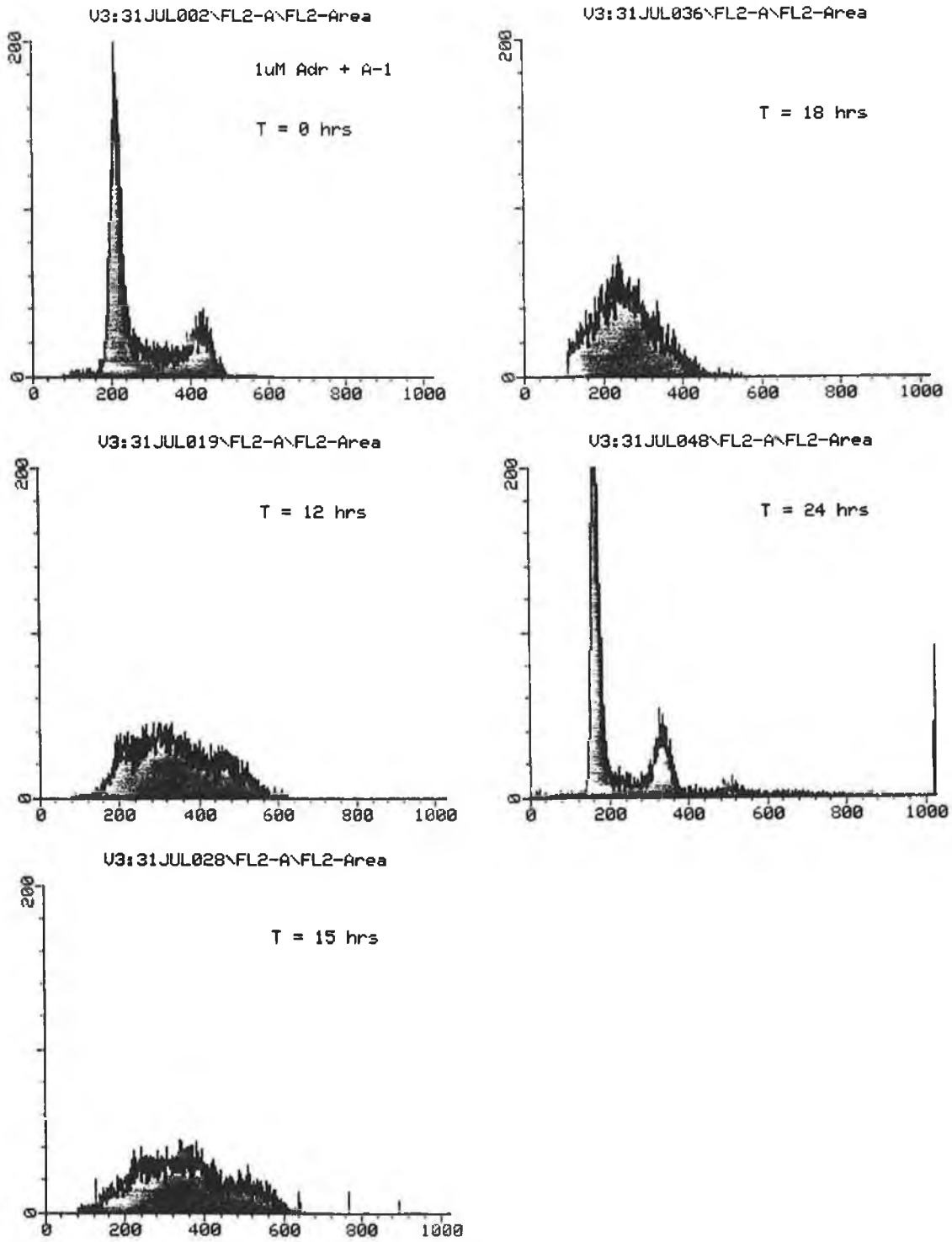

Figure 3.8.6 (a): Cell cycle distribution of DLKP-SQ treated 1μM adriamycin for 2 hours plus 200μM A-1 for 24 hours. The graphs represent the DNA fluorescence as measured by flow cytometry of 10, 000 individual cells taken at different time points. The x-axis represents relative DNA fluorescence and the y-axis represents cell number. The left-hand peak is the G_1 peak and represents diploid cells. The peak on the right-hand is the G_2/M peak and represents tetraploid cells before cytokinesis of mitosis. Cells between the two peaks are in the S phase, i.e. cells which are replicating their DNA and thus have an increasing amount of DNA fluoresence.

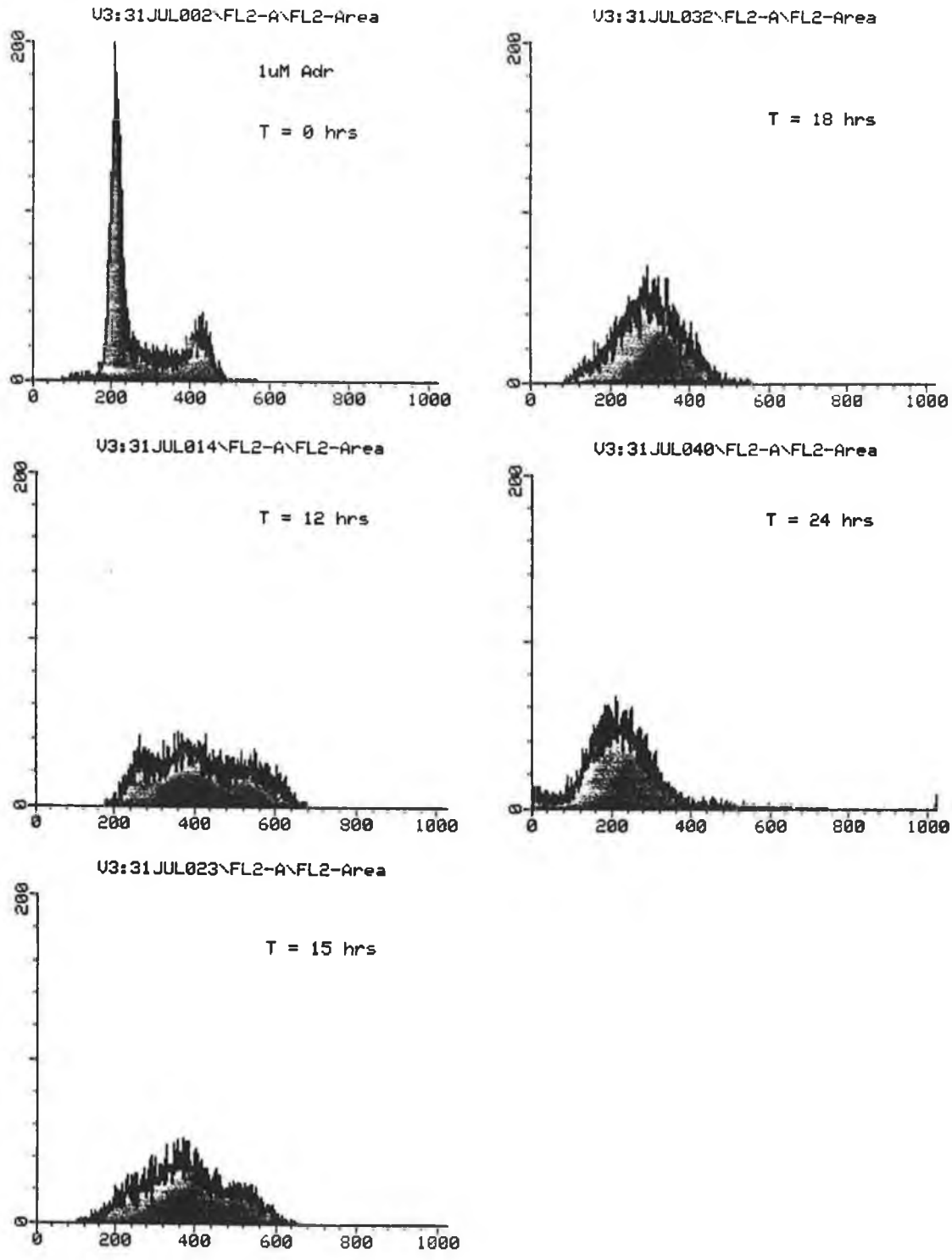

Figure 3.8.6 (b): Cell cycle distribution of DLKP-SQ treated with 1μM adriamycin for 2 hours. The graphs represent the DNA fluorescence as measured by flow cytometry of 10, 000 individual cells taken at different time points. The x-axis represents relative DNA fluorescence and the y-axis represents cell number. The left-hand peak is the G_1 peak and represents diploid cells. The peak on the right-hand is the G_2/M peak and represents tetraploid cells before cytokinesis of mitosis. Cells between the two peaks are in the S phase, i.e. cells which are replicating their DNA and thus have an increasing amount of DNA fluoresence.

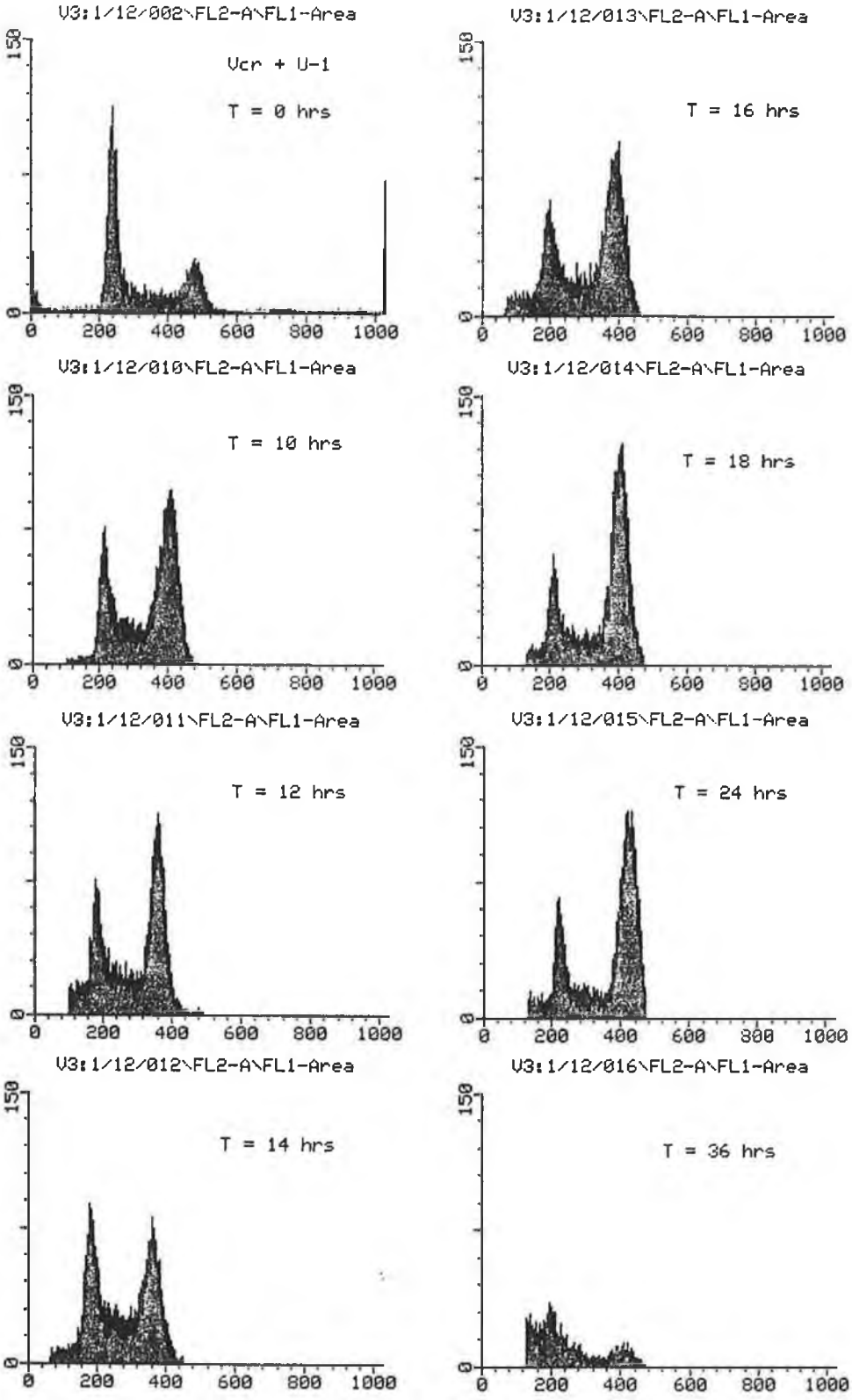

Figure 3.8.7 (a): Cell cycle distribution of DLKP-SQ treated with 50ng/ml vincristine for 2 hours plus 140μM U-1 for 24 hours. The graphs represent the DNA fluorescence as measured by flow cytometry of 10, 000 individual cells taken at different time points. The x-axis represents relative DNA fluorescence and the y-axis represents cell number. The left-hand peak is the G_1 peak and represents diploid cells. The peak on the right-hand is the G_2/M peak and represents tetraploid cells before cytokinesis of mitosis. Cells between the two peaks are in the S phase, i.e. cells which are replicating their DNA and thus have an increasing amount of DNA fluoresence.

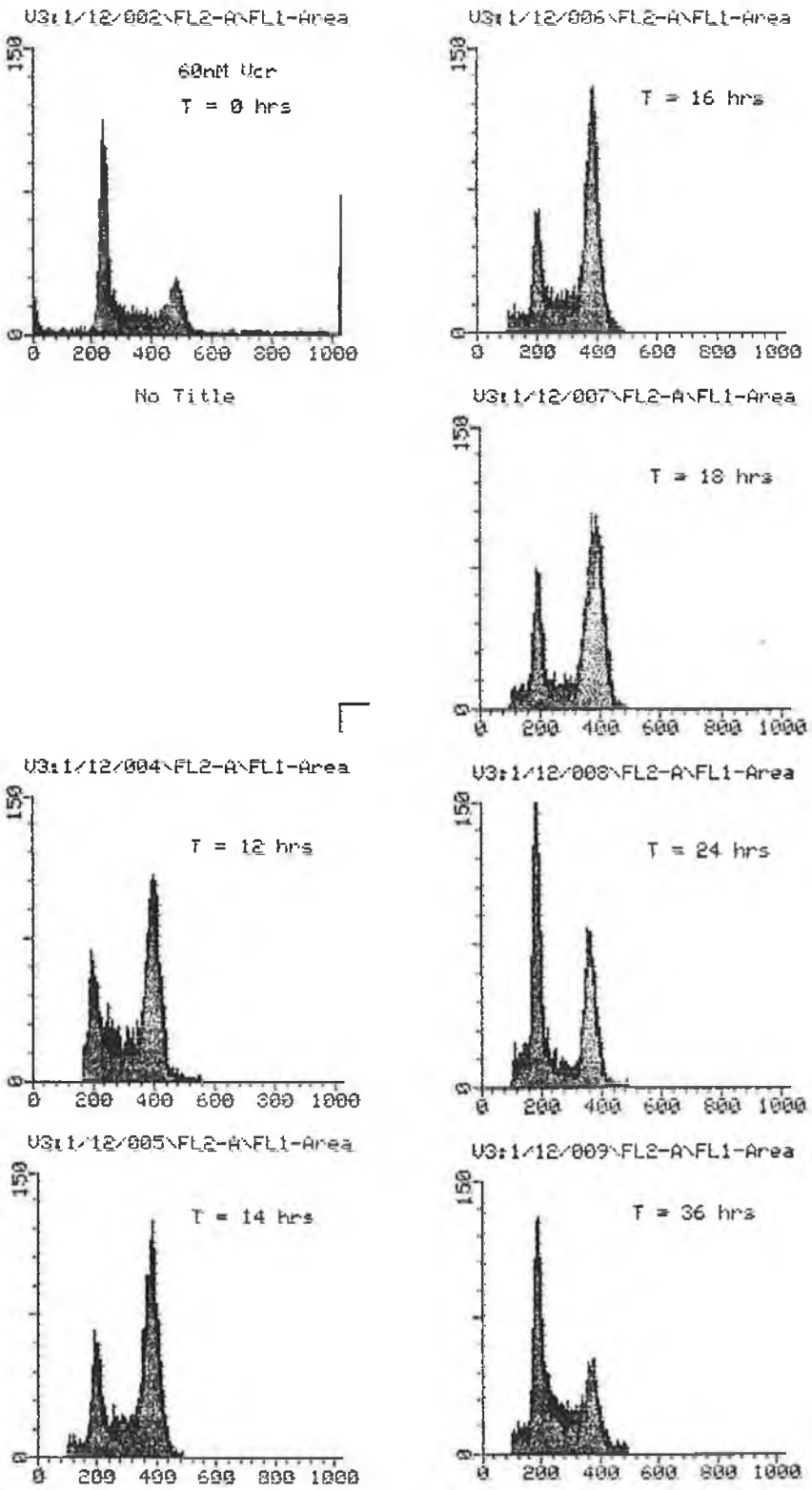

Figure 3.8.7 (b): Cell cycle distribution of DLKP-SQ treated with 50ng/ml vincristine for 2 hours. The graphs represent the DNA fluorescence as measured by flow cytometry of 10, 000 individual cells taken at different time points. The x-axis represents relative DNA fluorescence and the y-axis represents cell number. The left-hand peak is the G_1 peak and represents diploid cells. The peak on the right-hand is the G_2/M peak and represents tetraploid cells before cytokinesis of mitosis. Cells between the two peaks are in the S phase, i.e. cells which are replicating their DNA and thus have an increasing amount of DNA fluoresence.

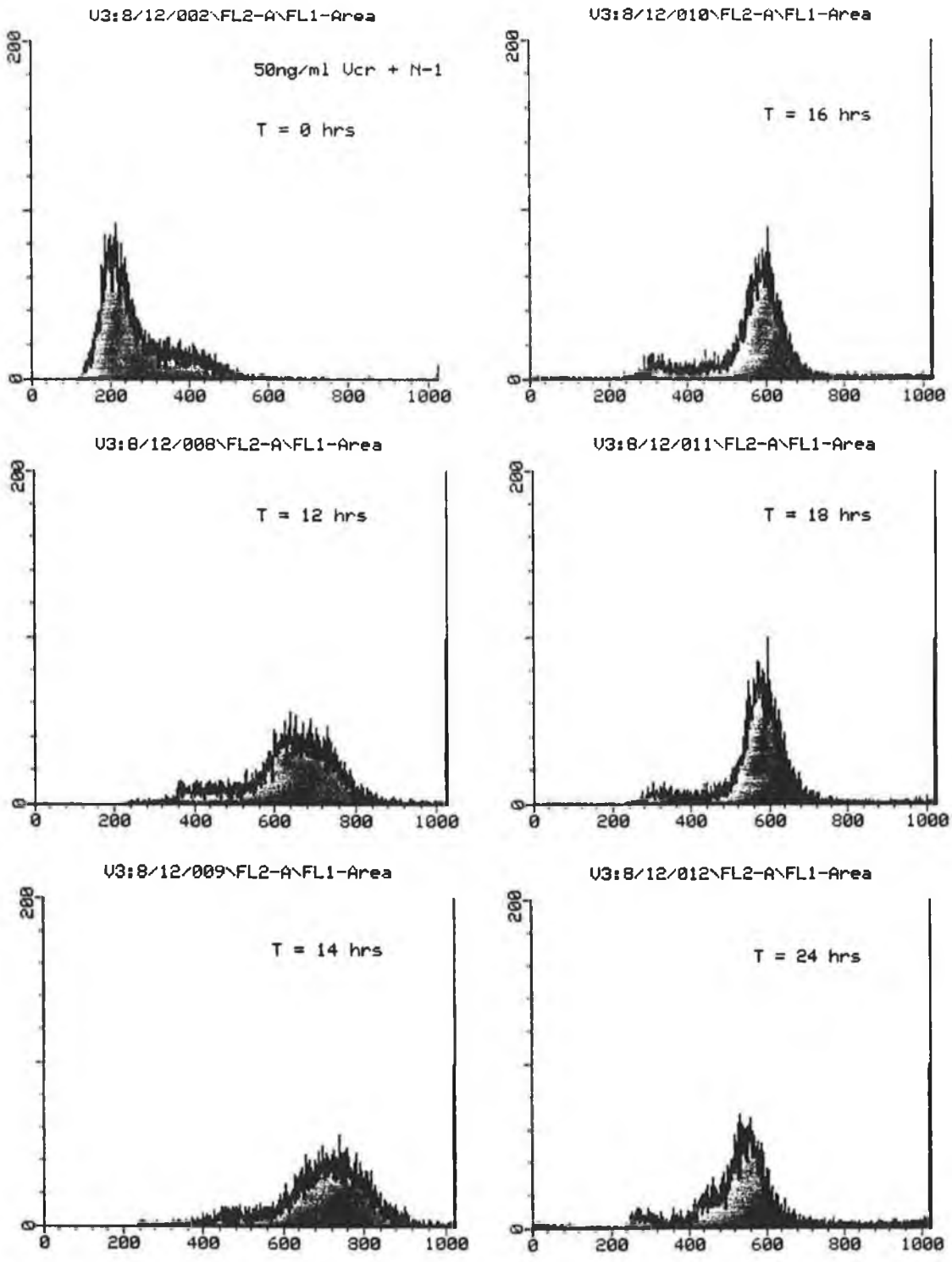

Figure 3.8.8 (a): Cell cycle distribution of DLKP-SQ treated with 50ng/ml vincristine for 2 hours plus 30μM N-1 for 24 hours. The graphs represent the DNA fluorescence as measured by flow cytometry of 10, 000 individual cells taken at different time points. The x-axis represents relative DNA fluorescence and the y-axis represents cell number. The left-hand peak is the G_1 peak and represents diploid cells. The peak on the right-hand is the G_2/M peak and represents tetraploid cells before cytokinesis of mitosis. Cells between the two peaks are in the S phase, i.e. cells which are replicating their DNA and thus have an increasing amount of DNA fluoresence.

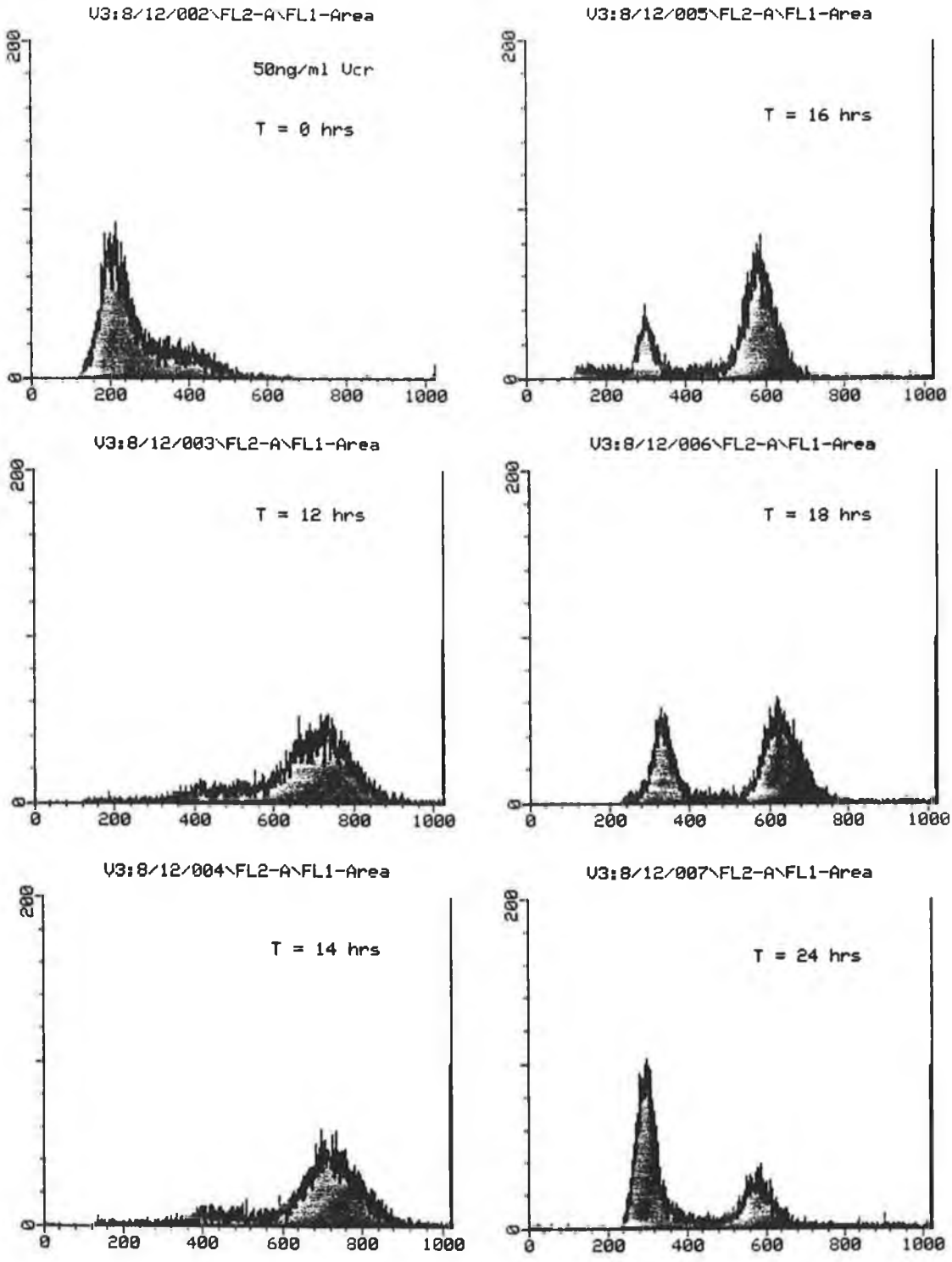

Figure 3.8.8 (b): Cell cycle distribution of DLKP-SQ treated with 50ng/ml vincristine for 2 hours. The graphs represent the DNA fluorescence as measured by flow cytometry of 10, 000 individual cells taken at different time points. The x-axis represents relative DNA fluorescence and the y-axis represents cell number. The left-hand peak is the G_1 peak and represents diploid cells. The peak on the right-hand is the G_2/M peak and represents tetraploid cells before cytokinesis of mitosis. Cells between the two peaks are in the S phase, i.e. cells which are replicating their DNA and thus have an increasing amount of DNA fluoresence.

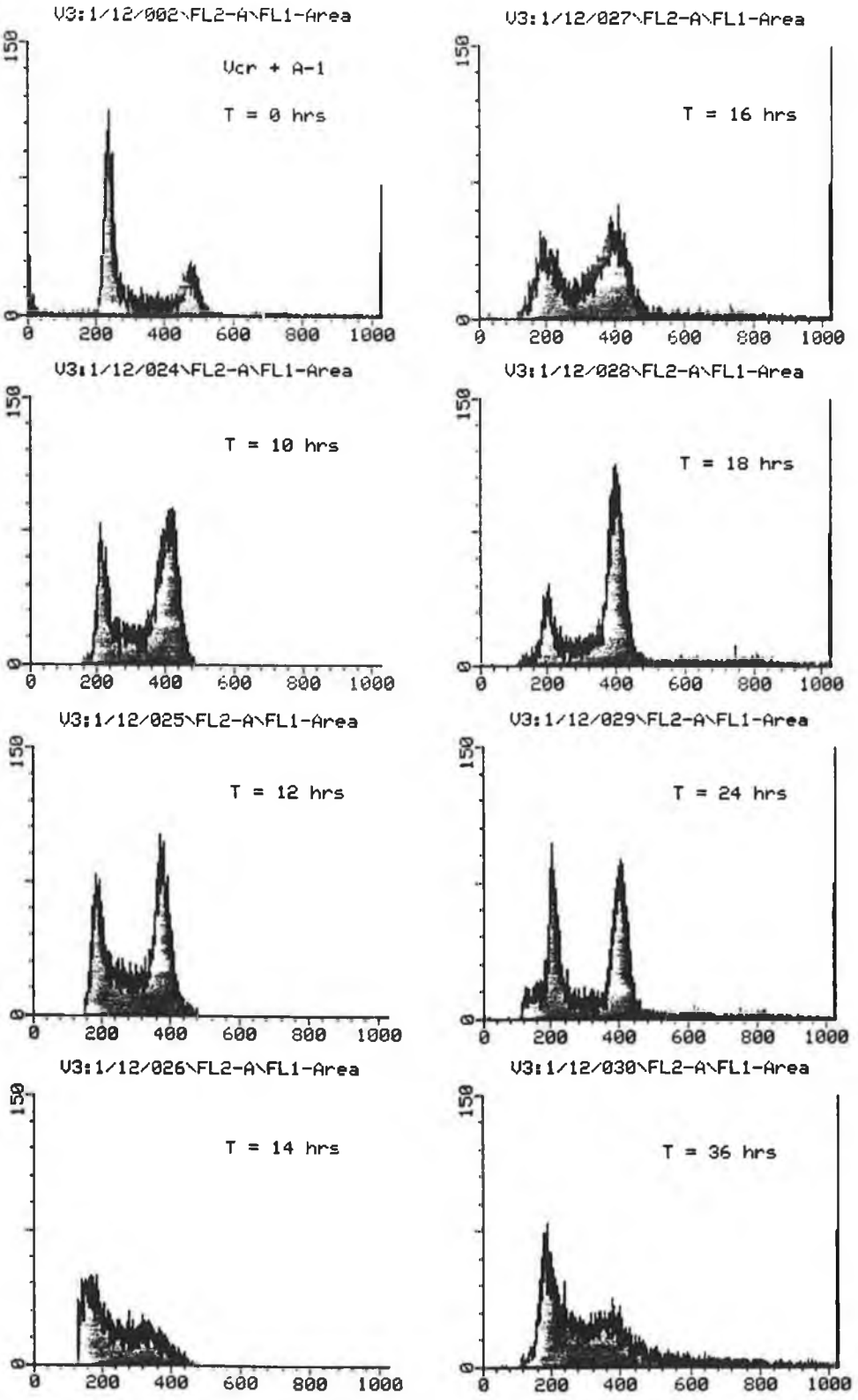

Figure 3.8.9: Cell cycle distribution of DLKP-SQ treated with 50ng/ml vincristine for 2 hours plus 200μM A-1 for 24 hours. The graphs represent the DNA fluorescence as measured by flow cytometry of 10, 000 individual cells taken at different time points. The x-axis represents relative DNA fluorescence and the y-axis represents cell number. The left-hand peak is the G_1 peak and represents diploid cells. The peak on the right-hand is the G_2/M peak and represents tetraploid cells before cytokinesis of mitosis. Cells between the two peaks are in the S phase, i.e. cells which are replicating their DNA and thus have an increasing amount of DNA fluoresence.

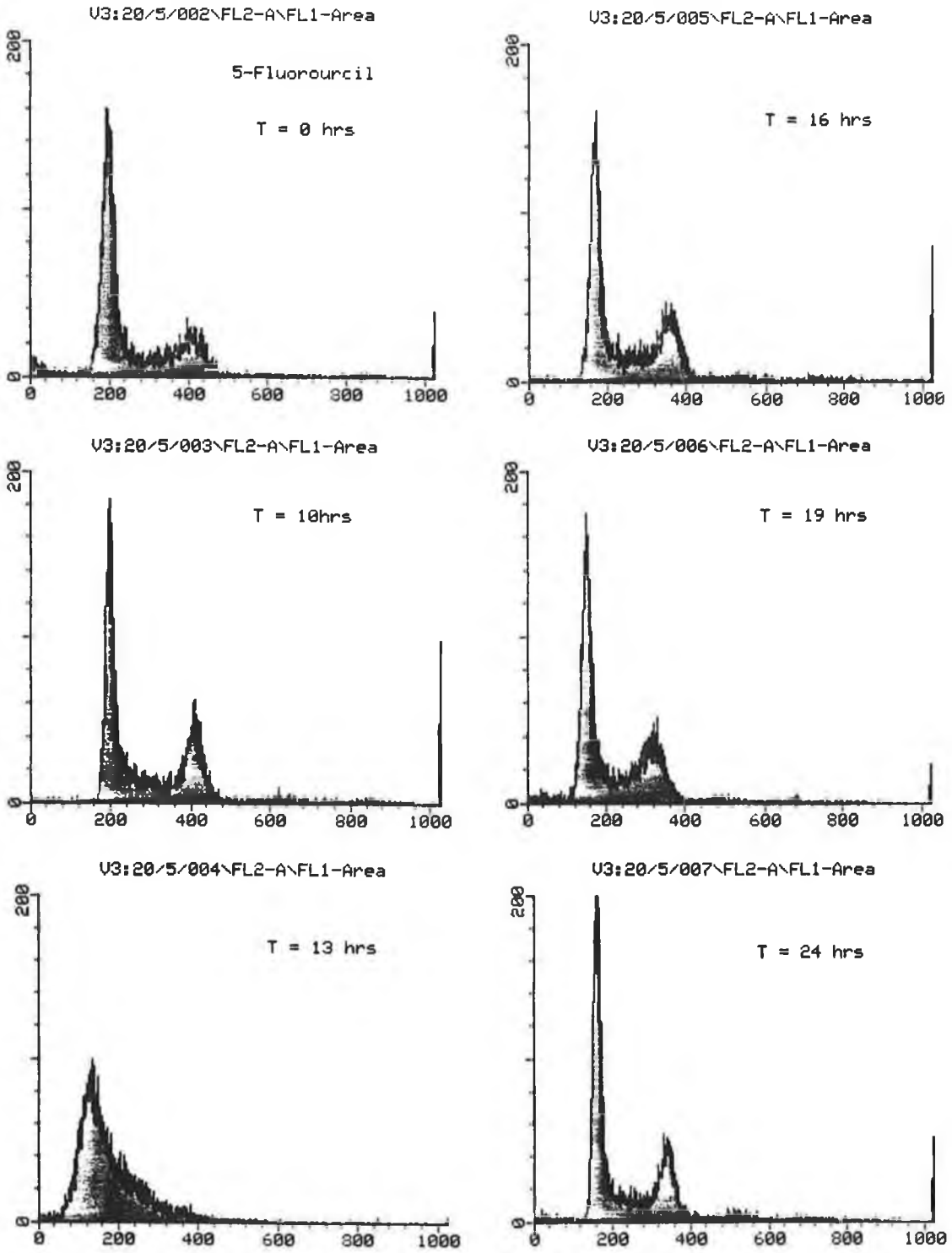

Figure 3.8.10: Cell cycle distribution of DLKP-SQ treated with 190μM 5-fluorouracil for 2 hours. The graphs represent the DNA fluorescence as measured by flow cytometry of 10, 000 individual cells taken at different time points. The x-axis represents relative DNA fluorescence and the y-axis represents cell number. The left-hand peak is the G_1 peak and represents diploid cells. The peak on the right-hand is the G_2/M peak and represents tetraploid cells before cytokinesis of mitosis. Cells between the two peaks are in the S phase, i.e. cells which are replicating their DNA and thus have an increasing amount of DNA fluoresence.

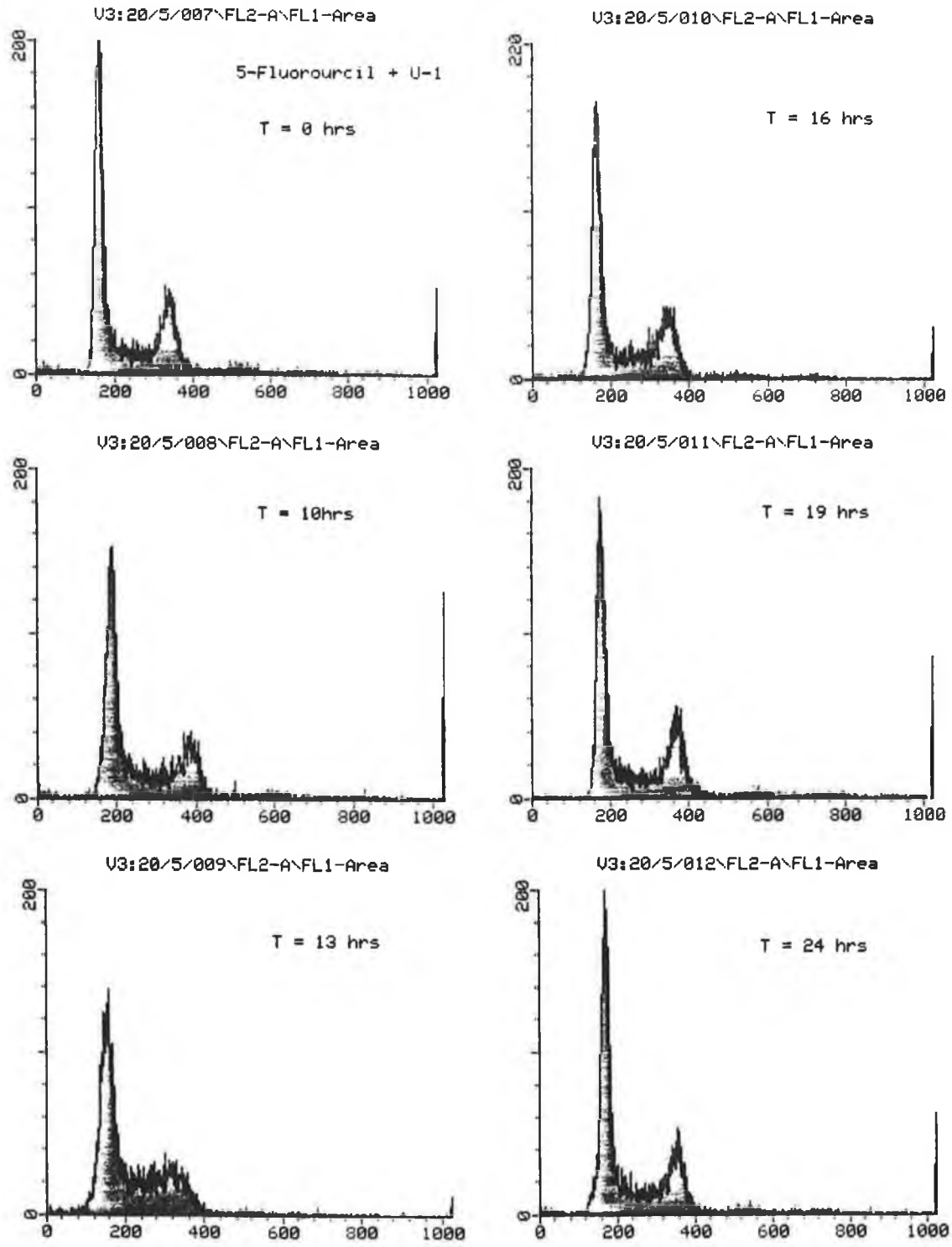

Figure 3.8.11: Cell cycle distribution of DLKP-SQ treated with 190μM 5-fluorouracil for 2 hours plus 140μM U-1 for 24 hours. The graphs represent the DNA fluorescence as measured by flow cytometry of 10, 000 individual cells taken at different time points. The x-axis represents relative DNA fluorescence and the y-axis represents cell number. The left-hand peak is the G_1 peak and represents diploid cells. The peak on the right-hand is the G_2/M peak and represents tetraploid cells before cytokinesis of mitosis. Cells between the two peaks are in the S phase, i.e. cells which are replicating their DNA and thus have an increasing amount of DNA fluoresence.

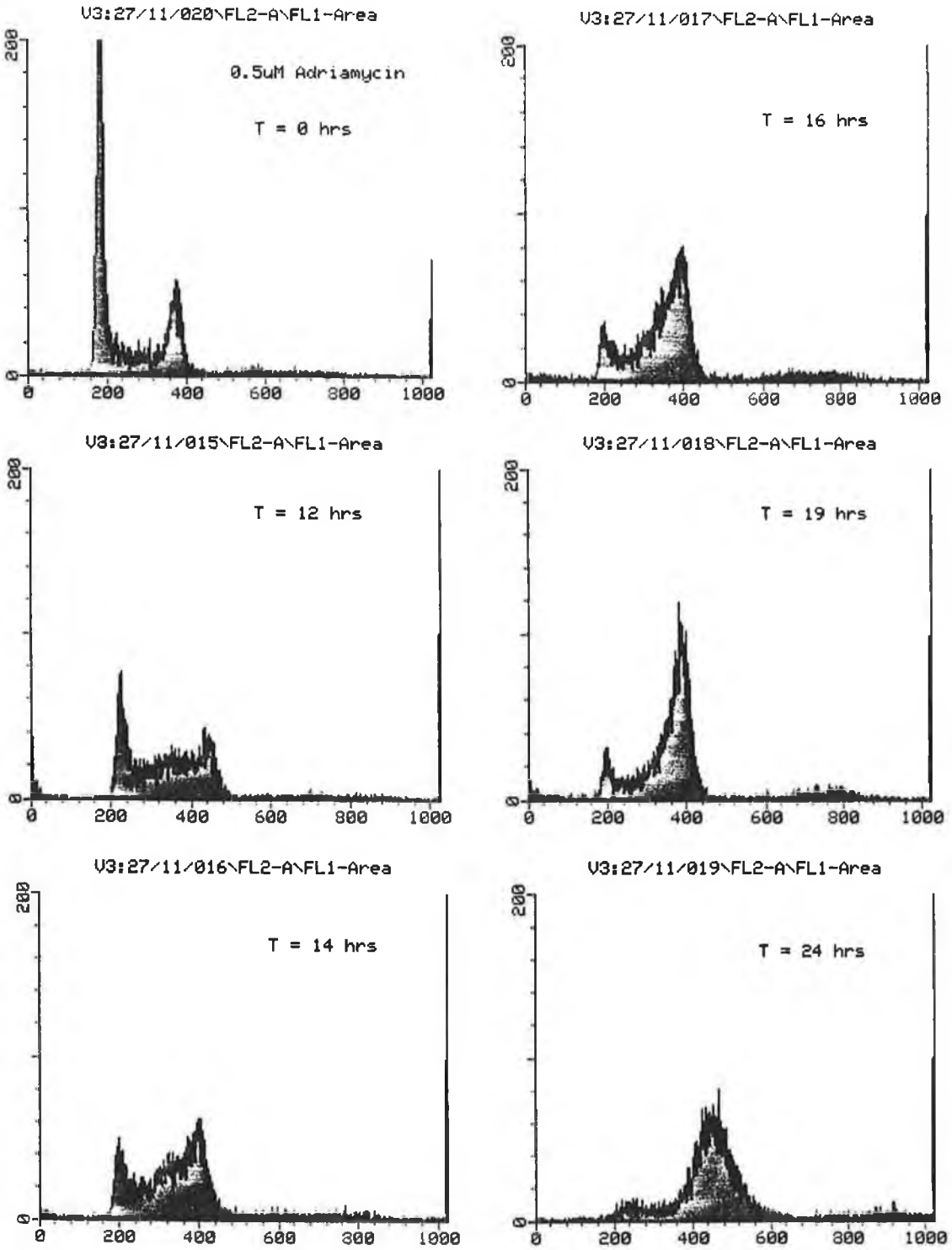

Figure 3.8.12: Cell cycle distribution of DLKP-SQ treated with 0.5μM adriamycin for 2 hours. The graphs represent the DNA fluorescence as measured by flow cytometry of 10, 000 individual cells taken at different time points. The x-axis represents relative DNA fluorescence and the y-axis represents cell number. The left-hand peak is the G_1 peak and represents diploid cells. The peak on the right-hand is the G_2/M peak and represents tetraploid cells before cytokinesis of mitosis. Cells between the two peaks are in the S phase, i.e. cells which are replicating their DNA and thus have an increasing amount of DNA fluoresence.

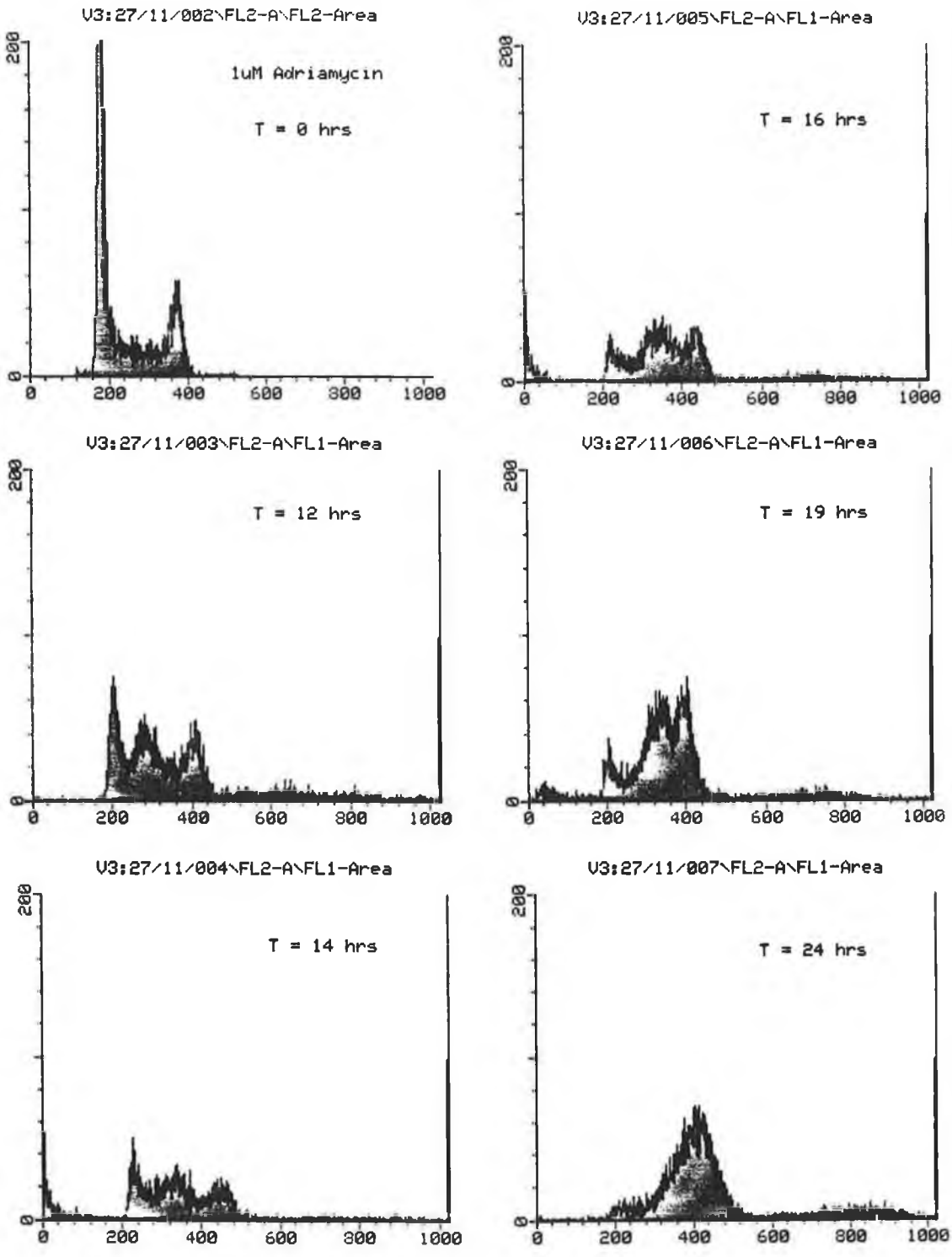

Figure 3.8.13: Cell cycle distribution of DLKP-SQ treated with 1μM adriamycin for 2 hours. The graphs represent the DNA fluorescence as measured by flow cytometry of 10, 000 individual cells taken at different time points. The x-axis represents relative DNA fluorescence and the y-axis represents cell number. The left-hand peak is the G_1 peak and represents diploid cells. The peak on the right-hand is the G_2/M peak and represents tetraploid cells before cytokinesis of mitosis. Cells between the two peaks are in the S phase, i.e. cells which are replicating their DNA and thus have an increasing amount of DNA fluoresence.

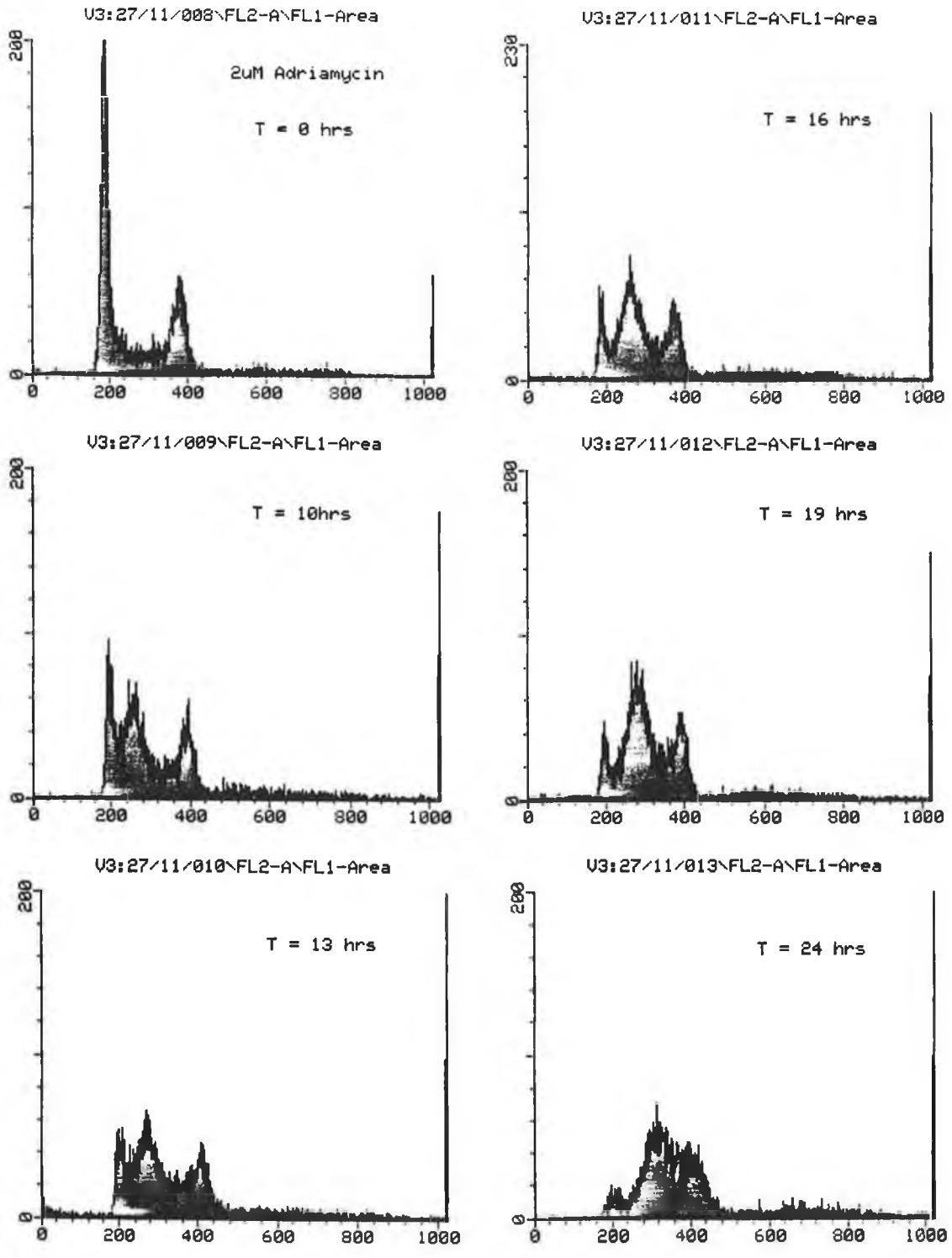

Figure 3.8.14: Cell cycle distribution of DLKP-SQ treated with 2μM adriamycin for 2 hours. The graphs represent the DNA fluorescence as measured by flow cytometry of 10, 000 individual cells taken at different time points. The x-axis represents relative DNA fluorescence and the y-axis represents cell number. The left-hand peak is the G_1 peak and represents diploid cells. The peak on the right-hand is the G_2/M peak and represents tetraploid cells before cytokinesis of mitosis. Cells between the two peaks are in the S phase, i.e. cells which are replicating their DNA and thus have an increasing amount of DNA fluoresence.

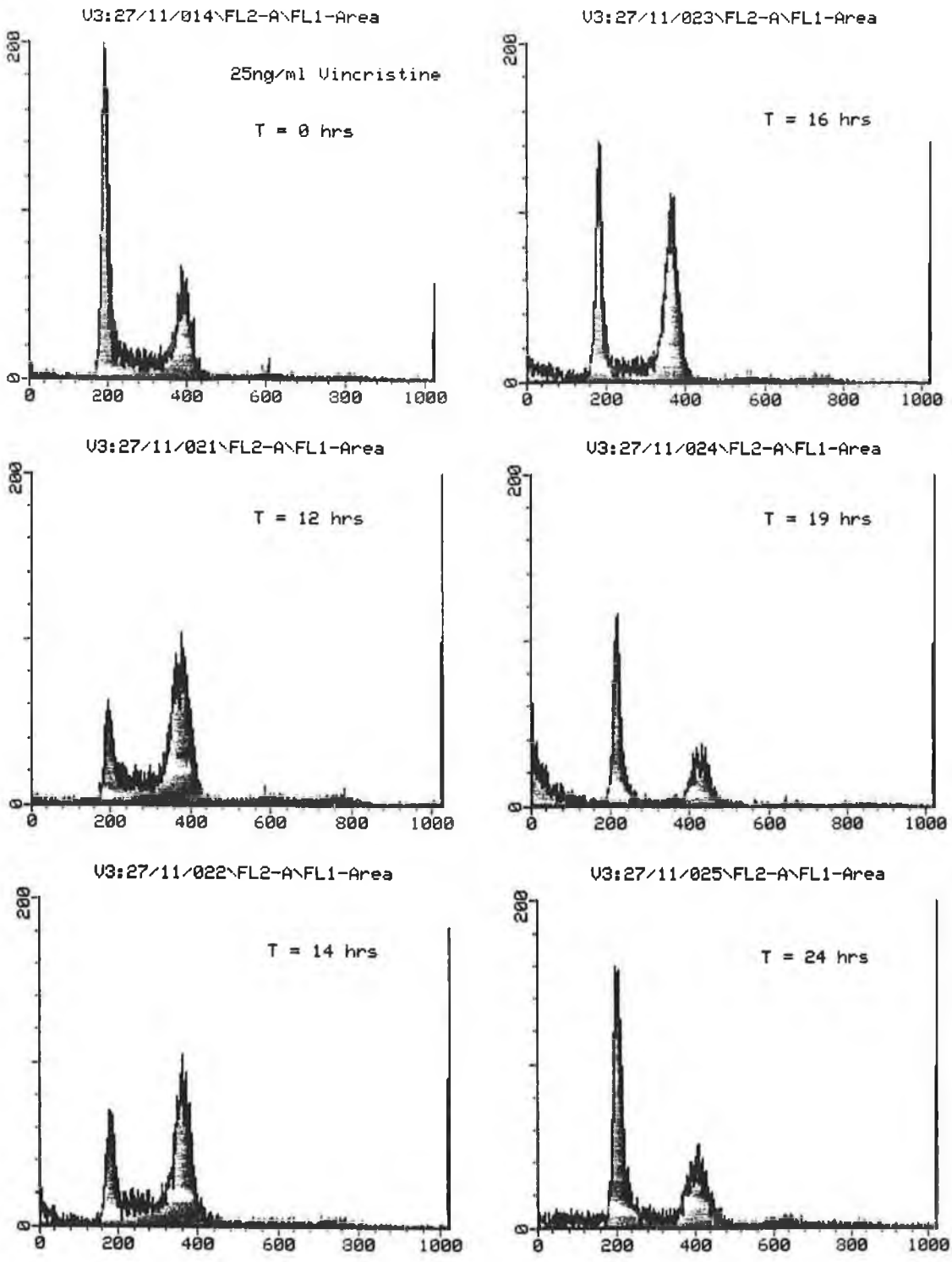

Figure 3.8.15: Cell cycle distribution of DLKP-SQ treated with 25ng/ml vincristine for 2 hours. The graphs represent the DNA fluorescence as measured by flow cytometry of 10, 000 individual cells taken at different time points. The x-axis represents relative DNA fluorescence and the y-axis represents cell number. The left-hand peak is the G_1 peak and represents diploid cells. The peak on the right-hand is the G_2/M peak and represents tetraploid cells before cytokinesis of mitosis. Cells between the two peaks are in the S phase, i.e. cells which are replicating their DNA and thus have an increasing amount of DNA fluoresence.

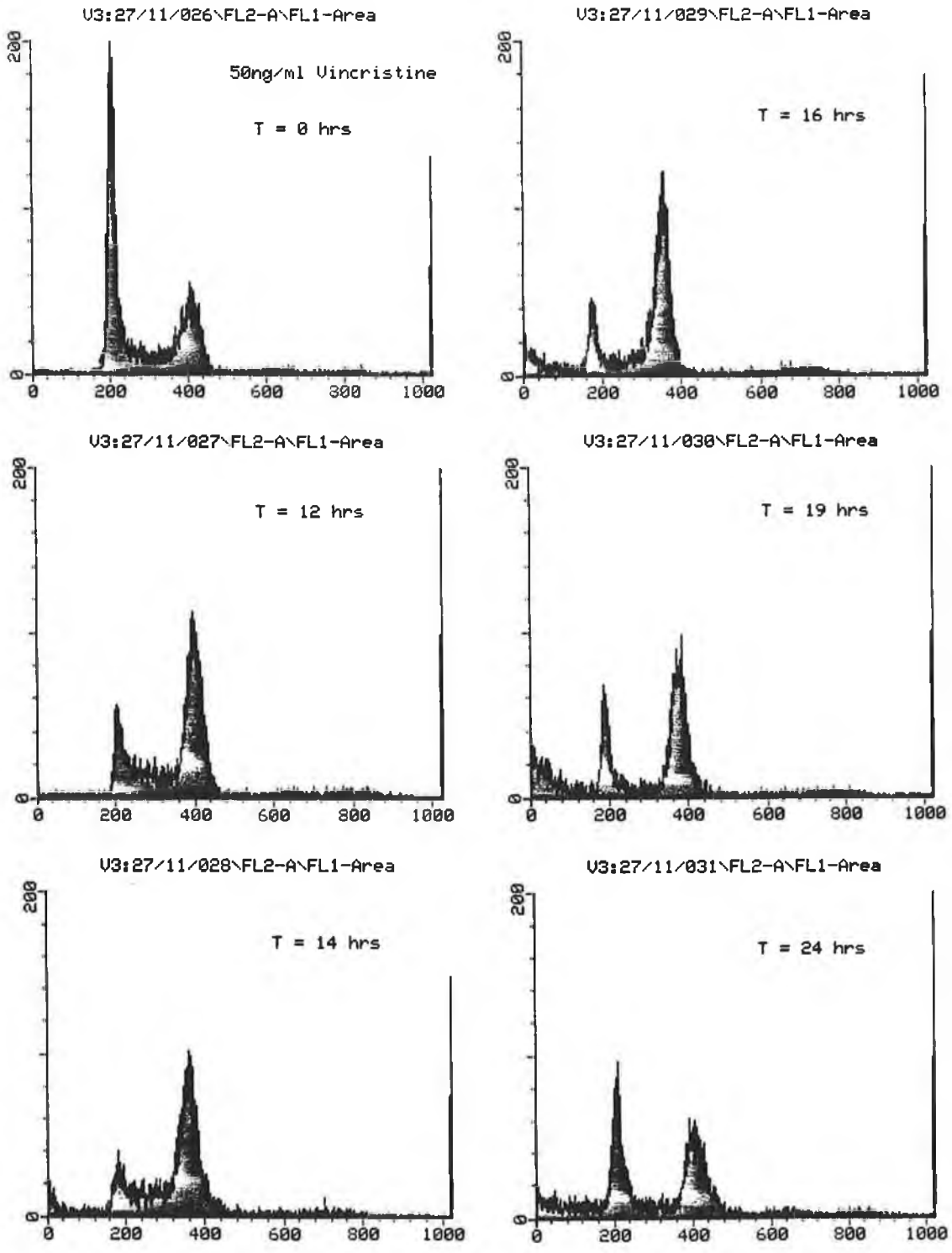

Figure 3.8.16: Cell cycle distribution of DLKP-SQ treated with 50ng/ml vincristine for 2 hours. The graphs represent the DNA fluorescence as measured by flow cytometry of 10, 000 individual cells taken at different time points. The x-axis represents relative DNA fluorescence and the y-axis represents cell number. The left-hand peak is the G_1 peak and represents diploid cells. The peak on the right-hand is the G_2/M peak and represents tetraploid cells before cytokinesis of mitosis. Cells between the two peaks are in the S phase, i.e. cells which are replicating their DNA and thus have an increasing amount of DNA fluoresence.

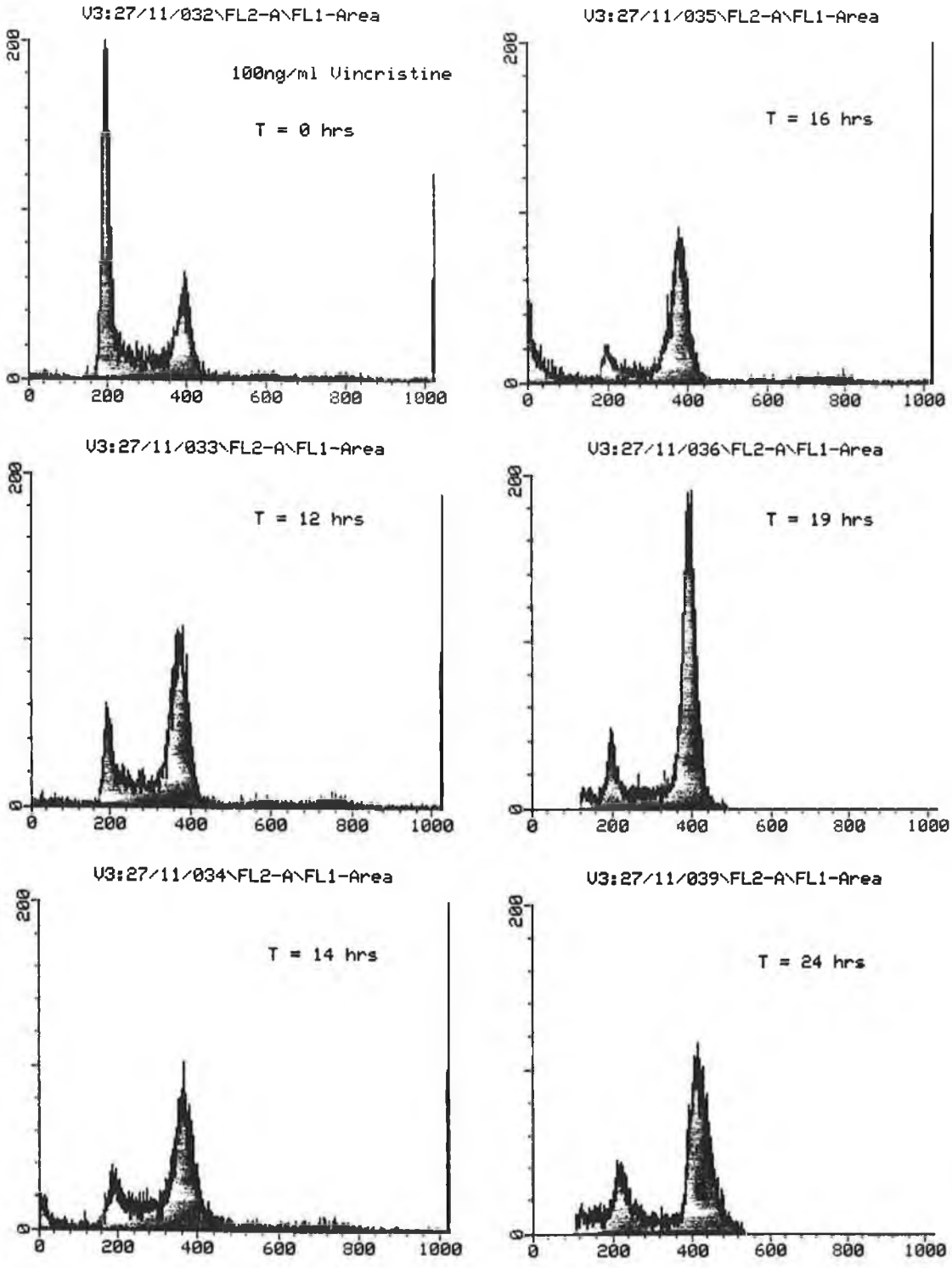

Figure 3.8.17: Cell cycle distribution of DLKP-SQ treated with 100ng/ml vincristine for 2 hours. The graphs represent the DNA fluorescence as measured by flow cytometry of 10, 000 individual cells taken at different time points. The x-axis represents relative DNA fluorescence and the y-axis represents cell number. The left-hand peak is the G_1 peak and represents diploid cells. The peak on the right-hand is the G_2/M peak and represents tetraploid cells before cytokinesis of mitosis. Cells between the two peaks are in the S phase, i.e. cells which are replicating their DNA and thus have an increasing amount of DNA fluoresence.

3.9 Time-Lapse Videomicroscopy

The results from Section 3.6 demonstrated that the test compounds, N-1, O-1 and U-1 exert their synergistic cytotoxic effect during the first 24 hours post-treatment with adriamycin or vincristine but not 5-fluorouracil. Flow cytometric analysis (Section 3.8) showed that there was a difference in cell cycle distribution during the first 24 hours after pulse exposure between adriamycin and adriamycin plus U-1 or N-1 and between vincristine and vincristine plus U-1 or N-1. Therefore, while there was an increased cytotoxicity in cells were exposed to N-1, O-1 or U-1 after adriamycin or vincristine exposure, and there was a difference in cell cycle distribution, there was no indication as to when the cells undergo cell death.

Time-lapse videomicroscopy permits the observation of the events which happen to cells following drug treatment. With this technique it was possible to follow in real time events such as cell rounding for mitosis and apoptosis. Mitosis was characterised by the rounding up of adherent cells followed by cytokinesis and reattachment of daughter cells to the surface of the flask. Cell death was classified as apoptotic on the basis of morphological events starting with rounding up of adherent cells, subsequent cell shrinkage and/or break-up into apoptotic bodies.

Using time-lapse videomicroscopy the kinetics of mitosis and apoptosis was followed in DLKP-SQ treated with U-1 alone for 24 hours, 2 hours pulse exposure to increasing concentrations of adriamycin, adriamycin and U-1 in combination, vincristine and vincristine plus U-1 in combination. Experiments were performed in 25cm^2 flasks and recording was started after cells were exposed to chemotherapeutic drug for two hours and washed twice with PBS (see Section 2.9).

Figure 3.9.1: DLKP-SQ exposed to 140μM U-1 for 24 hours and compared to the mitotic events in a drug-free control. Cell death was classified as apoptotic on the basis of morphological events starting with rounding up of adherent cells, subsequent cell shrinkage and/or break-up into apoptotic bodies. Cell death and mitosis were scored at the time when rounding up of the cells first occurred. Typically 100 cells in the microscope field were followed.

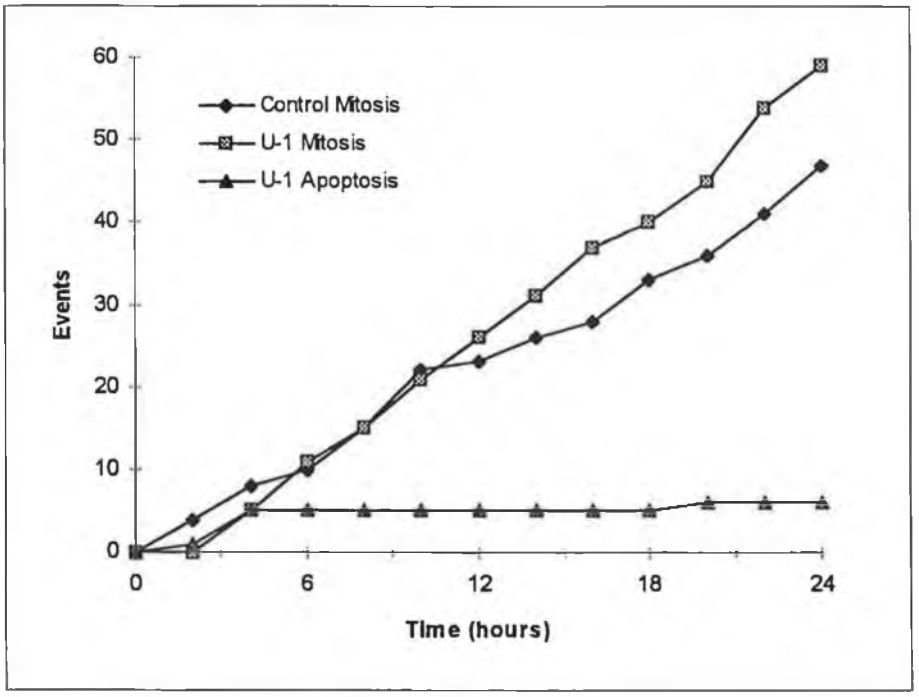

Treatment of DLKP-SQ with 140μM U-1 for 24 hours initially decreased the rate of mitosis (Figure 3.9.3). After 3 hours the rate increased to a rate similar to the drug free control. There was a low level of apoptosis during the first 6 hours of exposure.

Figure 3.9.2: Adriamycin alone and in combination with U-1. Cell death was classified as apoptotic on the basis of morphological events starting with rounding up of adherent cells, subsequent cell shrinkage and/or break-up into apoptotic bodies. Cell death and mitosis were scored at the time when rounding up of the cells first occurred. Typically 100 cells in the microscope field were followed.

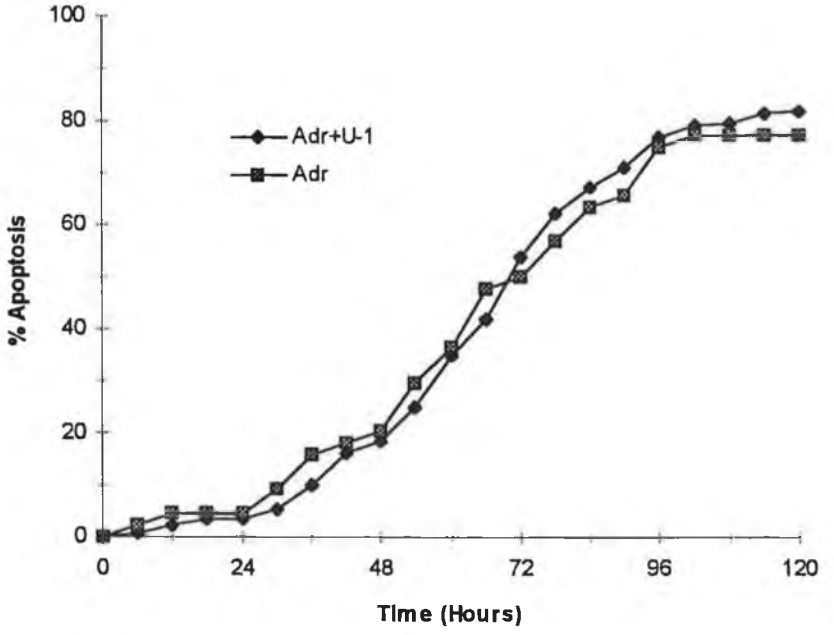

The apoptotic rate in 1μM treated adriamycin was low during the first 24 hours, the rate subsequently increased after 24 until 96 hours (Figure 3.9.2). The rate of apoptosis in 1μM treated samples exposed to 140μM U-1 for 24 hours followed a similar pattern to 1μM adriamycin alone i.e. the apoptotic rate was low during the first 24 hours and the rate increased after 24 until 96 hours. No mitotic events was observed in 1μM adriamycin or 1μM adriamycin plus 140μM U-1 treated samples.

Figure 3.9.3: Rate of apoptosis and mitosis in vincristine treated and vincristine plus U-1 treated DLKP-SQ. Cell death was classified as apoptotic on the basis of morphological events starting with rounding up of adherent cells, subsequent cell shrinkage and/or break-up into apoptotic bodies. Cell death and mitosis were scored at the time when rounding up of the cells first occurred. Typically 100 cells in the microscope field were followed.

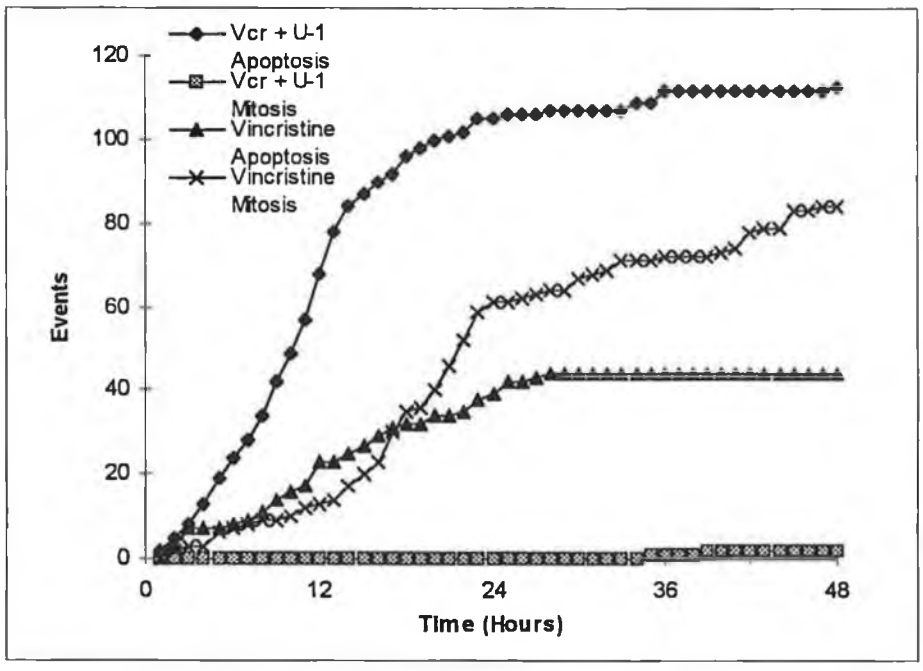

The rate of mitosis in 60nM vincristine treated DLKP-SQ cells was low up to 12 hours after exposure, the rate increased from 12 to 24 hours and then slowed from 24 to 48 hours (Figure 3.9.3). The rate of apoptosis steadily increased during the first 24 hours after exposure. After 24 hours there were no apoptotic events. In contrast to 60nM vincristine treated cells alone, subsequent exposure to 140μM U-1 resulted in an abolition of mitosis, with some mitosis occurring 36 hours after vincristine was removed. The rate of apoptosis increased dramatically during the first 12 hours of U-1 exposure, this rate decreased from 12 to 36 hours. No apoptosis was observed after 36 hours. U-1 alone induced a low level of apoptosis (Figure 3.9.1).

Figure 3.9.4: The rate of mitosis and apoptosis in 0.5μM adriamycin treated DLKP-SQ hours and compared to the mitotic events in a drug-free control. Cell death was classified as apoptotic on the basis of morphological events starting with rounding up of adherent cells, subsequent cell shrinkage and/or break-up into apoptotic bodies. Cell death and mitosis were scored at the time when rounding up of the cells first occurred. Typically 100 cells in the microscope field were followed.

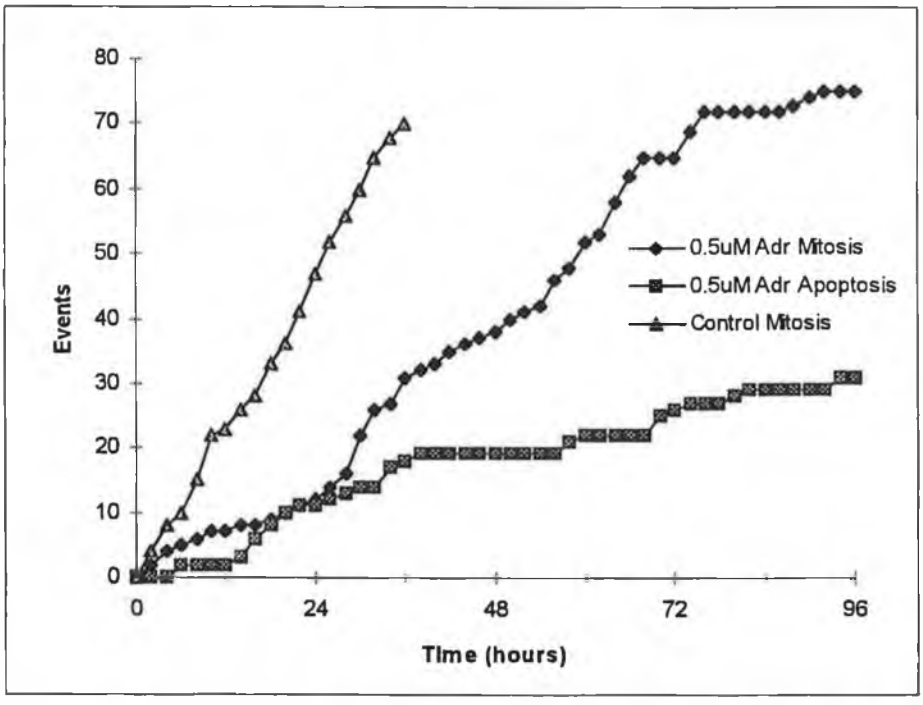

The rate of mitosis and apoptosis in 0.5μM adriamycin treated DLKP-SQ is given in Figure 3.9.4.

The rate of mitosis slowed during the initial 24 hours after exposure to 0.5μM adriamycin. After this time the rate of mitosis increased to that similar in the drug-free treated control. The rate of apoptosis increased 12 to 24 hours after adriamycin exposure and remained elevated until 36 hours.

Figure 3.9.5: Kinetics of cell death in DLKP-SQ treated with increasing concentrations of adriamycin. Cell death was classified as apoptotic on the basis of morphological events starting with rounding up of adherent cells, subsequent cell shrinkage and/or break-up into apoptotic bodies. Cell death and mitosis were scored at the time when rounding up of the cells first occurred. Typically 100 cells in the microscope field were followed.

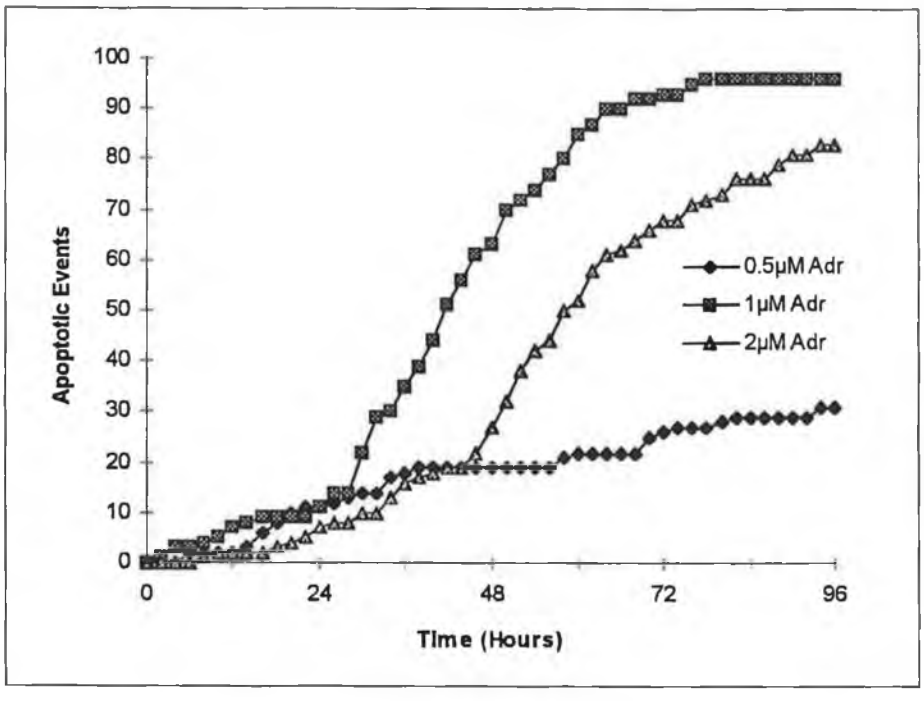

Kinetics of cell death in DLKP-SQ treated with increasing concentrations of adriamycin is given in Figure 3.9.5. In the 0.5μM adriamycin treated sample, the rate of apoptosis increased sharply 12 to 24 hours after adriamycin exposure and remained high until 36 hours. The apoptotic rate in 1μM treated adriamycin was similar to the rate for 0.5μM adriamycin during the first 24 hours. After this time the rate increased dramatically until 60 hours. 2μM adriamycin treatment resulted in apoptosis from 18 to 48 hours after exposure, after this time, the rate of apoptosis increased further. No mitotic events were observed in 1μM or 2μM adriamycin treated samples.

These results demonstrated that exposure of DLKP-SQ cells to increasing concentrations of adriamycin induced apoptosis predominantly 24 hours after drug removal. Mitosis was abolished with increasing concentrations. 140μM U-1 delayed mitosis for 12 hours and induced a low level of apoptosis during exposure. 1μM Adriamycin and U-1 in combination displayed no difference in the rate of apoptosis induced compared to adriamycin alone. This was surprising since the combination of adriamycin and U-1 demonstrated increased cytotoxicity to the cells. A 2 hour exposure to 60nM vincristine delayed mitosis for 12 hours; the rate increased from 12 to 24 hours and then slowed from 24 to 48 hours. The rate of apoptosis increased during the first 24 hours after exposure. 60nM vincristine treatment and subsequent exposure to 140μM U-1 resulted in an increased rate of apoptosis during the first 12 hours of U-1 exposure, which decreased from 12 to 36 hours, there were mitotic events until 12 hours after U-1 removal.

3.10 Cyclin E/CDK2 kinase activity

The adriamycin pulse exposure assays demonstrated that the enhanced cytotoxicity of adriamycin by N-1, O-1 and U-1 occurred during the first 24 hours after adriamycin removal (Section 3.7). Flow cytometric analysis (Section 3.8) also showed that by 24 hours the cells were arrested in the G_2/M phase. Previous to this arrest however was an increased delay in G_1/S and in the S phase transition.

To understand the effect of adriamycin and adriamycin plus U-1 in combination on the increased G_1/S delay, cyclin E/CDK2 complex kinase activity was studied. The transition from G_1 into S is controlled by the cyclin E/CDK2 complex and this is essential for the cell to begin DNA replication (see Section 1.3.1). The levels of cyclin E are regulated so that it is only transcribed during late G_1 and early S phase. Very little is known about the substrates of cyclin E but it is thought to activate E2F and thus transcription of S phase genes. Once cells enter the S phase cyclin E is rapidly degraded. Therefore by investigating the activity of the cyclin E/CDK2 complex it would be possible to examine the role that adriamycin plus U-1 in combination has on the increased G_1 arrest and delayed S phase transition as observed by flow cytometric analysis.

The kinase activity of the cyclin E/CDK2 complex was assayed as described in Section 2.12. Briefly, cells were set up in $25cm^2$ flasks 4 days before the experiment, they were then exposed to adriamycin or drug free media for two hours, washed twice with PBS, and drug-free media or U-1 added as appropriate. Samples were taken at various time points by trypsinising the cells and resuspending the resultant pellet in RIPA lysis buffer and stored at -80°C. The protein was quantified and 100μg of protein was immunoprecipated with cyclin E (Section 2.10), the immunoprecipitated cyclin E was resuspended in kinase buffer, and ^{32}P-labelled ATP and histone H1 (substrate) was added. The reaction mixture was left at 30°C for 30 minutes and stopped by adding loading buffer. Aliquots were run on a 15% acrylamide gel, the gel was dried and then exposed to autoradiographic film. Autoradiographs obtained during kinase assays were scanned using

a densitometer and all bands were compared to the control (treated with drug-free media for 2 hours) at 0 hours, which was arbitrarily taken as 1.

The cyclin E/CDK2 kinase activity of U-1 treated samples (see Figure 3.10.1) demonstrated that the activity increased steadily up to 19 hours and then decreased. Adriamycin treated samples (Figure 3.10.2) show a decrease at 0 hours, i.e. immediately following drug removal. The level of activity in this sample had increased at 10 hours but then decreased. Adriamycin plus U-1 (Figure 3.10.3) demonstrated an increase at 10 hours which then decreased steadily. A graph of the scanned autoradiographs is given in Table 3.10.1.

Table 3.10.1: Plot of the cyclin E/CDK2 kinase activity in U-1, adriamycin (Adr) and adriamycin plus U-1 treated samples. Autoradiographs were scanned using a densitometer and all bands were compared to the drug free treated control at 0 hours, which was arbitrarily taken as 1.

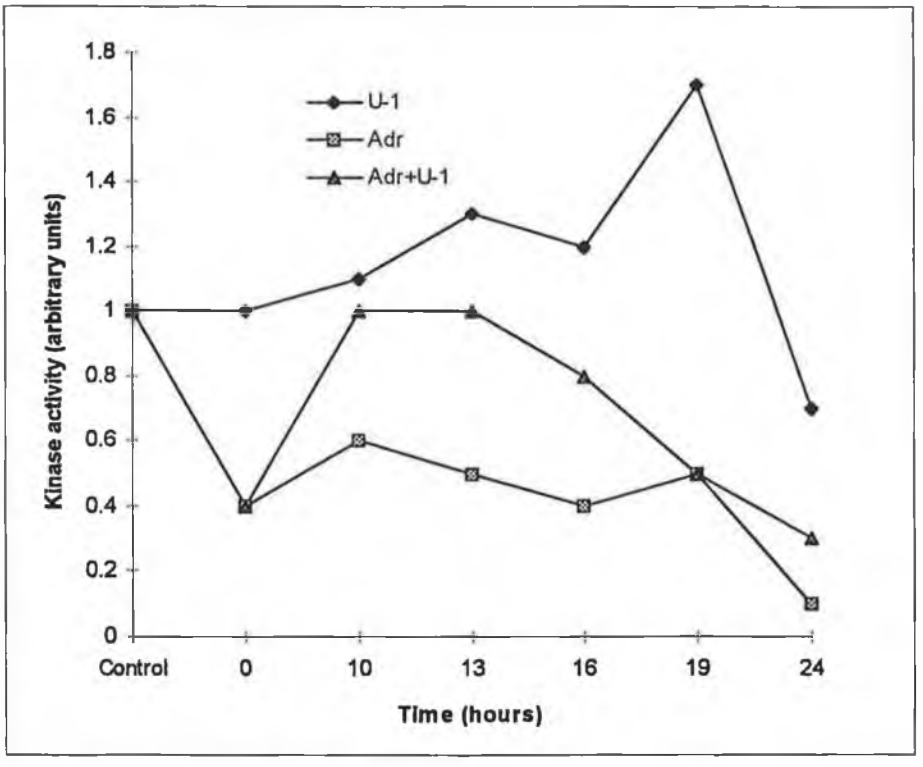

Figure 3.10.1: Cyclin E/CDK2 kinase activity in U-1 treated samples. Activity was measured as described in Section 2.11.

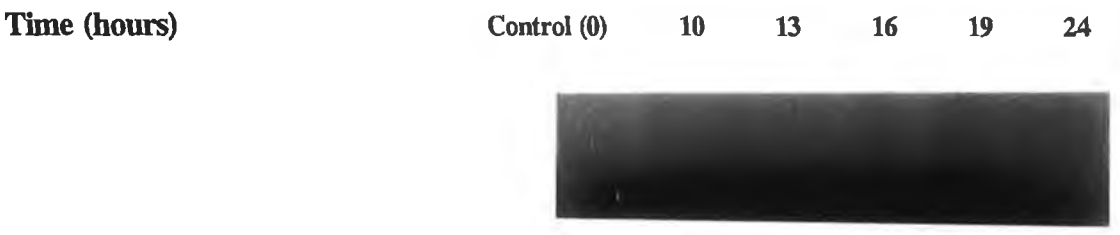

Figure 3.10.2: Cyclin E/CDK2 kinase activity in adriamycin treated samples. Activity was measured as described in Section 2.11.

Figure 3.10.3: Cyclin E/CDK2 kinase activity in adriamycin plus U-1 treated samples. Activity was measured as described in Section 2.11.

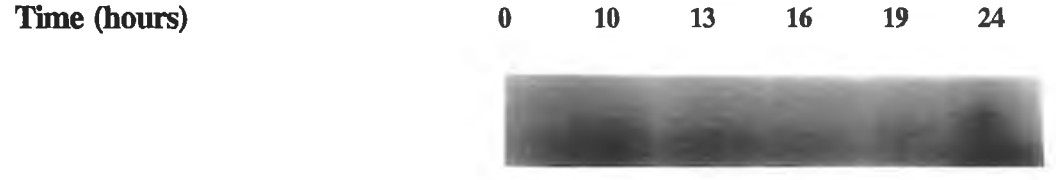

3.11 Cyclin E/CDK2 protein analysis

Cyclin E/CDK2 kinase activity results (Section 3.10) demonstrated that there was an effect on the activity in adriamycin alone versus the adriamycin plus U-1 treated samples. Therefore by investigating the levels of cyclin E and CDK2, it would be possible to examine the compare the proteins to the cyclin E/CDK2 complex kinae activity and investigate the role of these proteins an increased G_1 arrest and delayed S phase transition.

Cyclin E and cyclin dependent kinase 2 (CDK2) protein levels were analysed using western blotting. Experiments were performed as described in Section 2.10. Briefly, cells were set up in $25cm^2$ flasks 4 days before the experiment, they were then exposed to adriamycin or drug free media for two hours, washed twice with PBS and drug-free media or U-1 added as appropriate. Samples were taken at various time points by trypsinising the cells and resuspending the resultant pellet in RIPA lysis buffer and stored at -80°C. Protein quantification was performed on the samples and 10ug of loaded on a 15% acrylamide gel. The proteins were transferred onto a nitro-cellulose membrane and equal sample loading was confirmed by staining the membrane. They were then incubated overnight with anti-cyclin E or anti-CDK2 antibodies. The membranes were then developed using an enchanced chemiluminesence kit.

The levels of CDK2 in the drug-free control samples seemed to increased steadily from 0 hours to 16 hours, the level decreased at 19 hours and increased again at 24 hours (Figure 3.11.1). CDK2 levels in U-1 alone treated samples increased steadily until 13 hours but then decreased slowly at 16, 19 and 24 hours (Figure 3.11.2). Adriamycin treated samples showed an increase in levels until 10 hours, the levels decreased at 13 and 16 hours but increased again at 19 and 24 hours (Figure 3.11.3). Adriamycin plus U-1 in combination treated samples were similar to adriamycin alone (Figure 3.11.4). The samples showed an increase in levels until 13 hours, the levels decreased at 16 hours but increased again at 19 and 24 hours.

At least 3 forms of endogenous cyclin E protein have been detected in rat and human fibroblasts (Ohtsubo and Roberts, 1993) and HeLa cells (Dulic *et al.,* 1992). A 50kDa form is maximally expressed during late G_1 and early S phase of the cell cycle while a 40 kDa is thought to result from proteolytic degradation of over-expressed cyclin E. The higher molecular weight form (55kDa) has been observed in G_2 and early to mid-G_1.

The levels of cyclin E in drug-free control samples displayed an increase in levels of the higher molecular weight cyclin E at 10 hours with a large >67kDa band was gone by 13 hours. A band at >49kDa increased at 10 hours and remained elevated at 13 and 16 hours. A >37.5kDa band was observed at 0 hours. This band disappeared at 10 hours and the levels increased at 13 and 16 hours (Figure 3.11.5).

In U-1 samples, levels of the higher molecular weight cyclin E increased from 10 -13 hours, decreased by 16 hours and there was an increase in the 37.5kDa band from 16 hours (Figure 3.11.6).

In the adriamycin treated samples the level of the higher molecular weight cyclin E (67kDa) increased at 10 hours, decreased slightly at 13 hours and then disappeared until 24 hours. The lower molecular weight (≅37.5kDa) band disappeared at 10 hours but then reappeared at 13 hours. The level of the band increased at 16 and 19 hours and decreased at 24 hours (Figure 3.11.7). The ≅49kDa band increased from 0 hours to 13 hours and then decreased sharply. The levels increased again at 19 and 24 hours.

Cyclin E levels in adriamycin plus U-1 samples were similar to adriamycin alone but at 13 hours the high molecular weight band appears stronger while the <37.5kDa band has decreased compared to adriamycin (Figure 3.11.8). The level of the higher molecular weight cyclin E (67kDa) increased at 10 to 13 hours then disappeared until 24 hours. The lower molecular weight (≅37.5kDa) band remained at a low level until 16 and 19 hours and decreased at 24 hours. The ≅49kDa band increased from 0 hours to 13 hours and decreased sharply after 13 hours and increased again at 19 and 24 hours.

The above results show that the levels of CDK2 varied over a 24 hour period in untreated DLKP-SQ cells and cells treated with U-1, adriamycin and the adriamycin/U-1 combination. There seems to be no correlation between CDK2 levels and the cell cycle distribution. Cyclin E protein levels seem to indicate that an increased amount of the higher molecular weight form represents cells in G_1/G_1 arrest, the form around 49 kDa seems to represent active cyclin E, while the lower molecular weight form (37.5 kDa) represents cells in late S and G_2/M.

Figure 3.11.1: CDK2 protein levels in control, drug-free treated samples. Western blotting was performed as described in Section 2.10.

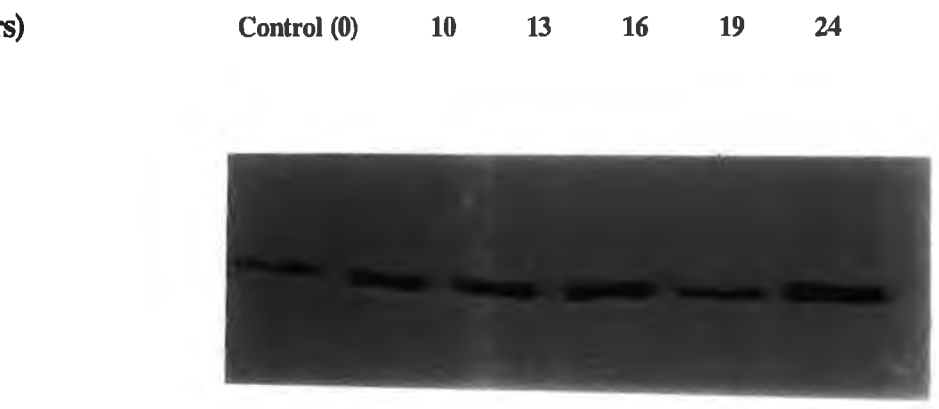

Figure 3.11.2: CDK2 protein levels in 140μM U-1 treated samples. Western blotting was performed as described in Section 2.10.

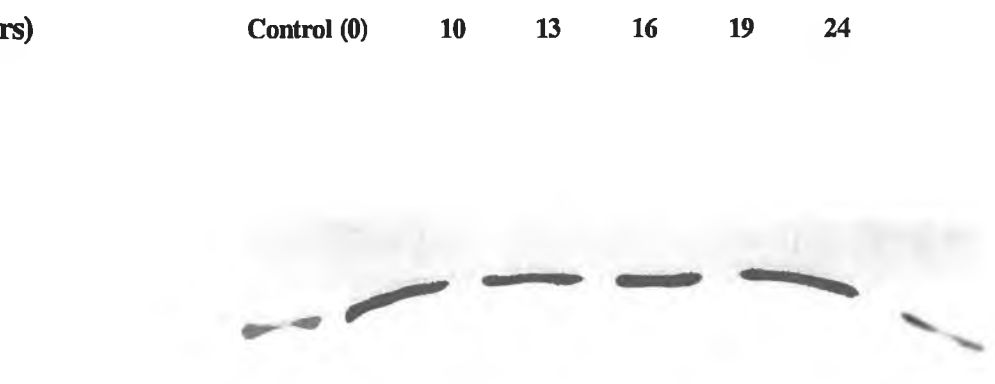

Figure 3.11.3: CDK2 protein levels in 1μM adriamycin treated samples. Western blotting was performed as described in Section 2.10.

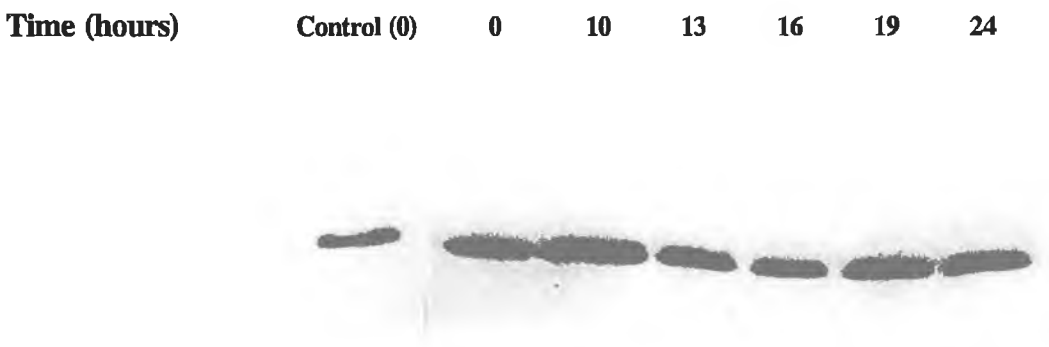

Figure 3.11.4: CDK2 protein levels in 1μM adriamycin plus 140μM treated samples. Western blotting was performed as described in Section 2.10.

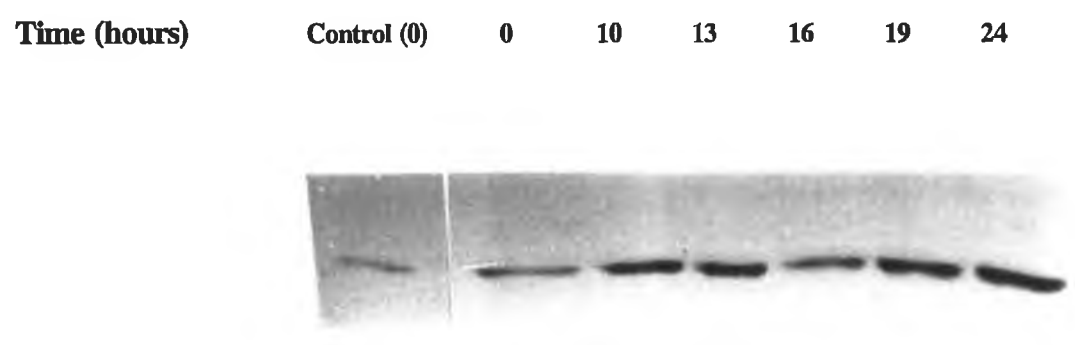

Figure 3.11.5: Cyclin E protein levels in control, drug-free treated samples. Western blotting was performed as described in Section 2.10.

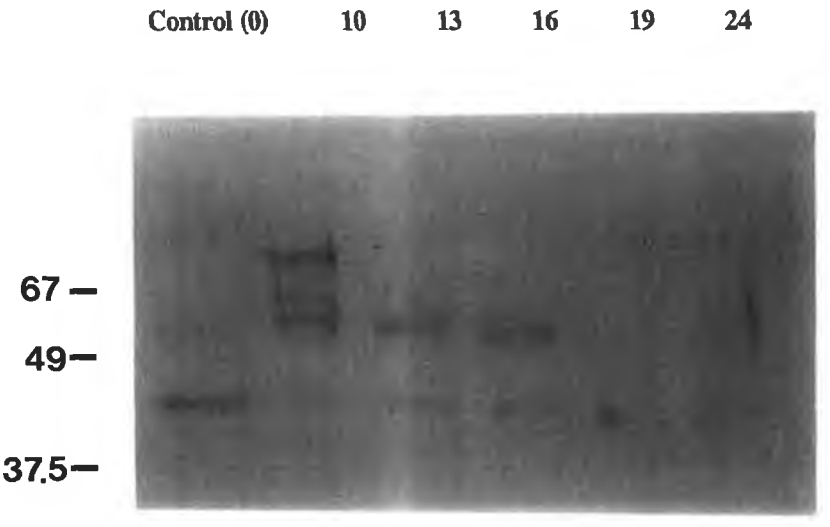

Figure 3.11.6: Cyclin E protein levels in 140μM U-1 treated samples. Western blotting was performed as described in Section 2.10.

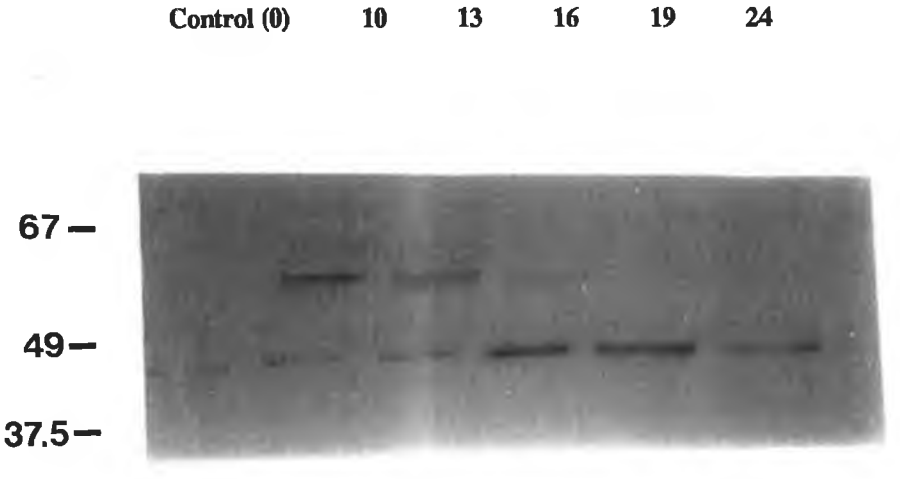

Figure 3.11.7: Cyclin E protein levels in 1μM adriamycin treated samples. Western blotting was performed as described in Section 2.10.

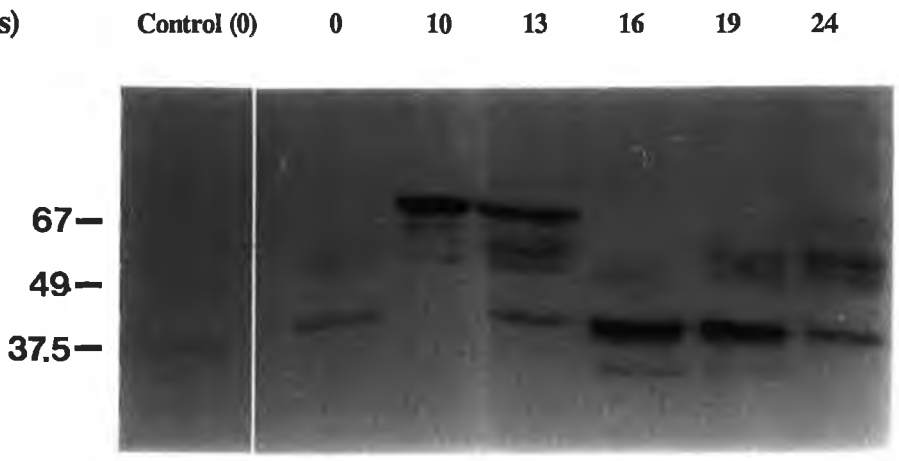

Figure 3.11.8: Cyclin E protein levels in 1μM adriamycin plus 140μM treated samples. Western blotting was performed as described in Section 2.10.

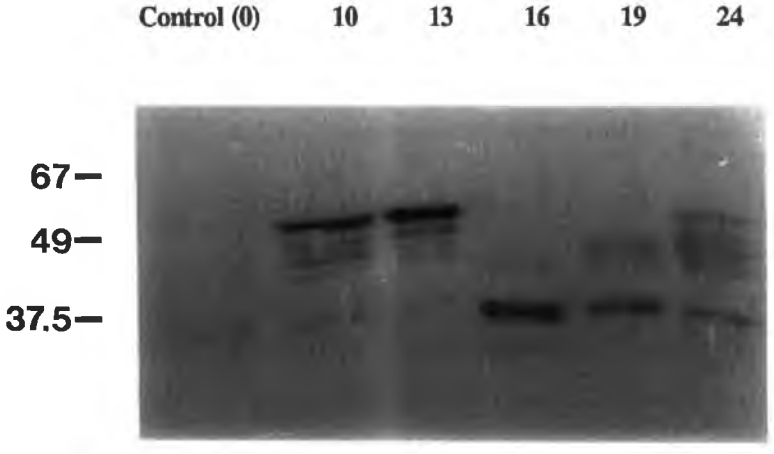

4.0 Discussion

The effect of combinations of different drugs on toxicity to cancer cells *in vitro* was examined in this thesis. Combinations of existing anticancer agents were first analysed. Combinations with the glutathione depleting agent, BSO, with and without verapamil were then studied. Cellular models transfected with the MDR1 gene and an anti-MDR1 ribozyme were also developed. The main part of the thesis concerned combinations of a known anticancer agent with one of a series of coded non-toxic compounds known to be safe for human use. These were examined in a number of cell lines and their mechanism of action further explored.

4.1 Chemotherapeutic drug combination

The use of multiple drugs in combination is a standard treatment for cancer patients (Patel and Rideout, 1992). Clinical studies have shown that drug combinations generally produce higher response rates than those produced by single agents alone. Agents active for a certain tumour type are first identified and the use of these active drugs in combination then depends on the predicted toxicity of the drug. This is to prevent overlapping of toxicity e.g. the relatively low toxicity of vincristine for normal marrow means it is often included in combination chemotherapy with other myelosuppressive agents (Pratt *et al.*, 1994). However, it is likely that for a given patient, some of the drugs in a combination are not effective and may be antagonistic to the effective agents.

This series of experiments was performed to investigate the efficacy of combining two common chemotherapeutic drugs at three different ratios and to investigate if the combination was synergistic, additive or antagonistic in DLKP and DLKP-A. DLKP is a human lung carcinoma cell line which is sensitive to chemotherapeutic drugs and DLKP-A is a MDR derivative of DLKP which overexpresses P-glycoprotein (Redmond, 1991; Cleary, 1995).

Adriamycin and carboplatin used in combination in DLKP (Table 3.1.1) were antagonistic at respective ratios of 1:10 and 1:100. The ratio of adriamycin to carboplatin at 1:40 displayed some additive effects at high concentrations of the combination. Combinations of adriamycin and carboplatin in DLKP-A (Table 3.1.2) were similar to combinations in DLKP. The combination in a 1:40 ratio in DLKP-A was additive although some concentrations did show synergy, while the combination at ratios of 1:10 and 1:100 were antagonistic. Carboplatin is not an P-glycoprotein substrate and this may explain the slight synergistic effect in DLKP-A.

Vincristine and carboplatin was assayed in DLKP-A (Table 3.1.3). The combination at ratios of 1:10 and 1:100 were antagonistic but the combination at the 1:40 ratio did show slight synergy at some concentrations, with an additive effect observed at the higher concentrations. These results are similar to those observed with the combination of adriamycin and carboplatin in DLKP-A. Other researchers have shown that carboplatin and etopside can be effective in breast cancer (Crown *et al.*, 1993).

Adriamycin and vincristine in DLKP (Table 3.1.4) were antagonistic initially but then showed some synergy at higher concentrations. However, at higher concentrations the percentage survival was very low (<20%). At ratios of 1:1, 4:1 and 1:4 in DLKP-A (Table 3.1.5), adriamycin and vincristine were antagonistic at the lower concentrations used but then showed some synergism at higher concentrations. Once again, at the higher concentrations the percentage survival was very low (<20%).

Vincristine and VP-16 were assayed at 1:1, 1:5 and 5:1 combinations in DLKP (Table 3.1.6). The combinations were antagonistic initially but were synergistic at higher concentrations of the combinations which had a very low percentage survival (<10%). Vincristine and VP-16 in combination in DLKP-A (Table 3.1.7) did show synergism in each combination at all concentrations used.

The above results demonstrated that a combination of carboplatin and adriamycin or vincristine was additive in DLKP-A but antagonistic in DLKP. The combinations of adriamycin plus vincristine were antagonistic to both cell lines. Vincristine plus VP-16 was antagonistic in DLKP but did show synergism in DLKP-A. This result was unexpected since vincristine and VP-16 are both P-glycoprotein substrates. However, VP-16 is a topoisomerase II inhibitor and vincristine is an inhibitor of the mitotic spindle (see Section 1.2), therefore, synergy may result from each drug targeting different cellular processes. Further work should be undertaken to confirm the synergy found.

Clinical studies have shown that drug combinations generally produce higher response rates in treated populations than those produced by single agents. Therefore, while the above results show an additive effect between carboplatin and adriamycin or vincristine in DLKP-A, the combination *in vivo* could have a limited applicability in cancers where chemotherapy efficacy is low e.g. colorectal cancer and non-small cell lung cancer. Therefore other approaches to improve chemotherapy must be undertaken.

4.2 Circumvention

The majority of metastatic cancers are not curable currently by chemotherapy or by any other form of therapy. This is because a population within a tumour displays resistance to a number of chemotherapy drugs, even if they are structurally dissimilar and have different mechanisms of action. This is called Multidrug Resistance (MDR). MDR may be intrinsic or induced in the tumour population and a variety of mechanisms have been described to account for this phenomenon (see Section 1.9 and 1.10). Currently the best characterised mechanism of MDR is the resistance mediated by the MDR1 gene product (P-glycoprotein) a 170 kDa glycoprotein which acts as an energy-dependent transmembrane efflux pump that actively transports chemotherapeutic agents out of the cell. Inhibition of this pump can lead to a restoration of the level of cytotoxic drug accumulation in MDR cells observed in sensitive cells.

A number of compounds have been identified which inhibit the efflux of chemotherapeutic drugs by P-glycoprotein and reverse cellular resistance in experimental systems, e.g. verapamil, a calcium antagonist, and cyclosporin A, an immunosuppressive drug.

However, there are a number of non-chemotherapeutic drugs which enhance chemotherapeutic cytotoxicity by mechanisms other than the inhibition of efflux pumps. One of these drugs, buthionine sulfoximine (BSO), reduces cellular glutathione levels by irreversibly inhibiting γ-glutamylcysteine synthetase, the first enzyme involved in *de novo* glutathione synthesis. Glutathione helps to protect cells both by conjugating with cytotoxic electrophile drug derivatives and by binding with drug generated reactive oxygen compounds such as peroxides (Pratt *et al.,* 1994). High glutathione levels were found to be associated with decreased DNA cross-link formation by some chemotherapy drugs. This reduction in DNA cross-link formation was probably due to intracellular drug inactivation by glutathione rather than an increased rate of DNA repair (Stewart and Evans, 1989). BSO also inhibits glutathione transferase activity, and inhibits the uptake of cysteine, a precursor of glutathione (Stewart and Evans, 1989). While BSO decreased glutathione concentrations in most normal tissues, the degree of glutathione reduction in these normal tissues has not been as great as in tumour tissues. Chemotherapeutic toxicity to normal tissues (including bone marrow) was generally not augmented at BSO doses that enhanced chemotherapy efficacy against tumours (Lee *et al.,* 1987; Stewart and Evans, 1989; Siemann and Beyers, 1993).

This series of experiments was performed to investigate the efficacy of BSO plus a P-glycoprotein inhibitor (verapamil) in combination with adriamycin in DLKP and DLKP-A cell lines.

The effect of BSO on the cytotoxicity of adriamycin in DLKP is given in Table 3.2.1 and the Combination Index (CI) values (see Section 2.7.6) are given in Table 3.2.2. These results show that at higher concentrations of BSO, the CI value was approximately 1.

This implies that there was an additive cytotoxic effect. A synergistic cytotoxic effect (i.e. CI value <1) was observed at 10ng/ml adriamycin when 1μg/ml of BSO was used.

Verapamil in combination with adriamycin showed little enhanced cytotoxic effect in DLKP (Table 3.2.5). At the lower concentrations of BSO (0.125μg/ml and 0.25μg/ml), there was synergism in toxicity (Table 3.2.6). However, BSO plus verapamil in combination with adriamycin did not enhance the toxicity of adriamycin compared to BSO with adriamycin (Table 3.2.7).

The effect of BSO on the cytotoxicity of adriamycin in DLKP-A is given in Table 3.2.3 and the Combination Index (CI) values are given in Table 3.2.4. These results show that at the lowest concentration of BSO, 1μg/ml, the CI values were less than 1, i.e. there was a synergistc toxic effect with all the concentrations of adriamycin used. At higher concentrations of BSO, the CI values were >1 thereby indicating an antagonistic combination.

Verapamil did show enhanced cytotoxicity in combination with adriamycin in DLKP-A (Table 3.3.8). This was expected because P-glycoprotein, which is inhibited by verapamil, is overexpressed in DLKP-A (Redmond, 1991; Cleary, 1995). However, BSO did not significantly affect adriamycin toxicity (Table 3.3.9). The combination of BSO plus verapamil was synergistic with adriamycin (Table 3.2.11); however, it was not clear if this effect was due to verapamil alone or the combination of BSO and verapamil. Therefore a more detailed experiment using a number of combinations of BSO and verapamil with adriamycin was performed (Table 3.2.11). This showed that the combination of BSO plus verapamil with adriamycin was synergistic. For example, when the 0.5mg/ml concentration of verapamil was used and the concentration of BSO was increased, the toxicity of adriamycin was enhanced from 63% to 43% cell survival. Conversely, when the 0.125mg/ml concentration of BSO was used and the concentration of verapamil was increased, the toxicity of adriamycin was also enhanced e.g. from 80% to 63% cell survival. This is in agreement with other researchers, who showed that BSO

plus verapamil in combination with daunorubicin, in myeloid leukaemic cells, further induced internucleosomal DNA fragmentation (Quilletmary *et al.*, 1996).

The above results demonstrate the effectiveness of BSO to enhance the toxicity of adriamycin in drug sensitive and drug resistant human lung carcinoma cell lines. BSO in combination with verapamil demonstrated an enhanced cytotoxicity and it would be interesting to repeat the experiment in DLKP-A using cyclosporin A instead of verapamil, in combination with BSO and adriamycin. While BSO may have a future role in enhancing chemotherapy in a resistant population, the results of other circumvention compounds in clinical trials have been disappointing due to non-specific effects (verapamil) or toxic effects (cyclosporin A) of the circumvention agent (Ford, 1995). Therefore, other alternatives need to be explored.

4.3 MDR1 ribozyme transfection

Currently the best understood mechanism of MDR is the resistance mediated by the MDR1 gene product, P-glycoprotein (see Section 4.2). Attempts at chemomodulation of P-glycoprotein have been investigated using various P-glycoprotein antagonists. The results of circumvention compounds in clinical trials have been disappointing due to non-specific effects (calcium antagonists) or toxic effects (cyclosporin A) of the circumvention agent (Ford, 1995). Therefore, a more specific modulation of MDR is necessary for an improved reduction in drug resistance. One alternative is to use antisense techniques such as ribozymes.

Ribozymes are RNA molecules which have catalytic activity. The hammerhead ribozyme is the smallest of the ribozymes and the target RNA cleavage sites have the least constraints with respect to sequence. Therefore, the hammerhead ribozyme has the most abundant target sites compared to other ribozyme types (Sullivan, 1994). To test the efficacy of antisense *in vitro*, a hammerhead ribozyme which cleaves the 3'-end of the

GUC sequence in codon 880 of mdr1 RNA was transfected into the adriamycin resistant human lung carcinoma cell line SK-MES-1/Adr (see Figure 4.3.1). SK-MES-1/Adr is a derivative of the chemotherapeutic drug sensitive cell line SK-MES-1, and was selected by exposure to increasing concentrations of adriamycin. Its mechanism of drug resistance is primarily thought to be due to P-glycoprotein overexpression (Redmond, 1991; Cleary, 1995).

Three clones were isolated when SK-MES-1/Adr was electroporated with the anti-MDR1 ribozyme plasmid. The clones were selected in 96-well plates by continuous exposure to 200μg/ml geneticin in ATCC media. These clones were assayed for their resistance to three chemotherapeutic drugs (adriamycin, vincristine and VP-16) and compared to the sensitive parent SK-MES-1 and the resistant parent SK-MES-1/Adr (Figures 3.3.1 - 3.3.3). These graphs demonstrate that each clone displays a decreased resistance to adriamycin, vincristine and VP-16 compared to the resistant parent cell line, SK-MES-1/Adr. Clone #2 is the most resistant of the three clones. Clone #3 and clone #4 showed a similar resistance profile.

RT-PCR analysis of RNA isolated from SK-MES-1, SK-MES-1/Adr and each ribozyme clone was performed (Figure 3.2.4). No MDR1 mRNA expression was detected in SK-MES-1. A decreased expression of MDR1 mRNA was detected in the three MDR1 ribozyme transfectants compared to the resistant parent. Of the ribozyme transfectants, clone #4 expressed the least amount of MDR1 mRNA while clone #2 expressed the greatest amount MDR1 mRNA. Therefore, clone #4, which showed the least amount of MDR1 mRNA expression, was also the clone most sensitive to adriamycin, vincristine and VP-16 as predicted.

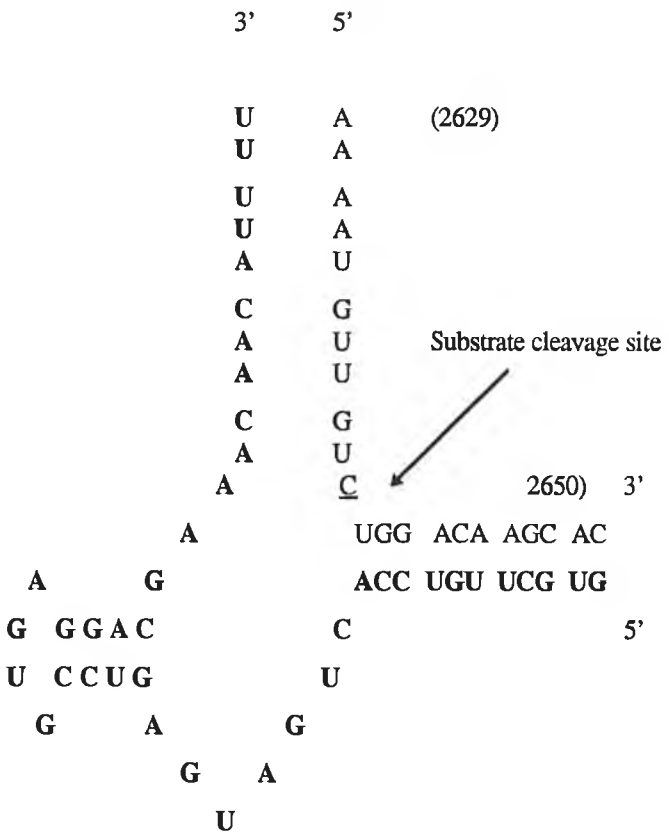

Figure 4.3.1 **Structure of the anti-MDR1 hammerhead ribozyme.**

The hammerhead ribozyme is in bold. The C represents the cleavage site of the mdr1 mRNA (Holm *et al.*, 1994). .

Fold resistance values found (Table 3.3.3) show that the ribozyme transfectant clones displayed a reduction of approximately 50% in resistance to adriamycin. Their resistance to vincristine and VP-16 varied, with clone #2, 60 and 4.9 fold resistant to vincristine and VP-16, clone #4 40 and 3.7 fold resistant respectively.

Further studies on these cell populations should include western blot analysis of the ribozyme transfectants compared to SK-MES-1 and SK-MES-1/Adr to establish the levels of P-glycoprotein being expressed. To further confirm that the chemosensitivity conferred on the transfectants was due to the ribozyme plasmid, PCR should be performed to establish that the plasmid is present in the cell lines and RT-PCR to confirm that the ribozyme is being expressed.

The use of ribozymes to control the expression of P-glycoprotein is a new technology and the experiments performed highlight some of the drawbacks of the technique. Transfection of the anti-MDR1 ribozyme does work as has been shown previously by other workers (Holm *et al.*, 1994; Kiehntopf *et al.*, 1994; Bertram *et al.*, 1995; Daly *et al.*, 1996). However, all of the clones isolated still expressed some MDR1 mRNA. Perhaps with the introduction of a site specific plasmid vector or the use of a retroviral vector this limitation may be overcome. This approach would allow the introduction of the ribozyme into a specific area of the genome where it would not be detrimental to the cell and where it could be under the control of a strong promoter. Although the ribozyme did not completely abrogate MDR1 expression, the use of ribozymes is a significant step forward since it bypasses the need for the repeated use of antisense oligonucleotides. In the future ribozyme technologies may surpass the use of pharmacological circumvention agents.

4.4 MDR1 transfection

MDR is generally a multifactorial phenomenon with a number of resistance mechanisms usually co-expressed within a cell. DLKP-A is an MDR cell line derived from DLKP by sequential exposure to increasing concentrations of adriamycin. Nine clones were isolated from DLKP-A, each with different levels of resistance and combinations of resistance mechanisms (Heenan, 1994). However, no clone expressed P-glycoprotein as the sole mechanism of resistance. Therefore, DLKP was electroporated with the pHaMDR1/A plasmid, which encodes the full cDNA for the human MDR1 gene (Pastan *et al.*, 1988),

to develop a low level resistant DLKP clone whose only mechanism of resistance would be the expression of P-glycoprotein. These clones would then be a realistic model of the *in vivo* situation and could be used for subsequent studies aimed at enhancing the effect of chemotherapy.

Two clones were isolated when DLKP was transfected with the pHaMDR1/A plasmid and selected by continuous exposure to 50ng/ml adriamycin in ATCC media. This adriamycin concentration represents approximately 3 times the IC50 value for DLKP. Control cells did not survive when exposed to this concentration and the clones selected were resistant to adriamycin.

Toxicity assays were performed on each clone using adriamycin, vincristine and VP-16 (Figures 3.4.1 - 3.4.3). These graphs demonstrate that each clone had an increased resistance to adriamycin, vincristine and VP-16 compared to the sensitive parent cell line, DLKP. Clone #1 demonstrated an increased resistance to adriamycin and vincristine compared to clone #2. In contrast, clone #2 showed a greater resistance to VP-16 than clone #1. The IC50 values for adriamycin, vincristine and VP-16 of each clone are given in Table 3.4.2 and are compared to DLKP and DLKP-A. The values show that the MDR1 transfectants were more resistant to each chemotherapeutic drug tested compared to DLKP but were not as resistant as DLKP-A . The fold resistance values (Table 3.4.3) showed that the clone #1 and clone #2 were 37 and 15 fold more resistant to adriamycin compared to DLKP but 8 fold and 13.6 fold more resistant to VP-16 respectively.

RT-PCR analysis of RNA isolated from DLKP, the two MDR1 transfectants and DLKP-A was performed (Figure 3.2.4). As expected no MDR1 expression was detected in DLKP. An increased expression of MDR1 mRNA was detected in DLKP-A and the two MDR1 transfectants with the expression of MDR1 in DLKP-A being much greater than in the two transfectant clones. Time did not permit western blot analysis of the MDR1 transfectants compared to DLKP and DLKP-A to establish the levels of P-glycoprotein being expressed. To further confirm that the resistance conferred to the transfectants was

due to the pHaMDR1/A plasmid, PCR should be performed to establish that the plasmid is present in the cell lines.

The toxicity data also demonstrated that clone #1 was more resistant to adriamycin and vincristine than clone #2 but that clone #2 was more resistant to VP-16 than clone #1. Thus, even though these clones were derived from the same parent cell line and were transfected with the same plasmid, they displayed different resistance profiles to the chemotherapeutic drugs tested. This may be due to plasmid insertion at different locations of the genome. Alternatively, DLKP has previously been shown to be polyclonal and to be composed of three cell distinguishable populations (McBride, 1995). Therefore, the difference in resistance profiles of the two MDR1 transfectants may be due to the transfection of two different clones within DLKP, although there was little difference between each clone and chemotherapeutic drug sensitivity (McBride, 1995). Examining the morphology of each transfectant and comparing them to the known morphology of the subclones of DLKP may verify this theory. Transfection of the different clones of DLKP with pHaMDR1/A would establish if MDR1 expression within different clones displays a different resistance profile to chemotherapeutic drugs.

4.5 Test compound screening

There are a number of non-chemotherapeutic drugs which enhance chemotherapeutic cytotoxicity by mechanisms other than the reversal of drug resistance (reviewed in Stewart and Evans, 1989). These include buthionine sulfoximine (BSO) and other glutathione depletors, the nitroimidazoles and the methylxanthines. However, none of these are in common clinical use. Thus, the need to test new non-chemotherapeutic drugs which enhance the cytotoxicity of chemotherapeutic drugs is essential. This series of experiments investigated possible cytotoxic synergy between an anticancer agent with one of a series of coded non-toxic test compounds known to be safe for human use (A-1, N-1, O-1, U-1 and U-2).

Seven cell lines were tested to investigate the presence of any synergistic toxic effect between adriamycin and the five test compounds in drug sensitive and drug resistant cell lines. These cell lines were resistant variants derived from 2 parental cell lines, DLKP and SK-MES-1 both lung carcinoma cell lines. DLKP-SQ is a clone of DLKP a human lung carcinoma cell line, which is sensitive to chemotherapeutic drugs (McBride, 1995); DLKP pHaMDR1/A #2 is a clone of DLKP which was transfected with the MDR1 gene and has been found to overexpress MDR1 mRNA (see Section 3.4); DLKP-A-2B is a low level resistant clone derived from the MDR cell line DLKP-A (Heenan, 1994), and expresses a number of MDR mechanisms including overexpression of P-glycoprotein; DLKP-A-2B IC7 is a MDR1 ribozyme transfectant of DLKP-A-2B, in which the expression of P-glycoprotein mRNA is inhibited (McBride, 1995). SK-MES-1 is also a human lung carcinoma cell line, which is sensitive to chemotherapeutic drugs, but whose resistance to adriamycin is approximately 3 fold that of DLKP; SK-MES-1/Adr is an MDR derivative of SK-MES-1, which was exposed to increasing concentrations of adriamycin; SK-MES-1/Adr MDR1 ribozyme clone #4 was the most sensitive clone obtained after transfection of SK-MES-1/Adr with a MDR1 ribozyme, although P-glycoprotein mRNA expression was not completely inhibited (see Section 3.2).

The results demonstrated that the test compounds N-1, O-1 and U-1, at non-toxic concentrations, were found to enhance the toxicity of adriamycin in three cell lines; DLKP (Table 3.5.1), DLKP-A-2B IC7 (Table 3.5.4) and SK-MES-1 (Table 3.5.5). No test compound demonstrated any enhanced toxic effect in DLKP-A-2B (Table 3.5.3), DLKP pHaMDR1/A#2 (Table 3.5.2), SK-MES-1/Adr (Table 3.5.6) and SK-MES-1/Adr mdr1 ribozyme #4 (Table 3.5.7). A brief summary of these results is given in Table 4.5.1.

Therefore, the cell lines which were found to be sensitive to the synergistic effect of the test compounds were drug sensitive, DLKP and SK-MES-1 or a low level resistant variant which does not express MDR1 (DLKP-A-2B IC7). All cell lines found to be unresponsive to the test compounds were multidrug resistant P-glycoprotein overexpressing cell lines.

These results show that the enhanced toxicity of adriamycin by N-1, O-1 and U-1 occurred in those cell lines where there was no P-glycoprotein expression i.e. DLKP, SK-MES-1 and DLKP-A-2B IC7. It is interesting that DLKP-A-2B IC7 continues to exhibit a low level of resistance, this may in part be due to decreased levels of topoisomerase II which is found in DLKP-A-2B (Heenan, 1994). DLKP which was sensitive to the above effect was rendered insensitive when transfected with the MDR1 gene. All of the cell lines tested in which the test compounds had no effect all over-expressed P-glycoprotein. This suggests that adriamycin may not be present in the cell in sufficient quantity or the test compounds may also be P-glycoprotein substrates. However N-1 has been shown to accumulate in P-glycoprotein positive cells within minutes of being added to media (C.Elliot, personal communication). Thus, while the test compounds may not be P-glycoprotein substrates, P-glycoprotein does affect their ability to enhance the cytotoxicity of adriamycin presumably by decreasing its intracellular concentration. This effect may not be related to the test compounds but the effect could be due to efflux of adriamycin from the cells.

Table 4.5.1: Summary of the effect on cell lines screened for synergy between the test compounds and adriamycin.

Cell Line	Synergy	Comment
DLKP-SQ	Yes	Sensitive
DLKP pHaMDR1/A	No	MDR1 transfectant
DLKP-A-2B	No	Low level resistant
DLKP-A-2B IC7	Yes	MDR1 ribozyme transfectant
SK-MES-1	Yes	Sensitive
SK-MES-1/Adr	No	Resistant
SK-MES-1/Adr ribo #4	No	MDR1 ribozyme transfectant

4.6 Scheduling

The results of Section 3.5 described the effect of combining five test compounds with adriamycin. Three of these compounds were found to enhance the toxicity of adriamycin in three of seven cell lines assayed. The standard circumvention assay used allowed the screening of test compounds in combination with adriamycin. However it did not provide an insight into the mechanism of the synergistic action. An assay was developed to analyse how synergy was affected when cells were exposed to the test compounds at different times relative to adriamycin exposure. Cells were pulse treated with adriamycin for 2 hours which resulted in approximately 50% cell survival. When the adriamycin was washed off, the cells were exposed to high non-toxic levels of a test compound for short periods of time (24 hours).

Using these assays, non-toxic levels of N-1, O-1 and U-1 were shown to enhance adriamycin toxicity in DLKP (Table 3.6.1) and DLKP-SQ (a sub-clone of DLKP). A-1, I-1 and U-2 as expected had no effect (Table 3.6.2). During the first 24 hours after adriamycin exposure, DLKP-SQ cells were sensitive to the effect of N-1, O-1 and U-1 but not during any other 24 hour time period following the initial 24 hours. Pretreatment for 24 hours had no effect (Table 3.6.5). Treating cells with adriamycin and a test compound together did not enhance the cytotoxic effect of adriamycin possibly due to the short duration of co-exposure (Table 3.6.6). While a synergistic toxic response might have been expected with this combination, the test compound exposure with adriamycin was only for 2 hours compared to the other assays which did display synergy, where exposure was for 24 hours. Exposure to N-1 for shorter periods (10 hours) was assayed after pulse exposure with different concentrations of adriamycin (Table 3.6.6). The toxic effect of N-1 was evident during the initial two 10 hour periods after adriamycin exposure. However, while there was a consistent trend, the results from these experiments were just outside the error values. The clonogenic assay, which determines the number of colonies formed after drug exposure, could be used instead of the growth assay used in this thesis. This assay may be more sensitive and thus could indicate shorter time periods when exposure to a test compound may be important.

Since the active test compounds exerted their synergistic effect during the first 24 hours following drug removal, cycloheximide and actinomycin D were used to try and block the synergistic effect. Cycloheximide, a protein synthesis inhibitor, was used in combination with U-1 after adriamycin exposure (Table 3.6.7). A relatively non-toxic level of cycloheximide was used (75% cell survival). However at this concentration of cycloheximide, there was no inhibition of the enhanced toxic effect of U-1. This would suggest that the synergistic effect of U-1 is independent of protein synthesis. Actinomycin D, an inhibitor of transcription and translation, was also used at non-toxic concentrations in combination with U-1 after adriamycin exposure (Table 3.6.8). Actinomycin D did not inhibit the toxic effect of U-1. This would suggest that the synergistic effect of U-1 is also independent of transcription and translation. To prove conclusively that protein synthesis, transcription and translation do not prevent the effect of U-1, studies to confirm that the level of cycloheximide used does inhibit protein synthesis and that the level of actinomycin D does inhibit transcription and translation in DLKP-SQ would need to be performed in these cell lines.

Two active (N-1 and U-1) and one inactive (A-1) test compounds were further studied in combination with two other commonly used chemotherapeutic drugs:- vincristine and 5-fluorouracil. O-1 and U-1 continued to cause an increase in observed toxicity during the first 24 hours after vincristine exposure (Table 3.6.3). It is interesting that there was a greater cytotoxic effect observed with vincristine in combination with the active test compounds as compared to adriamycin. No enhanced cytotoxic effect was observed with vincristine plus A-1 in combination. No test compound showed any effect with 5-fluorouracil (Table 3.6.4).

These results show that O-1 and U-1 at non-toxic levels enhance the toxicity of adriamycin and vincristine but not 5-fluorouracil. Interestingly, adriamycin and vincristine are both P-glycoprotein substrates while 5-fluorouracil is not. This seems to correlate with the results from Section 3.5, which show that cell lines expressing P-glycoprotein do not exhibit enhanced toxicity to adriamycin using any of the test compounds. However it raises the

question as to why the test compounds do not work with 5-fluorouracil. One possibility is that chemotherapeutic drugs may induce different apoptotic pathways within a sensitive cell. Further studies screening other chemotherapeutic drugs and other cell lines expressing alternative resistance mechanisms, for example P-glycoprotein related proteins like MRP and LRP, would also be relevant.

One of the advantages of the assay developed is that pulse exposure of the cells *in vitro* mimics the treatment of a patient *in vivo*. The high concentration (1μM adriamycin) and short time exposure (2 hours) is an approximate imitation of the initial adriamycin concentration in the body (Piscitelli *et al.*, 1993). Thus, the test compounds could be used concurrently with chemotherapeutic drug treatment *in vivo* and for an extended period after the chemotherapeutic agent has been metabolised. This is unlike other circumvention agents such as verapamil or cyclosporin A which must be present during chemotherapeutic drug exposure in order to exert their effect.

Further studies could be performed to investigate the effect of synchronising cells in specific phases of the cell cycle, pulse treated with a chemotherapeutic drug, followed by exposure to an active test compound, would there be an increase or decrease in sensitivity? In these experiments the cell cycle progression could be followed using flow cytometry and apoptotic events could be examined by time-lapse videomicroscopy.

4.7 DLKP pHaMDR1/A #2 Scheduling

The results from Section 3.6 demonstrate that the active test compounds, N-1, O-1 and U-1 exert their synergistic cytotoxic effect during the first 24 hours post-treatment with adriamycin. Previous results also demonstrated that the test compounds N-1, O-1 and U-1 were shown to have no synergistic effect in combination with adriamycin in DLKP pHaMDR1/A #2 or any other P-glycoprotein over-expressing cell line using the standard circumvention assay. Therefore, DLKP pHaMDR1/A #2 was assayed using the modified

assay, i.e. pulse treating with adriamycin and then exposing to a high concentration of a test compound for 24 hour periods.

DLKP pHaMDR1/A #2 was pulse treated with adriamycin and exposed to 6 test compounds for 24 hour periods (Table 3.7.1). No synergistic effect with adriamycin was observed with any of the six test compounds assayed.

Because the test compounds had displayed no synergy with adriamycin in the P-glycoprotein positive cells inhibitors of P-glycoprotein were used to try and restore the synergistic effect of the test compounds. Verapamil inhibits P-glycoprotein associated energy-dependent drug-efflux in MDR cells, apparently by blocking the binding of drugs to P-glycoprotein (Ford, 1995). Using the test compounds and verapamil in combination with adriamycin, there was no restoration of the synergistic effect induced by the test compounds as observed in DLKP (Table 3.7.2). These experiments were repeated using cyclosporin A instead of verapamil. Cyclosporin A is an immunosuppressive peptide which has been found to act as an MDR substrate and antagonise MDR at least in part through inhibition of P-glycoprotein-mediated efflux of cytotoxic drugs (Ford, 1995). Again the synergistic effect observed between the test compounds and adriamycin was not restored.

Even in the presence of P-glycoprotein inhibitors, there was no restoration in chemosensitivity caused by the test compounds. During the assay, various cytotoxic levels of adriamycin were used. Therefore, even though there was cytotoxic injury to the MDR cells, exposure to the test compounds, which are apparently P-glycoprotein-mediated transport independent substrates (C.Elliot, personal communication), did not enhance cytotoxicity even when P-glycoprotein inhibitors were used in combination. One possibility is that chemotherapeutic drugs may induce different types of cytotoxic damage in sensitive versus resistant cells. This could be investigated by analysing the toxic effect of a chemotherapeutic drug on cell lines with different drug sensitivities. Therefore, treatments which induce 75% or 50% cell survival could be compared between the cell lines to ascertain a difference in cell cycle distribution by flow cytometry. Alternatively

chemotherapeutic drugs may induce different apoptotic pathways in sensitive and drug resistant cell lines.

4.8 Cell cycle distribution

The results from Section 3.6 demonstrated that the test compounds, N-1, O-1 and U-1 exert their synergistic cytotoxic effect during the first 24 hours post-treatment with adriamycin or vincristine but not 5-fluorouracil. In order to further investigate the role of these test compounds on DLKP-SQ, flow cytometric analysis was used to determine the cell cycle distribution of treated samples. Using a flow cytometer the amount of DNA fluorescence from propidium iodide stained cells (which intercalates with DNA), can be measured and this can be used to determine the position of a cell in the cell cycle.

Flow cytometric analysis was used to determine the cell cycle distribution in DLKP-SQ pulse treated with adriamycin, vincristine or 5-fluorouracil for 2 hours alone and in combination with a test compound (A-1, N-1 or U-1) for 24 hours.

U-1 on its own was shown to induce a G_1/S arrest for up to 10 hours (Figure 3.8.1). There was no apparent effect on the cell cycle distribution using A-1 or N-1 (Figure 3.8.2 and Figure 3.5.3).

The active test compounds (U-1 or N-1) in combination with adriamycin displayed an increased G_1/S arrest with a delayed S peak evident at 13 to 19 hours compared to adriamycin alone (Figure 3.8.4 and Figure 3.8.5). Thus the addition of an active test compound causes an increased delay in the G_1 phase and the S phase compared to adriamycin alone. This delay was not observed with A-1 (inactive) and adriamycin treatment (Figure 3.8.6). Because of the increased G_1/S phase arrest and an increased S phase transition in DLKP-SQ treated with adriamycin plus N-1 or U-1, increasing concentrations of adriamycin alone were analysed. These results show that there was an increased G_1/S phase arrest, a delay in S and a G_2/M arrest approximately 24 hours after

drug removal, when increasing drug concentrations were used to pulse treat cells (Figure 3.8.12 - 3.8.14). It is known that low concentrations of adriamycin induce G_2 arrest, and that higher concentrations or exposure to drug for longer periods of time induces a G_1 arrest and a delay in S phase traverse (Barlogie *et al.*, 1976).

U-1 or N-1 in combination with vincristine (Figure 3.8.7 (a) and 3.8.8 (a) respectively), showed an increased G_2/M arrest compared to vincristine treated cells alone (Figure 3.8.7 (b) and 3.8.8 (b)). In each combination, there was a large increase in the G_1 peak at 24 hours in vincristine treated cells compared to the large G_2/M peak when U-1 or N-1 were combined in combination with vincristine. This G_2/M arrest was expected since vincristine is a mitotic inhibitor. This means (in vincristine treated cells) that by 24 hours the G_2/M arrest was overcome, while in the N-1/U-1 plus vincristine combination there was still a G_2/M arrest. Therefore, the addition of an active compound after vincristine exposure causes an increased delay in G_2/M. Vincristine and A-1 in combination did show a slight cell cycle delay in G_1/S at 12 - 15 hours but this was not as striking as in U-1 or N-1 treated cells (Figure 3.8.9). Increasing concentrations of vincristine were analysed to investigate if increasing concentrations increased G_2/M arrest as found when 50ng/ml plus U-1 or N-1 were used in combination (Figure 3.8.15 - 3.8.17). Increasing concentrations of vincristine showed a decrease in the G_1 peak and an increased G_2/M peak representing an increased G_2/M arrest as compared to untreated cells.

DLKP-SQ treated with 5-fluorouracil alone and in combination with U-1 showed no effect on the cell cycle distribution (Figure 3.8.10 and Figure 3.8.11). These results were expected since there was no synergy between any test compound and 5-fluorouracil when previously assayed (Table 3.6.4).

These results seem to suggest that the effect of U-1 and N-1 in combination with a chemotherapeutic drug (adriamycin and vincristine but not 5-fluorouracil), may mimic higher chemotherapeutic drug combinations. For example, the cell cycle distribution of 1μM adriamycin and U-1 in combination seems similar to 2μM adriamycin alone (Figure 3.8.4 (a) and Figure 3.8.14) and 50ng/ml vincristine and U-1 in combination (Figure

3.8.7(a)) seems similar to 100ng/ml vincristine alone (Figure 3.8.17). This effect may be the result of increased cytotoxic action due to the higher concentration causing a greater cytotoxic insult to the cell and thus the increased G_1/S delay, S phase traverse and G_2/M delay. It is interesting to note that cells which have been synchronised in the S or the G_2 phase are more sensitive to adriamycin cytotoxicity than cells in G_1 (Krishan and Frei, 1976). These above results show that the active test compounds have an effect on the cell cycle which is different from the pulsed chemotherapeutic drug alone and this effect may mimic increased concentrations of the chemotherapeutic drug alone. HPLC analysis of cells treated with drug could be used to determine the intracellular levels of a chemotherapeutic drug and the test compound. This would demonstrate if there was an increased accumulation of chemotherapeutic drug in samples treated with chemotherapy and an active test compound.

4.9 Cell death kinetics

The test compounds, N-1, O-1 and U-1 exert their synergistic cytotoxic effect during the first 24 hours post-treatment with adriamycin or vincristine. Flow cytometric analysis (Section 3.8) showed that there was a difference in cell cycle distribution during the first 24 hours after pulse exposure between adriamycin and adriamycin plus U-1 or N-1 and between vincristine and vincristine plus U-1 or N-1. Therefore, while there was an increased cytotoxicity in cells which were exposed to N-1, O-1 or U-1 after adriamycin or vincristine exposure, and there was a difference in cell cycle distribution, there was no indication as to why or when the cells undergo cell death.

Time-lapse videomicroscopy permits the continuous observation of cells following drug treatment. With this technique it was possible to follow, in real time events such as cell rounding for mitosis or apoptosis. Mitosis was characterised by the rounding up of adherent cells followed by cytokinesis and reattachment of daughter cells to the surface of the flask. Cell death was classified as apoptotic on the basis of morphological events

starting with rounding up of adherent cells, subsequent cell shrinkage and/or break-up of the cell into apoptotic bodies.

Using time-lapse videomicroscopy the kinetics of mitosis and apoptosis was followed in DLKP-SQ treated with U-1 alone for 24 hours, 2 hours pulse exposure to increasing concentrations of adriamycin, adriamycin and U-1 in combination, 2 hours pulse exposure to vincristine, and vincristine plus U-1 in combination.

The results show that exposure of DLKP-SQ to 140μM U-1 has no detrimental effect on the cells, although initially there was a low level of apoptosis and a temporary inhibition of mitosis compared to the drug free control (Figure 3.9.3). Apoptosis was induced 24 hours after 1μM adriamycin removal, however, when U-1 was used in combination with adriamycin there was no difference in the rate at which apoptosis was induced compared to adriamycin alone (Figure 3.9.2). In the adriamycin plus U-1 treated sample, apoptosis was also induced after 24 hours and the rate of apoptosis was similar to adriamycin alone. Mitosis was abolished in both samples. This result was unexpected since it was thought that apoptosis may have been induced sooner when U-1 was used because of the observed synergy, although a similar rate of apoptosis in both samples may be related to the effect of adriamycin on the cell cycle. In contrast, vincristine exposure induced a different response (Figure 3.9.3). 60nM vincristine exposure inhibited mitosis for 12 hours but induced apoptosis continuously for the first 24 hours following exposure which then stopped. Vincristine followed by U-1 exposure inhibited mitosis completely and induced a high level of apoptosis for approximately the first 12 to 18 hours after vincristine removal.

Therefore the above results show that different chemotherapeutic drugs induce apoptosis at different times. This seems to suggest that different chemotherapeutic drugs induce different apoptotic pathways.

Further analysis of a range of adriamycin concentrations was performed to investigate if varying the concentrations induced different rates of apoptosis. 2 hour exposure to 0.5μM adriamycin, delayed mitosis for 24 hours and induced a low rate of apoptosis from 12

hours (Figure 3.9.4). 1μM and 2μM adriamycin concentrations inhibit mitosis completely and induce apoptosis 24 to 48 hours after exposure. It is interesting that with the 1μM adriamycin concentration, apoposis was induced 24 hours after exposure and continued until 72 hours, while 2μM adriamycin induced apoptosis after 48 hours which continued until the experiment finished i.e. 96 hours. Therefore, there is a possibility that higher concentrations of adriamycin "shock" or cause so much damage to the cell that it delays the induction of apoptosis.

It is interesting to correlate these microscopical results with the flow cytometric data. A two hour 1μM adriamycin exposure induced apoptosis 24 hours after it was removed. By this time, most of the cells would be arrested in the G_2/M phase. In contrast, vincristine treated cells arrest almost immediately in the G_2/M phase. Further work could be undertaken to try and determine at what stage of the cell cycle DLKP-SQ cells undergo apoptosis. These results might also explain why the active test compounds enhance the toxicity of vincristine to a greater extent than adriamycin and why there seemed to be no difference in the rate of apoptosis in adriamycin only as compared to adriamycin plus U-1 treated samples. However it seems that the active test compounds do not need to be present in order for apoptosis to occur. Apoptosis occurs 24 hours after the removal of adriamycin, while it has already been shown that exposure to an active test compound is necessary during the first 24 hours subsequent to adriamycin exposure to enhance the toxicity of adriamycin. This suggests that the active test compounds may enhance apoptosis at an early stage in the apoptotic pathway. This could be further investigated by determining the levels of proteins involved in early stages of apoptosis e.g. members of the bcl-2 family.

It has previously been shown in human B-cell lymphoma cells that an inhibition of DNA fragmentation (one of the early stages of apoptosis) occurs at high concentrations of adriamycin and this was closely linked to the inhibition of S phase traverse (Smith *et al.*, 1994). The authors concluded that the presence of drug or DNA damage is not sufficient to induce DNA fragmentation but that the unregulated commitment to S phase traverse is

an important factor in the activation of apoptosis. Since increasing concentrations of adriamycin disrupt the S phase in DLKP-SQ, deregulation of the S phase traverse could be a factor in the activation of apoptosis.

The adriamycin pulse exposure assays (Section 4.7) demonstrated that the enhanced cytotoxicity of N-1, O-1 and U-1 occurred during the first 24 hours after adriamycin removal. Flow cytometric analysis (Section 4.8) displayed an increased delay in the G_1 phase and in the S phase transition until there was a G_2/M arrest approximately 24 hours after adriamycin removal. Time-lapse videomicroscopy demonstrated that apoptosis was induced 24 hours after 1μM adriamycin removal. In the adriamycin plus U-1 treated sample, apoptosis was also induced after 24 hours but the rate of apoptosis was similar to adriamycin alone (Figure 3.9.2). However it is thought that the unregulated commitment to S phase traverse in response to adriamycin is an important factor for the activation of apoptosis (Smith *et al.*, 1994). Since increasing concentrations of adriamycin disrupt the S phase in DLKP-SQ, deregulation of the S phase traverse and the proteins that control the transition from G_1 into the S phase may have an important role in the activation of apoptosis.

4.10 Cell cycle proteins

To understand the effect of adriamycin and adriamycin plus U-1 in combination on the increased G_1/S delay, the kinase activity of the cyclin E/CDK2 complex (Section 3.10) and the levels of cyclin E and CDK2 were studied (Section 3.11). The transition from G_1 into S is controlled by the cyclin E/CDK2 complex and this is essential for the cell to begin DNA replication (see Section 1.3.1). Therefore, the cyclin E/CDK2 complex must be activated to overcome G_1 arrest. The level of cyclin E is regulated so that it is only transcribed during late G_1 and early S phase. Very little is known about the substrates of the cyclin E/CDK2 complex but it is thought to activate E2F and thus transcription of S phase genes. Once cells enter the S phase cyclin E is rapidly degraded. Therefore, by

investigating the role of cyclin E and CDK2 it would be possible to see if alterations in their levels are responsible for the G1 arrest and delayed S phase transition caused by adriamycin and adriamycin plus U-1 in combination as observed by flow cytometric analysis.

At least 3 forms of endogenous cyclin E protein have been detected in rat and human fibroblasts (Ohtsubo and Roberts, 1993) and HeLa cells (Dulic *et al.*, 1992). A 50kDa form is maximally expressed during late G_1 and early S phase while a 40 kDa form is thought to result from proteolytic degradation of overexpressed cyclin E or from translation initiation at an internal methionine residue (Ohtsubo and Roberts, 1993). A higher molecular weight form (55kDa) has been observed in G_2 and early to mid-G_1 when kinase activity is low but from late-G_1 the 50 kDa form is expressed.

The cyclin E/CDK2 kinase activity of U-1 treated samples demonstrated that the activity increased steadily up to 19 hours and then decreased at 24 hours. Adriamycin treated samples show a decrease in activity at 0 hours, which was when drug was removed after two hours drug exposure, compared to a control sample treated with drug free media for 2 hours. The activity increased slightly at 10 hours but then decreased gradually until 24 hours. When adriamycin and U-1 were combined there was an increase in activity at 10 hours which then decreased steadily until 24 hours (see Table 3.10.1). The kinase activity of cells treated with adriamycin plus U-1 was elevated compared to adriamycin alone. Activity treated with adriamycin may have peaked at an earlier time and then decreased, while activity in cells treated with adriamycin plus U-1 peaked at 10 hours. This could correlate to the observed delay in the cell cycle studies where the adriamycin plus U-1 samples enter the S phase later than adriamycin samples alone.

The levels of CDK2 varied over a 24 hr period in untreated DLKP-SQ cells and cells treated with U-1, adriamycin and the adriamycin plus U-1 combination (Figure 3.11.1 - 3.11.4). The levels increased initially, then decreased and subsequently increased again in each case. However, there seems to be no correlation between CDK2 levels and the cell cycle distribution (Figure 3.8.2, 3.8.4 and 3.8.7).

Untreated control samples showed an increase in levels of a higher molecular weight cyclin E (67kDa) at 10 hours; a 49 kDa band was evident from 10 to 16 hours which decreased with time until 24 hours (Figure 3.11.5). In U-1 treated samples, levels of another high molecular weight cyclin E (≅49kDa) increased from 10-13 hours, but had then decreased by 16 hours. There was also an increase in a 37.5 kDa band from 16 hours onwards (Figure 3.11.6). The level of the higher molecular weight (67kDa) cyclin E in adriamycin treated cells increased at 10-13 hours. A lower molecular weight band (37.5kDa) increased at 16 and 19 hours but decreased by 24 hours (Figure 3.11.7). Cyclin E levels in adriamycin and U-1 treated samples were similar to adriamycin treatment alone but at 13 hours the high molecular weight band (67kDa) appears stronger while the 37.5 kDa band has decreased compared to adriamycin (Figure 3.11.8).

Thus, the western blots of cyclin E in Figures 3.11.5 - 3.11.8 seem to indicate that an increased amount of the higher molecular weight form (67kDa) represents cells in G_1 or G_1 arrest; the form around 49 kDa seems to represent active cyclin E, while the lower molecular weight form (37.5 kDa) represents cells in late S and G_2/M. This would seem to correlate with the flow cytometry results and entry from G_1 into S. These results would also seem to indicate that the G_1/S delay is released when the higher molecular weight form of cyclin E decreases.

Levels of cyclin E were not elevated in U-1 treated samples compared to the control, while the kinase activity of the cyclin E/CDK2 did increase over time. However these results do not show the cyclinE/CDK2 kinase activity levels of control samples for each time point. Thus it is assumed that the activity of the control samples are approximately the same as or higher than U-1 treated samples. In contrast, the levels of cyclin E in adriamycin and adriamycin plus U-1 treated samples increased significantly compared to the control and U-1 samples. When cyclin E is overexpressed in cells, the cells progress through G_1 and into the S phase at a faster rate (Ohtsubo and Roberts, 1993). Thus, overexpression of cyclin E above would be expected to decrease the length of time a cell remained in G_1. Even though there were elevated levels of cyclin E there was no corresponding increase in kinase activity, in fact the kinase activity decreased. Therefore

the increase in protein levels but decrease in kinase activity suggests that cyclin E/CDK2 activity was inhibited. It has been previously shown that the activation of the cyclin E/CDK 2 complex appears to be the point at which radiation damage in the G_1 phase can delay the cell cycle (Dulic *et al.*, 1994). Therefore inhibition of cyclin E/CDK2 would lead to an arrest in G1 and a delay in the S phase transition.

Due to the increased rate of apoptosis during the initial 24 hours after vincristine treatment in U-1 treated samples, work investigating the role of cyclin E and CDK2 proteins in vincristine treated cells would be very interesting. Although cyclin E is one protein that controls the G_1/S transition (see Section 1.3.1), G_1 arrest may also be due to the inhibition of Rb, cyclin D1-CDK4/6 and/or due to the induction of p21, p27, p16 and other CKIs which inhibit cyclin-CDK complexes. Some of these proteins may be involved in the G_1/S delay induced by adriamycin and they would be interesting proteins to investigate.

5.0 Conclusions

This thesis examined the effect of combinations of different drugs on toxicity to cancer cells *in vitro*. The effects of combining existing anticancer agents were analysed first. A combination of carboplatin and adriamycin or vincristine was found to be additive in DLKP-A but antagonistic in DLKP. The combinations of adriamycin plus vincristine were antagonistic in both cell lines. Vincristine plus VP-16 was antagonistic in DLKP but did show synergism in DLKP-A. This synergy may result from each drug targeting different cellular processes.

Combinations with the glutathione depleting agent, BSO, with and without verapamil were also studied in DLKP and DLKP-A. The effect of BSO on the cytotoxicity of adriamycin in DLKP-A showed a synergistic toxic effect at the lowest concentration of BSO. At higher concentrations of BSO, the CI values were, in general, antagonistic. BSO plus verapamil in combination with adriamycin did not enhance the toxicity of adriamycin compared to a combination of BSO and adriamycin only, in DLKP. The combination of BSO plus verapamil in combination was synergistic with adriamycin in DLKP-A.

Different cellular models were also developed by transfection of the mdr-1 cDNA into sensitive cells, and by transfection of an anti-mdr-1 ribozyme into a P-glycoprotein over-expressing cell line.

The main part of the thesis concerned combinations of a known anticancer agent (adriamycin, vincristine and 5-fluorouracil) with one of a series of coded non-toxic compounds known to be safe for human use. Seven cell lines were tested. These cell lines were resistant variants derived from 2 parental human lung carcinoma cell lines, DLKP and SK-MES-1. These assays demonstrated that three of the test compounds N-1, O-1 and U-1, at non-toxic concentrations were found to enhance the toxicity of adriamycin in three cell lines; DLKP, DLKP-A-2B IC7 and SK-MES-1. No test compound demonstrated any enhanced toxic effect in DLKP-A-2B, DLKP pHaMDR1/A#2, SK-MES-1/Adr and SK-MES-1/Adr mdr1 ribozyme #4. Therefore the cell lines which were found to be sensitive to the synergistic effect of the test compounds were all drug sensitive (DLKP and SK-MES-1) or a low level resistant variant which does not express MDR1

(DLKP-A-2B IC7). All cell lines found to be insensitive to the test compounds were multidrug resistant P-glycoprotein overexpressing cell lines. Thus the mechanism of the test compounds involved was not inhibition of the P-glycoprotein drug efflux pump. Further studies, to characterise the effect of the test compounds should be performed in cell lines with different mechanisms of resistance. DLKP-A-2B IC7 has a low level of resistance possibly due to decreased levels of topoisomerase II (Heenan, 1994). Therefore the test compounds may be active in cell lines with mechanisms of resistance other than P-glycoprotein. It would be interesting to undertake similar investigations in cell lines overexpressing other drug efflux pumps including MRP and LRP. One derivative of DLKP developed by pulse exposure to adriamycin displays a five fold resistance to adriamycin compared to the sensitive parent (R. NicAmhlaoibh, personal communication). This cell line is a better *in vitro* model of drug resistance as it develops *in vivo* and examining effects of the test compounds on this cell line would be interesting.

Significant enhancement of toxicity with vincristine but not 5-fluorouracil, was observed with the three active test compounds. Interestingly, adriamycin and vincristine are both P-glycoprotein substrates while 5-fluorouracil is not. This seems to correlate with the results which show that cell lines expressing P-glycoprotein do not exhibit enhanced toxicity to adriamycin using any of the test compounds.

The standard circumvention assay used allowed the screening of test compounds in combination with adriamycin but did not provide an insight into the mechanism of the synergistic action. An assay was developed to analyse how synergy was affected when cells were exposed to the test compounds at different times relative to adriamycin exposure. Cells were pulse treated with adriamycin for 2 hours, adriamycin removed and the cells exposed to high levels of a test compound for short periods of time. Activity of the active test compounds was observed only during the 24 hours subsequent to drug exposure. Pre-treatment or treatment at later times was ineffective. When exposure for shorter periods (10 hours) was assayed the enhanced toxic effect of N-1 was evident during each 10 hour period for the initial 20 hours following adriamycin

exposure. However, while there was a consistent trend, the results were just outside the error values. To improve on these results, the clonogenic assay could be used instead of the growth assay used in this thesis. This assay may be more sensitive and thus could be used to quantify shorter time periods when exposure to a test compound may be important.

Since the active test compounds exerted their synergistic effect during the first 24 hours after drug removal, cycloheximide, a protein synthesis inhibitor, and actinomycin D, an inhibitor of transcription and translation, were used to try and block the synergistic effect. However, there was no inhibition of the enhanced toxic effect when they were used, separately, in combination with an active test compound after adriamycin exposure.

Further studies could be performed to investigate the effect of synchronising cells in specific phases of the cell cycle. If cells were synchronised in, for example, mitosis and pulse treated with a chemotherapeutic drug, followed by exposure to an active test compound, would there be an increase or decrease in sensitivity? In these experiments the cell cycle progression could be followed using flow cytometry and apoptotic events could be examined by time-lapse videomicroscopy.

In order to further investigate the role of these test compounds, flow cytometric analysis was used to determine the cell cycle distribution in DLKP-SQ, a human lung carcinoma clonal cell line, pulse treated with adriamycin, vincristine or 5-fluorouracil for 2 hours alone or with subsequent exposure to the test compounds for 24 hours. U-1 (active in the combination assay) on its own was shown to induce a transient G_1/S arrest but there was no apparent effect on the cell cycle distribution using A-1 (inactive) or N-1 (active). U-1 or N-1 in combination with adriamycin caused an increased delay in the G_1 phase and the S phase compared to adriamycin alone. This delay was not observed with adriamycin plus A-1 treatment. U-1 or N-1 in combination with vincristine, showed an increased G_2/M arrest compared to vincristine treated cells alone. This G_2/M arrest was expected since vincristine is a mitotic inhibitor. Vincristine plus A-1 in combination did show a slight cell cycle delay in G_1/S at 12 - 15 hours but this was not as striking as in U-1 or N-1 treated

cells. DLKP-SQ treated with 5-fluorouracil alone and in combination with U-1 showed no effect on the cell cycle distribution.

These pulse treatment experiments were repeated using increasing concentrations of adriamycin or vincristine. These results showed that there was an increased G_1/S phase arrest, a delay in S and a G_2/M arrest, with increasing concentrations of adriamycin. Increasing concentrations of vincristine showed a decrease in the G_1 peak and an increased G_2/M peak representing an increased G_2/M arrest as compared to untreated cells. These results suggest that the effect of U-1 and N-1 in combination with a chemotherapeutic drug (adriamycin and vincristine but not 5-fluorouracil), may mimic higher chemotherapeutic drug combinations. HPLC analysis of cells treated with drug could be used to assay the levels of a chemotherapeutic drug and the test compound. This would demonstrate if there was an increased accumulation of chemotherapeutic drug in samples treated with chemotherapic drug plus an active test compound as compared to chemotherapeutic treatment alone.

Time lapse videomicroscopic studies of the above combinations were also undertaken, and the rates of apoptosis and mitosis measured. Apoptosis occurred within 24 hours with vincristine and the rate of apoptosis was higher in the combination. Cells underwent apoptosis 24 hours after treatment with adriamycin but there was no significant difference between the apoptotic rate of the cells treated with adriamycin alone compared to the combination. This was surprising given the observed enhancement of toxicity in the 7 day toxicity assay.

Further investigations could be performed to try to determine at what stage of the cell cycle DLKP-SQ undergo apoptosis. These experiments would attempt to explain the observation that the active test compounds enhanced the toxicity of vincristine to a greater extent than adriamycin, and why there seemed to be no difference in the rate of apoptosis in adriamycin alone and adriamycin plus U-1 treated samples. An observation that could be further investigated is the fact that apoptosis begins 24 hours following adriamycin exposure, however the test compounds only enhance adriamycin toxicity during the initial

24 hours after adriamycin is removed. A possible explanation is that the active test compounds may enhance apoptosis at an early stage in the apoptotic pathway. This could be investigated by determining the expression of proteins involved in early stages of apoptosis e.g. members of the bcl-2 family.

To study if the combination effect was due to interference with proteins controlling cell cycle progress, cyclin E/CDK2 kinase activity was assayed and the levels of cyclin E and CDK2 were determined using western blotting. The levels of cyclin E were not elevated in U-1 treated samples as compared to the control, while the kinase activity of the cyclin E/CDK2 did increase over time. In contrast, the levels of cyclin E in adriamycin alone and adriamycin plus U-1 treated samples increased significantly compared to the control and U-1 samples but the kinase activity of adriamycin and adriamycin plus U-1 decreased. This increase in protein levels but decrease in kinase activity suggests that cyclin E/CDK2 activity was inhibited. Inhibition of cyclin E/CDK2 activity would lead to an arrest in G1 and a delay in the S phase transition. Future work investigating the role of cyclin E and CDK2 proteins in vincristine treated cells would be very interesting. Although cyclin E is one protein that controls the G_1/S transition (see Section 1.3.1), G_1 arrest may also be due to the inhibition of Rb, cyclin D1-CDK4/6 and/or by the induction of p21, p27, p16 and other CKIs which inhibit cyclin-CDK complexes. Some of these proteins may be involved in the G_1/S delay induced by adriamycin and would be interesting proteins to investigate.

6.0 References

Abbadie, C., Kabrun, N., Bouali, F., Smardova, J., Stehlin, D. and Vandenbunder, B. **(1993)** High levels of c-rel expression are associated with programmed cell death in the developing avian embryo and in bone marrow cell *in vitro*. *Cell* 75 899-912.

Ackerman, P., Glover, C. V. and Osheroff, N. **(1985)** Phosphorylation of DNA topoisomerase II by casein kinase II: modulation of eukaryotic topoisomerase II activity *in vitro*. *PNAS* 82 3164-3168.

Ackerman, P., Glover, C. V. and Osheroff, N. **(1988)** Phosphorylation of DNA topoisomerase II *in vivo* and total homogenates of Drosophila Kc cells. The role of casein kinase II. *J. Biol. Chem.* 263 12653-12660.

Alberts, B., Bray, D., Lewis, J., Raff, M., Roberts, K. and Watson, J. D. **(1994)** *Molecular Biology of the Cell*, Garland Publishing Inc.

Allsopp, T. E., Wyatt, S., Paterson, H. F. and Davies, A. M. **(1993)** The proto-oncogene bcl-2 can selectively rescue neurotrophic factor-dependent neurons from apoptosis. *Cell* 73 295-307.

Asiedu, C., Biggs, J., Lilly, M. and Kraft, A. S. **(1995)** Inhibition of leukemic cell growth by the protein kinase C activator bryostatin 1 correlates with the dephosphorylation of cyclin-dependent kinase 2. *Can. Res.* 55 3716-3720.

Barlogie, B., Drewinko, B., Johnston, D. A. and Freireich, E. J. **(1976)** The effect of adriamycin on the cell cycle traverse of a human lymphoid cell line. *Can. Res.* 36 1975-1979.

Barr, P. J. and Tomei, L. D. **(1994)** Apoptosis and its role in human disease. *Bio/technology* 12 487-493.

Bernhard, E. J., Maity, A., Muschel, R. J. and McKenna, W. G. **(1994)** Increased expression of cyclin B1 mRNA coincides with diminished G_2-phase arrest in irradiated HeLa cells treated with staurosporine or caffeine. *Radiat. Res.* 140 393-400.

Bertram, J., Palfner, K., Killian, M., Brysch, W., Schlingensiepen, K. H., Hiddemann, W. and Kneda, M. **(1995)** Reversal of multiple drug resistance *in vitro* by phosphorothioate oligonucleotides and ribozymes. *Anti-Canc. D.* 6 124-134.

Bertrand, R., Kerrigan, D., Sarang, M. and Pommier, Y. **(1991)** Cell death induced by topoisomerase inhibitors: role of calcium in mammalian cells. *Bioch. Pharm.* 42(1) 77-85.

Bisset, D., McLaughlin, K., Kelland, L. R. and Brown, R. **(1993)** Cisplatin-DNA damage recognition proteins in human tumour extracts. *Br. J. Canc.* 67 742-748.

Blight, M. A. and Holland, I. B. **(1990)** Structure and function of hemolysin B, P-glycoprotein and other members of a novel family of membrane translocators. *Molecular Microbiol.* 4 873-880.

Boise, L. H., Gonzalez-Garcia, M., Postema, C. E., Ding, L., Lindsten, T., Turka, L. A., Mao, X., Nunez, G. and Thompson, C. **(1993)** Bcl-x, a bcl-2-related gene that functions as a dominant regulator of apoptotic death. *Cell* 74 597-608.

Boyd, J. M., Gallo, G. J., Elangovan, B., Houghton, A. B., Malstrom, S., Avery, B. J., Ebb, R. G., Subramanian, T., Chittenden, T., Lutz, R. J. and Chinnadurai, G. **(1995)** Bip1, a novel death-inducing protein shares a distinct sequence motif with Bcl-2 family proteins and interacts with viral and cellular survival-promoting proteins. *Oncogene* 11(9) 1921-1928.

Bunch, R. T., Creswell, D. and Eastman, A. **(1994)** The effect of caffeine on G_2/M transition in CHO/UV41 cells. *Proceedings of the American Association for Cancer Research* 35 26.

Burt, R. K. and Thorgeirsson, S. S. **(1988)** Coinduction of MDR1 multidrug resistance and cytochrome P450 in rat liver by xenobiotics. *J. Nat. Canc.* 80 1383-1386.

Byfield, J. E., Murnane, J., Ward, J. F., Calabro-Jones, P., Lynch, M. and Kulhanian, F. **(1981)** Mice, men, mustards and methylated xanthines: the potential role of caffeine and related drugs in the sensitization of human tumours by alkylating agents. *Br. J. Canc.* 43 669-683.

Campain, J. A., Padmanabhan, R., Hwang, J., Gottesman, M. M. and Pastan, I. **(1993)** Characterisation of an unusual mutant of human melanoma cells resistant to anticancer drugs that inhibit topoisomerase II. *J. Cell Physiol.* 155 414-425.

Canman, C. E., Wolff, A. C., Chen, C. Y., Fornace, A. J. J. and Kastan, M. B. **(1994)** The p53-dependent G_1 cell cycle checkpoint pathway and ataxia-telangiectasia. *Can. Res.* 54 5054-5058.

Chan, V. T. W., Ng, S., Eder, J. P. and Schnipper, L. E. **(1993)** Molecular cloning and identification of a point mutation in the topoisomerase II cDNA from an etopside-resistant Chinese hampster ovary cell line. *J. Biol. Chem.* 268 2160-2165.

Chellappan, S. P., Hiebert, S., Mudryj, M., Horowitz, J. M. and Nevins, J. R. **(1991)** Independent binding of the retinablastoma protein and p107 to the transcription factor E2F. *Cell* 65 1053-1061.

Chen, C. J., Clark, D., Ueda, K., Pastan, I., Gottesman, M. M. and Roninson, I. B. **(1986)** Internal duplication and homology with bacterial transport proteins in the MDR1 (P-glycoprotein) gene from MDR cells. *Cell* 47 381-389.

Chen, C. Y., Oliner, J. D., Zhan, Q., Fornace, A. J. J., Vogelstein, B. and Kastan, M. B. **(1994)** Interactions between p53 and MDM2 in a mammalian cell cycle checkpoint pathway. *PNAS* 91 2684-2688.

Chen, G., Shi, L. F., Litchfield, D. W. and Greenburg, A. H. **(1995)** Rescue from granzyme B-induced apoptosis by wee1 kinase. *J. Exp. Med.* 181(6) 2295-2300.

Chen, J., Jackson, P. K., Kirschner, M. W. and Dutta, A. **(1995)** Separate domains of p21 involved in the inhibition of Cdk kinases and PCNA. *Nature* 374 386-388.

Chen, X., Bargotti, J. and Prives, C. **(1995)** p53,through p21 (WAF1/CIP1), induces cyclin D1 synthesis. *Can. Res.* 55 4257-4263.

Chen, Y. Q., Cipriano, S. C., Sarkar, F. H., Ware, J. L. and Arenkiel, J. M. **(1995)** p53-independent induction of p21 (WAF1) pathway is preserved during tumor progression. *Int. J. Oncol.* 7 889-893.

Chen-Levy, X. and Cleary, M. L. **(1990)** Membrane topology of the bcl-2 proto-oncogenic protein demonstrated *in vitro*. *J. Biol. Chem.* 265 4929-4933.

Cheng, X., Pantelias, G. E., Okayasu, R., Cheong, N. and Iliakis, G. **(1993)** Mitosis-promoting factor activity of inducer mitotic cells may affect radiation yield of interphase chromosome breaks in the premature chromosome condensation assay. *Can. Res.* 53 5592-5596.

Chittenden, T., Flemmington, C., Houghton, A. B., Chinnadurai, G. and Lutz, R. J. **(1995)** A conserved domain in bak, distinct from BH1 and BH2, mediates cell death and protein binding functions. *EMBO J.* 14(22) 5589-5596.

Chittenden, T., Harrington, E. A., O'Connor, R., Flemington, C., Lutz, R. J., Evan, G. I. and Guild, B. C. **(1995)** Induction of apoptosis by the bcl-2 homologue Bak. *Nature* 374 733-736.

Chou, J. and Chou, T. C. **(1987)** *Dose-effect analysis with microcomputers.* Cambridge, England, Biosoft.

Chou, T. C. and Talalay, P. **(1983)** Analysis of combined drug effects: a new look at a very old problem. *Trends Phar.* 4 450-454.

Chou, T. C. and Talalay, P. **(1984)** Quantitiative analysis of dose-effect relationships: the combined effects of multiple drugs or enzyme inhibitors. *Adv. Enzyme* 22 27-55.

Chugani, D. C., Rome, L. H. and Kedersha, N. L. **(1993)** Evidence that vault ribonucleoprotein particles localise to the nuclear pore complex. *J. Cell Sci.* 106 23-29.

Clarke, A. R., Purdie, C. A., Harrison, D. J., Morris, R. G., Bird, C. C., Hooper, M. L. and Wyllie, A. H. **(1993)** Thymocyte apoptosis induced by p53-dependent and independent pathways. *Nature* 362 849-852.

Cleary, I. **(1995)** Drug accumulation studies in multiple drug resistant human cell lines. *PhD* Dublin City University.

Cole, S. P. C., Bhardwaj, G., Gerlach, J. H., Mackie, J. E., Grant, C. E., Almquist, K. C., Stewart, A. J., Kurz, E. U., Duncan, A. M. V. and Deeley, R. G. **(1992)** Overexpression of a transporter gene in a multidrug-resistant human lung cancer cell line. *Science* 258 1650-1653.

Cole, S. P. C., Sparks, K. E., Fraser, K., Loe, D. W., Grant, C. E., Wilson, G. M. and Deeley, R. G. **(1994)** Pharmacological characterisation of multidrug resistant MRP-transfected human tumor cells. *Can. Res.* 54 5902-5910.

Connolly, D. T., Knight, M. B., Harakas, N. K., Wittwer, A. J. and Feder, J. **(1986)** Determination of the number of endothelial cells in culture using an acid phosphatase assay. *Analyt. Bioc.* 152 136-140.

Corcoran, G. B., Fix, L., Jones, D. P., Treinen Moslen, M., Nicotera, P., Oberhammer, F. A. and Buttyan, R. **(1994)** Apoptosis: Molecular control point in toxicity. *Tox. Appl. Ph.* 128 169-181.

Cordon-Cardo, C., O'Brien, J. P., Boccia, J., Casals, D., Bertino, J. R. and Melamed, M. R. **(1990)** Expression of the multidrug resistance gene product (P-glycoprotein) in human normal and tumor tissues. *J. Hist. Cyto.* 38 1277-1287.

Cross, S. M., Sanchez, C. A., Morgan, C. A., Schimke, M. K., Ramel, S., Idzerda, R. L., Raskind, W. H. and Reid, B. J. **(1995)** A p53-dependent mouse spindle checkpoint. *Science* 267 1353-1356.

Crown, J., Hakes, T., Reichman, B., Lebwohl, D., Gilewski, T., Surbone, A., Currie, V., Yao, T. J., Hudis, C., Seidman, A. and Norton, L. **(1993)** Phase II trial of carboplatin and etopside in metastatic breast cancer. *Cancer* 71(4) 1254-1257.

D'Arpa, P., Beardmore, C. and Liu, L. F. **(1990)** Involvement of nucleic acid synthesis in cell killing mechanisms of topoisomerase poisons. *Can. Res.* 50 6919-6924.

Daly, C., Coyle, S., McBride, S., O'Driscoll, L., Daly, N., Scanlon, K. and Clynes, M. **(1996)** *mdr*1 Ribozyme mediated reversal of the multi-drug resistant phenotype in human lung cell lines *Cytotechnology* 19(3) 199-205.

Danks, M. K., Schmidt, C. A., Deneka, D. A. and Beck, W. T. **(1989)** Increased ATP requirement for activity of and complex formation by DNA topoisomerase II from human leukemic CCRF-CEM cells selected for resistance to tenopside. *Cancer Commun.* 1 101-109.

Dano, K. **(1973)** Active outward transport of daunomycin in resistant Ehrlich ascites tumor cells *Biochim. Biophys. Acta* 323 466-483.

Darkin, S. J. and Ralph, R. K. **(1989)** A protein factor that enhances amsacrine-mediated formation of topoisomerase II-DNA complexes in murine mastocytoma cell nuclei. *Biochim. Biophys. Acta* 1007 295-300.

Darkin-Rattray, S. J. and Ralph, R. K. **(1991)** Evidence that a protein kinase enhances amsacrine mediated formation of topoisomerase II-DNA complexes in murine mastocytoma cell nuclei. *Biochim. Biophys. Acta* 1088 285-291.

Das, S. K., Lau, C. C. and Pardee, A. B. **(1982)** Abolition by cycloheximide of caffeine-enhanced lethality of alkylating agents in hampster cells. *Can. Res.* 42 4499-4504.

Datta, R., Hass, R., Gunji, H., Weichselbaum, R. and Kufe, D. **(1992)** Down-regulation of cell cycle control genes by ionizing radiation. *Cell Growth* 3 637-644.

De Isabella, P., Capranico, G., Binaschi, M., Tinelli, S. and Zunnio, F. **(1990)** Evidence of DNA-topoisomeraseII-dependent mechanisms of multidrug resistance in P388 leukemia cells. *Mol. Pharmacol.* 37 11-16.

De Tinguy-Moreaud, E., Pourquier, P., Montaudon, D. and Robert, J. **(1994)** Relationships between DNA damage and growth inhibition induced by topoisomerase II-interfering drugs in doxorubicin-sensitive and -resistant rat glioblastoma cells. *AnticancerRes.* 14 99-104.

Deffie, A. M., McPherson, J. P., Gupta, R. S., Hedley, D. W. and Goldenberg, G. J. **(1992)** Multifactorial resistance to antineoplastic agents in drug-resistant P388 murine leukemia, Chinese hampster ovary and human HeLa cells, with emphasis on the role of DNA topoisomerase II. *Biochem. Cell Biol.* 70 354-364.

DeGraff, W., Hahn, S. M., Mitchell, J. B. and Krishna, M. C. **(1994)** Free radical modes of cytotoxicity of adriamycin and streptonigrin. *Bioch. Pharm.* 48(7) 1427-1435.

Del Bino, G., Skierski, J. S. and Darzynkiewicz, Z. **(1991)** The concentration-dependent diversity of effects of DNA topoisomerase I and II inhibitors on the cell cycle of HL-60 cells. *Exp. Cell Re.* 195 485-491.

Demarcq, C., Bunch, R. T., Creswell, D. and Eastman, A. **(1994)** The role of cell cycle progression in cisplatin-induced apoptosis in chinese hampster ovary cells. *Cell Growth* 5 983-993.

DeVore, R. F., Corbett, A. H. and Osheroff, N. **(1992)** Phosphorylation of topoisomerase II by casein kinase II and protein kinase C: Effects on enzyme mediated DNA cleavage/religation and sensitivity to the antineoplastic drugs etopside and 4'-(9-acridinylamino)methane-sulfon-m-anisidide. *Can. Res.* 52 2156-2161.

DeWitt, D. and Smith, W. L. **(1995)** Yes, but do they still get headaches? *Cell* 63 345-348.

Dive, C. and Hickman, J. A. **(1991)** Drug-target interactions: only the first step in the commitent to programmed cell death? *Br. J. Canc.* 64 192-196.

Dive, C. and Wyllie, A. H. Apoptosis and cancer chemotherapy. Oxford, Blackwell Scientific. 21-56.

Dole, M. G., Jasty, R., Cooper, M. J., Thompson, C. B., Nunez, G. and Castle, V. P. **(1995)** Bcl-xL is expressed in neuroblastoma cells and modulates chemotherapy-induced apoptosis. *Can. Res.* 55 2576-2582.

Dole, M. G., Nunez, G., Merchant, A. K., Maybaum, J., Rode, C. K., Bloch, C. A. and Castle, V. A. **(1994)** Bcl-2 inhibits chemotherapy-induced apoptosis in neuroblastoma. *Can. Res.* 54 3253-3259.

Donaldson, K. L., Goolsby, G., Kiener, P. A. and Wahl, A. F. **(1994)** Activation of p34cdc2 coincident with taxol-induced apoptosis. *Cell Growth* 5 1041-1050.

Donaldson, K. L., Goolsby, G. L. and Wahl, A. F. **(1994)** Cytotoxicity of the anticancer agents cisplatin and taxol during cell proliferation and the cell cycle. *Int. J. Cancer* 57 847-855.

Dou, Q. P., An, B. and Yu, C. **(1995)** Activation of cyclin E-dependent kinase by DNA-damage signals during apoptosis. *Biochemical and Biophysical Research Communications* 214(3) 771-780.

Downes, C. S., Clarke, D. J., Mullinger, A. M., Gimmenez-Ablan, J. F., Creighton, A. M. and Johnson, R. T. **(1994)** A topoisomerase II-dependent G_2 cycle checkpoint in mammalian cells. *Nature* 372 467-470.

Drake, F. H., Zimmerman, J. P., McCabe, F. L., Bartus, H. F., Per, S. R., Sullivan, D. M., Ross, W. E., Mattern, M. R., Johnson, R. K., Crooke, S. T. and Mirabelli, C. K. **(1987)** Purification of topoisomerase II from amsacrine-resistant P388 leukemia cells. *J. Biol. Chem.* 262 16739-16747.

Dubrez, L., Goldwasser, F., Genne, P., Pommier, Y. and Solary, E. **(1995)** The role of cell cycle regulation and apoptosis triggering in determining the senstivity of leukemic cells to topoisomerase I and II inhibitors. *Leukemia* 9 1013-1024.

Dulic, V., Kaufmann, W. K., Wilson, S. J., Tisty, T. D., Lees, E., Harper, W. J., Elledge, S. J. and Reed, S. I. **(1994)** p53-dependent inhibition of cyclin-dependent kinase activities in human fibroblasts during radiation-induced G_1 arrest. *Cell* 76 1013-1023.

Dulic, V., Lees, E. and Reed, S. I. **(1992)** Association of human cyclin E with a periodic G_1-S phase protein kinase. *Science* 257 1958-1961.

Eblen, S. T., Fautsch, M. P., Burnette, R. J., Snyder, M. and Leof, E. B. **(1995)** Dissociation of p34cdc2 complex formation from phosphorylation and histone H1 kinase activity. *Can. Res.* 55 1994-2000.

Enoch, T. and Norbury, C. **(1995)** Cellular responses to DNA damage: cell-cycle checkpoints, apoptosis and the roles of p53 and ATM. *TIBS* 20 426-430.

Erlichman, C., Moore, M., Thiessen, J. J., Kerr, I. G., Walker, S., Goodman, P., Bjarnason, G., DeAngelis, C. and Bunting, P. **(1993)** Phase I pharmacokinetic study of cyclosporin A combined with doxorubicin. *Can. Res.* 53 4837-4842.

Evan, G., Harrington, E., Fanidi, A., Land, H., Amati, B. and Bennett, M. **(1994)** Integrated control of cell proliferation and cell death by the c-myc oncogene. *Phil. Trans. R. Soc. Lond. B. Biol. Sci.* 345 269-275.

Evan, G., Wyllie, A. H., Gilbert, C. S., Littlewood, T. D., Land, H., Brooks, M., Waters, C. M., Penn, L. Z. and Hancock, D. C. **(1992)** Induction of apoptosis in fibroblasts by c-myc protein. *Cell* 69 119-128.

Evans, H. J. **(1993)** Molecular genetics aspects of human cancers: The 1993 Frank Rose lecture. *Br. J. Canc.* 68 1051-1060.

Ewen, M. E., Sluss, H. K., Whitehouse, L. L. and Livingston, D. M. **(1993)** TGF-ß inhibition of Cdk4 synthesis is linked to cell cycle arrest. *Cell* 74 1009-1020.

Fan, S., El-Deiry, W. S., Bae, I., Freeman, J., Jondle, D., Bhatia, K., Fornace, A. J. J., Magrath, I., Kohn, K. W. and O'Connor, P. M. **(1994)** p53 gene mutations are associated with decreased sensitivity of human lymphoma cells to DNA damaging agents. *Can. Res.* 54 5824-5830.

Farrow, S. N., White, J. H. M., Martinou, I., Raven, T., Pun, K.-T., Grinham, C. J., Martinou, J.-C. and Brown, R. **(1995)** Cloning of a bcl-2 homologue by interaction with adenovirus E1B 19K. *Nature* 374 731-733.

Felmelee, T., Pellett, S. and Welch, R. A. **(1985)** Nucleotide sequence of an Escherichia coli chromosomal hemolysin. *J. Bacteriol.* 163 94-105.

Ferguson, P. J., Fisher, M. H., Stephenson, J., Li, D., Zhou, B. and Cheng, Y. **(1988)** Combined modalities of resistance in etopside-resistant human KB cells. *Can. Res.* 48 5956-5964.

Fernandes, D. J., Danks, M. K. and Beck, W. T. **(1990)** Decreased nuclear matrix DNA topoisomerase II in human leukemia cells resistant to VM-26 and m-AMSA. *Biochem.* 29 4235-4241.

Fernandes, R. S. and Cotter, T. G. **(1994)** Apoptosis or necrosis - Intracellular levels of glutathione influence mode of cell death. *Bioch. Pharm.* 48(4) 675-681.

Fingert, H. J., Chang, J. D. and Pardee, A. B. **(1986)** Cytotoxic, cell cycle, and chromosomal effects of methylxanthines in human tumor cells treated with alkylating agents. *Can. Res.* 46 2463-2467.

Fisher, R. P. and Morgan, D. O. **(1994)** A novel cyclin associates with MO15/CDK7 to form the CDK activating kinase. *Cell* 78 713-724.

Fojo, A. T., Ueda, K., Salmon, D. J., Poplack, D. G., Gottessman, M. M. and Pastan, I. **(1987)** Expression of a multidrug resistance gene in human tumors and tissues. *Proceedings of the American Association for Cancer Research* 84 265-259.

Foote, S. T., Thompson, J. K., Cowman, A. F. and Kemp, D. J. **(1989)** Amplification of the multidrug resistance gene in some chloroquine resistant isolates of P.falciparum. *Cell* 57 921-930.

Ford, J. M. **(1995)** Modulators of multidrug resistance. *Oncology and Hematology* 9(2) 337-361.

Fotedar, R., Fitzgerald, P., Rousselle, T., Cannella, D., Doree, M., Messier, H. and Fotedar, A. **(1996)** p21 contains independent binding sites for cyclin and cdk2: Both sites are required to inhibit cdk2 kinase activity. *Oncogene* 12 2155-2164.

Fotedar, R., Flatt, J., Gupta, S., Margolis, R. L. and Fitzgerald, P. **(1994)** *Molecular & Cell Biology* 15 932-.

Fotedar, R., Flatt, J., Gupta, S., Margolis, R. L., Fitzgerald, P., Messier, H. and Fotedar, A. **(1995)** Activation-induced T-cell death is cell cycle dependent and regulated by cyclin B *Mol. Cell Biol.* 15(2) 932-942.

Freeman, R. S., Estus, S. and Johnson Jr., E. M. **(1994)** Analysis of cell cycle-related gene expression in postmitotic neurons: Selective induction of cyclin D1 during programmed cell death. *Neuron* 12 343-355.

Friedberg, E. C. **(1985)** *DNA Repair* New York, Freeman.

Gekeler, V., Frese, G. and Noller, A. **(1992)** Mdr1/P-glycoprotein, topoisomerase, and glutathione-S-transferase-π gene expression in primary and relapsed state adult and childhood leukaemia. *Br. J. Canc.* 66 507-517.

Gewirtz, D. A. **(1993)** DNA damage, gene expression, growth arrest and cell death. *Oncol. Res.* 5(10/11) 397-408.

Girinsky, T., Koumenis, C., Graeber, T. G., Peehl, D. M. and Giaccia, A. J. **(1995)** Attenuated response of p53 and p21 in primary cultures of human prostatic epithelial cells exposed to DNA-damaging agents. *Can. Res.* 55 3726-3731.

Glisson, B. R., Gupta, R., Smallwood-Kentro, S. and Ross, W. **(1986)** Characterization of acquired epipodophyllotoxin resistance in chinese hampster ovary cell line: Loss of drug-stimulated DNA cleavage activity. *Can. Res.* 46 1934-1938.

Gorbsky, G. J. **(1994)** Cell cycle progression and chromosome segregation in mammalian cells cultured in the presence of the topoisomerase inhibitors ICRF-187 [(+)-1,2-bis(3,5-dioxopiperazinyl-1-yl)propane; ADR-529] and ICRF-159 (Razoxane). *Can. Res.* 54 1042-1048.

Gorczyca, W., Gong, J., Ardelt, B., Traganos, F. and Darzynkiewicz, Z. **(1993)** The cell cycle related differences in susceptibility of HL-60 cells to apoptosis induced by various antitumor agents. *Can. Res.* 53 3186-3192.

Gros, P., Neriah, Y. B., Croop, J. M. and Housman, D. E. **(1986)** Isolation and expression of a complementary DNA that confers multidrug resistance. *Nature* 323 728-731.

Hain, J., Crompton, N. E. A., Burkart, W. and Jaussi, R. **(1993)** Caffeine release of radiation induced S and G_2 phase arrest in V79 hampster cells: Increase of histone messenger RNA levels and p34cdc2 activation. *Can. Res.* 53 1507-1510.

Hain, J., Jaussi, R. and Wurgler, F. E. **(1994)** Effects of ionizing radiation and caffeine treatment on cyclin dependent kinase complexes in V79 hampster cells. *Cell Signal* 6(5) 539-550.

Hall, P. A. and Lane, D. P. **(1994)** Genetics of growth arrest and cell death: Key determinants of tissue homeostasis. *Eur. J. Canc.* 30A(13) 2001-2012.

Han, J., Sabbatini, P., Perez, D., Rao, L., Modha, D. and White, E. **(1996)** The E1B 19K protein blocks apoptosis by interacting with and inhibiting the p53-inducible and death-promoting Bax protein. *Genes & Development* 10(4) 461-477.

Han, J. and White, E. **(1995)** Induction of apoptosis by the E1B 19K binding protein, Nbk. *In preparation* .

Hannon, G. J., Demetrick, D. and Beach, D. **(1993)** Isolation of Rb-related p130 through its interaction with CDK2 and cyclins. *Genes & Development* 7 2378-2391.

Harrison, D. J. **(1995)** Molecular mechanisms of drug resistance in tumours *J. Pathology* 175 7-12.

Heenan, M. **(1994)** Clonal variation in multidrug resistant human cell populations *PhD* Dublin City University.

Hengartner, M. O. and Horwitz, H. R. **(1994)** C.elegans cell survival gene ced-9 encodes a functional homolog of the mammalian proto-oncogene bcl-2. *Cell* 76 665-676.

Hermeking, H., Funk, J. O., Reichert, M., Ellwart, J. W. and Eick, D. **(1995)** Abrogation of p53-induced cell cycle arrest by c-myc: evidence for an inhibitor of p21,WAF1. *Oncogene* 11 1409-1415.

Heusel, J. W., Wesselschmidt, R. L., Shresta, S., Russell, J. H. and Ley, T. J. **(1994)** Cytotoxic lymphocytes require granzyme B for the rapid induction of DNA fragmentation and apoptosis in allogeneic target cells. *Cell* 70 977-987.

Higgins, C. **(1989)** Export import family expands. *Nature* 340 342-346.

Hoang, A. T., Cohen, K. J., Barrett, J. F., Bergstrom, D. A. and Dang, C. V. **(1994)** Participation of cyclin A in Myc-induced apoptosis. *PNAS* 91 6875-6879.

Holm, P. S., Scanlon, K. J. and Dietal, M. **(1994)** Reversion of multidrug resistance in the P-glycoprotein-positive human pancreatic cell line (EPP85-181RDB) by introduction of a hammerhead ribozyme. *Br. J. Canc.* 70 239-243.

Hsiang, Y. H. **(1989)** Arrest of replication forks by drug-stabilised topoisomerase I-DNA cleavable complexes as a mechanism of cell killing by campothecin. *Can. Res.* 49 5077-5082.

Hyde, S. C., Emsley, P., Hartshorn, M. J., Mimmach, M. M., Gileadi, U., Pearce, S. R., Gallagher, M. P., Gill, D. R., Hubbard, R. E. and Higgins, C. F. **(1990)** Structural model of ATP-binding proteins associated with cycstic fibrosis, multidrug resistance and bacterial transport. *Nature* 346 362-365.

Ishida, R., Sato, M., Narita, T., Utsumi, K. R., Nishimoto, T., Morita, T., Nagata, H. and Andoh, T. **(1994)** Inhibition of DNA topoisomerase II by ICRF-193 induces polyploidization by uncoupling chromosome dynamics from other cell cycle events. *J. Cell Biol.* 126(6) 1341-1351.

Izquierdo, M. A. **(1996)** Non-Pgp related multidrug resistance *PhD.* Vrije Universiteit.

Izquierdo, M. A., Scheffer, G. L., Flens, M. J., Giaccone, G., Broxterman, H. J., Meijer, C. J. L. M., van der Valk, P. and Scheper, R. J. **(1996)** Broad distribution of the multidrug resistance related vault protein LRP in normal human tissues and tumors. *American Journal of Pathology* In Press.

Izquierdo, M. A., Shoemaker, R. H., Flens, M. J., Scheffer, G. L., Wu, L., Prather, T. R. and Scheper, R. J. **(1996)** Overlapping phenotypes of multidrug resistance among panels of human cancer-cells lines. *Int. J. Cancer* 65 1-8.

Izquierdo, M. A., van der Zee, A. G. J., Vermorken, J. B., van der Valk, P., Belien, J. A. M., Giaccone, G., Scheffer, G. L., Flens, M. J., Pinedo, H. M., Kenemans, P., Meijer, C. J. L. M., de Vries, E. G. E. and Scheper, R. J. **(1995)** Drug resistance-associated marker LRP for prediction of response to chemotherapy and prognoses in advanced ovarian carcinoma. *J. Nat. Canc.* 87 1230-1237.

Jedlitschky, G., Leier, I., Buchholz, U., Barnouin, K., Kurz, G. and Keppler, D. **(1996)** Transport of glutathione, glucuronate, and sulfate conjugates by the MRP gene-encoded conjugate export pump. *Can. Res.* 56 988-994.

Jordan, M. A., Thrower, D. and Wilson, L. **(1992)** Effects of vinblastine, podophyllotoxin and nocodazole on mitotic spindles. *J. Cell Sci.* 102 401-416.

Jordan, M. A., Thrower, D. and Wilson, S. **(1991)** Mechanism of inhibition of cell proliferation by vinca alkaloids. *Can. Res.* 51 2212-2222.

Kalwinsky, D. K., Look, A. T., Ducore, J. and Fridland, A. **(1983)** Effects of the epipodophyllotoxin VP-16-213 on cell cycle traverse, DNA synthesis, DNA strand size in cultures of human leukemic lymphoblasts. *Can. Res.* 43 1592-1597.

Kastan, M. B., Canman, C. E. and Leonard, C. J. **(1995)** p53, cell cycle control and apoptosis: Implications for cancer. *Canc. Metast.* 14 3-15.

Kastan, M. B., Onyekwere, O., Sidransky, D., Vogelstein, B. and Craig, R. W. **(1991)** Participation of p53 protein in the cellular response to DNA damage. *Can. Res.* 51 6304-6311.

Kastan, M. B., Zhan, Q., El-Deiry, W. S., Carrier, F., Jacks, T., Walsh, W. V., Plunkett, B. S., Vogelstein, B. and Fornace, A. J. **(1992)** A mammalian cell cycle checkpoint pathway utilising p53 and GADD45 is defective in ataxia-telangiectasia. *Cell* 71 587-597.

Kedersha, N. L., Heuser, J. E., Chugani, D. C. and Rome, L. H. **(1991)** Vaults III. Vault ribonucleoprotein particles open into flower-like structures with octagonal symmetry. *J. Cell Biol.* 112 225-235.

Kedersha, N. L., Miquel, M.-C., Bittner, D. and Rome, L. H. **(1990)** Vaults II. Ribonucleoprotein structures are highly conserved among higher and lower eukaryotes. *J. Cell Biol.* 110 895.

Kedersha, N. L. and Rome, L. H. **(1986)** Isolation and characterisation of a novel ribonucleoprotein particle: large structures contain a single species of small RNA. *J. Cell Biol.* 103 699-709.

Kiehntopf, M., Brach, M. A., Licht, T., Petschauer, S., Karawajew, L., Kirschning, C. and Herrman, F. **(1994)** Ribozyme-mediated cleavage of the MDR-1 transcript restores chemosensitivity in previously resistant cancer cells. *EMBO J.* 13(19) 4645-4652.

King, R. W., Jackson, P. K. and Kirschner, M. W. **(1994)** Mitosis in transition *Cell* 79 563-571.

Knoblich, J. A., Sauer, K., Jones, L., Richardson, H., Saint, R. and Lehner, C. F. **(1994)** Cyclin E controls S phase progression and its down-regulation during Drosophila embryogenesis is required for the arrest of cell proliferation. *Cell* 77 107-120.

Korsmeyer, S. J. **(1992)** Bcl-2 initiates a new category of oncogenes: regulators of cell death. *Blood* 80 879-886.

Kozopas, K. M., Yang, T., Buchan, H., Zhou, P. and Craig, R. W. **(1993)** MCL1, a gene expressed in programmed myeloid cell differentiation, has sequence similiarity to BCL-2. *PNAS* 90 3516-3520.

Kranenburg, O., van der Eb, A. and Zantema, A. **(1996)** Cyclin D1 is an essential mediator of apoptotic neuronal cell death. *EMBO J.* 15(1) 46-54.

Krek, W., Ewen, M. E., Shirodkar, S., Arany, S., Kaelin, W. G. and Livingstone, D. M. **(1994)** Negative regulation of the growth-promoting transcription factor E2F-1 by a stably bound cyclin A-dependent protein kinase. *Cell* 78 161-172.

Krek, W. and Nigg, E. A. **(1991)** Differential phosphorylation of vertebrate p34cdc2 kinase at the G_1/S and G_2/M transitions of the cell cycle: identification of major phosphorylation sites. *EMBO J.* 10 305-316.

Krishan, A. and Frei, E. **(1976)** Effect of adriamycin on the cell cycle traverse and kinetics of cultured human lymphocytes. *Can. Res.* 36 143-150.

Krishnamachary, N. and Center, M. S. **(1993)** The MRP gene associated with a non-P-glycoprotein multidrug resistance encodes a 190-kDa membrane bound glycoprotein. *Can. Res.* 53 3658-3661.

Kumar, S., Kinoshita, M., Noda, M., Copeland, N. G. and Jenkins, N. A. **(1994)** Induction of apoptosis by the mouse Nedd2 gene, which encodes a protein similar to the product of the Caenorhabditis elegans cell death gene ced-3 and the mammalian IL-1ß-converting enzyme. *Genes & Development* 8 1613-1626.

Kung, A. L., Zetterburg, A., Sherwood, S. W. and Schimke, R. T. **(1990)** Cytotoxic effects of the cell cycle phase specific agents: Result of cell cycle perturbation. *Can. Res.* 50 7307-7317.

La Thangue, N. **(1994)** DP and E2F proteins: components of a heterodimeric transcription factor implicated in cell cycle control. *Curr. Op. Cel.* 6 443-450.

Lahti, J. M., Xiang, J., Heath, L. S., Campana, D. and Kidd, V. J. **(1995)** PITSLRE protein kinase activity is assaoiated with apoptosis. *Mol. Cell Biol.* 15(1) 1-11.

Lee, F. Y. F., Allalunis-Turner, M. J. and Siemann, D. W. **(1987)** Depletion of tumour versus normal glutathione by buthionine sulfoximine. *Br. J. Canc.* 56 33-38.

Lees, E., Faha, B., Dulic, V., Reed, S. I. and Harlow, E. **(1992)** Cyclin E/cdk2 and cyclin A/cdk2 kinases associate with p107 and E2F in a temporally distinct manner. *Genes & Development* 6 1874-1885.

Lew, D. J., Dulic, V. and Reed, S. I. **(1991)** Isolation of three novel human cyclins by rescue of G_1 cyclin (Cln) function in yeast. *Cell* 66 1197-1206.

Li, C. J., Friedman, D. J., Wang, C., Metelev, V. and Pardee, A. B. **(1995)** Induction of apoptosis in uninfected lymphocytes by HIV-1 tat protein. *Science* 268 429-431.

Lin, E. Y., Orlofsky, A., Berger, M.-S. and Prystowsky, M. B. **(1993)** Characterisation of A1, a novel hemopoietic-specific early response gene with sequence similarity to bcl-2. *J. Immunol.* 151 1979-1988.

Lin, Y. and Benchimol, S. **(1995)** Cytokines inhibit p53-mediated apoptosis but not p53-mediated G_1 arrest. *Mol. Cell Biol.* 15(11) 6045-6054.

Ling, Y. H., Priebe, W. and Perez-Soler, R. **(1993)** Apoptosis induced by anthracycline antibiotics in P388 parent and multidrug-resistant cells. *Can. Res.* 53 1845-1852.

Liu, L. F. **(1989)** DNA topoisomerase poisons as antitumour drugs. *Annu. Rev. Biochem.* 58 351-375.

Liu, S. Y., Hwang, B. D., Haruna, M., Imakura, Y., Lee, K. H. and Cheng, Y. C. **(1989)** Podophyllotoxin analogs: effects on DNA topoisomerase II, tubulin polymerization, human tumor KB cells, and their VP-16-resistant variants. *Mol. Pharmacol.* 36 78-82.

Lock, R. B. **(1992)** Inhibition of p34cdc2 kinase activation, p34cdc2 tyrosine dephosphorylation, and mitotic progression in chinese hampster ovary cells exposed to etopside *Can. Res.* 52 1817-1822.

Lock, R. B., Galperina, O. V., Feldhoff, R. C. and Rhodes, L. J. **(1994)** Concentration-dependent differences in the mechanisms by which caffeine potentiates etopside cytotoxicity in HeLa cells *Can. Res.* 54 4933-4939.

Lock, R. B. and Keeling, P. K. **(1993)** Responses of HeLa and chinese hampster ovary p34cdc2/cyclin-B kinase in relation to cell cycle perturbations induced by etopside *Int. J. Oncol.* 3 33-42.

Lock, R. B. and Ross, W. E. **(1990)** Inhibition of p34cdc2 kinase activity by etopside or irradiation as a mechanism of G_2 arrest in chinese hampster ovary cells. *Can. Res.* 50 3761-3766.

Lock, R. B. and Ross, W. E. **(1990)** Possible role for p34cdc2 kinase in etopside-induced cell death of chinese hampster ovary cells *Can. Res.* 50 3767-3771.

Lotem, J. and Sachs, L. **(1993)** Regulation of bcl-2, c-myc, and p53 of susceptibility to induction of apoptosis by heat shock and cancer chemotherapy compounds in differentiation-competent and -defective myeloid leukemic cells. *Cell Growth* 4 41-47.

Lowe, S. W., Schmitt, E. M., Smith, S. W., Osborne, B. A. and Jacks, T. **(1993)** p53 is required for radiation-induced apoptosis in mouse thymocytes. *Nature* 362 847-849.

Lücke-Huhle, C. **(1982)** α-Irradiation-induced G_2 delay: a period of cell recovery. *Radiat. Res.* 89 298-308.

Ludlow, J. W., Shon, J., Pipas, J. M., Livingston, D. M. and DeCaprio, J. A. **(1990)** The retinablastoma susceptibility gene product undergoes cell cycle dependent dephosphorylation and binding to and release from SV40 large T. *Cell* 60 387-396.

Maity, A., McKenna, W. G. and Muschel, R. J. **(1995)** Evidence for post-translational regulation of cyclin B1 mRNA in the cell cycle following irradiation in HeLa cells. *EMBO J.* 14(3) 603-609.

Marks, D. I. and Fox, R. M. **(1991)** DNA damage, poly(ADP-ribosyl)ation and apoptotic cell death as a potential common pathway of cytotoxic drug action. *Bioch. Pharm.* 42 1859-1867.

Martin, A. and Clynes, M. **(1991)** Acid phosphatase: Endpoint for *in vitro* toxicity assays. *In vitro Cell. Dev. Biol.* 27A 183-184.

Martin, S. J., McGahon, A. J., Nishioka, W. K., La Face, D., Guo, X., Th'ng, J., Bradbury, E. M. and Green, D. G. **(1995)** p34cdc2 and apoptosis. *Science* 269 106-107.

Matsushime, H., Roussel, M. F., Ashmun, R. A. and Sherr, C. J. **(1991)** Colony-stimulating factor 1 regulates novel cyclins during the G_1 phase of the cell cycle. *Cell* 65 701-713.

Mattern, J. and Volm, M. **(1995)** Resistance mechanisms in human lung cancer. *Invas. Metas.* 15 81-94.

McBride, S. **(1995)** Characterisation of clonal variants in a human lung carcinoma cell line: investigations into control of cell growth and differentiation. *PhD* Dublin City University.

McGahon, A., Bissonnette, R., Schmitt, M., Cotter, K. M., Green, D. R. and Cotter, T. G. **(1994)** BCR-ABL maintains resistance of chronic myelogenous leukemia cells to apoptotic cell death. *Blood* 83 1179-1187.

McIlwrath, A. J., Vasey, P. A., Ross, G. M. and Brown, R. **(1994)** Cell cycle arrests and radiosensitivity of human tumor cell lines: Dependence on wild-type p53 for radiosensitivity. *Can. Res.* 54 3718-3722.

McKenna, W. G., Iliakis, G., Weiss, M. C., Bernhard, E. J. and Muschel, R. J. **(1991)** Increased G_2 delay in radiation-resistant cells obtained by transformation of primary rat embryo cells with the oncogenes H-ras and v-myc. *Radiat. Res.* 125 283-287.

Meikrnatz, W., Gisselbrecht, S., Tam, S. and Schlegel **(1994)** Activation of cyclin A-dependent kinases during apoptosis. *PNAS* 91 3754-3758.

Merry, D. E., Veis, D. J., Hickey, W. F. and Korsmeyer, S. J. **(1994)** Bcl-2 protein expression is widespread in the developing nervous system and retained in the adult PNS. *Development* 120 301-311.

Minn, A. J., Rudin, C. M., Boise, L. H. and Thompson, C. B. **(1995)** Expression of Bcl-x_L can confer a multidrug resistance phenotype. *Blood* 86(5) 1903-1910.

Miura, M., Zhu, H., Rotello, R., Hartwieg, E. A. and Yuan, J. **(1993)** Induction of apoptosis in fibroblasts by IL-1ß-converting enzyme, a mammalian homolog of the C.elegans cell death gene ced 3. *Cell* 75 653-660.

Miyashita, T., Krajewski, S., Krajewska, M., Wang, H. G., Lin, H. K., Liebermann, D. A., Hoffman, B. and Reed, J. C. **(1994)** Tumor suppressor p53 is a regulator of bcl-2 and bax gene expression *in vitro* and *in vivo*. *Oncogene* 9 1709-1805.

Miyashita, T. and Reed, J. C. **(1993)** Bcl-2 oncoprotein blocks chemotherapy-induced apoptosis in a human leukemia cell line. *Blood* 81 151-157.

Miyashita, T. and Reed, J. C. **(1995)** Tumor suppressor p53 is a direct transcriptional activator of the human bax gene. *Cell* 80 293-299.

Muller, R. **(1995)** Transcriptional regulation during the mammalian cell cycle. *Trends Gen.* 11(5) 173-178.

Muschel, R. J., Zhang, H. B., Iliakis, G. and McKenna, W. G. **(1991)** Cyclin B expression in HeLa cells during the G_2 block induced by ionizing radiation. *Can. Res.* 51 5113-5117.

Muschel, R. J., Zhang, H. B. and McKenna, W. B. **(1993)** Differential effect of ionizing radiation on the expression of cyclin A and cyclin B in HeLa cells. *Can. Res.* 53 1128-1135.

Musk, S. R., Downes, C. S. and Johnson, R. T. **(1988)** Caffeine induces uncoordinated expression of cell cycle functions after ultraviolet irradiation. Accelerated cycle transit, sister chromatid exchanges, and premature chromosome condensation in a transformed Indian muntjac cell line. *J. Cell Sci.* 90 591-599.

Nagata, S. and Suda, T. **(1995)** Fas and Fas ligand: lpr and gld mutations. *Immunology Today* 16(1) 39-42.

Neefjes, J. J., Momburg, F. and Hammerling, G. J. **(1993)** Selective and ATP-dependent translocation of peptides by the MHC-encoded transporter. *Science* 261 769-771.

Nguyen, M., Millar, D. G., Yong, V. W., Korsmeyer, S. J. and Shore, G. C. **(1993)** Targeting of bcl-2 to the mitochondrial outer membrane by a COOH-terminal signal anchor sequence. *J. Biol. Chem.* 268 25265-25268.

Norbury, C., MacFarlane, M., Fearnhead, H. and Cohen, G. M. **(1994)** Cdc2 activation is not required for thymocyte apoptosis. *Biochemical and Biophysical Research Communications* 202(3) 1400-1406.

Norbury, C. and Nurse, P. **(1992)** Animal cell cycles and their control. *Annu. Rev. Biochem.* 61 441-470.

O'Connor, P. M., Ferris, D. K., Hoffmann, I., Jackman, J., Draetta, G. and Kohn, K. W. **(1994)** Role of the cdc25C phosphatase in G_2 arrest induced by nitrogen mustard. *PNAS* 91 9480-9484.

O'Connor, P. M., Ferris, D. K., Pagano, M., Draetta, G., Pines, J., Hunter, T., Longo, D. L. and Kohn, K. W. **(1993)** G_2 delay induced by nitrogen mustard in human cells affects cyclin A/cdk2 and cyclin B1/cdc2-kinase complexes differently. *J. Biol. Chem.* 268(11) 8298-8308.

O'Connor, P. M., Ferris, D. K., White, G. A., Pines, J., Hunter, T., Longo, D. L. and Kohn, K. W. **(1992)** Relationships between cdc2 kinase, DNA cross-linking, and cell cycle perturbations induced by nitrogen mustard. *Cell Growth* 3 43-52.

O'Connor, P. M., Jackman, J., Jondle, D., Bhatia, K., Magrath, I. and Kohn, K. W. **(1993)** Role of the p53 tumor suppressor gene in cell cycle arrest and radiosensitivity of burkitt's lymphoma cell lines. *Can. Res.* 53 4776-4780.

O'Connor, P. M., Wassermann, K., Sarang, M., Magrath, I., Bohr, V. A. and Kohn, K. W. **(1991)** Relationship between DNA cross-links, cell cycle, and apoptosis in burkitt's lymphoma cell lines differing in sensitivity to nitrogen mustard. *Can. Res.* 51 6550-6557.

Oberhammer, F. A., Hochegger, K., Froschl, G., Tiefenbacher, R. and Pavelka, M. **(1994)** Chromatin condensation during apoptosis is accomanied by degradation of lamin A + B, without enhanced activation of cdc2 kinase. *J. Cell Biol.* 126(4) 827-837.

Ohtsubo, M. and Roberts, J. M. **(1993)** Cyclin-dependent regulation of G_1 in mammalian fibroblasts. *Science* 259 1908-1912.

Oliner, J. D., Pietenpol, J. A., Thiagalingam, S., Gyuris, J., Kinzler, K. W. and Vogelstein, B. **(1993)** Oncoprotein mdm2 conceals the activation domain of the tumor suppressor p53. *Nature* 362 857-860.

Oltvai, Z. N. and Korsmeyer, S. J. **(1994)** Checkpoints of dueling dimers foil death wishes. *Cell* 79 189-192.

Oltvai, Z. N., Milliman, C. L. and Korsmeyer, S. J. **(1993)** Bcl-2 heterodimerises *in vivo* with a conserved homolog, Bax, that accelerates programmed cell death. *Cell* 74 609-619.

Pardee, A. B. **(1989)** G_1 events and regulation of cell proliferation. *Science* 246 603-608.

Parker, L. L. and Piwnica-Worms, H. **(1992)** Inactivation of p34cdc2-cyclin B complex by the human Weel tyrosine kinase. *Science* 257 1955-1957.

Parker, L. L., Walter, S. A., Young, P. G. and Piwnica-Worms, H. **(1993)** Phosphorylation and inactivation of the mitotic inhibitor Weel by the nim1/cdr1 kinase. *Nature* 363 736-738.

Pastan, I. and Gottesman, M. M. **(1991)** Multidrug resistance. *Ann. Rev. Med.* 42 277-286.

Pastan, I., Gottesman, M. M., Ueda, K., Lovelace, E., Rutherford, A. V. and Willingham, M. C. **(1988)** A retrovirus carrying an MDR1 cDNA confers multidrug resistance and polarized expression of P-glycoprotein in MDCK cells. *Proceedings of the American Association for Cancer Research* 85 4486-4490.

Patel, J. and Rideout, D. **(1992)** Synergism and antagonism in cancer chemotherapy. *Canc. J.* 5(5) 254-266.

Perez, C., Pelayo, F., Vilaboa, N. E. and Aller, P. **(1994)** Caffeine attenuates the action of amsacrine and etopside in U-937 cells by mechanisms which involve inhibition of RNA synthesis. *Int. J. Cancer* 57 889-893.

Perry, M. E., Piette, J., Zawadzki, J. A., Harvey, D. and Levine, A. J. **(1993)** The mdm-2 gene is induced in response to UV light in a p53-dependent manner. *PNAS* 90 11623-11627.

Peter, M. and Herskowitz, I. **(1994)** Joining the complex: cyclin-dependent kinase inhibitory proteins and the cell cycle. *Cell* 79 181-184.

Pines, J. **(1993)** Cyclins and cyclin-dependent kinases: take your partners. *TIBS* 18 195-197.

Piscitelli, S. C., Rodvold, K. A., Rushing, D. A. and Tewksbury, D. A. **(1993)** Pharmokinetics and pharmacodynamics of doxorubicin in patients with small cell lung cancer. *Clin. Pharm.* 53(5) 555-561.

Polyak, K., Kato, J. Y., Solomon, M. J., Sherr, C. J., Massagué, J., Roberts, J. M. and Koff, A. **(1994)** p27Kip1, a cyclin-Cdk inhibitor, links transforming growth factor-ß and contact inhibition to cell cycle arrest. *Genes & Development* 8 9-22.

Pratt, W. B., Ruddon, R. W., Ensminger, W. D. and Maybaum, J. **(1994)** *The Anticancer Drugs* Oxford, Oxford University Press.

Price, B. and Park, S. J. **(1994)** DNA damage increases the levels of MDM2 messenger RNA in wtp53 human cells. *Can. Res.* 54 896-899.

Quilletmary, A., Mansat, V., Duchayne, E., Come, M. G., Allouche, M., Bailly, J. D., Bordier, C. and Laurent, G. **(1996)** Daunorubicin-induced internucleosomal DNA fragmentation in acute myeloid cell lines. *Leukemia* 10(3) 417-425.

Rao, P. N. **(1980)** The molecular basis of drug-induced G_2 arrest in mammmalian cells. *Molec. Cell Biochem.* 29 47-57.

Redmond, A. **(1991)** Multiple drug resistance in human tumor cells. *PhD* Dublin City University.

Reed, J. C. **(1994)** Bcl-2 and the regulation of programmed cell death. *J. Cell Biol.* 124 1-6.

Riordan, J. R., Rommens, J. M., Kerem, B. S., Alon, N., Rozmahel, R., Grzelczak, J. and Zielenski, J. **(1989)** Identification of the cycstic fibrosis gene: cloning and characterisation of complementary DNA. *Science* 245 1066-1073.

Roninson, I. B., Chin, J. E., Choi, K., Gros, P., Housman, D. E., Fojo, A., Gottesman, M. M. and Pastan, I. **(1986)** Isolation of human MDR sequences amplified in multidrug resistant KB carcinoma cells. *Proceedings of the American Association for Cancer Research* 83 4538-4542.

Rottmann, M., Schroder, H. C., Gramzow, M., Renneisen, K., Kurelec, B., Dorn, A., Friese, U. and Muller, W. E. **(1987)** Specific phosphorylation of proteins in pore complex laminas from the sponge Geodia cydonium by the homologue aggregation factor and phorbol ester. Role of protein kinase C in the phosphorylation of DNA topoisomerase II. *EMBO J.* 6 3939-3944.

Rowley, R., Hudson, J. and Young, P. G. **(1992)** The wee1 protein kinase is required for radiation-induced mitotic delay. *Nature* 356 353-355.

Russell, K. J., Wiens, L. W., Demers, G. W., Galloway, D. A., Plon, S. E. and Groudine, M. **(1995)** Abrogation of the G_2 checkpoint results in differential radiosensitization of G_1 checkpoint-deficient and G_1 checkpoint-competent cells. *Can. Res.* 55 1639-1642.

Russo, P., Cimoli, G., Valenti, M., De Sessa, F., Parodi, S. and Pommier, Y. **(1994)** Induction of DNA double-strand breaks by 8-methoxycaffeine: cell cycle dependence and comparison with topoisomerase II inhibitors. *Carcinogene.* 15(11) 2491-2496.

Safa, A. R., Glover, C. J., Sewell, J. L., Meyers, M. B., Biedler, J. K. and Felsted, R. L. **(1987)** Identification of the multidrug resistance related membrane glycoprotein as an acceptor for calcium channel blockers. *J. Biol. Chem.* 262 7884-7888.

Sander, M., Nolan, J. M. and Hsieh, T. S. **(1984)** A protein kinase activity tightly associated with Drosophila type II DNA topoisomerase *PNAS* 81(22) 6938-6942.

Scanlon, K. J., Ishida, H. and Kashani-Sabet, M. **(1994)** Ribozyme-mediated reversal of the multidrug-resistant phenotype. *Proceedings of the American Association for Cancer Research* 91 11123-11127.

Scheffer, G. L., Wijngaard, P. L. J., Flens, M. A., Izquierdo, M. A., Slovak, M. L., Pinedo, H. M., Meijer, C. J. L. M., Clevers, H. C. and Scheper, R. J. **(1995)** The drug resistance-related protein LRP is the human major vault protein. *Nature Med.* 1 578-582.

Scheper, R. J., Broxterman, H. J., Scheffer, G. L., Kaaijk, P., Dalton, W. S., van Heijningen, T. H. M., van Kalken, C. K., Slovak, M. L., de Vries, E. G. E., van der Valk, P., Meijer, C. J. L. M. and Pinedo, H. M. **(1993)** Overexpression of a Mr 110,000 vesicular protein in non-P-glycoprotein-mediated multidrug resistance *Can. Res.* 53 1475-1479.

Schiano, M. A., Sevin, B. U., Perras, J., Ramos, R., Wolloch, E. H. and Averette, H. E. **(1991)** *In vitro* enhancement of cis-platinum antitumor activity by caffeine and pentoxifylline in a human ovarian cell line *Gynecol. Oncol.* 43 37-45.

Schlegel, R. and Pardee, A. B. **(1986)** Caffeine-induced uncoupling of mitosis from the completion of DNA replication in mammalian cells. *Science* 232 1264-1266.

Serrano, M., Hannon, G. J. and Beach, D. **(1993)** A new regulatory motif in cell-cycle control causing specific inhibition of cyclin D/CDK4. *Nature* 366 704-707.

Sherr, C. J. **(1993)** Mammalian G_1 cyclins. *Cell* 73 1059-1065.

Shi, L., Nishioka, W. K., Th'ng, J., Morton Bradbury, E., Litchfield, D. W. and Greenberg, A. H. **(1994)** Premature p34cdc2 activation required for apoptosis. *Science* 263 1143-1145.

Shimizu, T., O'Connor, P. M., Kohn, K. W. and Pommier, Y. **(1995)** Unscheduled activation of cyclin B1/cdc2 kinase in human promyelocytic leukemia cell line HL60 cells undergoing apoptosis induced by DNA damage. *Can. Res.* 55 228-231.

Siemann, D. W. and Beyers, K. L. **(1993)** *In vivo* therapeutic potential of combination thiol depletion and alkylating chemotherapy. *Br. J. Canc.* 68 1071-1079.

Simon, S. M. and Schindler, M. **(1994)** Cell biological mechanisms of multidrug resistance in tumors. *PNAS* 91 3497-3504.

Skladanowski, A. and Konopa, J. **(1993)** Adriamycin and Daunomycin induce programmed cell death (apoptosis) in tumour cells. *Bioch. Pharm.* 46(3) 375-382.

Smeets, M. F. M. A., Mooren, E. H. M., Abdel-Wahab, A. H. A., Bartelink, H. and Begg, A. C. **(1994)** Differential repair of radiation-induced DNA damage in cells of human squamous cell carcinoma and the effect of caffeine and cysteamine on induction and repair of DNA double-strand breaks. *Radiat. Res.* 140 153-160.

Smeyne, R. J., Vendrell, M., Hayward, M., Baker, S. J., Miao, G. G., Schilling, K., Robertson, L. M., Curran, T. and Morgan, J. I. **(1993)** Continuous c-fos expression precedes programmed cell death *in vivo*. *Nature* 363 166-169.

Smith, M. L., Chen, I., Bae, I., Chen, C., Gilmer, T., Kastan, M. B., O'Connor, P. M. and Fornace, A. J. **(1994)** Physical and functional interaction of the p53-regulated protein Gadd45 with proliferating cell nuclear antigen. *Science* 266 1376-1380.

Smith, P. J., Rackstraw, C. and Cotter, F. **(1994)** DNA fragmentation as a consequence of cell cycle traverse in doxorubicin- and idarubicin-treated human lymphoma cells. *Ann. Hematol.* 69 S7-S11.

Smith, P. J., Soues, S., Gottlieb, T., Falk, S. J., Watson, J. V., Osborne, R. J. and Bleenan, N. M. **(1994)** Etopside-induced cell cycle delay and arrest-dependent modulation of DNA topoisomerase II in small-cell lung cancer cells. *Br. J. Canc.* 70 914-921.

Solary, E., Bertrand, R. and Pommier, Y. **(1994)** Apoptosis induced by DNA topoisomerase I and II inhibitors in human leukemic HL-60 cells. *Leukemia & Lymphoma* 15 21-32.

Solomon, M., Glotzer, M., Lee, T. H., Phillipe, M. and Kirschner, M. **(1990)** Cyclin activation of p34cdc2. *Cell* 63 1013-1024.

Sorenson, C. M. and Eastman, A. **(1988)** Mechanism of cis-diamminedichloroplatinum(II)-induced cytotoxicity: Role of G_2 arrest and DNA double-strand breaks. *Can. Res.* 48 4484-4488.

Sorger, P. K. and Murray, A. W. **(1992)** S-phase feedback control in budding yeast independent of tyrosine phosphorylation of p34cdc28. *Nature* 355 365-368.

Spoelstra, E. C., Westerhoff, H. V., Pinedo, H. M., Dekker, H. and Lankelma, J. **(1994)** The multidrug-resistance-reverser verapamil interferes with cellular P-glycoprotein-mediated pumping of daunorubicin as a non-competing substrate. *Eur. J. Biochem.* 221 363-373.

Staunton, M. J. and Gaffney, E. F. **(1995)** Tumor type is a determinant of susceptibility to apoptosis. *A.J.C.P.* 103(3) 300-307.

Steinmann, K. E., Belinsky, G. S., Lee, D. and Schlegel, R. **(1991)** Chemically induced premature mitosis: Differential response in rodent and human cells and the relationship to cyclin B systhesis and p34cdc2/cyclin B complex formation. *PNAS* 88 6843-6847.

Stewart, D. J. and Evans, W. K. **(1989)** Non-chemotherapeutic agents that potentiate chemotherapy efficacy. *Cancer Treatment Reviews* 16 1-40.

Stoilov, L. M., Mullenders, L. H. F. and Natarajan, A. T. **(1994)** Caffeine potentiates or protects against radiation-induced DNA and chromosomal damage in human lymphocytes depending on temperature and concentration. *Mut. Res.* 311 169-174.

Sugawara, I., Kataoka, I., Morishita, Y., Hamada, H., Tsuruo, T., Itoyama, S. and Mori, S. **(1988)** Tissue distribution of P-glycoprotein encoded by the multidrug resistant gene as revealed by a monoclonal antibody, MRK16. *Can. Res.* 48 4611-4614.

Sugawara, I., Nakahama, M., Hamada, H., Tsuruo, T. and Mori, S. **(1988)** Apparent stronger expression in the human adrenal cortex than in the human adrenal medulla of Mr170,000-180,000 P-glycoprotein. *Can. Res.* 32 4611-4614.

Sullivan, D. M., Rowe, T. C., Latham, M. D. and Ross, W. E. **(1989)** Purification and characterization of an altered topoisomerase II from a drug-resistant Chinese hampster ovary cell line. *Biochem.* 28 5680-5687.

Sullivan, S. M. **(1994)** Development of ribozymes for gene therapy. *J. Inves. Der.* 103 85S-89S.

Sumantran, V. N., Ealovega, M. W., Nunez, G., Clarke, M. F. and Wicha, M. S. **(1995)** Overexpression of bcl-x_S sensitizes MCF-7 cells to chemotherapy-induced apoptosis. *Can. Res.* 55 2507-2510.

Symthe, C. and Newport, J. W. **(1992)** Coupling of mitosis to the completion of S phase in Xenopus occurs via the modulation of the tyrosine kinase that phosphorylates p34cdc2. *Cell* 68 787-797.

Takayama, S., Sato, T., Krajewski, S., Kochel, K., Irie, S., Millan, J. A. and Reed, J. C. **(1995)** Cloning and functional analysis of Bag-1: a novel Bcl-2-binding protein with anti-cell death activity. *Cell* 80 279-284.

Tam, S. W. and Schlegel, R. **(1992)** Staurosporine overrides checkpoints for mitotic onset in BHK cells. *Cell Growth* 3 811-817.

Tan, K. B., Mattern, M. R., Eng, W. K., McCabe, F. L. and Johnson, R. K. **(1989)** Nonproductive rearrangement of DNA topoisomerase I nad II genes. *J. Nat. Canc.* 81 1732-1735.

Thiebaut, F., Tsuruo, T., Hamada, H., Gottesman, M. M., Pastan, I. and Willingham, M. C. **(1987)** Cellular localisation of the multidrug resistant gene product P-glycoprotein in normal tissues. *Proceedings of the American Association for Cancer Research* 84 7735-7738.

Thornberry, N. A., Bull, H. G., Calaycay, J. R., Chaoman, K. T., Howard, A. D., Kostura, M. J., Miller, D. K., Molineaux, S. M., Weidner, J. R., Aunins, J., Elliston, K. O., Ayala, J. M., Casano, F. J., Chin, J., Ding, G. J.-F., Egger, L. A., Gaffney, E. P., Lumoco, G., Palyha, O. C., Raju, S. M., Rolando, A. M., Salley, J. P., Yamin, T.-T., Lee, T. D., Shively, J. E., MacCross, J. E., Mumford, R. A., Schmidt, J. A. and Tocci, M. J. **(1992)** A novel heterodimeric cysteine protease is required for interleukin-1ß processing in monocytes. *Nature* 356 768-774.

Traganos, F., Kapuscinski, J. and Darnzynkiewicz, Z. **(1991)** Caffeine modulates the effects of DNA-intercalating drugs *in vitro*: A flow cytometric and spectrophotometric analysis of caffeine interaction with novantrone, doxorubicin, ellipticine, and the doxorubicin analogue AD 198. *Can. Res.* 51 3682-3689.

Traganos, F., Kapuscinski, J., Gong, J., Ardelt, B., Darzynkiewicz, R. J. and Darzynkiewicz, Z. **(1993)** Caffeine prevents apoptosis and the cell cycle effects induced by camptothecin or topotecan in HL-60 cells. *Can. Res.* 53 4613-4618.

Tsao, Y. P., D'Arpa, P. and Liu, L. F. **(1992)** The involvement of active DNA synthesis in campothecin-induced G_2 arrest: Altered regulation of p34cdc2/cyclin B. *Can. Res.* 52 1823-1829.

Tsujii, M. and DuBois, R. N. **(1995)** Alterations in cellular adhesion and apoptosis in epithelial cells overexpressing prostaglandin endoperoxide synthase 2. *Cell* 83 493-501.

Ueda, K., Cardarelli, C., Gottesman, M. M. and Pastan, I. **(1987)** The multidrug resistance (MDR1) gene: cDNA cloning and transcription initiation. *J. Biol. Chem.* 262 505-508.

Van der Bliek, A. M., Van der Velds-Koerts, T., Ling, V. and Borst, P. **(1986)** Overexpression and amplification of five genes in a multidrug resistant chinese hampster ovary cell line. *Mol. Cell Biol.* 6 1671-1678.

van der Graaf, W. T. A., de Vries, E. G. E., Timmer-Bosscha, H., Meersma, G. J., Mesander, G., Vellenga, E. and Mulder, N. H. **(1994)** Effects of amiodarone, cyclosporin A and PSC 833 on the cytotoxicity of mitoxantrone, doxorubicin and vincristine in non-P-glycoprotein human small cell lung cancer cell lines. *Can. Res.* 54 5368-5373.

Vaux, D. L., Weissman, I. L. and Kim, S. K. **(1992)** Prevention of programmed cell death in Caenorhabditis elegans by human bcl-2. *Science* 258 1955-1957.

Veis, D. J., Sorenson, C. M., Shutter, J. R. and Korsmeyer, S. J. **(1993)** Bcl-2-deficient mice demonstrate fulminant lymphoid apoptosis, polycystic kidneys, and hypopigmented hair. *Cell* 75 229-240.

Walton, M. L., Whysong, D., O'Connor, P. M., Hockenbury, D., Korsmeyer, S. J. and Kohn, K. W. **(1993)** Constitutive expression of human bcl-2 modulates nitrogen mustard and campothecin induced apoptosis. *Can. Res.* 53 1853-1861.

Wang, H.-G., Milan, J. A., Cox, A. D., Der, C. J., Rapp, U. R., Beck, T., Zha, H. and Reed, J. C. **(1995)** R-ras promates apoptosis caused by growth factor deprivation via a Bcl-2 suppressible mechanism. *J. Cell Biol.* 129 1103-1114.

Wang, L., Miura, M., Bergeron, L., Zhu, H. and Yuan, J. **(1994)** Ich-1, an ICE/ced-3-related gene, encodes both positive and negative regulators of programmed cell death. *Cell* 78 739-750.

Weinberg, R. A. **(1995)** The retinablastoma protein and cell cycle control *Cell* 81 323-330.

Whitacre, C. M., Hashimoto, H., Tsai, M. L., Chatterjee, S., Berger, S. J. and Berger, N. A. **(1995)** Involvement of NAD-poly(ADP-ribose) metabolism in p53 regulation and its consequences. *Can. Res.* 55 3697-3701.

Williams, G. T. and Smith, C. A. **(1993)** Molecular regulation of apoptosis: genetic controls on cell death. *Cell* 74 777-779.

Wood, A. C., Elvin, P. and Hickman, J. A. **(1995)** Induction of apoptosis by anti-cancer drugs with disparate modes of action: kinetics of cell death and changws in c-myc expression. *Br. J. Canc.* 71 937-941.

Xu, M., Sheppard, K. A., Peng, C. Y., Yee, A. S. and Piwnica-Worms, H. **(1994)** Cyclin A/CDK2 binds directly to E2F-1 and inhibits the DNA-binding activity of E2F-1/DP-1 by phosphorylation. *Mol. Cell Biol.* 14 8420-8431.

Yamaizumi, M. and Sugano, T. **(1994)** U.V.-induced nuclear accumulation of p53 is evoked through DNA damage of actively transcribed genes independentof the cell cycle. *Oncogene* 9 2775-2784.

Yang, E., Zha, J., Jockel, J., Boise, L. H., Thompson, C. B. and Korsmeyer, S. J. **(1995)** Bad, a heterodimeric partner for Bcl-xL and Bcl-2, displaces Bax and promote cell death. *Cell* 80 285-291.

Yin, X.-M., Oltvai, Z. N. and Korsmeyer, S. J. **(1994)** BH1 and BH2 domains of Bcl-2 are required for inhibition of apoptosis and heterodimerisation with Bax. *Nature* 369 321-323.

Zaman, G. J. R., Versantvoort, C. H. M., Smit, J. J. M., Eijdems, W. H. M., de Haas, M., Smith, A. J., Broxterman, H. J., Mulder, N. H., de Vries, E. G. E., Baas, F. and Borst, P. **(1993)** Analysis of the expression of MRP, the gene for a new putative transmembrane drug transporter, in human multidrug resistant lung cancer cell lines. *Can. Res.* 53 1747-1750.

Zhan, Q., Bae, I., Kastan, M. B. and Fornace, A. J. **(1994)** The p53-dependent gamma-Ray response of GADD45. *Can. Res.* 54 2755-2760.

Zhan, Q., Carrier, F. and Fornace, A. J. **(1993)** Induction of cellular p53 activity by DNA-damaging agents and growth arrest. *Mol. Cell Biol.* 13 4242-4250.

Zhan, Q., El-Deiry, W., Bae, I., Alamo, I., Kastan, M. B., Vogelstein, B. and Fornace, A. J. J. **(1995)** Similarity of the DNA-damage responsiveness and growth-suppresssive properties of WAF1/CIP1 and GADD45. *Int. J. Oncol.* 6 1-9.

Zhan, Q., Lord, K. A., Alamo, I., Hollander, M. C., Carrier, F., Ron, D., Kohn, K. W., Hoffman, B., Liebermann, D. A. and Fornace, A. J. **(1994)** The gadd and MyD genes define a novel set of mammalian genes encoding acidic proteins that synergistically suppress cell growth. *Mol. Cell Biol.* 14 2361-2371.